

WORKING GROUP ON THE INTEGRATED ASSESSMENTS OF THE BARENTS SEA (WGIBAR)

VOLUME 2 | ISSUE 30

ICES SCIENTIFIC REPORTS

RAPPORTS
SCIENTIFIQUES DU CIEM



International Council for the Exploration of the Sea Conseil International pour l'Exploration de la Mer

H.C. Andersens Boulevard 44-46
DK-1553 Copenhagen V
Denmark
Telephone (+45) 33 38 67 00
Telefax (+45) 33 93 42 15
www.ices.dk
info@ices.dk

The material in this report may be reused for non-commercial purposes using the recommended citation. ICES may only grant usage rights of information, data, images, graphs, etc. of which it has ownership. For other third-party material cited in this report, you must contact the original copyright holder for permission. For citation of datasets or use of data to be included in other databases, please refer to the latest ICES data policy on ICES website. All extracts must be acknowledged. For other reproduction requests please contact the General Secretary.

This document is the product of an expert group under the auspices of the International Council for the Exploration of the Sea and does not necessarily represent the view of the Council.

ISSN number: 2618-1371 | © 2020 International Council for the Exploration of the Sea

ICES Scientific Reports

Volume 2 | Issue 30

WORKING GROUP ON THE INTEGRATED ASSESSMENTS OF THE BARENTS SEA (WGIBAR)

Recommended format for purpose of citation:

ICES. 2020. Working Group on the Integrated Assessments of the Barents Sea (WGIBAR).
ICES Scientific Reports. 2:30. 206 pp. <http://doi.org/10.17895/ices.pub.5998>

Editors

Elena Eriksen • Anatoly Filin

Authors

Espen Bagøien • Bjarte Bogstad • Padmini Dalpadado • Andrey Dolgov • Elena Eriksen • Johanna Fall
Per Fauchald • Anatoly Filin • Sylvia Frantzen • Harald Gjørseter • Cecilie Hansen • Daniel Howell Bé-
rengère Husson • Randi Ingvaldsen • Edda Johannesen • Lis Lindal Jørgensen • Roman Klepikovskiy
Vidar Lien • Gro van der Meeren • Nils Øyen • Tatiana Prokhorova • Irina Prokopchuk • Dmitry
Prozorkevich • Alexey Russkihk • Hein Rune Skjoldal • Hiroko Solvang • Nataliya Strelkova • Aleksandr
Trofimov • Denis Zakharov



ICES
CIEM

International Council for
the Exploration of the Sea
Conseil International pour
l'Exploration de la Mer

Contents

i	Executive summary	ii
ii	Expert group information.....	iii
1	Terms of Reference a) – f)	1
2	Summary of Work plan.....	2
3	List of Outcomes and Achievements of the WG in this delivery period.....	3
4	Progress report of ToR a) - f)	5
4.1	Progress report on ToR a	5
4.2	Progress report on ToR b	5
4.3	Progress report on ToR c.....	5
4.4	Progress report on ToR d	7
4.5	Progress report on ToR e	10
4.6	Progress report on ToR f.....	11
4.7	Cooperation	11
5	Revisions to the work plan and justification	13
6	Next meeting.....	14
Annex 1:	List of participants.....	15
Annex 2:	WGIBAR recommends.....	17
Annex 3:	Agenda for the WGIBAR 2020 meeting	18
Annex 4:	The state and trends of the Barents Sea ecosystem in 2019.....	20

i Executive summary

The Working Group on the Integrated Assessments of the Barents Sea (WGIBAR) conducts and develops integrated ecosystem assessments for the Barents Sea.

In this report the group updated and extended historical time-series used for the integrated assessments. New spatial time-series for mesoplankton and 0-group fish were added to the existing time-series. Trend analysis was performed and the application of ecosystem models to assessment of the Barents Sea ecosystem was discussed. The annual report “The state and trends of the Barents Sea ecosystem” was updated. This provides information on the status and changes in the Barents Sea ecosystems for the Joint Russian-Norwegian Fisheries Commission, the Joint Russian-Norwegian Environmental Commission, the Norwegian Ministry of Climate and Environment.

The group discussed the current state and changes of the Barents Sea ecosystem and concluded that:

- The Barents Sea has become colder since 2015–2016, and the cooling continued from 2018 to 2019. However, the air and water temperatures are still typical of warm years. Mesozooplankton biomass in the Barents Sea in autumn 2019 was approximately the same as in recent years, and krill biomass has shown an increasing trend in recent decades. Temperatures in 2020–21 are expected to decline slightly but will remain relatively high; the plankton are anticipated to therefore provide good feeding conditions for planktivorous consumers.
- In 2019, total biomass of pelagic fish in the Barents Sea was estimated to be at the lowest level in the last 20 years. The main demersal fish stocks in the Barents Sea are in a healthy state and at a level at or above the long-term mean. Diet composition of cod has been relatively stable in recent years. The stock of northern shrimp is relatively stable in the last years. The snow crab population is still spreading, and its abundance is increasing in the Barents Sea.
- The white-beaked dolphin was the most common species of marine mammal in 2019 during the ecosystem survey. Summer abundance of minke whales and humpback whales in the Barents Sea has increased recently.
- The main stocks are fished sustainably, without violations of fisheries regulations. Concentrations of most contaminants in fish and crustaceans in the Barents Sea are relatively low in comparison to other sea areas. The amount of plastic and other litter in the sea is also relatively low. Levels of the anthropogenic radionuclides Cs-137, Sr-90 and Pu-239,240 in seawater, sediments, fish and seaweed are currently low.

The WGIBAR provides background ecosystem information on stock development of relevance to assessment expert groups. This report also identifies vulnerable and valuable areas in the Barents Sea.

ii Expert group information

Expert group name	Working Group on the Integrated Assessments of the Barents Sea (WGIBAR)
Expert group cycle	Multiannual
Year cycle started	2020
Reporting year in cycle	1/3
Chair(s)	Elena Eriksen, Norway
	Anatoly Filin, Russia
Meeting venue(s) and dates	24-28 February 2020, Bergen, Norway (29 participants)

1 Terms of Reference a) – f)

ToR	Description	Background	Science Plan codes	Duration	Expected Deliverables
a	Prepare relevant datasets that can be used for the integrated assessments of the Barents Sea	Science and advisory requirements	6.1	Year 1,2, 3	Updated datasets
b	Perform an integrated analysis of multivariate datasets and other relevant information including model outputs	Science and advisory requirements	1.3; 1.4	Year 1, 2, 3	Annual reports
c	Analyse spatial patterns and trends with special emphasis on shifting distribution of communities and species, and valuable and vulnerable areas	Science and advisory requirements	2.2; 2.4	Year 1, 2, 3	Annual reports
d	Prepare an annual report on the status and trends of the Barents Sea ecosystem	Science and advisory requirements	1.3; 2.1; 6.5	Year 1, 2, 3	Annual reports
e	Provide support to ongoing ecosystem assessments and evaluations in the Barents Sea	Science and advisory requirements	2.2; 2,7; 6.1	Year 1, 2, 3	Annual report
f	Evaluate the current monitoring of the Barents Sea ecosystem	Science and advisory requirements	3.1; 3.2	Year 1,2,3	Annual reports

2 Summary of Work plan

Year	Description
Year 1	<p>Prepare relevant datasets and other relevant information, including biotic and abiotic ecosystem components and human pressure that can be used for the integrated assessment of the Barents Sea.</p> <p>Perform an integrated analysis of multivariate datasets and other relevant information including model outputs</p> <p>Prepare an annual report on the Barents Sea ecosystem status and describe fluctuations and changes based on trend analyses and integrated analysis of multivariate datasets</p> <p>Evaluate the current monitoring of the Barents Sea ecosystem</p> <p>Provide support to ongoing ecosystem assessments and evaluations in the Barents Sea</p>
Year 2	<p>Prepare relevant datasets and other relevant information, including biotic and abiotic ecosystem components and human pressure that can be used for the integrated assessment of the Barents Sea.</p> <p>Perform an integrated analysis of multivariate datasets and other relevant information including model outputs</p> <p>Prepare an annual report on the Barents Sea ecosystem status and describe fluctuations and changes based on trend analyses and integrated analysis of multivariate datasets</p> <p>Evaluate the current monitoring of the Barents Sea ecosystem</p> <p>Provide support to ongoing ecosystem assessments and evaluations in the Barents Sea</p>
Year 3	<p>Prepare relevant datasets and other relevant information, including biotic and abiotic ecosystem components and human pressure that can be used for the integrated assessment of the Barents Sea.</p> <p>Perform an integrated analysis of multivariate datasets and other relevant information including model outputs</p> <p>Prepare an annual report on the Barents Sea ecosystem status and describe fluctuations and changes based on trend analyses and integrated analysis of multivariate datasets</p> <p>Evaluate the current monitoring of the Barents Sea ecosystem</p> <p>Provide support to ongoing ecosystem assessments and evaluations in the Barents Sea</p> <p>Revise the Barents Sea ecoregion description in the ICES Ecosystem Overview, including overview of the ecosystem, its current state and changes under the environmental and anthropogenic impacts</p>

3 List of Outcomes and Achievements of the WG in this delivery period

- WGIBAR prepared relevant datasets to describe status and analyse of long-term changes in the Barents Sea ecosystem.
- The annual report “The state and trends of the Barents Sea ecosystem” has been updated. Two new subchapter describes organic contaminants in marine organisms and radioactive contamination state and changes were included.
- Trend analysis of historical datasets was performed and main changes in the Barents Sea ecosystem were identified. The main points for 2019 are listed in the executive summary.
- WGIBAR started processes with identification of valuable areas in the Barents Sea with 1) preparation of a general description of the ecosystem, important species (biology and vulnerable stages or habitat) and important interactions, and 2) evaluation of the Arctic Monitoring and Assessment Program (AMAP) identification of the vulnerable areas.
- WGIBAR used results of ecosystem models to improve “Interaction” chapter in the report “The state and trends of the Barents Sea ecosystem” and build a bridge between IEA and modelers.
- Most of the scientific work relevant for WGIBAR is done by other projects at IMR/PINRO or other institutions. Because of the way WGIBAR is funded there is little intersessional work done by WGIBAR as a group.

List of relevant publications

- Dupont, N., Durant, J. M., Langangen, O., Gjøsæter, H., and Stige, L. C. (Accepted). Sea ice, temperature, and prey effects on annual variations in mean lengths of a key Arctic fish, *Boreogadus saida*, in the Barents Sea. *ICES J. Mar. Sci.*
- Eriksen, E., Bogstad, B., Dolgov, A.V., and Beck, I.M. 2017. Cod diet as an indicator of Ctenophora abundance dynamics in the Barents Sea. *Marine Ecology Progress Series*, <https://doi.org/10.3354/meps12199>
- Eriksen, E., Skjoldal, H.R., Gjøsæter, H. and Primicerio R. 2017. Spatial and temporal changes in the Barents Sea pelagic compartment during the recent warming. *Progress in Oceanography* 151: 206-226, <http://dx.doi.org/10.1016/j.pocean.2016.12.009>
- Eriksen, E., Huserbråten, M., Gjøsæter, H., Vikebø, F. and Albretsen, J. 2019. Polar cod egg and larval drift patterns in the Svalbard archipelago. *Polar Biology*, <https://doi.org/10.1007/s00300-019-02549-6>
- Eriksen, E., Benzik, A.N., Dolgov, A.V., Skjoldal, H.R., Vihtakari, M., Johannesen, E., Prokhorova, T.S., Keulder-Stenevik, F., Prokopchuk, I., Strand, E. 2020. Diet and trophic structure of fishes in the Barents Sea: the Norwegian-Russian program “Year of stomachs” 2015 -establishing a baseline. *Progress in Oceanography*. <https://doi.org/10.1016/j.pocean.2019.102262>
- Eriksen, E., Gjøsæter, H., Prozorkevich, D., Shamray, E., Dolgov, A., Skern-Mauritzen, M., Stiansen, J.E., Kovalev, Yu., Sunnanaa K. 2017. From single species surveys towards monitoring of the Barents Sea ecosystem. *Progress in Oceanography* <http://dx.doi.org/10.1016/j.pocean.2017.09.007>
- Grøsvik, B.E., Prokhorova, T., Eriksen, E., Krivosheya, P., Horneland, P.A., Prozorkevich, D. 2018. Assessment of marine litter in the Barents Sea, a part of the joint Norwegian-Russian ecosystem survey. *Front. Mar. Sci.*, 06 March 2018. <https://doi.org/10.3389/fmars.2018.00072>
- Huserbråten, M., Eriksen, E., Gjøsæter, H., Vikebø, F. 2019. Polar cod in jeopardy under the retreating Arctic sea ice. *Communications Biology*, 2. <https://www.nature.com/articles/s42003-019-0649-2>
- Jørgensen, L. L., Primicerio, R., Ingvaldsen, R. B., Fossheim, M., Strelkova, N., Thangstad, T. H., & Zakharov, D. (2019). Impact of multiple stressors on seabed fauna in a warming Arctic. *Marine Ecology Progress Series*, 608, 1-12.

- [Skaret, G., Johansen, G. O., Johnsen, E., Fall, J., Fiksen, Ø., Englund, G., Fauchald, P., Gjosæter, H., Macaulay, G., Johannesen, E. \(in press\). Diel vertical movements determine spatial interactions between cod, pelagic fish and krill on an Arctic shelf bank. Marine Ecology Progress Series](#)
- [Fall, J., Ciannelli, L., Skaret, G., & Johannesen, E. \(2018\). Seasonal dynamics of spatial distributions and overlap between Northeast Arctic cod \(*Gadus morhua*\) and capelin \(*Mallotus villosus*\) in the Barents Sea. PLoS One, 13\(10\), e0205921. doi:10.1371/journal.pone.0205921](#)
- [Fall, J. \(2019\). Drivers of variation in the predator-prey interaction between cod and capelin in the Barents Sea. PhD thesis, University of Bergen.](#)
- [Fall, J., & Fiksen, Ø. \(2019\). No room for dessert: A mechanistic model of prey selection in gut-limited predatory fish. Fish and Fisheries, 21\(1\), 63-79. doi:10.1111/faf.12415](#)

4 Progress report of ToR a) - f)

4.1 Progress report on ToR a

The historical time-series that are used for the integrated assessments of the Barents Sea ecosystem were updated and extended. New spatial time-series for mesoplankton and 0-group fish were used in addition to traditional time-series.

4.2 Progress report on ToR b

The trend analysis was performed using the updated historical data. The time-series were standardized to zero mean and unit variance. Results of the trend analysis are presented in the Annex 4.

H.Solvang presented analyses for common trend estimation and warning signal for WGIBAR time-series data. Common trend analysis includes two procedures - trend estimation and classification as groups presenting similar configurations. The results for common trends are communicated in an easily accessible form by using 'icons', which could give general references to the needs of stakeholders. Warning signal analysis also includes two procedures – trend estimation and prediction using data in a specific time period. By comparing the observations with the prediction (and the confidence intervals), it is useful to investigate whether the recent observations follow the estimated trend or are away from the trend. This may make an assessment whether the observation is a sign of something 'unusual' going on in the ecosystem that may represent a warning signal.

C. Hansen presented results of using the NoBa Atlantis model for evaluation of snow crab impact on fish stocks in the Barents Sea. NoBa is a large, complex end-to-end model implemented for the Nordic and Barents Seas, representing the ecosystems in the area by 53 species and functional groups. In the study, the ecosystem impact of snow crab was explored. A set of scenarios was run for the period of 1995-2035, including changes in recruitment, predation, distribution and harvest. Preliminary results show that it is not necessarily that the direct predator-prey links that are the most important. The indirect predation pressure relief for some of the small pelagic stocks (capelin, polar cod, Norwegian spring-spawning herring) is more important than the direct predation effects of snow crab on benthos and on large predators on snow crab. It has to be emphasized that some of the effects that we do not see (e.g. predation effects on benthos), is most likely due to the resolution of the benthos functional groups in the model. Until now, these have been implemented as extremely large functional groups, with huge biomass, and the predation from a relatively small snow crab population in comparison, will have no or very small effects.

4.3 Progress report on ToR c

Results from study on impact of cod-capelin spatial overlap on cod's consumption of capelin were presented by Johanna Fall. The overlap between the species was quite low in both summer and winter, which were interpreted as a weak aggregative response of cod to capelin. Increasing population sizes (particularly of cod) and water temperature have influenced a northeastward shift of the late summer overlap area. The correlation between spatial overlap and consumption was examined for summer and found to be very low, both at the scale of sampling and when scaled up to the larger overlap area. Within the overlap area, individual consumption of capelin

was highly variable. This had little to do with variation in capelin density, as the relationship between capelin consumption and capelin density was relatively flat. In contrast, the vertical distribution of capelin explained more variation, especially at the Great and Central banks where the main feeding interaction took place. Here, cod were found in relatively high densities, and had more capelin in their stomachs when capelin stood closer to the seafloor. Vertical overlap, rather than horizontal, therefore has potential as an indicator of cod-capelin interaction strength and should be further explored. Finally, a potential mechanism behind cod's weak aggregative response to capelin was suggested; once capelin is present, it is present in densities that allow cod to reach satiation. If this is the case, cod may not get any additional benefit from aggregating in areas with high capelin density.

P. Fauchald presented results on modelling of spatial interactions between seabirds, predatory fish, pelagic fish, 0-group fish, krill and mesolankton. Ecosystem survey data from the Barents Sea were used for this. The data were aggregated on a coarse spatial scale (100km), and the spatial interactions were addressed by the spatial overlap among the different organism groups. The data were fitted to Structural Equation Models (SEM). Specifically, we used the Piecewise SEM package in R which allows complex model structures and the specification of generalized linear mixed models. Temperature (10m), temperature fronts and salinity were used as exogeneous variables, and the models were controlled for year and spatial autocorrelation. The results from the final model are described in the following. There were strong effects of temperature on the distribution of the different species. The relationships were both positive and negative, suggesting that the species are distributed in temperature niches along the temperature gradient in the Barents Sea. There were numerous positive paths from capelin, zero-group fish, polar cod and herring to the top predators, suggesting predator-aggregation on prey patches. Capelin and 0-group fish were the most important and structuring prey groups. Negative paths were found between capelin and meso-zooplankton and between capelin and krill, suggesting that high concentrations of capelin have a negative impact on the abundance of these prey groups. We found several positive paths between top predators, suggesting that predators tend to be attracted by each other and that facilitation among predators is important for the spatial structure. Finally, there were negative paths from capelin to Atlantic puffin and from capelin to little auk. Capelin, puffin and little auk have overlapping diets, and the results suggest that the two seabird species avoid areas with high concentrations of capelin, presumably to avoid detrimental competition. In sum, these preliminary analyses suggest that the spatial organization of the Barents Sea ecosystem is related both to the dominating temperature gradient and to spatial interactions among species. In general, capelin was found to be a central structuring species following a "wasps-waist" organization with positive spatial relationship with top-predators and negative relationships with krill, zooplankton and seabird competitors. Facilitation was important among top-predators with cod and Brünnich's guillemot as dominating structuring species.

E. Eriksen presented results of study on biologically and ecologically significant areas in the Barents Sea. The assessment of this areas from an ecosystem structure and function perspective requires a broad evaluation of biological/ecological components and processes. In 2019 ICES has been hold a workshop on ecological valuing of areas of the Barents Sea (WKBAR). The outcome of this workshop were a definition and development of the ecological values, criteria and framework to identify areas of special ecological value, as well as an evaluation of potential of their using for management (ICES, 2019). This provides a scientific basis for evaluation of biologically and ecologically significant areas in the Barents Sea. To perform this the group start preparation of a background document on description of the Barents Sea ecosystem, main processes and key species (Appendix 5).

E. Eriksen presented also an international work done by AMAP (AMAP 2007, 2009,) and PAME (2009) aimed to identify ecologically and biologically important areas in the Arctic, including the Barents Sea.

References

- AMAP 2007 <https://www.amap.no/documents/doc/assessment-2007-oil-and-gas-activities-in-the-arctic-effects-and-potential-effects.-volume-1/776>
- AMAP 2009 <https://oaarchive.arctic-council.org/handle/11374/54>
- PAME 2009 <https://www.amap.no/documents/download/1548/inline>
- ICES. 2019. Workshop on ecological valuing of areas of the Barents Sea (WKBAR)/ ICES Scientific Reports. 1:39. 34 pp. <http://doi.org/10.17895/ices.pub.5444>

4.4 Progress report on ToR d

The followed presentations focusing of status of different ecosystem components and pressures were given during the meeting:

Hydrography, Alexander Trofimov and Vidar Lien

The situation for 2019 was presented for the following parameters: temperature (air and water), salinity, sea ice coverage, NAO index, index for storm activity, Atlantic waters inflow and areas of Atlantic, Arctic and mixed waters. In the western entrance of the Barents Sea, the Atlantic Water temperatures in 2019 were at the same level as in the early 2000s. Coastal and Atlantic waters in the Kola Section were fresher than in 2018. In autumn, the area of Atlantic waters ($>3^{\circ}\text{C}$) decreased slightly and the area of Arctic waters near bottom ($<0^{\circ}\text{C}$) increased slightly compared to 2018, whereas the area of cold bottom waters ($<0^{\circ}\text{C}$) almost tripled compared to the previous year. Ice coverage has increased since 2016 due to lower temperatures and lower inflow of Atlantic Water. In 2019, the ice coverage was below average but higher than in 2018; its seasonal maximum (51%) was in March, a month earlier than usual, its seasonal minimum (1%) was in September, as usual.

Plankton, Espen Bagøien and Irina Prokopchuk

The plankton status based on the most recent data available was presented. This includes time-series for satellite-based estimates of net primary production, time-series and spatial distributions of mesozooplankton biomass, abundances of *Calanus spp.* and other dominant copepod species, as well as biomass and distributions of macroplankton. Estimated net primary production has shown an increasing trend with a doubling over the last twenty years for the Barents Sea as a whole. The mesozooplankton biomass in autumn 2019 was at approximately the same level as in recent years for the Barents Sea as a whole. The biomass in the western inflow area of Atlantic water was higher in 2019, and also somewhat higher on the Central and Great Banks, than in preceding years. The biomass in the eastern and northern areas remained at a relatively high level comparable to the long-term mean. Krill biomass has shown an increasing trend in recent decades and remained high in 2019. Pelagic amphipods were nearly absent in 2012-2013, but have since shown increased abundances and expanded distributions in the area east of Svalbard. The plankton situation in 2019 indicated good feeding conditions for planktivorous consumers.

0-group fish, Elena Eriksen

Abundance estimates and mean length were calculated for the new strata system (15 subareas) using MatLab. It was done for period 1980-2018 and that summarized for the entire Barents Sea (ICES 2019). The «new» 0-group indices are very close to those calculated before by other software (SAS, ICES 2017). A new standard software, StoX software (Johnsen et al. 2019), was used to calculate indices in 2019. These indices were not checked for comparability with previous calculations. Thus, the 2019 indices are preliminary and will be verified later.

The main distribution of most of 0-group species were covered well in 2019. The 2019-year class of capelin was estimated as a strong. The 2019-year class of redfish was close to long-term mean level. The 2019-year classes of cod, haddock, polar cod and herring were estimated as weak. Abundance indices of saithe, long rough dab, sandeel and Greenland halibut were not calculated.

Pelagic fish, Dmitry Prozorkevich

Status and development of the pelagic fish stocks in the Barents Sea were presented. The distribution area of juvenile herring, capelin and blue whiting in the Barents Sea was covered enough well in the survey of 2019 but the distribution of polar cod was only partially covered. The survey indices for these species were calculated. Polar cod index shows a low level of its stock in the Barents Sea, but the estimate is more uncertain than for the other pelagic species. In 2019, the total biomass of pelagic fish in the Barents Sea was below 2 million tons, this is less than long-term mean and is lowest level in the last 23 years. The biomass of young herring (age 1-2) in 2019 in the Barents Sea decreased compare to 2018 and was close to the long-term level. This estimation is based on the ICES assessment by VPA. The total capelin stock was estimated at 0.41 million tonnes, it is significantly below the long-term average and represents a 75% decrease compare to 2018. In 2019 about 73% (0.3 million tonnes) of the capelin stock was represented by maturing individuals. Distribution of blue whiting in the Barents Sea depends on both of stock state and sea temperatures. Abundance of blue whiting in the Barents Sea in 2019 was very low, and dominated by older fish.

Demersal fish, Bjarte Bogstad and Alexey Russkikh

Most of the main demersal fish stocks (cod, haddock, Greenland halibut, *Sebastes mentella*, long rough dab, saithe) in the Barents Sea are in a healthy state and at a level at or above the long-term mean. The exception is *S. norvegicus*, which is still depleted.

The northern limit of the cod distribution in autumn in the area between Spitsbergen and Franz Josef Land has moved southwards from 2017 to 2019. An increase in the haddock stock in the near future is expected due to the strong 2016-year class. The other stocks are expected to be relatively stable in the near future.

Non-commercial fish, Edda Johannesen, Tatiana Prokhorova and Bérengère Husson

Non-commercial demersal fish species were grouped according to their biogeography to assess their relative abundance, trends and suitable habitats. Abundance of Arctic species seems to have increased in 2019 compared to the two previous years. This is probably due to high catches of Liparids. Zoogeographic grouping is consistent with their suitable habitats with temperature is a major driver of the suitable habitats

Trophic interactions, Bjarte Bogstad and Andrey Dolgov

Temporal distribution of cod stomach sampling decreased from 2018 to 2019, and the coverage in 2019 was very limited in the second and fourth quarters. Diet composition, growth and maturation of cod has been relatively stable in recent years, however cod fatness (liver weight in % of body weight) in 2019 (3.9 %) was lower than in previous years (4.8 % in 2018 and 5.2-5.5 % in 2016-2017). Capelin importance in cod diet was slightly higher than in 2018, despite decreasing capelin stock. Consumption of shrimp by cod increased from 2018 to 2019, this is consistent with the increase in the shrimp stock. Weight percent of snow crab in cod diet remains similar to two previous years. Stomach fullness for capelin and polar cod was somewhat above the long-term average in 2018. Stomach fullness and growth rate is positively related for capelin, while for polar cod there is no such relationship.

Benthos, Lis Lindal Jørgensen/Natalia Strelskova

The results of 2019 showed a highest number of megabenthic taxa for the whole period of BESS. Average value of megabenthos biomass and abundance were in range of the interannual fluctuation (for the period 2006-2018). Time-series of the megabenthos biomass distribution during this period shows relative stable large-scale patterns.

The fourteen years monitoring (2006-2019) shown a moderate linear positive trend of increasing mean megabenthos biomass for the total Barents Sea. According to average estimates, the mean biomass of megabenthos in the Barents Sea has approximately doubled during this period. Interannual biomass fluctuations show moderate positive correlation with the water temperature on the Kola Sections with a time-lag of 7 years. This is in accordance with latest data on macrobenthos in the Barents Sea and size-age characteristics of the dominant megabenthic taxa populations.

Snow crab, Dmitry Prozorkevich

The experimental calculation of stock size index of snow crab in the Barents Sea was presented. The assessment methodology is based on investigation of the snow crab catchability by Campeleen trawl in Canada's waters (*E.G. Dawe at all., 2002*). The data on trawl catches of snow crab from the Barents Sea ecosystem survey were used for the stock index calculation. According to the to the last data the snow crab stock continues to increase and its distribution area is extended. However, available estimations of snow crab abundance associated with a high level of uncertainties and it needs in further improvement.

Marine mammals, Nils Øyen and Roman Klepikovskiy

The presentation was based on data collected during the Barents Sea Ecosystem Survey in 2019 and summarized over the period 2004-2019. Total individuals of 10 species of marine mammals were observed in 2019. The white-beaked dolphin was the most common species and is seen all over the Barents Sea. Especially minke whales, but also fin whales, are distributed over large parts of the survey area. Humpback whales had much more aggregated distributions north and west of Hopen and around Bear Island, and these locations were also shared by the other baleen whale species. A major difference compared to earlier years was that most of the cetacean observations were made south of 78°N, probably due to the low capelin abundance in the north. From dedicated cetacean sighting surveys, the summer abundance of minke and humpback whales within the Barents Sea have increased in recent years, correspondently to 70,000 and 4,000 individuals.

Summarized over the years 2004-2019, the odontocete species white-beaked dolphin and the baleen whale species minke, fin and humpback whales have completely dominated the cetacean fauna in the Barents Sea. However, different regions of the area can be characterized in different ways: In northwest (Svalbard area) we find the highest densities of cetaceans and especially the baleen whales besides the white-beaked dolphin; this is also an important capelin and euphausiid area. In southwest (Bear Island, coastline Norway-Russia) we find a productive area with high concentrations of euphausiids and juvenile fish of haddock, cod, herring, redfish and capelin. The white-beaked dolphin is dominant here but also minke and fin whales are abundant here. Along the slopes we also find sperm whales. In northeast (Novaya Zemlya, Franz Josef Land) the area is dominated by polar cod, cod and capelin. This area has a lower abundance of cetaceans, mostly represented by white-beaked dolphins, minke and humpback whales; however, harp seals are important part of the fauna here. In southeast (Pechora Sea) there has been a lower number of observations than in the other subareas and the characteristic species are white-beaked dolphins, minke whale and harbour porpoises.

Sea birds, Per Fauchald

In total, the Barents Sea holds a breeding population of more than 10 million adult seabirds. Several of the populations have been declining the last 30 years. Most importantly, the populations of Atlantic puffin, Brünnich's guillemot and black-legged kittiwake have decreased by 20% to 50%. The population of common guillemot is still recovering from the population crash in 1986-87. In addition to being an important breeding area for seabirds, data from tracking studies show that the Barents Sea is an important feeding area in early autumn. During this period, birds from breeding colonies in the Norwegian Sea, and even birds from as far south as the North Sea, migrate into the Barents Sea to feed. This is also a period when the auk species moult and become flightless for several weeks. More than 50% of the seabirds leave the Barents Sea during the darkest months from November to January. The birds return gradually from early February.

The spatial distribution of seabirds in September has been monitored by the Barents Sea ecosystem cruise since 2004. The distribution of species reflects the climatic gradient from a boreal Atlantic climate, dominated by common guillemots, Atlantic puffins, herring gull and black-backed gull in the south and west, to an Arctic climate with little auks, Brünnich's guillemots and kittiwakes in the north and east. The data from the cruise can be used to identify pagophilic species and consequently which species that are most at risk from diminishing sea ice. Analyses show that ivory gull, black guillemot, Arctic tern, little auk, glaucous gull, Brünnich's guillemot, northern fulmar, black-legged kittiwake and pomarine skua are associated with Arctic waters influenced by ice. Analyses of the centre of gravity of the most common species during the autumn cruise show a northward displacement for several species the last ten years. The centre of gravity of Little auks, Brünnich's guillemot, glaucous gull, black-legged kittiwake, northern fulmar and black-backed gull has moved from 150 to 500 km northward from 2008 to 2019, suggesting that seabirds are displaced toward the north following a period of warming.

Contaminants in marine organisms, Sylvia Frantzen

Status and trends for contaminants in marine organisms were presented. Concentrations of most contaminants in fish and crustaceans in the Barents Sea are relatively low compared to other sea areas, and always below EU and Norway's maximum levels set for food safety, where these exist.

Based on above presentations and trend analysis the annual status report "The state and trends of the Barents Sea ecosystem" (Annex 4) has been updated.

United Nations a Decade of Ocean Science for Sustainable Development, Elena Eriksen

The United Nations General Assembly proclaimed the Decade of Ocean Science for Sustainable Development to mobilise ocean stakeholders worldwide behind a common framework that will ensure ocean science can fully support countries in the achievement of the 2030 Agenda for Sustainable Development. The Decade will stimulate action over the next ten years in areas of critical importance for the planet, people, prosperity, peace and partnership (<https://en.unesco.org/ocean-decade>). Involving of WGIBAR in it was discussed. It was agreed that WGIBAR contribution would be related with updating of the ecosystem overview and accumulating of knowledge about ecosystem functioning and its responds to different disturbances and pressures, including climate change and anthropogenic impacts.

4.5 Progress report on ToR e

B. Husson presented the Barents Risk project, which is funded by the Norwegian Research Council. It aims at developing and implementing the ecosystem risk assessment for the Barents Sea ecosystem, assessing cumulative impacts across sectors within one and unified framework including direct and indirect, foodweb mediated responses. The focus is on the risk caused by

human activities and climate on the ecosystem and ecosystem services. The involved sectors include among others fisheries, aquaculture, offshore windmills, petroleum and shipping, tourism and NGOs. It is divided in three steps:

1. A first qualitative assessment of the risks relying on a strong and dynamic stakeholder involvement in scoping, identifying objectives and setting research priorities. An expert survey is also being conducted, aiming to flag high risks interactions and the impacted ecosystem services.
2. The second step combines analysis based on qualitative and quantitative data to provide a basis for further quantitative analysis at level 3. The stakeholder panel will review and validate the results and prioritize high-risk impacts in collaboration with scientists.
3. Appropriate numerical and statistical models are applied in step three, based on inputs from the two previous steps

Last year (2019) was the first year of the project and the work is still at the first step. This project is interested in cooperating with WGIBAR regarding the information and methodological supports. The WGIBAR is a group with many of various experts and therefore it may be an excellent platform for expertise and evaluation of studies within the Barents Risk project.

B. Husson also presented the literature review on integrated ecosystem assessments in USA and compared it with studies within the Barents Risk project and WGIBAR.

H. Solvang and A. Filin presented preliminary results of generating environmental scenarios for the ecosystem risk assessments in the Barents Sea (explorative “what if” scenarios). To construct them different approaches may be applied. This study is devoted to development of a statistical-based method that will allow to choose of environmental scenarios for the ecosystem risk assessment in best way. This work will be continued and a final aim is producing a suit of the explorative environmental scenarios that will be based on the WGIBAR database and will be available at the WGIBAR SharePoint.

4.6 Progress report on ToR f

The joint Russian-Norwegian ecosystem survey is running annually in August-October since 2004. Its experiences in the 2019 were considered. It was recognized the negative tendencies in the monitoring of the Barents Sea ecosystem during the last years. It related with decreasing in the survey efforts that led to a deterioration in quality of the collected data. This situation is a reason for concern of the group, but it beyond the powers of scientists to change it. The issues related with management of the ecosystem monitoring in the Barents Sea have to be solved by joint decisions of the Russian and Norwegian authorities.

4.7 Cooperation

Cooperation with other WGs

- Stock assessment groups in particular AFWG and WGWIDE
- Other IEA groups in particular WGINOR and WGICA
- WGSAM
- At the moment the continental slope is not comprehensively covered by the ecoregion working groups WGINOR, WGIBAR and WGICA in ICES, and this should be addressed.

Cooperation with Management structures

- The Joint Russian-Norwegian Fisheries Commission, in charge of joint fisheries management in the Barents Sea.
- The Joint Russian-Norwegian Environmental Commission, in charge of joint environmental management in the Barents Sea.
- The Norwegian Ministry of Climate and Environment, in charge of Norwegian holistic ecosystem-based management plan for the Norwegian part of the Barents Sea.

Cooperation with other IGOs

- Relevant groups within the Arctic Council.
- Norwegian monitoring group under the Norwegian Management Plan
- Norwegian Fishery reference fleet (coastal and sea)

5 Revisions to the work plan and justification

No any revision of the work plan, but it was decided to focus on study of effects of possible climate changes on the Barents Sea ecosystem and the role of top predations on the ecosystem structure and functioning. The group recognized of these issues as the most important for the IEA of the Barents Sea in the current situation.

6 Next meeting

Next WGIBAR meeting is planned to be held in Murmansk in February-March 2021.

Annex 1: List of participants

Name	Address	Phone/Fax	E-mail
Espen Bagøien	PO Box 1870, 5817 Bergen, Norway	+47 911 27 273	espen.bagoien@hi.no
Bjarte Bogstad	PO Box 1870, 5817 Bergen, Norway	+4792422352	bjarte.bogstad@hi.no
Elena Eriksen	PO Box 1870, 5817 Bergen, Norway	+47318781	elena.eriksen@hi.no
Anatoly Filin	6 Knipovich St., 183038 Murmansk, Russia	+78152472231	filin@pinro.ru
Andrey Dolgov	6 Knipovich St., 183038 Murmansk, Russia		dolgov@pinro.ru
Dmitry Prozorkevich	6 Knipovich St., 183038 Murmansk, Russia	+78152472147	dvp@pinro.ru
Alexey Russkikh	6 Knipovich St., 183038 Murmansk, Russia		russkikh@pinro.ru
Hein Rune Skjoldal	PO Box 1870, 5817 Bergen, Norway	+90572356	hein.rune.skjoldal@hi.no
Aleksandr Trofimov	6 Knipovich St., 183038 Murmansk, Russia	+78152402621	trofimov@pinro.ru
Harald Gjøsæter	PO Box 1870, 5817 Bergen, Norway	+4741479177	harald@hi.no
Vidar Lien	PO Box 1870, 5817 Bergen, Norway		vidar.lien@hi.no
Hiroko Solvang, Kato	PO Box 1870, 5817 Bergen, Norway	+47 482 20 478	hiroko.solvang@hi.no
Nils Øyen	PO Box 1870, 5817 Bergen, Norway	+47 910 02 344	nils.oyen@hi.no
Gro van der Meeren	PO Box 1870, 5817 Bergen, Norway	+47 941 68 742	GroM@hi.no
Irina Prokopchuk	6 Knipovich St., 183038 Murmansk, Russia		irene_pr@pinro.ru
Padmini Dalpadado	PO Box 1870, 5817 Bergen, Norway	+47 936 34 035	padmini.dalpadado@hi.no
Bérengère Husson	PO Box 1870, 5817 Tromsø, Norway		
Nataliya Strelkova	6 Knipovich St., 183038 Murmansk, Russia		n_anisim@pinro.ru
Denis Zakharov by correspondance	6 Knipovich St., 183038 Murmansk, Russia		zakharov@pinro.ru
Per Fauchald	Norwegian Institute for Nature Research, Tromsø, Norway	+47 452 76 808	per.fauchald@nina.no
Edda Johannesen	PO 1870 Nordnes, 5817 Bergen, Norway	+47 470 26 913	edda.johannesen@hi.no

Daniel Howell	PO Box 1870, 5817 Bergen, Norway	daniel.howell@hi.no
Lis Lindal Jørgensen	PO Box 1870, 5817 Tromsø, Norway	lis.lindal.joergensen@hi.no
Randi Ingvaldsen	PO Box 1870, 5817 Bergen, Norway	randi.ingvaldsen@hi.no
Johanna Fall	PO Box 1870, 5817 Bergen, Norway	johanna.fall@hi.no
Sylvia Frantzen	PO Box 1870, 5817 Bergen, Norway	Sylvia.Frantzen@hi.no
Cecilie Hansen By skype	PO Box 1870, 5817 Bergen, Norway	cecilieha@hi.no
Tatiana Prokhorova by correspondance	6 Knipovich St., 183038 Murmansk, Russia	alice@pinro.ru
Roman Klepikovskiy by correspondance	6 Knipovich St., 183038 Murmansk, Russia	rom@pinro.ru

Annex 2: WGIBAR recommends

The WGIBAR “State and trends of the Barents Sea ecosystem 2020” report will be useful for ICES assessment WG’s (AFWG, WGWIDE, WGHARP and NIPAG) as background ecosystem information for the stock development. It will be also appropriate for identification of vulnerable and valuable areas in the Barents Sea and will contribute to the United Nations a Decade of Ocean Science for Sustainable Development (2021—2030).

Annex 3: Agenda for the WGIBAR 2020 meeting

February 24, Monday

Arrival of the Russian delegation.

February 25, Tuesday (Bergen, IMR, meeting room “Pynten”)

09:30 – 16.00 Plenary

Opening of the meeting, adopting of the agenda and practical information (E. Eriksen/A. Filin)

ToR (d) – Prepare an annual report on the status and trends of the Barents Sea ecosystem

Ecosystem status and trends: (15 min per presentation + 5 min discussion)

Oceanography (V. Lien, A. Trofimov)

Plankton (E. Bagøien, I. Prokopchuk)

Fish recruitment (E. Eriksen, T. Prokhorova)

11:00 – 12:00 Lunch

Pelagic fish (G. Skaret/D. Prozorkevich)

Demersal fish (B. Bogstad, A. Russkikh)

Benthos (N. Strelkova, L. Jørgensen)

Sea birds (P. Fauchald)

Marine mammals (N. Øyen, R. Klepikovskiy)

14:00-14:30 Coffee & Tea break

Non-commercial fish (E. Johannesen, T. Prokhorova)

Fish trophic interactions (B. Bogstad, A. Dolgov)

Pollution, including marine litter (B.E Grøsvik/T. Prokhorova)

Contaminants in fish and invertebrates (S. Frantzen)

Discussion of the current state and long-term trends of the Barents Sea ecosystem

How WGIBAR can contribute to the United Nations Decade of Ocean Science for Sustainable Development

February 26, Wednesday (IMR)

09:00 – 12:00 Plenary

ToR (b) – Perform an integrated analysis of multivariate datasets and other relevant information including model outputs

Evaluation of snow crab impact on fish stocks by Atlantis model (C. Hansen)

Time-series analyses (H. Solvang)

Integrated analyses and models in ICES IEA groups (B. Husson)

ToR (c) – Analyse spatial patterns and trends with special emphasis on shifting distribution of communities and species and valuable and vulnerable areas

Is spatial overlap a good indicator of cod-capelin interaction strength? (J. Fall)

Sea birds and trophic interactions (P. Fauchald)

10:40-11:00 Coffee & Tea break

Making sense of Barents Sea foodweb data with RCaN (B. Husson)

Biologically and ecologically significant areas in the Barents Sea (E. Eriksen and H.R Skjoldal)

ToR (e) – Provide support to ongoing ecosystem assessments and evaluations in the Barents Sea

Presentation of the BARENTS-RISK project (B. Husson)

“Generating environmental scenarios for the Ecosystem Risk Assessment in the Barents Sea” (H. Solvang and A. Filin)

ToR (f) – Evaluate the current monitoring of the Barents Sea ecosystem

Experiences with ecosystem monitoring in the 2019 (D. Prozorkevich)

12:00 – 13:00 Lunch

ToR (a) – Prepare relevant datasets that can be used for the integrated assessments of the Barents Sea

13:00-17:00 Practical work by groups

Updating the WGIBAR database

Integrated analysis of multivariate datasets and time-series analyses

Prepare description of ecosystem status and long-term trends to the report (Anex 5)

Dinner 17:00 Meeting room “Pynten”

February 27, Thursday (IMR)

09.00 – 15:00 Practical work by groups

Summing up the results of the meeting

Future work, next meeting

Prepare the status description of the Barents Sea ecosystem to the report

Writing the WG report

11:30-12:00 Lunch

15:00-16:00 Plenary

February 28, Friday

Departure of the Russian delegation.

Annex 4: The state and trends of the Barents Sea ecosystem in 2019

Edited by Elena Eriksen and Anatoly Filin

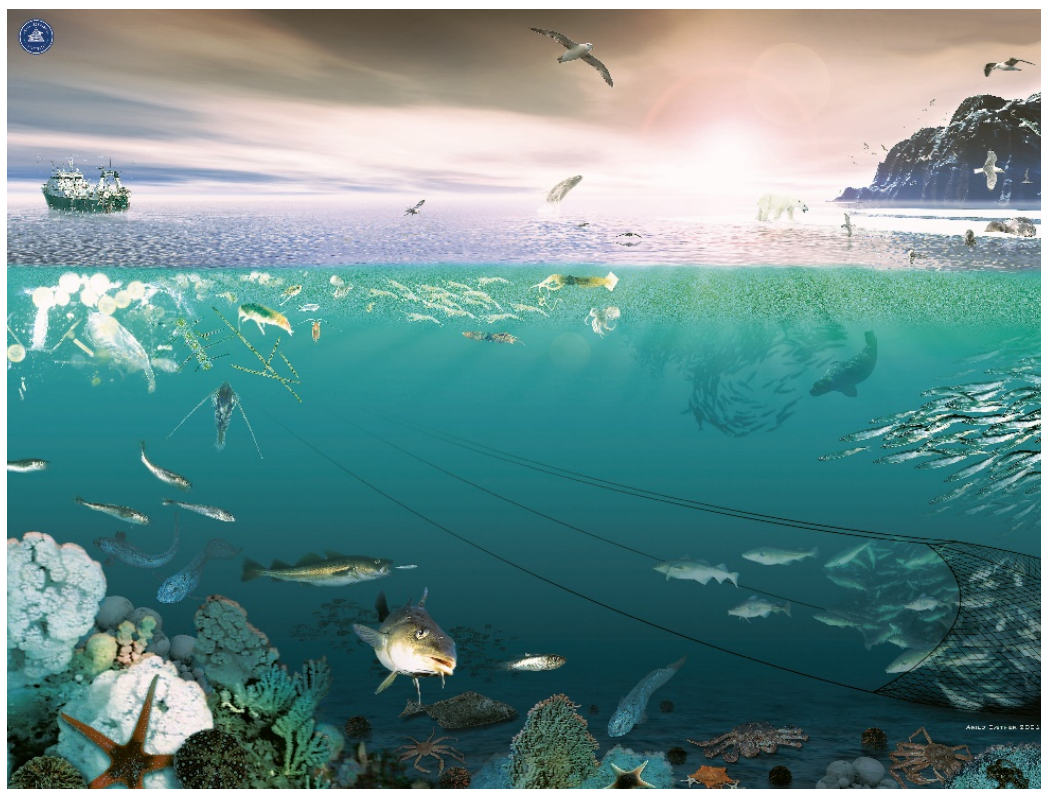
Contributing Authors (Alphabetic):

Espen Bagøien¹, Bjarte Bogstad¹, Anatoly Chetyrkin², Padmini Dalpadado¹, Andrey Dolgov², Elena Eriksen¹, Johanna Fall¹, Per Fauchald³, Anatoly Filin², Sylvia Frantzen¹, Harald Gjørseter¹, Bjørn Einar Grøsvik¹, Hilde Elise Heldal¹, Bérengère Husson¹, Randi Ingvaldsen¹, Edda Johannesen¹, Lis Lindal Jørgensen¹, Roman Klepikovskiy², Pavel Krivosheya², Vidar Lien¹, Anna Mikhina², Valentina Nesterova¹, Tatiana Prokhorova², Irina Prokopchuk², Dmitri Prozorkevich², Alexey Russkikh², Jon Rønning¹, Hein Rune Skjoldal¹, Hiroko Solvang¹, Natalia Strelkova², Alexander Trofimov², Gro van der Meeren¹, Denis Zakharov², Ksenia Zaytseva²

¹*Institute of Marine Research (IMR), Norway*

²*Polar Branch of the Federal State Budget Scientific Institution, Russian Federal Research Institute of Fisheries and Oceanography ("PINRO" named after N. M. Knipovich), Russia.*

³*The Norwegian Institute for Nature Research (NINA), Norway*



Summary

Since the 1980s, the Barents Sea has gone from a situation with high fishing pressure, cold conditions and low demersal fish stock levels, to the current situation with high levels of demersal fish stocks, reduced fishing pressure and warm conditions.

Ecosystem state: The Barents Sea experienced warming with a record warm temperature condition in 2016. Since that the Barents Sea has become colder and the cooling continued in 2019. However, the air and water temperatures are still being typical of warm years. The mesozooplankton and krill biomass was slightly higher than in recent years most likely due to low biomasses of planktivorous consumers. The total biomass of pelagic fish (capelin, polar cod, young herring and blue whiting) was at the lowest level in the last 20 years. Most of the main demersal fish stocks (cod, haddock, Greenland halibut, *Sebastes mentella*, long rough dab, saithe) are in a healthy state and at a level at or above the long-term mean. The exception is *S. norvegicus*, which is still depleted. Diet composition, of cod has been relatively stable in recent years. Megabenthos biomass and abundance were at the long-term mean level. The stock of the northern shrimp is relatively stable in the last years. The snow crab population is still increasing and spreading over larger area. The Barents Sea is important feeding area for habiting and visiting sea birds and marine mammals. In step with warming, birds follow the retreating sea ice and showed northern redistribution (centre of mass for auks, gulls and fulmar moved 150-300 km further north) in recent decade. Number of individuals and species of marine mammals increased during last decades. The white-beaked dolphin was the most common species in 2019 during the ecosystem survey. The summer abundance of minke whales and humpback whales increased and were about 70,000 and 4,000, respectively.

Human pressure: The assessment for several commercial important stocks indicated that the stocks has been fished sustainably and has remained well above precautionary reference limits. The present (2016–2021) minke whale quota is considered precautionary, conservative, and protective for the minke whale population in the Northeast Atlantic. The AIS tracking of vessel, 2012 to 2019, indicated decreased fisheries effort in the northern area, while an increase in passenger vessels to the Svalbard area. Anthropogenic litter were observed at each fourth (pelagic) and each second (bottom) stations during the ecosystem survey, and plastic dominated among all observations. Amount of plastic and other litters are relatively low in comparison to other sea areas. Concentrations of most contaminants in fish and crustaceans in the Barents Sea are relatively low in comparison to other sea areas. Levels of the anthropogenic radionuclides Cs-137, Sr-90 and Pu-239,240 in seawater, sediments, fish and seaweed in the Barents Sea area are currently low. In recent decades, there has been a slow decrease in the levels of most anthropogenic radionuclides in the Barents Sea.

Expected changes in the coming years: Oceanic systems have a “longer memory” than atmospheric ones. According to the expert evaluation, the Atlantic water temperature is expected to decline slightly but remain typical of warm years. Due to high

temperatures and low sea-ice extent in recent years, the ice coverage of the Barents Sea is expected to remain below normal. Most of the commercial fish stocks in the Barents Sea are at or above the long-term mean level. The exceptions are capelin, polar cod and gold redfish (*Sebastes norvegicus*). Concerning shellfish, the shrimp abundance has increased in 2018-2019 and is close to the highest observed. The abundance and distribution area of snow crab is also increasing, the stock of the red king crab is relatively stable in the last years.

Contents

1	Summary.....	19
2	Temporal development.....	23
2.1	Trend analysis.....	23
2.1.1	Trend estimation and classification analyses (TREC)	23
2.1.2	Warning signal analysis.....	25
2.2	Preliminary study of generating environmental scenarios for the Ecosystem Risk Assessment in the Barents Sea.....	26
3	Current state of the Barents Sea ecosystem components.....	28
3.1	Meteorological and oceanographic conditions	28
3.2	Phytoplankton and primary production.....	44
3.2.1	Satellite data	44
3.2.2	Spatial and temporal patterns of Chl <i>a</i> in spring	45
3.2.3	Net Primary Production (NPP)	46
3.3	Zooplankton.....	46
3.3.1	Mesozooplankton biomass and distribution	47
3.3.2	Macroplankton biomass and distribution.....	56
3.4	Benthos and shellfish	64
3.4.1	Benthos.....	64
3.4.2	State of selected benthic species	71
3.5	Pelagic fish.....	77
3.5.1	Total biomass	77
3.5.2	Capelin	79
3.5.3	Herring.....	86
3.5.4	Polar cod	89
3.5.5	Blue whiting	92
3.6	Demersal fish	94
3.6.1	Cod.....	95
3.6.2	NEA haddock.....	99
3.6.3	Long rough dab	103
3.6.4	Greenland halibut.....	105
3.6.5	Deepwater redfish	106
3.7	Zoogeographical groups of non-commercial species.....	109

3.8	Marine mammals and sea birds	117
3.8.1	Marine mammals.....	117
3.8.2	Sea birds.....	124
3.9	Anthropogenic impact.....	131
3.9.1	Fisheries	131
3.9.2	Catches of shellfish.....	131
3.9.3	Whaling and seal hunting	138
3.9.4	Fishing activity.....	139
3.9.5	Discards.....	141
3.9.6	Shipping activity.....	141
3.9.7	Oil and gas.....	142
3.9.8	Marine litter.....	144
3.9.9	Contaminants in marine organisms.....	146
3.9.10	Radioactive contamination.....	160
4	Interactions, drivers and pressures.....	161
4.1	Feeding and growth of capelin and polar cod	161
4.2	Feeding, growth, and maturation of cod	166
4.3	Causes of capelin stock fluctuations	173
4.4	Causes of polar cod stock fluctuations	176
4.5	Cod-capelin-polar cod interaction	178
5	Expected changes in the coming years.....	183
5.1	Sea temperature	183
5.2	Possible development of some fish, shellfish and sea mammal stocks (near future)	183

2 Temporal development

2.1 Trend analysis

By Hiroko Solvang

2.1.1 Trend estimation and classification analyses (TREC)

Common trends refer to trends that are similar across ecosystem components. Identifying common trends can be useful as a diagnostic tool to reveal past changes and to explore the relationships among biological communities and between these communities and environmental conditions. For the investigation, trend estimation and classification analyses (TREC) are applied to WGIBAR time series data including 7 abiotic components, 18 biotic components, and 8 human impacts. The estimates obtained by polynomial trend model are shown in Fig. 2.2.1.1. Using trends for 1 and 6, two-category discrimination is applied to roughly classify them as three groups (Fig. 2.2.1.2).

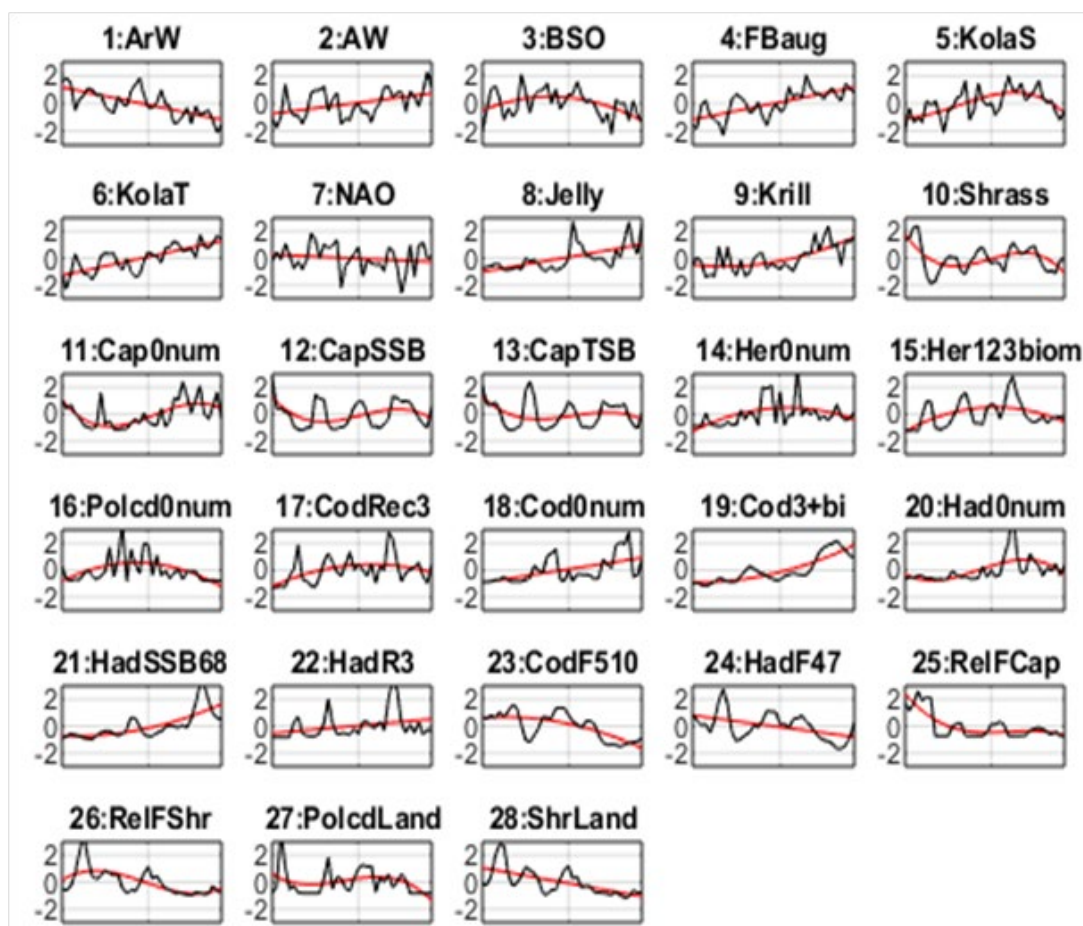


Figure 2.2.1.1. Estimated trend (red) and observation (black). X-axis indicates years (1980-2019) and y-axis indicates standardized values for each data

In the classified groups, some precise common configurations are still shown, e.g. linear, exponentially or saturation curves in upward. These trends become references to apply more than two-category discrimination. The reference is corresponding to the

representative icon figure, which serve general reference for the needs of stakeholders. The details for classified each category and assigned icons are shown in Fig.2.2.1.3.

The ongoing warming were associated with increased trend in water temperature, larger area covered by Atlantic warm water masses and decreased trend ice coverage since 1980s. The warming was also associated with increased macro zooplankton such as krill and jellyfish biomass, increased fish recruitment (age 0) which trigger positive development of fish stocks (cod, haddock and herring).

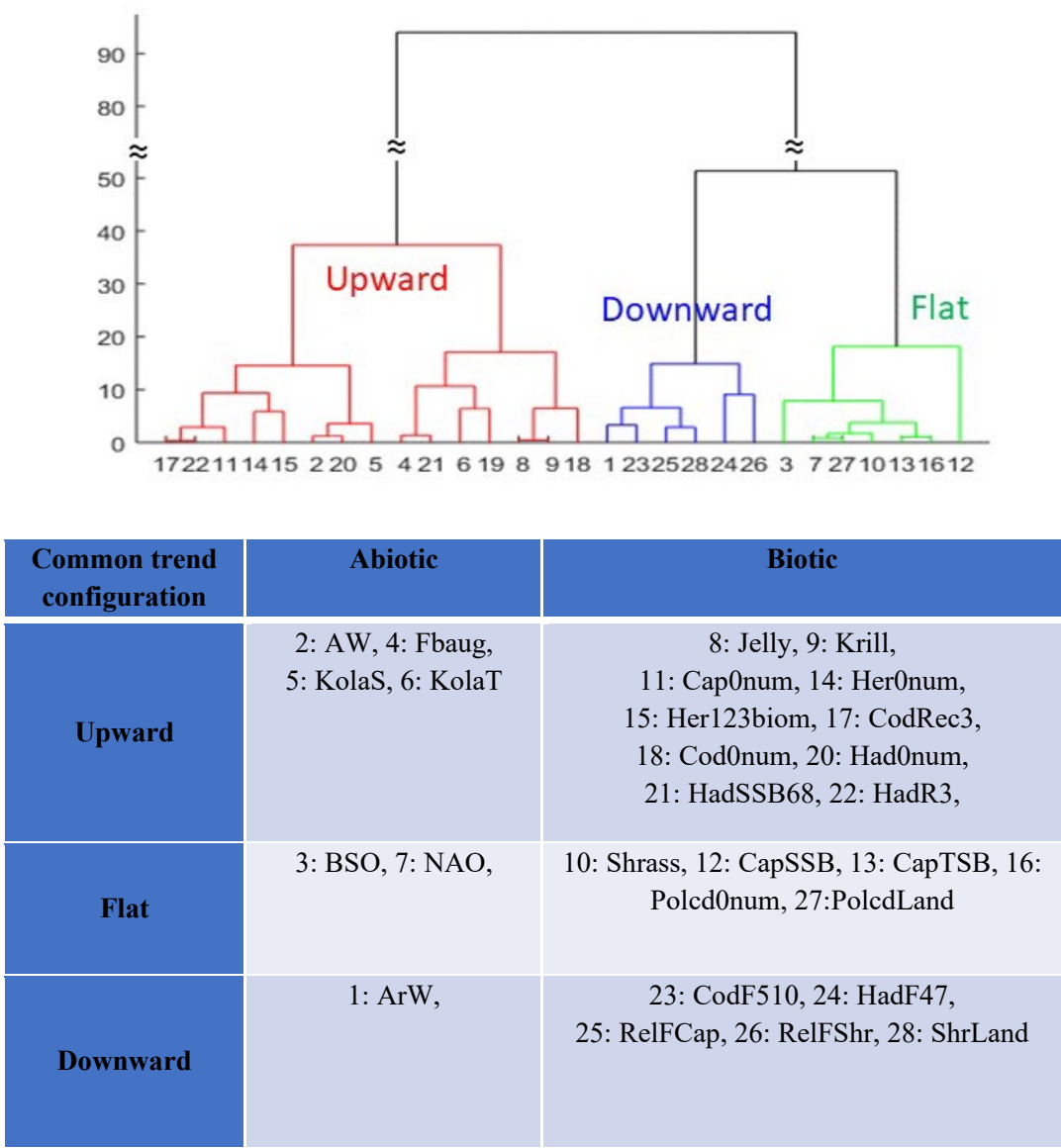


Figure 2.2.1.2. Dendrogram obtained by 2-category-discriminant analysis procedure (upper panel) and the classified groups (roughly three, upward, flat and downward) (lower table).























Common trend	category	Classified data	Icon
Upward		2: AW, 4: FBaug, 6: KolaT, 8: Jelly, 18: Cod0num, 22: HadR3	
		9: Krill, 19: Cod3+bi, 21: HadSSB68	
		20: Had0num	
		11: Cap0num	
		5: KolaS, 14: Her0num, 15: Her123blom, 17: CodRec3	
Flat		7: NAO, 27: PolcodLand	
		10: SHrass, 12: CapSSB, 13: CapTSB	
		3: BSO, 16: Polcd0num	
Downward		1: ArW, 24: HadF47, 26: RelFSshr, 28: ShrLand	
		25: RelFCap	
		23: CodF510	

Figure 2.2.1.3. The details for classified data in each category.

2.1.2 Warning signal analysis

To investigate whether the most recent observation follow the recent trend or is away from the trend, one (or more) years ahead predictions are calculated. The trend in this case is estimated by stochastic trend model. Stochastic trend model is presented by a class of auto-regressive model and is easily set in state space representation. Kalman filter algorithm is applied to estimate trend component and to calculate the prediction. The trend estimates look more fluctuated rather than estimates by polynomial trend. This is because of that stochastic trend follows the data variation in each time point. We run the algorithm using the data recording until 2016 and calculate the prediction for 2017-2019. In Fig.2.2.2.1, the estimated trend and prediction with the confidence interval are plotted by red line. Real observations for 2017-2019 are plotted by black dots. Existing black dots inside/outside the confidence intervals gives the statistical criteria to know the distance between observation and predicted value by trend model. This may make an assessment whether the observation is a sign and something 'unusual' going on the ecosystem that may represent a warning signal.

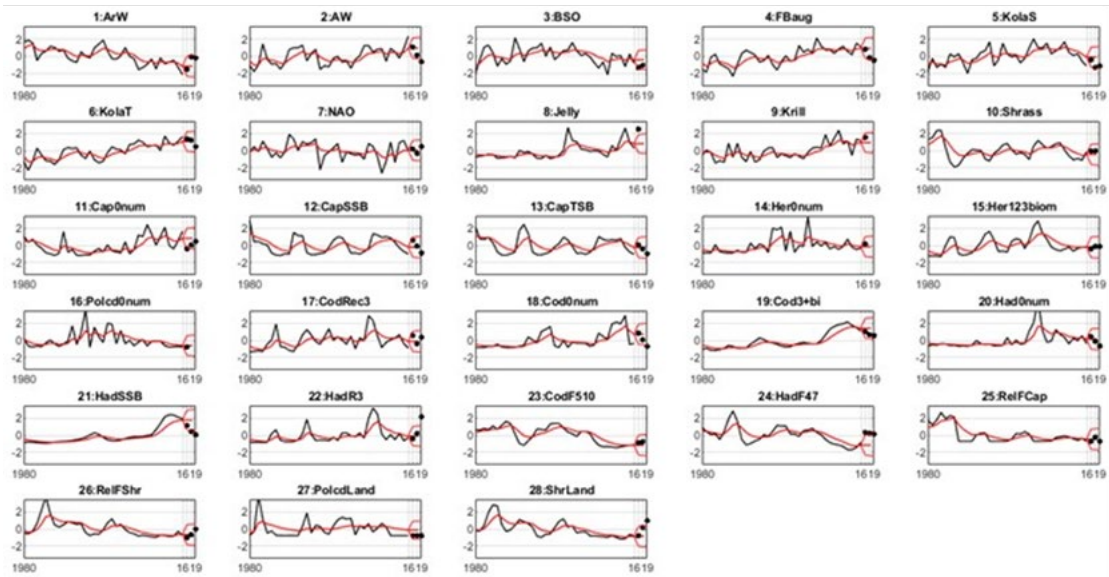


Figure 2.2.2.1. 3-years-ahead prediction and the confidence intervals (red line) for the trend obtained by the data recording for 1980-2016 (black line). Black dots indicate real observations recording on 2017-2019.

Status of outside of or border on the confidence intervals	2017	2018	2019
Higher (or border of the upper confidence interval)		1:ArW	
	8: Jelly		
			22: HadR3
	24: HadF47	24: HadF47	24: HadF47
Lower (or border of the lower confidence interval)			28: ShrLand
			2: AW
	3: BSO		
		5; KolaS	
	11: Cap0num		
			18: Cod0num
		21: HadSSB	21: HadSSB

Table 2.2.1.2. Observations for abiotic and biotic variables located outside of or the just border of the confidence intervals for the prediction values in the period 2017-2019, which were calculated by the trend and observation noise using the observations until 2016.

2.2 Preliminary study of generating environmental scenarios for the Ecosystem Risk Assessment in the Barents Sea

By Hiroko Solvang (IMR), Anatoly Filin (PINRO)

Climate change and annual fluctuations of environmental conditions strongly affect fish stocks and all biological ecosystem components. Evaluating fisheries management strategies should include environmental information as part of the decision basis. Estimation of how often an undesirable event may occur, and what the consequences would be of such an event needs to be estimated through a risk analysis using stochastic simulations. Regarding the ecosystem risk assessments, it requires the

application of ecosystem models and environmental scenarios. In order to investigate these scenarios, different numerical approaches are applied and evaluated to select the appropriate scenarios to represent the features of the observations. This study is devoted to a choice of environmental scenarios that corresponds to the ecosystem risk assessments in the best way.

The proposed procedure includes three stages: 1. Methodological study of producing the stochastic environmental scenarios for the long-term model runs; 2. Making a decision on which scenarios are required; 3. Creating a set of environmental scenarios for potential users. The focus was on the first item, and temperature scenario was considered as an environmental scenario in this study. The simulation data were generated based on two kinds of temperature scenarios, STOCOBAR-based and Auto-regressive (AR) model. The generated simulation data were compared with the real temperature time series data observed at the Kola section during the period 1951 – 2016. The dissimilarity between the observations and the simulated data was evaluated by two distance measurements for time series data, where one was based on the estimated autocorrelation for 30-time lags and another was based on the estimated periodogram. The outputs from this preliminary study indicated that the AR model scenario was closer to the observations than the STOCOBAR-based scenario.

What we expect in this study is creating a suit of the environmental scenario, which will be based on the WGIBAR database and may be available at the site of WGIBAR. Furthermore, we consider the statistical methodology to evaluate not only time series data but also spatial data including many environmental metrics.

3 Current state of the Barents Sea ecosystem components

3.1 Meteorological and oceanographic conditions

A. Trofimov (PINRO), R. Ingvaldsen (IMR), V. Lien (IMR)

The Barents Sea has become colder since 2015–2016, and the cooling continued from 2018 to 2019. However, the air and water temperatures are still being typical of warm years. In the western entrance of the Barents Sea, the Atlantic Water temperatures in 2019 were at the same level as in the early 2000s. Coastal and Atlantic waters in the Kola Section were fresher than in 2018. In autumn, the area of Atlantic waters ($>3^{\circ}\text{C}$) decreased slightly and the area of Arctic waters near bottom ($<0^{\circ}\text{C}$) increased slightly compared to 2018, whereas the area of cold bottom waters ($<0^{\circ}\text{C}$) almost tripled compared to the previous year. Ice coverage has increased since 2016 due to lower temperatures and lower inflow of Atlantic Water. In 2019, the ice coverage was below average but higher than in 2018; its seasonal maximum (51%) was in March, a month earlier than usual, its seasonal minimum (1%) was in September, as usual.

The Barents Sea is a shelf sea of the Arctic Ocean. Being a transition area between the North Atlantic and the Arctic Basin, it plays a key role in water exchange between them. Atlantic waters enter the Arctic Basin through the Barents Sea and the Fram Strait (Figure 3.1.1). Variations in volume flux, temperature and salinity of Atlantic waters affect hydrographic conditions in both the Barents Sea and the Arctic Ocean and are related to large-scale atmospheric pressure systems.

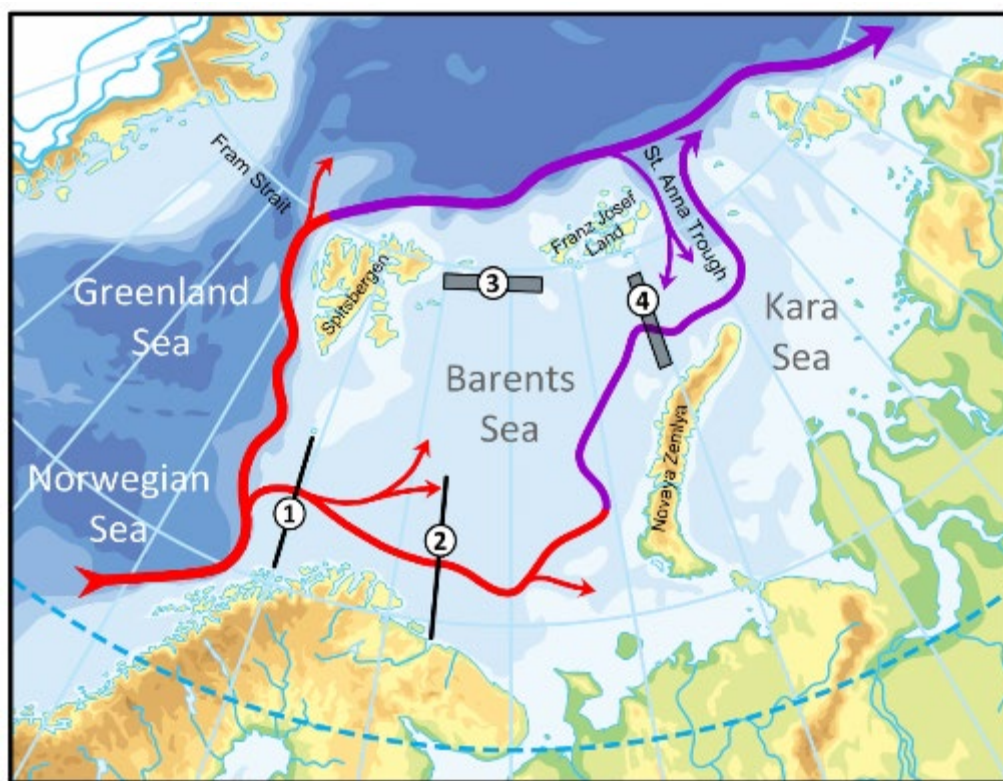


Figure 3.1.1. The main paths of Atlantic waters in the Barents Sea as well as Fugløy–Bear Island Section (1), Kola Section (2) and boxes in the northwestern (3) and northeastern (4) Barents Sea.

Air pressure, wind and air temperature

In 2019, the winter (December–March) NAO index was 2.09 that was much higher than in 2018 (0.30). Over the Barents Sea, southerly and southeasterly winds prevailed in January–March 2019, easterly and northeasterly winds – during the rest of the year. The number of days with winds more than 15 m/s was higher than usual most of the year. It was lower than or close to the long-term average (1981–2010) in the western part of the sea in January, April and October, in the central part in January, February, April, August and December, in the eastern part in January, April and December. In June (in the east) and July (in the east and center), the storm activity was a record high since 1981.

Air temperature (<http://nomad2.ncep.noaa.gov>) averaged over the western (70–76°N, 15–35°E) and eastern (69–77°N, 35–55°E) Barents Sea dropped significantly in 2019 compared to the previous year and its annual mean value was the lowest since 2011 (Fig. 3.1.2). The air temperature in the western part of the sea was close to the long-term average (1981–2010) for most of the year; negative anomalies of -0.4 and -1.2°C were found in May and October respectively; positive anomalies of more than 1.0°C were only observed in April, September and December. The air temperature in the eastern part of the sea exceeded the average for most of the year and was close to it only in May, June, July, October and November. In the east, the largest positive anomalies ($>2.0^{\circ}\text{C}$) were observed in January, March, April and December (Fig. 3.1.2).

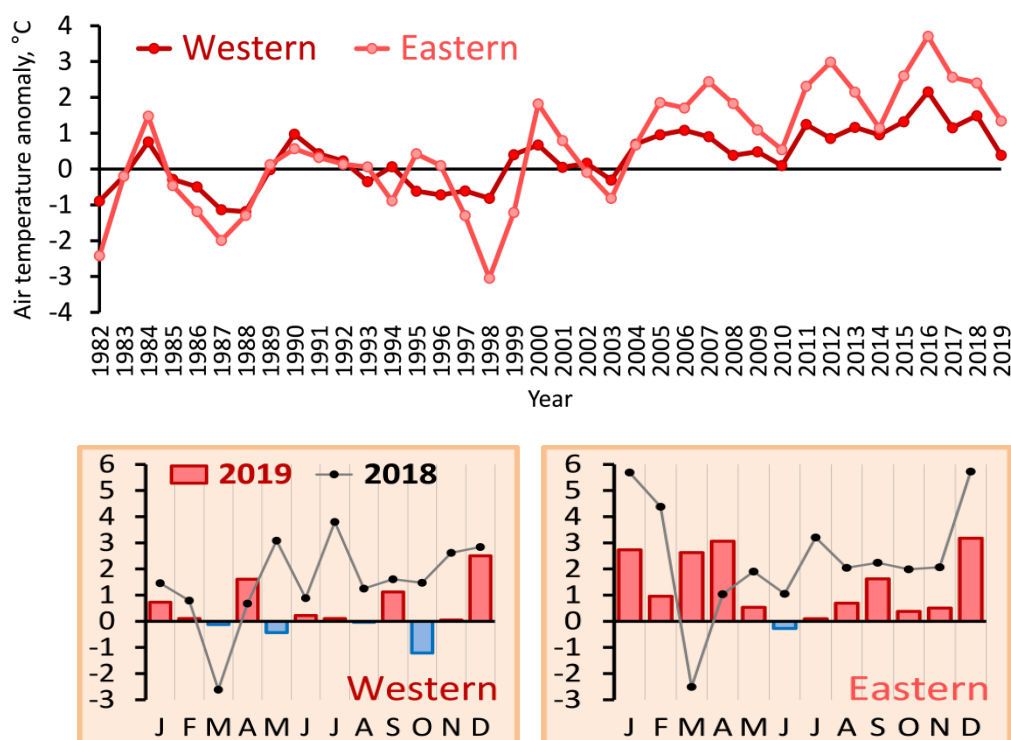


Figure 3.1.2. Annual (upper) and monthly (lower) air temperature anomalies in the western and eastern Barents Sea.

Ice conditions

In December 2018, the Barents Sea ice extent (expressed as a percentage of the total sea area) equaled 15% and was the lowest since 1951. However, in January–March 2019, ice formation accelerated significantly, and in March (a month earlier than usual), the ice-covered area reached a seasonal maximum of 51% and was close to the long-term average (1981–2010) (Fig. 3.1.3). The ice extent reduction began in April, not in May, as usual, but intensive ice melting started only in June. During the low-ice season (August–October), ice coverage equaled 1–4% that was 3–9% below average but 1–4% higher compared to the previous year. Freezing began in October and ice formation went much faster than in 2018. The November and December ice coverage were respectively 10 and 9% lower than average but 9 and 16% higher than in 2018. Overall, the 2019 annual mean ice coverage of the Barents Sea was 10% below average but 4% higher than in the previous year.

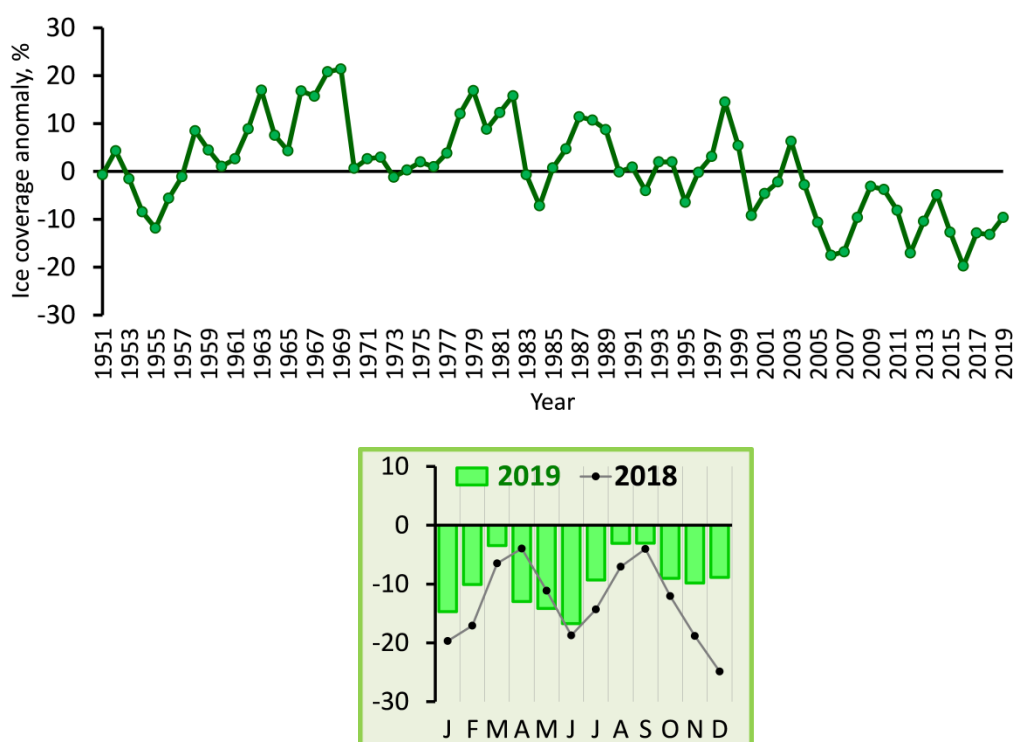


Figure 3.1.3. Annual (upper) and monthly (lower) ice coverage anomalies in the Barents Sea.

Currents and transports

The volume flux into the Barents Sea varies with periods of several years. The annual volume flux was relatively high during 2003–2006 (Fig. 3.1.4). From 2006 to 2014, the inflow was relatively stable before it increased substantially in 2015 to about 1 Sv above the long-term average. The year of 2016 had relatively low inflow. Since 2017 the annual volume inflow to the Barents Sea has decreased, but the data series presently stops in May 2019 thus the annual value of 2019 should presently be considered a rough estimate. There is no statistically significant trend in the annual volume fluxes.

Volume fluxes split into quarterly periods show that volume flux has decreased in winter (January–March) and spring (April–June) during the last 5 years (since 2015), while it has increased in summer (July–September) and fall (October–December) (Fig.

3.1.4). The inflow in spring 2019 was about 1 Sv lower than in 2018, but these number might change when the time series (which presently stop in May 2019) is updated.

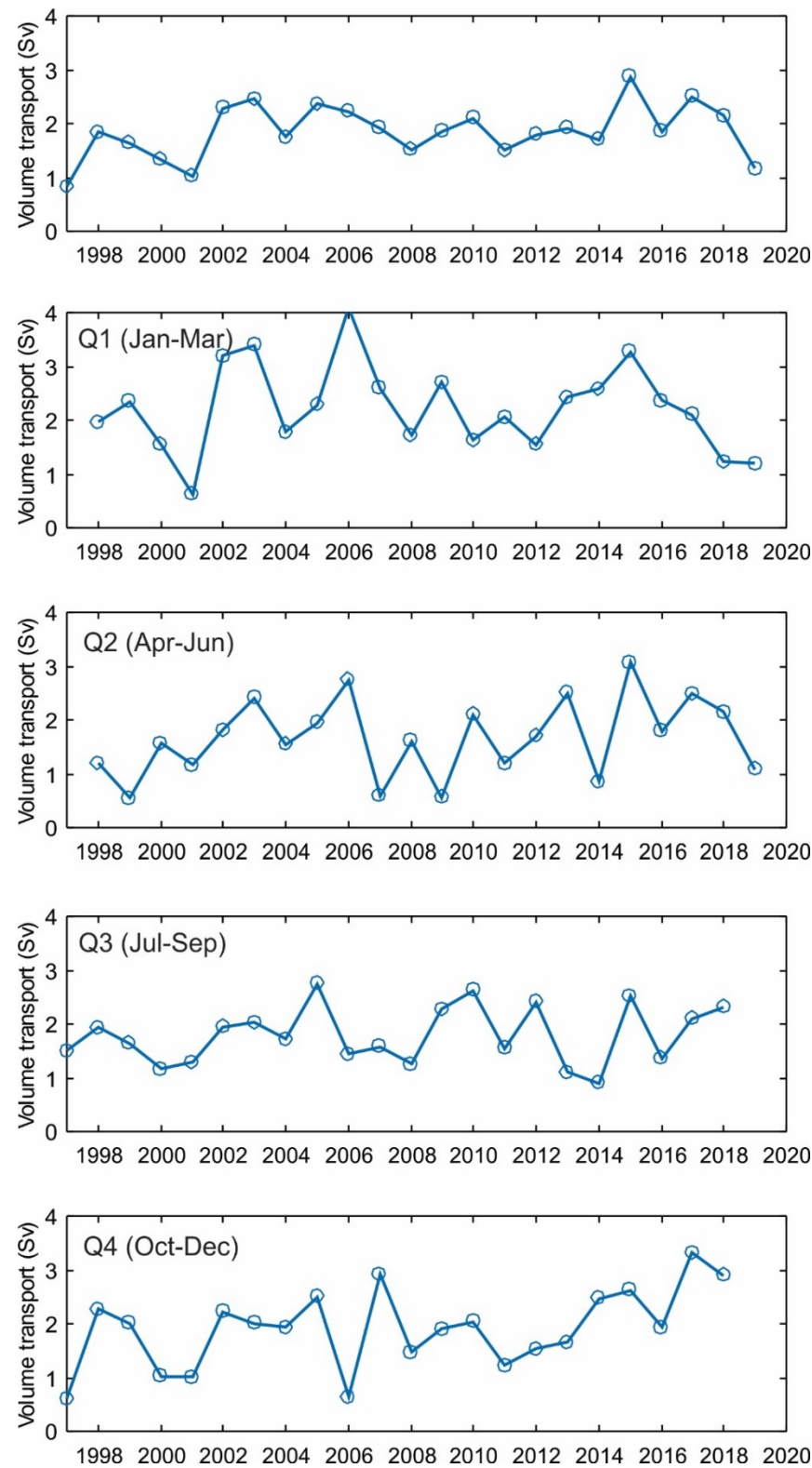


Figure 3.1.4. Observation-based annual volume flux anomalies (in Sverdrups) through the Fugløya–Bear Island Section. Upper panel show annual mean volume flux, while the four lower panels show quarterly volume flux. The volume flux is calculated for the area 71°15' to 73°45'N, and include all waters flowing inside this area.

Temperature and salinity in standard sections and northern boundary regions

The Fugløya–Bear Island Section covers the inflow of Atlantic and Coastal water masses from the Norwegian Sea to the Barents Sea, while the Kola Section covers the same waters in the southern Barents Sea. Note a difference in the calculation of the temperatures in these sections; in the Fugløya–Bear Island Section the temperature is averaged over the 50–200 m depth layer while in the Kola Section the temperature is averaged from 0 to 200 m depth.

Since 2015, the temperatures in the inflowing Atlantic Water to the Barents Sea has decreased by more than 1°C (Fig. 3.1.5). At the Fugløya–Bear Island section, which is in the far western entrance, the temperatures of the inflowing Atlantic Water was in 2019 at the same level as in the early 2000s. The decrease in the Atlantic Water temperatures are linked to lower temperatures upstream in the Norwegian Sea. The lower temperatures, in combination with lower inflow during winter (Fig. 3.1.4) has caused the increases in winter sea ice observed the resent years. The decrease in temperatures were lower when progressing into the Barents Sea (at Vardø–North).

The salinity of the inflowing Atlantic Water has decreased since 2011 and were in 2019 at the same level as during the very fresh (and cold) period in the late 1970s (Fig. 3.1.5).

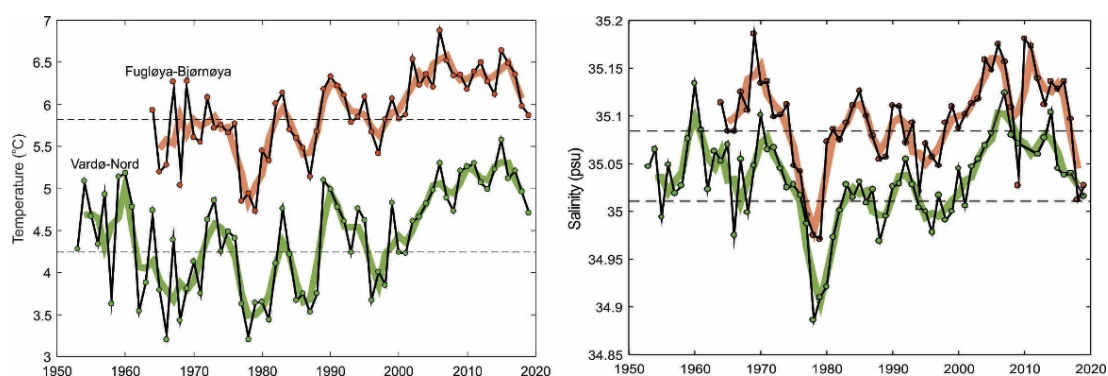


Figure 3.1.5. Average temperature (left) and salinity (right) in August–September in the 50–200 m layer in the Fugløya–Bear Island and Vardø–North Sections. Black lines show annual August–September values, while thick coloured lines show three years running means. Horizontal lines show average over the period 1981–2010.

Temperature of coastal and Atlantic waters in the Kola Section in 2019 was typical of warm years in general. During the 2019 observation period, positive temperature anomalies in the 0–200 m layer in coastal waters and Atlantic waters of the central part of the section (Murman Current) were decreasing from 0.9°C in March to 0.2–0.3°C in November–December (Fig. 3.1.6). In Atlantic waters in the outer part of the section (Central branch of the North Cape Current), a temperature anomaly first increased from 0.2°C in March to 0.6°C in June and then decreased to a value close to average in October and to a negative value (–0.2°C) in November; in December, it grew again up to 0.4°C. Compared to 2018, coastal waters had almost the same temperature in March–June 2019, whereas Atlantic waters in March–August 2019 were colder by 0.2–0.5°C in the central part of the section and by 0.3–1.0°C in the outer part (Fig. 3.1.6).

Salinity of coastal and Atlantic waters in the Kola Section in 2019 was lower than average and, in general, close to that in 2018 (Fig. 3.1.6). In coastal waters (0–200 m), a negative salinity anomaly was decreasing from -0.22 in March–May to -0.02 in December. In Atlantic waters in the central part of the section (Murman Current), it was also decreasing from -0.17 in March to -0.05 in December but with a less pronounced trend. In Atlantic waters in the outer part of the section (Central branch of the North Cape Current), a negative salinity anomaly varied slightly from -0.04 to -0.09 during the 2019 observation period. March–December averaged negative salinity anomaly decreased from -0.14 in coastal waters to -0.09 in Atlantic waters of the central part of the section and to -0.06 in Atlantic waters of the outer part (Fig. 3.1.6).

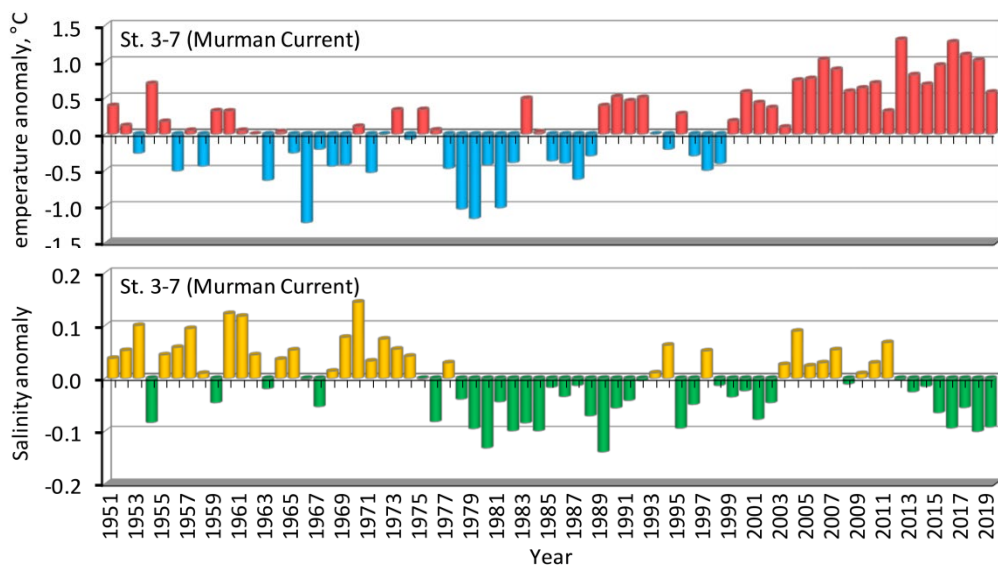
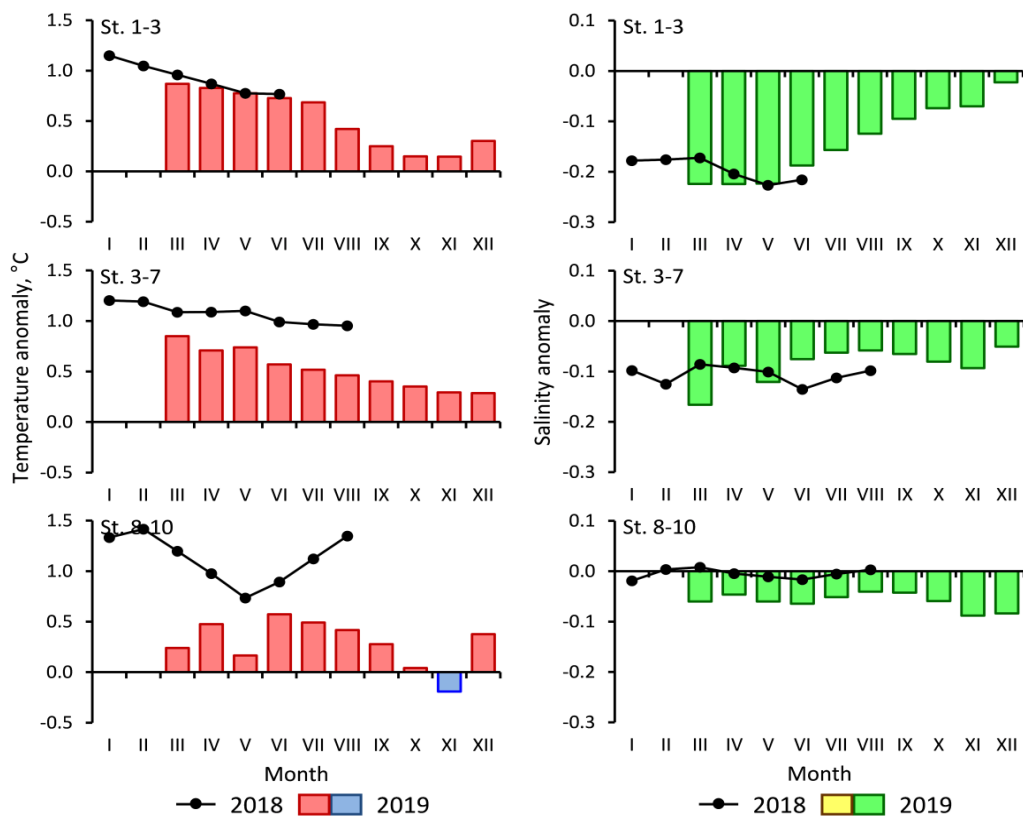


Figure 3.1.6. Monthly and annual temperature and salinity anomalies in the 0–200 m layer in the Kola Section. St. 1–3 – Coastal waters, St. 3–7 – Murman Current, St. 8–10 – Central branch of the North Cape Current (Anon., 2019). Annual mean values for 2016–2019 were recovered.

In the northern Barents Sea (NW) there was a strong temperature decrease from 0.30°C in 2018 to –1.20°C in 2019. No temperature could be calculated for the northeastern Barents Sea due to data coverage.

Spatial variation in temperature and salinity (surface, 100 m and bottom)

Sea surface temperature (SST) (<http://iridl.ldeo.columbia.edu>) averaged over the southwestern (71–74°N, 20–40°E) and southeastern (69–73°N, 42–55°E) Barents Sea dropped significantly in 2019 compared to the previous year and its annual mean value was the lowest since 2011 (Fig. 3.1.7). The SST in the southwestern part of the sea was close to the long-term average (1982–2010) for most of the year; small negative anomalies of –0.2, –0.3 and –0.1°C were found in July, August and November respectively; positive anomalies of more than 0.5°C were only observed in January, February and September. The SST in the southeastern part of the sea exceeded the average for most of the year and was close to it only in June, July, November and December; while July and November anomalies were slightly negative (–0.1 and –0.2°C respectively). In the southeast, the largest positive anomalies (>0.8°C) were observed in January, April, May and September (Fig. 3.1.7).

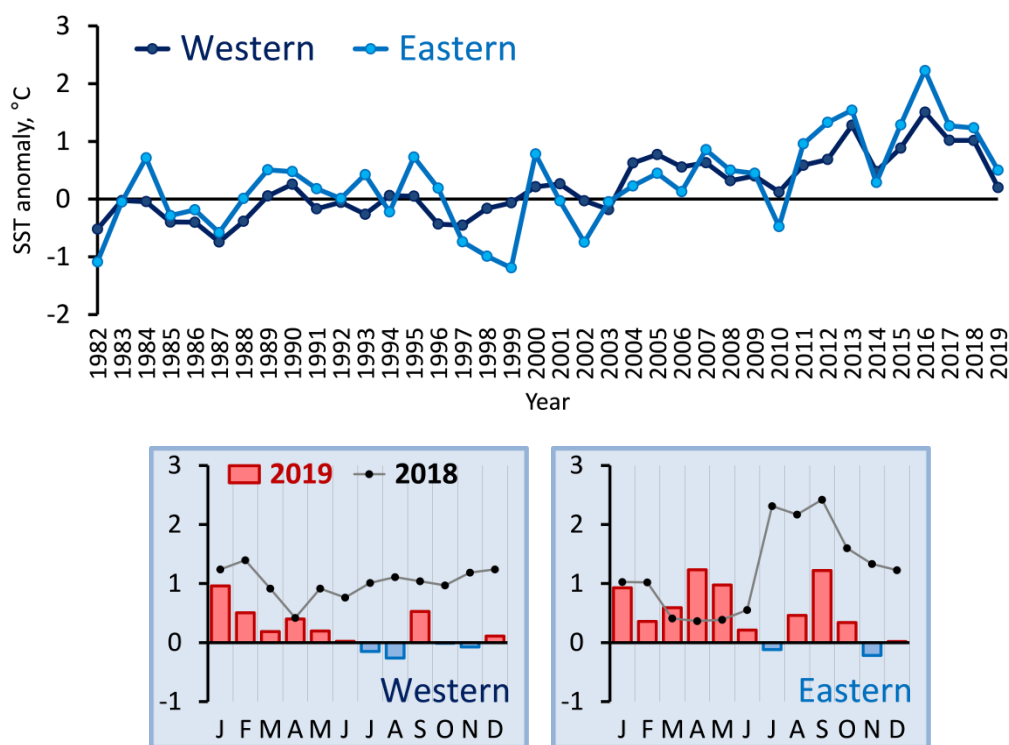


Figure 3.1.7. Annual (upper) and monthly (lower) sea surface temperature anomalies in the western and eastern Barents Sea.

During August–September 2019, the joint Norwegian-Russian ecosystem survey was carried out in the Barents Sea. Surface temperature was on average 0.7°C higher than the long-term (1931–2010) mean in about two thirds of the surveyed area (Fig. 3.1.8).

Negative anomalies (about -0.5°C on average) took place mostly in the northernmost and south-western Barents Sea. Compared to 2018, the surface temperature in 2019 was much lower (by 1.1°C on average) in most of the surveyed area ($\sim 80\%$), with the largest negative differences ($>2^{\circ}\text{C}$) in the south-eastern and south-westernmost parts of the sea as well as north and east of the Spitsbergen Archipelago (Fig. 3.1.8).

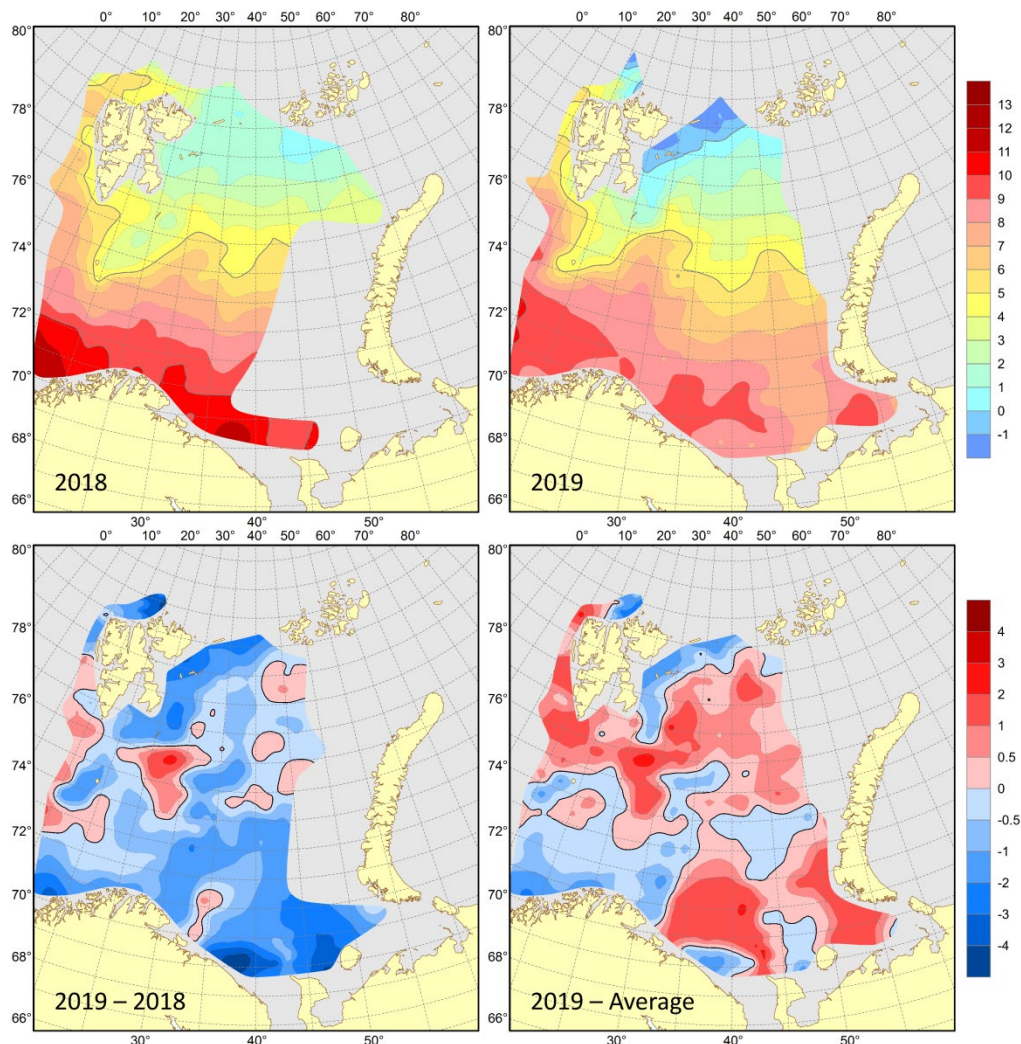


Figure 3.1.8. Surface temperatures ($^{\circ}\text{C}$) in August–September 2018 (upper left) and 2019 (upper right), their differences between 2019 and 2018 (lower left, $^{\circ}\text{C}$) and anomalies in August–September 2019 (lower right, $^{\circ}\text{C}$).

Arctic waters were mainly found, as usual, in the 50–100 m layer north of 77°N . Temperatures at depths of 50 and 100 m were higher than the long-term (1931–2010) means (on average, by 1.1 and 0.7°C respectively) in about two thirds of the surveyed area with the largest positive anomalies in the east, especially at 50 m depth (Fig. 3.1.9). Negative anomalies (about -0.4°C on average) were mainly found in the northern and south-western Barents Sea with the largest values in the north at a depth of 100 m. Compared to 2018, the 50 and 100 m temperatures in 2019 were lower (on average, by 0.9 and 0.7°C respectively) in most of the surveyed area (80 and 85% respectively) with the largest negative differences in the northern Barents Sea at 50 m depth; positive differences were mainly observed in the south-eastern part of the sea (Fig. 3.1.9).

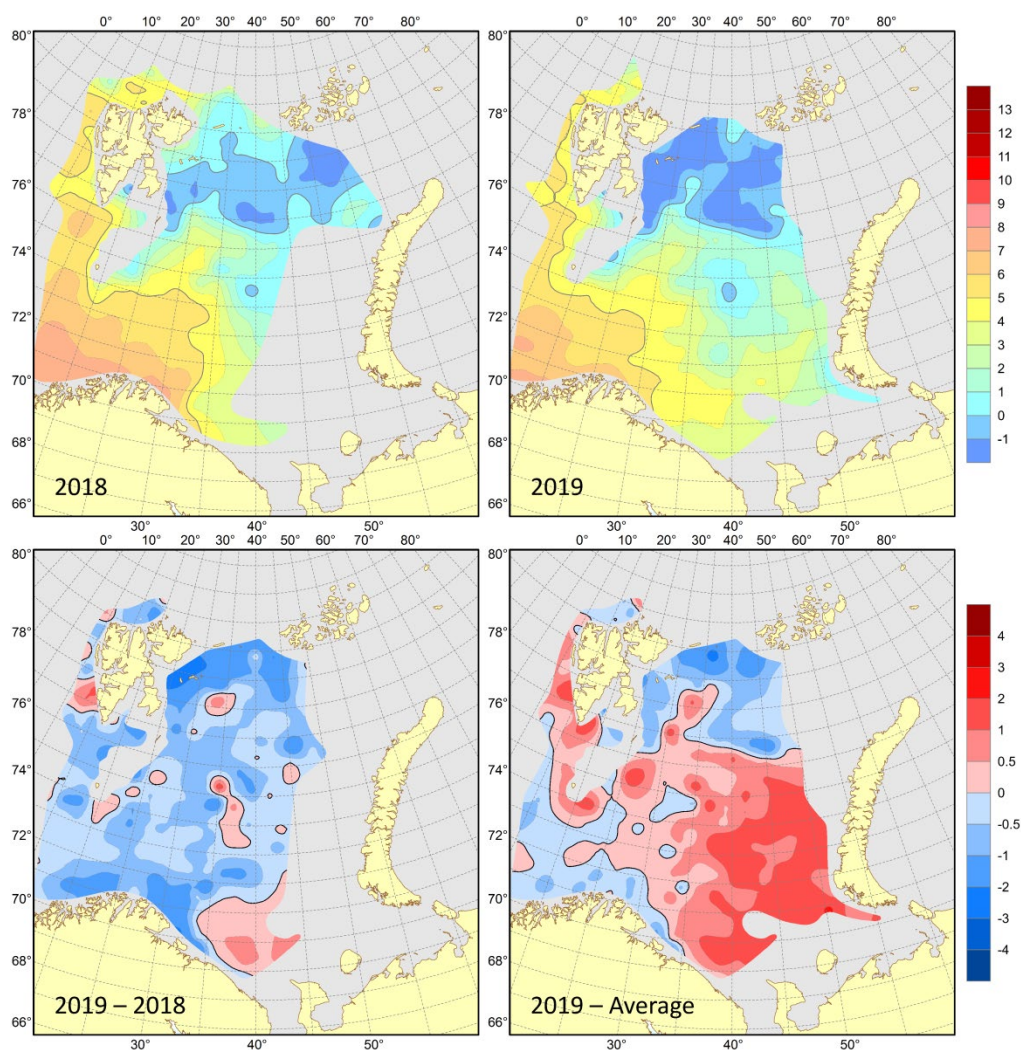


Figure 3.1.9. 100 m temperatures (°C) in August–September 2018 (upper left) and 2019 (upper right), their differences between 2019 and 2018 (lower left, °C) and anomalies in August–September 2019 (lower right, °C).

Bottom temperature was in general 0.8°C above average (1931–2010) in most of the Barents Sea (~70% of the surveyed area) with the largest positive anomalies in the south-east (Fig. 3.1.10). Negative anomalies (–0.8°C on average) were mainly observed in the northern part of the sea with the largest values east of the Spitsbergen Archipelago. Compared to 2018, the bottom temperature in 2019 was on average 0.7°C lower in 75% of the surveyed area with the largest differences in the north (Fig. 3.1.10). Bottom waters were warmer (on average, by 0.5°C) than in 2018 mainly in the south-eastern part of the sea.

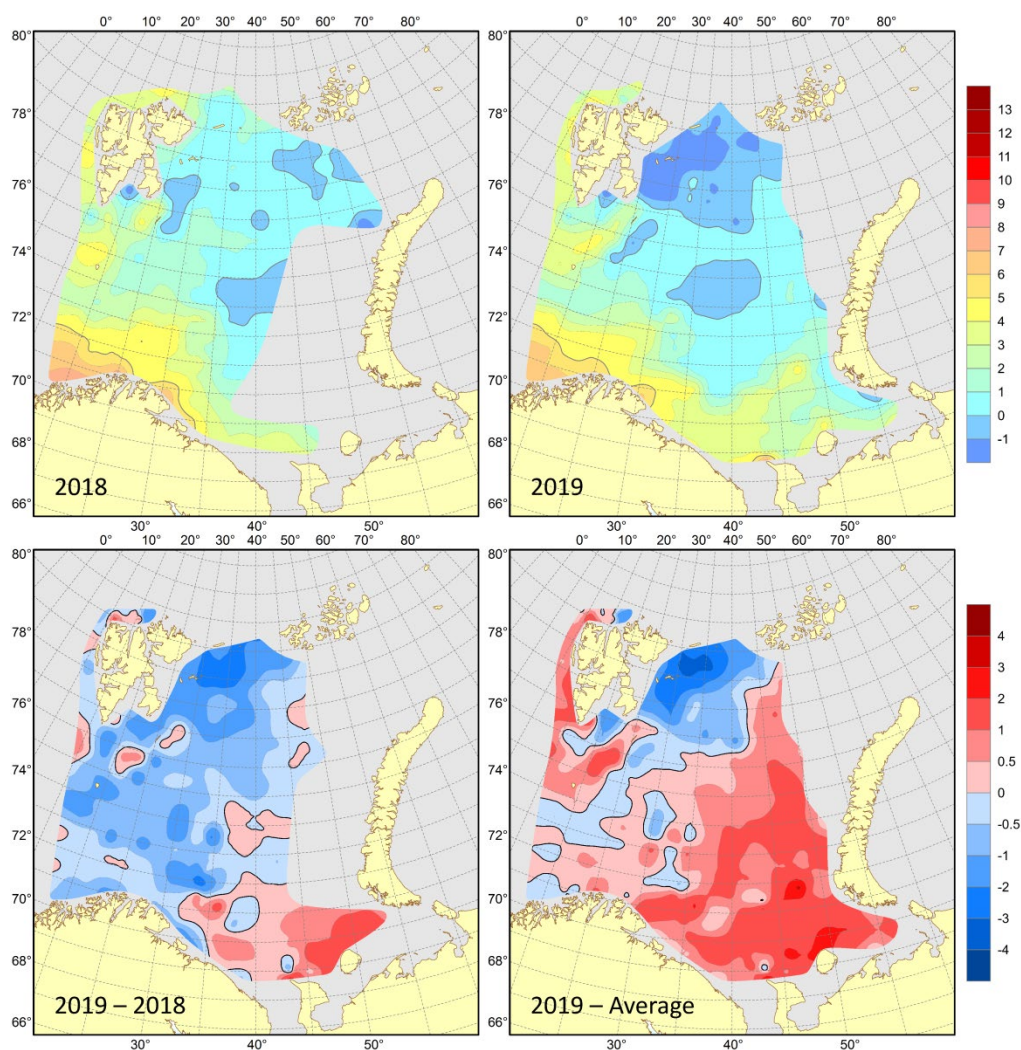


Figure 3.1.10. Bottom temperatures (°C) in August–September 2018 (upper left) and 2019 (upper right), their differences between 2019 and 2018 (lower left, °C) and anomalies in August–September 2019 (lower right, °C).

Surface salinity was on average 0.3 higher than the long-term (1931–2010) mean mainly in the central and northern parts of the surveyed area with the largest positive anomalies (>0.8) mostly in the northern Barents Sea (Fig. 3.1.11). Negative anomalies (about -0.3 on average) were mainly observed in the western, southern and south-eastern parts of the sea with the largest values in some areas in the south-east. In August–September 2019, the surface waters were on average 0.4 fresher than in 2018 almost all over the surveyed area (87%) with the largest negative differences east of the Spitsbergen Archipelago and in the south-eastern Barents Sea (Fig. 3.1.11).

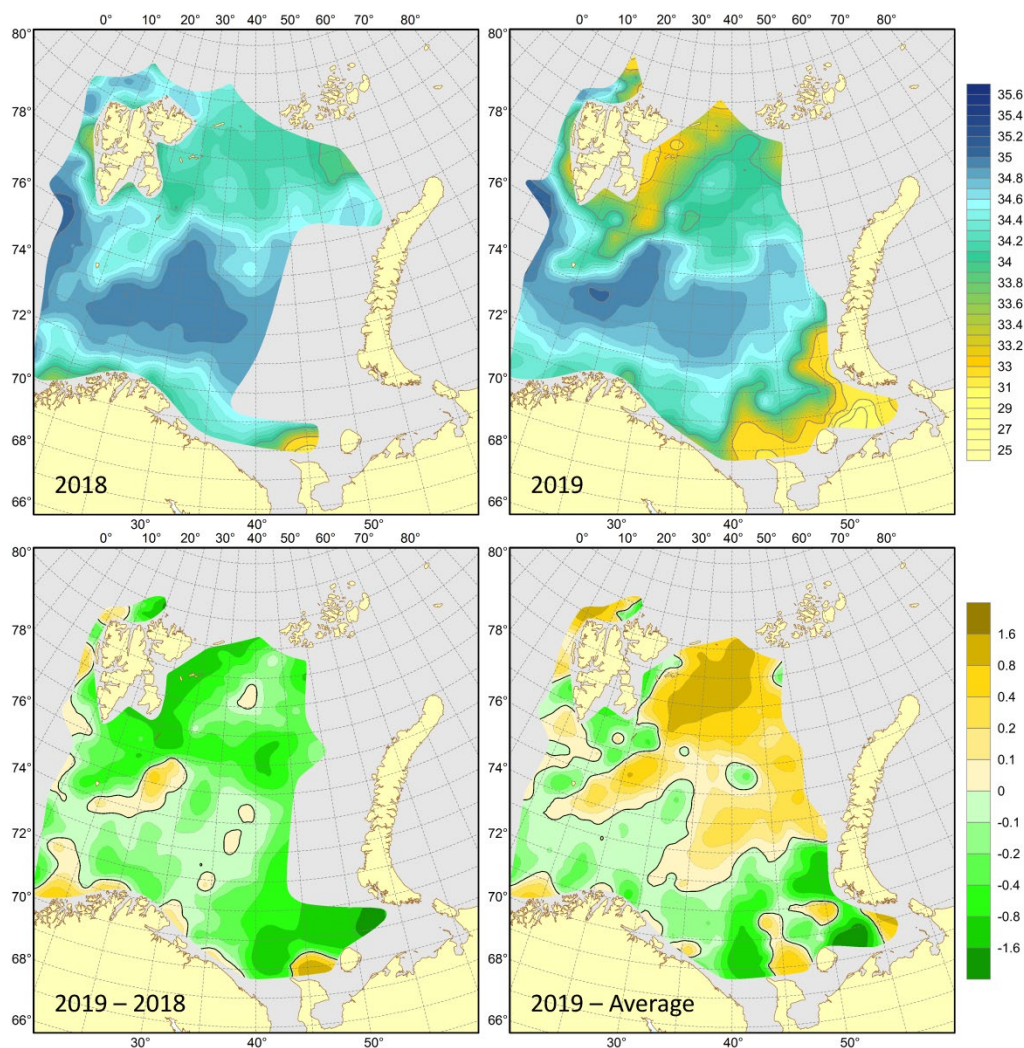


Figure 3.1.11. Surface salinities in August–September 2018 (upper left) and 2019 (upper right), their differences between 2019 and 2018 (lower left) and anomalies in August–September 2019 (lower right).

The 50 and 100 m salinity was lower than average (1931–2010) (by about 0.1 on average) in two thirds of the surveyed area with the largest negative anomalies in the south-eastern part of the Barents Sea (Fig. 3.1.12). Positive anomalies were mainly observed in the north-western part of the sea with the largest values east of the Spitsbergen Archipelago. In August–September 2019, waters at 50 and 100 m were fresher (by 0.1 on average) than in 2018 in most of the surveyed area (58 and 67% respectively) with the largest negative differences in the east of the area (Fig. 3.1.12). Significant positive differences (>0.1) in salinity between 2019 and 2018 were mainly observed in the northern Barents Sea and in the coastal waters of its south-western part. At a depth of 100 m, salinity anomalies and differences of less than 0.1 occupied about 80 and 90% of the surveyed area respectively (Fig. 3.1.12).

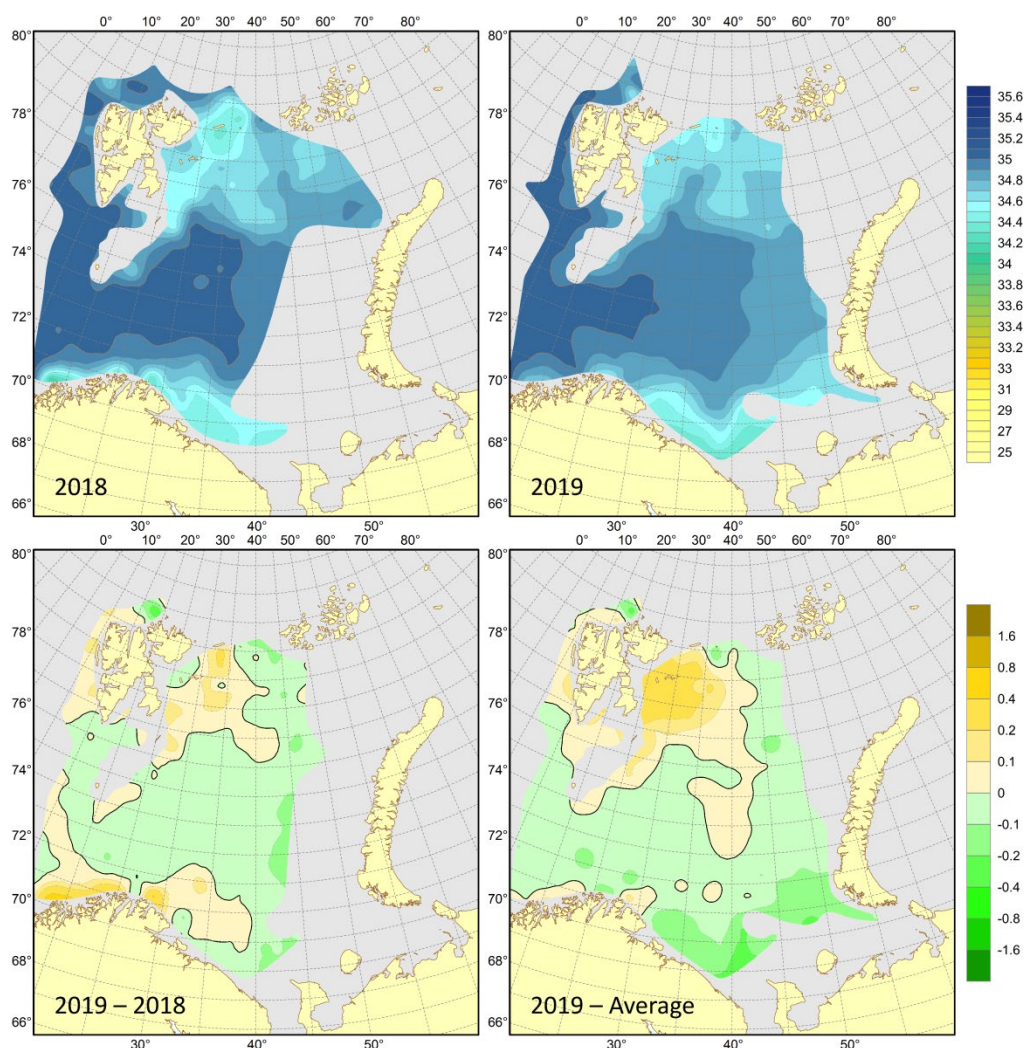


Figure 3.1.12. 100 m salinities in August–September 2018 (upper left) and 2019 (upper right), their differences between 2019 and 2018 (lower left) and anomalies in August–September 2019 (lower right).

Bottom salinity was slightly lower than average (1931–2010) in two thirds of the surveyed area with the largest negative anomalies (>0.1) in the south-eastern and northernmost Barents Sea (Fig. 3.1.13). Slightly positive anomalies were found in the central part of the sea and anomalies of more than 0.1 took place mainly south and south-east of the Spitsbergen Archipelago as well as in shallow waters in the south-easternmost part of the sea. In August–September 2019, the bottom waters were a bit fresher than in 2018 in most of the surveyed area (80%) (Fig. 3.1.13). The largest negative differences (>0.1) in bottom salinity between 2019 and 2018 were mostly found in small areas north of the White Sea Opening and Kanin Peninsula as well as north of Bear Island. Only coastal waters in the south-western Barents Sea and waters around the Spitsbergen Archipelago were saltier than in 2018. As a whole, bottom salinity anomalies and differences were small (<0.1) almost all over the surveyed area (78 and 86% respectively) (Fig. 3.1.13).

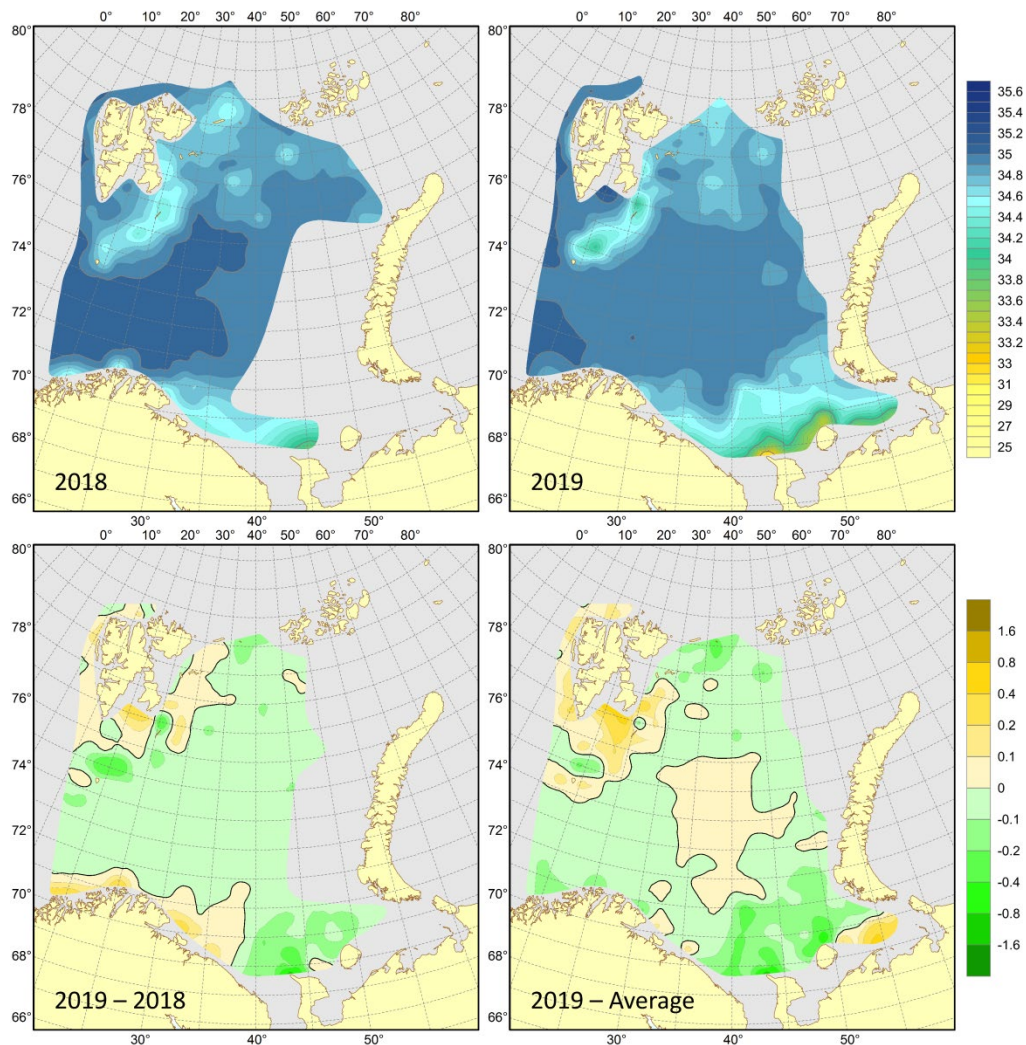


Figure 3.1.13. Bottom salinities in August–September 2018 (upper left) and 2019 (upper right), their differences between 2019 and 2018 (lower left) and anomalies in August–September 2019 (lower right).

Water masses

Time series of area covered by Arctic Water masses in 50–200 m depth show a strong shift occurring around 2006 (Fig. 3.1.14), with substantially larger extent of Arctic Water before than after. The extent of the Atlantic Water masses show a more gradual increase over the period from 1970 to 2019, and vary to a large extent in synchrony with the temperature of the inflowing Atlantic Water in the western Barents Sea (Fig. 3.1.14). Largest extent of Atlantic Water, and least extent of Arctic Water, were observed in 2016. After that the extent of Atlantic Water has decreased and the extent of Arctic Water decreased. The areas of the two water masses were in 2019 at about the same level as in 2004–2005.

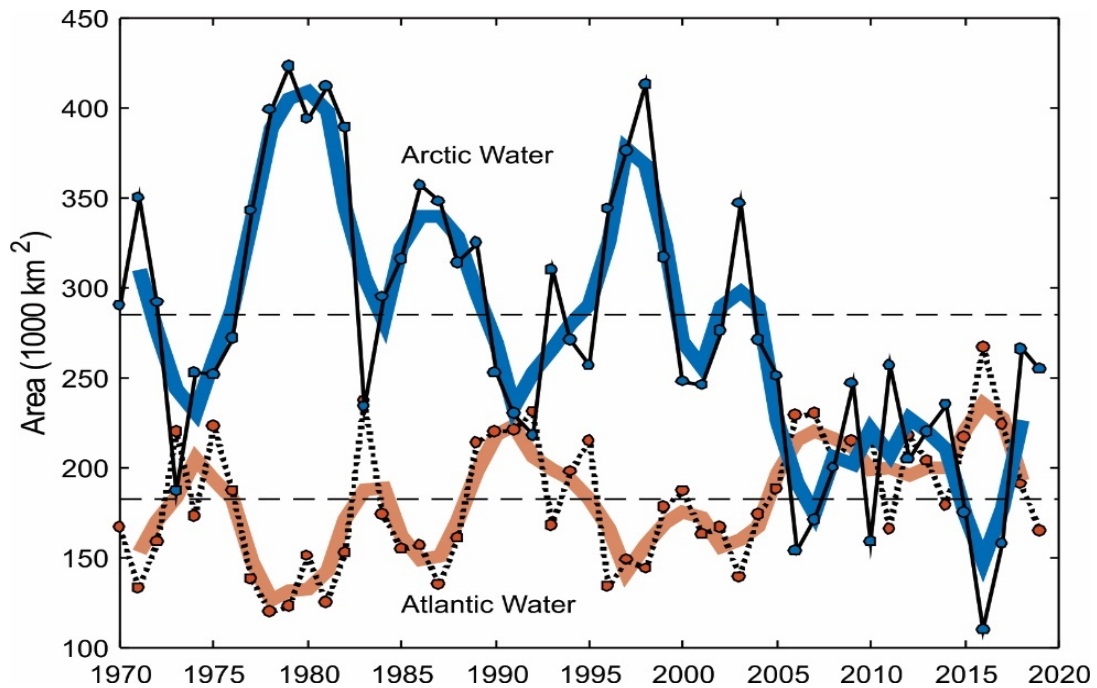


Figure 3.1.14. Area of Atlantic Water ($T > 3^{\circ}\text{C}$) and Arctic Water ($T < 0^{\circ}\text{C}$) masses in the Barents Sea ($71\text{--}79^{\circ}\text{N}$, $25\text{--}55^{\circ}\text{E}$) in August–September 1970–2019 (based on 50–200 m averaged temperature). Black lines show annual August–September values, while thick coloured lines show three years running means. Horizontal lines show average over the period 1981–2010.

Focusing in on the different depth levels, the area covered by warm water (above 4, 3 and 1°C at 50, 100 m and near the bottom respectively) in August–September 2019 was 7, 4 and 23% smaller than in 2018 at 50, 100 m and near the bottom respectively (Fig. 3.1.15). The area covered by cold water (below 0°C) was 6% larger than in 2018 at 50 and 100 m and 21% larger near the bottom. Since 2000, the area covered by cold bottom water was the largest in 2003 and rather small in 2007, 2008, 2012, 2016–2018; in 2016, it reached a record low value since 1965 and then it has been increasing for the past three years; in 2019, it almost tripled compared to the previous year.

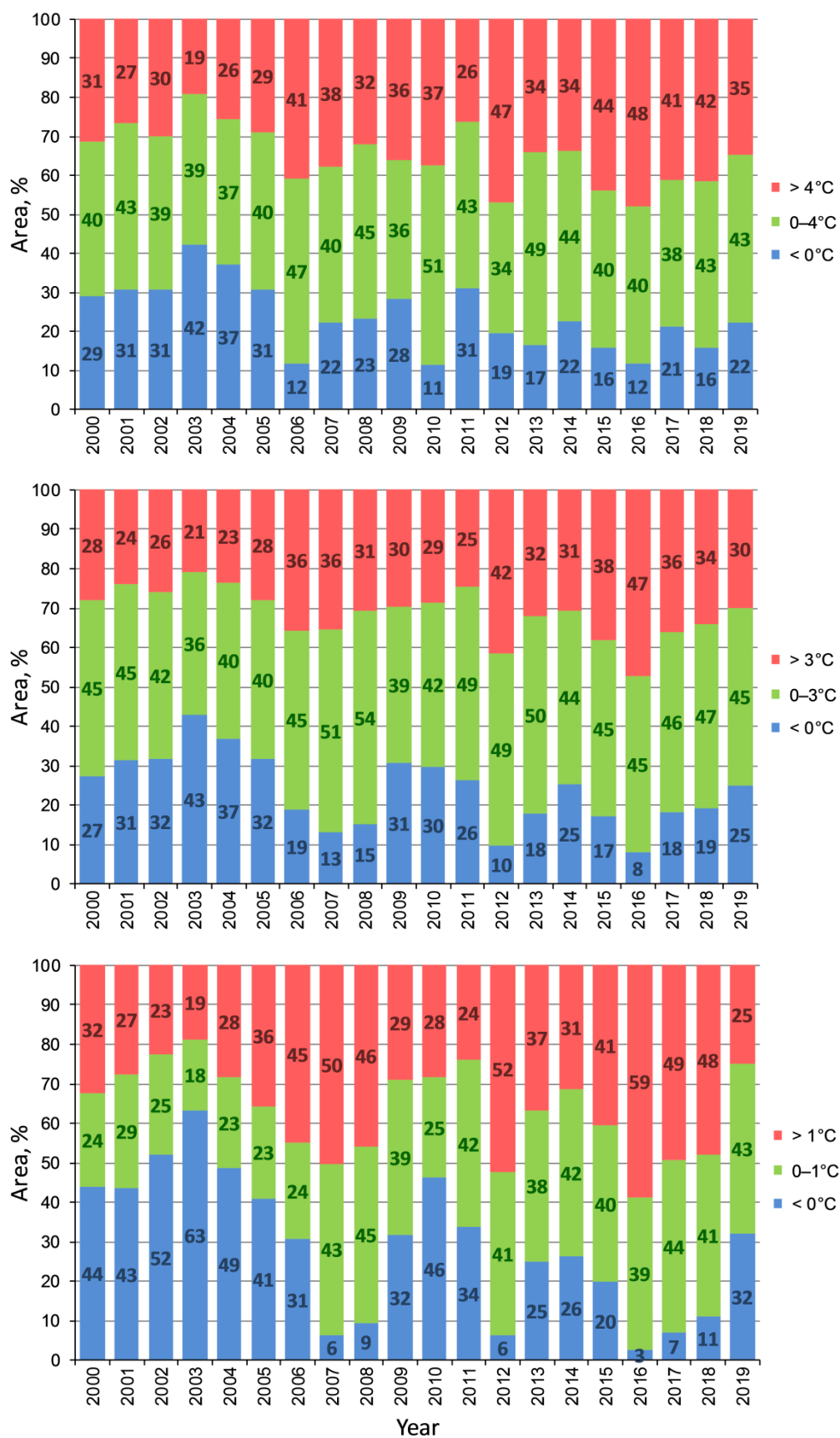


Figure 3.1.15. Areas covered by water with different temperatures at 50 m (upper panel), 100 m (middle panel) and near the bottom (lower panel) in the Barents Sea (71–79°N, 25–55°E) in August–September 2000–2019.

Mean temperature in polygons

Mean temperature in the upper, intermediate and deep waters were calculated for polygons for possible inclusion in multivariate analysis (Fig. 3.1.16). The polygons series show that the temperature in the upper, intermediate and deep waters in August–September 2019 were higher than the mean (1981–2010) in most subregions. The exceptions were the outer boundary subregions; the South West and the Franz Victoria Trough, where they were slightly below the mean. At Great Bank, the temperatures at bottom were in 2019 below the mean.

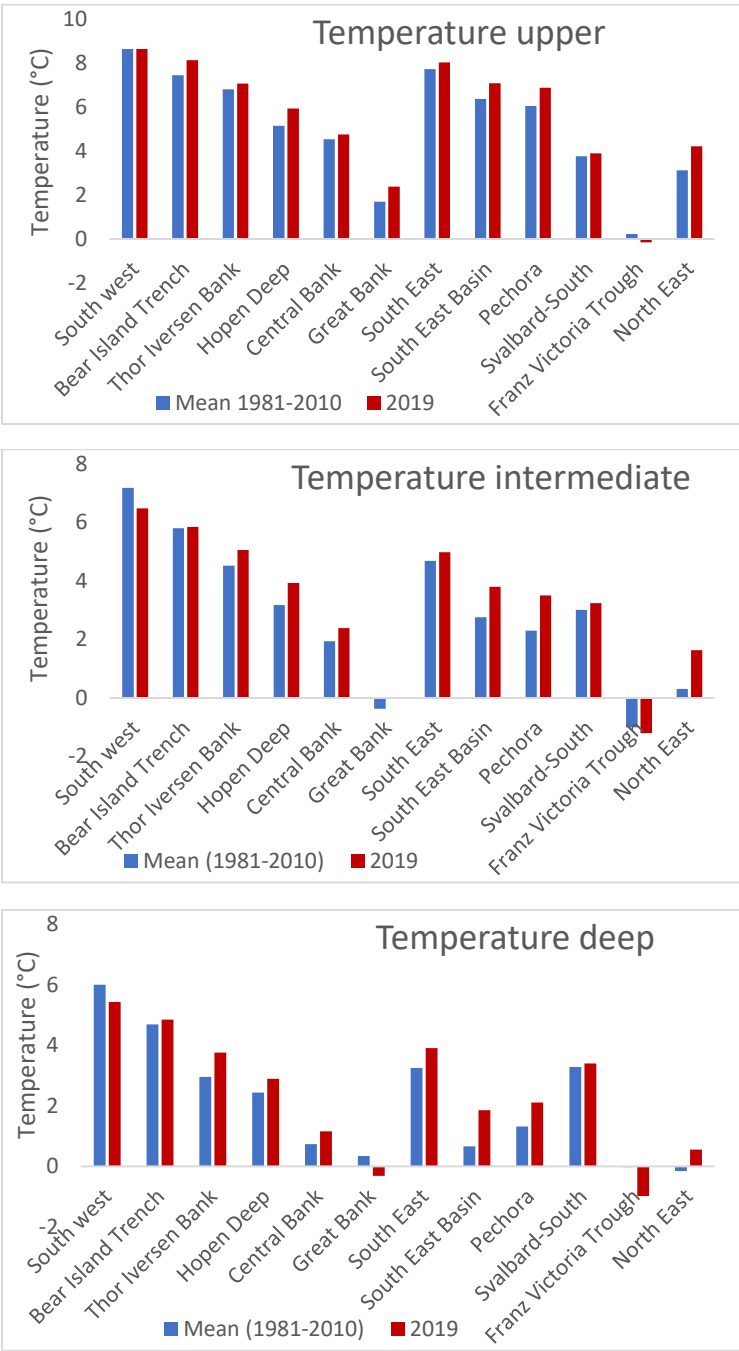


Figure 3.1.16. Average temperature in the polygons with data coverage in 2019 (red bars) and mean temperature for the period 1981–2020 (blue bars).

3.2 Phytoplankton and primary production

By Padmini Dalpadado

Satellite-based annual net primary production in the Barents Sea has shown an increasing trend with a doubling over the last twenty years, due to increased temperatures leading to reduced ice-coverage and prolonged open water period.

The phytoplankton development in the Barents Sea is typical for a high latitude region with a pronounced maximum in biomass and productivity during spring. During winter and early spring (January-March) both phytoplankton biomass and productivity are quite low. The spring bloom is initiated during mid-April to mid-May and may vary strongly from one year to another. The bloom duration is typically about 3-4 weeks and it is followed by a reduction of phytoplankton biomass mainly due to the exhaustion of nutrients and grazing by zooplankton. Later in the fall when the increasing winds start to mix the upper layer and bring nutrients to the surface, a short autumn bloom can be observed. However, the time development of this general description can vary geographically. The spring bloom in the Atlantic water domain without sea-ice is thermocline-driven, whereas in the Arctic domain with seasonal sea-ice, stability from ice-melt determines the bloom (Skjoldal and Rey 1989, Hunt et al. 2012). Thus, the spring bloom at the ice edge in the Barents Sea can sometimes take place earlier than in the southern regions due to early stratification from ice melting.

3.2.1 Satellite data

Remote sensing data having high spatial and temporal resolution were used in obtaining Chl *a* concentration (mg m^{-3}) and mean daily NPP ($\text{g C m}^{-2} \text{ day}^{-1}$). Daily net primary production (NPP) and open water area (OWA) were calculated from satellite data as described in detail in Arrigo and Van Dijken (2015). Satellite-derived surface Chl *a* (Sat Chl *a*, Level 3, 8 days binned) was based on SeaWiFS and MODIS/Aqua sensors. SeaWiFS was used in 1998-2002, and MODIS/Aqua in 2003-2017. Data were updated using NASA's latest reprocessing - version R2018.0. For the years where data was available for both sensors (2003-2007), SeaWiFS Chl was consistently higher than MODIS/Aqua Chl. Therefore, we used a correction factor for SeaWiFS Chl to create a comparable 20-year time series. The values for the South-East and Pechora polygons were recalculated excluding the regions most influenced by river inflow (18% and 41% of the total area, respectively). The work done here is in collaboration with Professor Kevin Arrigo and Gert van Dijken from the Stanford University, USA.

Validation of satellite Chl *a* using *in situ* data showed significant correlations between the two variables in the Barents Sea (Dalpadado et al. 2014, ICES/WGIBAR 2017, this study) and thus, the NPP model based on satellite data by Arrigo et al. (2015) gives reasonable results that compare well with sea ground truthing measurements. Also, estimates of new production from phytoplankton based on nitrogen consumption (seasonal draw-down of nitrate in the water column) for the Fugløya - Bear Island (FB) and Vardø-Nord (VN) sections, representing the western and central Barents Sea

respectively, from March to June resulted in values comparable to satellite NPP estimates (Rey et al. in prep, pers. com.).

3.2.2 Spatial and temporal patterns of Chl *a* in spring

Remote sensing data, providing good spatial and temporal coverage, were used to explore the seasonal and interannual variability in Chl *a* distribution. Satellite data from the Barents Sea during 2016–2018 showed large interannual variability with the highest Chl *a* concentration generally observed in May (Fig. 3.2.2.1). There was much less sea ice in 2016, and north- and eastward expansion of the Chl *a* distribution. Furthermore, earlier blooming and higher concentrations in the eastern regions in April and May were observed in this year. 2017 was a colder year with more ice especially compared to 2016. Chl *a* was much lower during April to July in 2017 compared to the previous year. The ice cover was larger in April 2017 and 2018, than in 2016. Though the Chl *a* in April in 2018 was lower compared to 2016, high concentration was observed in May for both years.

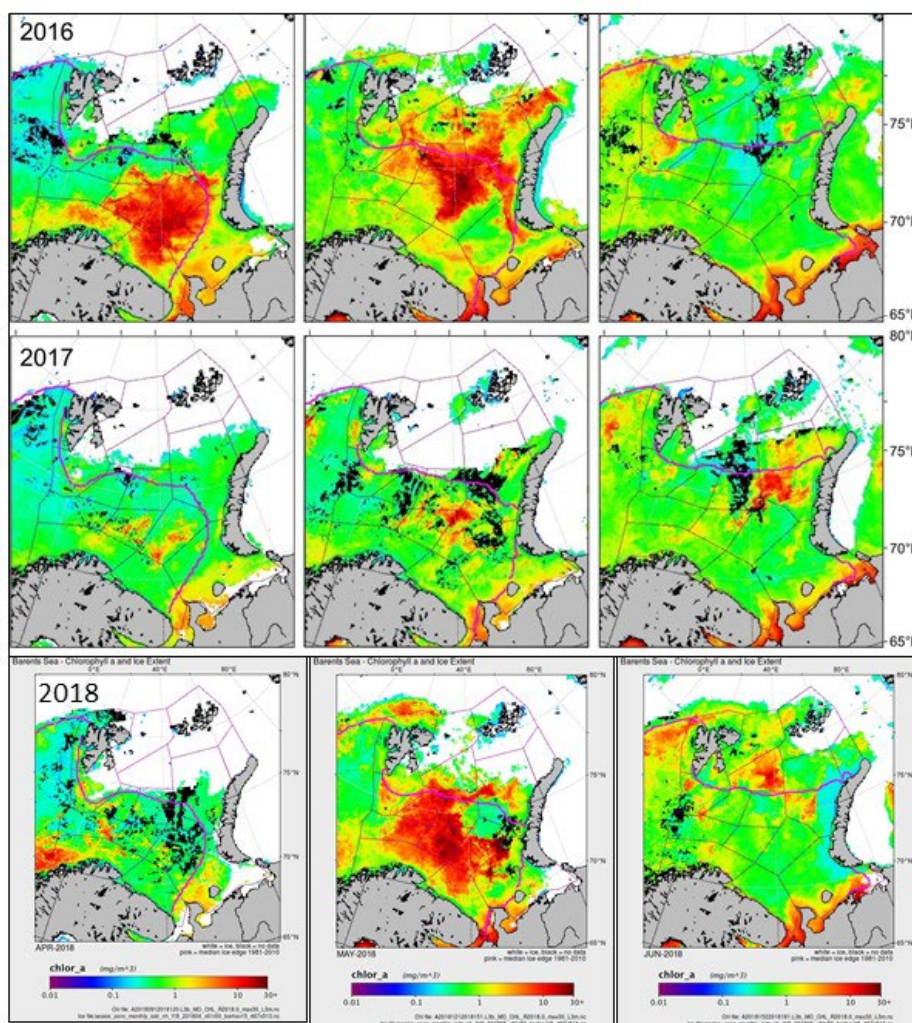


Figure 3.2.2.1. Spatial distributions of Chl *a* (mg m^{-3}) in April, May and June for 2016, 2017 and 2018. White areas indicate ice-coverage. The black areas indicate no data. The pink lines show the climatological (average 1981–2010) position of the ice edge.

3.2.3 Net Primary Production (NPP)

Although the NPP of the whole Barents Sea showed substantial interannual variability, there was a marked significant increase during the study period, 1998-2018 (Fig. 3.2.3.1, $p = 0.001$). Average NPP for the whole Barents Sea was much lower in years 1998-2008 than in the more recent decade 2009-2018 (64.8 and 93.8 Tg C, respectively). Though the NPP in the western and eastern regions of the Barents Sea increased significantly during the study period ($p < 0.01$), the increase in the northeastern region was up to 5 times larger compared to the south west region.

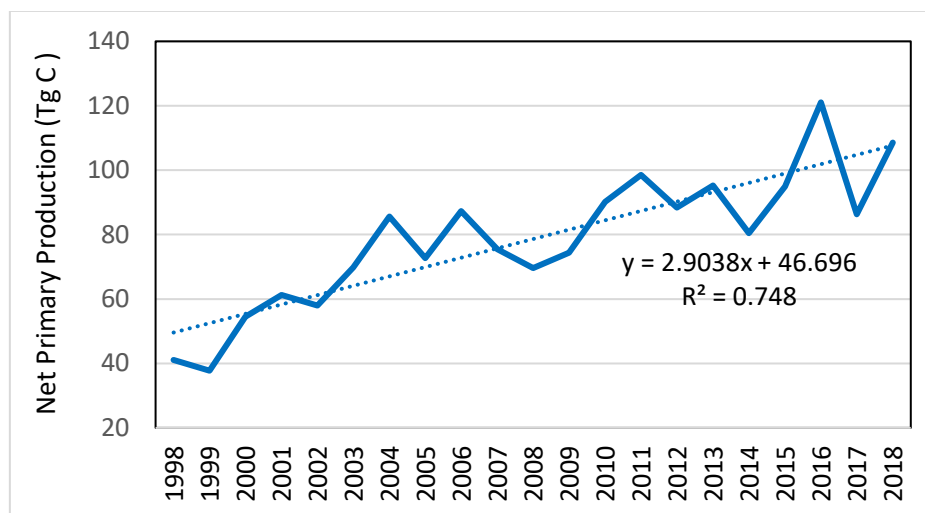


Figure 3.2.3.1. Annual net primary production (satellite based NPP) for the whole Barents Sea.

References

- Arrigo K.R. and van Dijken G. (2015). Continued increases in Arctic Ocean primary production. *Progress in Oceanography* 136:60-70
- Dalpadado P., Arrigo, A.R., Hjøllø, S., Rev, F., Ingvaldsen R.B., Sørø, E., Dijken G.L.V., Olsen, A., Ottersen, G. (2014). Productivity in the Barents Sea - response to recent climate variability. *PLoS ONE* 9(5):e95273 doi:10.1371/journal.pone.0095273
- Hunt G.L., Blanchard A.L., Boveng P., Dalpadado P., Drinkwater K., Eisner L., Hopcroft R., Kovacs K.M., Norcross B.L., Renaud P., Reigstad M., Renner M., Skioldal H.R., Whitehouse A., Woodgate R. A 2012. The Barents and Chukchi Seas: Comparison of two Arctic shelf ecosystems. *Journal of Marine Systems*: 43-68
- Rev et al. (in press). Interannual variability of new and net primary production in the Barents Sea.
- Sakshaug E., Johnsen G., Kristiansen S. et al (2009). Phytoplankton and primary production. 2009. In *Ecosystem Barents Sea*. Eds. Sakshaug E, Johnsen G, Kovacs K. Tapir Academic Press, Norway. pp: 167- 208
- Skioldal, H.R., Rev, F., 1989. pelagic production and variability of the Barents Sea ecosystem. In: Sherman, K., Alexander, L.M. (Eds.), *Biomass yields and geography of large marine ecosystems*, AAAS Selected Symposium, vol. 111. Westview Press, pp. 241-286.

3.3 Zooplankton

By Espen Bagøien, Irina Prokopchuk, Andrey Dolgov, Padmini Dalpadado, Hein Rune Skjoldal, Elena Eriksen, Jon Rønning, Valentina Nesterova, Ksenia Zaytseva, Tatyana Prokhorova and Pavel Krivosheya

The mesozooplankton biomass in autumn 2019 was at approximately the same level as in recent years for the Barents Sea as a whole. The biomass in the western inflow area of Atlantic water was higher in 2019, and also somewhat higher on the Central and Great Banks, than in preceding years. The biomass in the eastern and northern areas remained at a relatively high

level comparable to the long-term mean. Krill biomass has shown an increasing trend in recent decades and remained high in 2019. Pelagic amphipods were nearly absent in 2012-2013 but have since shown increased abundances and expanded distributions in the area east of Svalbard. The plankton situation in 2019 indicates good feeding conditions for planktivorous consumers.

3.3.1 Mesozooplankton biomass and distribution

Mesozooplankton biomass – large scale distributions

By Espen Bagøien (IMR), Irina Prokopchuk (PINRO), Andrey Dolgov (PINRO), Padmini Dalpadado (IMR), Jon Rønning (IMR), Valentina Nesterova (PINRO)

Mesozooplankton play a key role in the Barents Sea ecosystem by transferring energy from primary producers to animals higher in the foodweb. Geographic distribution patterns for mesozooplankton biomass show similarities over a multiannual time-scale, although some interannual variability is apparent.

Differing geographical survey-coverages between years will impact biomass estimates both for territorial waters and the Barents Sea as a whole, particularly as the ecosystem is characterized by large-scale heterogeneous distributions of biomass. One way to address this challenge, is to perform interannual comparisons of estimated biomass within well-defined and consistent spatial subareas (polygons).

During August-October 2019, relatively high biomass ($>10 \text{ g m}^{-2}$) was observed in the area of the Bear Island Trench, north and northeast of Svalbard/Spitsbergen, south of Franz Josef Land, and in the basin of the south-eastern Barents Sea. Relatively low biomass ($<4 \text{ g m}^{-2}$) was observed in mainly in the south-eastern corner of the Barents Sea, but also west and south-east of Svalbard including the Great and Central Banks (Figure 3.3.1.1). The large-scale horizontal distribution of plankton in the Barents Sea during autumn 2019 resembled that of 2018, not considering the large unsurveyed areas in south-eastern region in 2018 and in the north-eastern region in 2019.

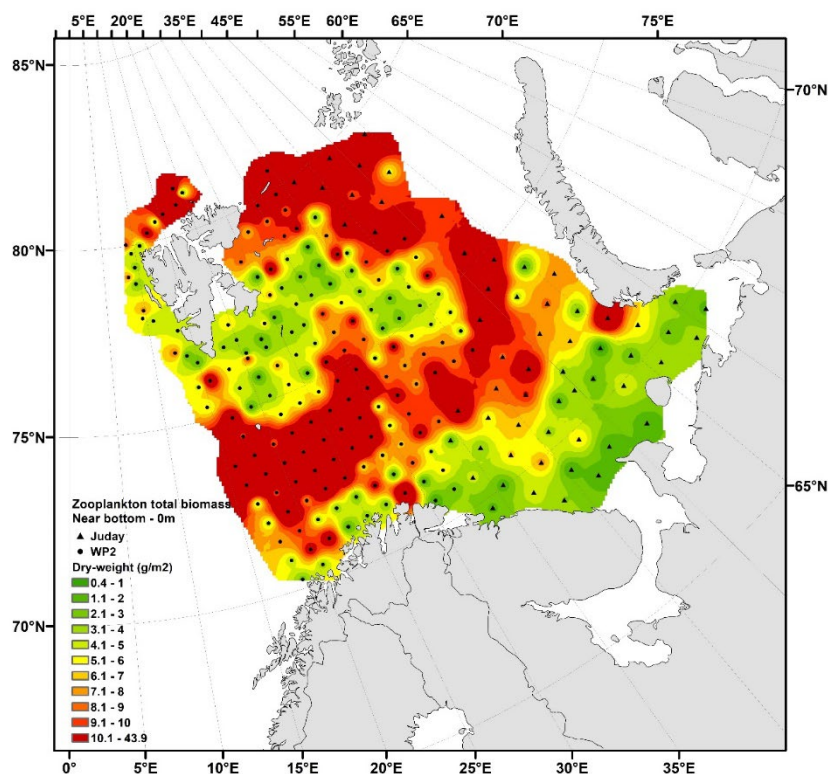


Figure 3.3.1.1. Distribution of total mesozooplankton biomass (dry-weight, g m^{-2}) from seafloor to surface. Data based on 229 samples collected during BESS in mid August – early-October 2019. A WP2 net was applied by IMR and a Juday net by PINRO; both nets with mesh-size $180 \mu\text{m}$. Interpolation made in ArcGIS v.10.6.1, module Spatial Analyst, using inverse distance weighting (default settings).

In the Norwegian sector of the Barents Sea, mesozooplankton biomass was size-fractionated ($180\text{--}1000 \mu\text{m}$, $1000\text{--}2000 \mu\text{m}$, and $>2000 \mu\text{m}$) before weighing. The biomass for the intermediate size-fraction in 2019 was above the 20-year (1999–2018) long-term average. In contrast, the biomasses for smallest and largest size-fractions were slightly lower than the long-term averages (1999–2018) (Figure 3.3.1.2). Regarding the largest size-fraction, average values have shown a decreasing tendency during the ca. last 15 years, even if the 2019 value was not particularly low.

Based only on Norwegian data, which represent the spatially most consistent time-series, average zooplankton biomass (summing all size-fractions) during August–October 2019 was 8.0 (SD 6.2) $\text{g dry-weight m}^{-2}$ for the western part of the Barents Sea. This estimate is based on 171 observations and is higher than in 2018 ($7.2 \text{ g dry-weight m}^{-2}$), and also above the long-term (1999–2018) average ($7.0 \text{ g dry-weight m}^{-2}$) (Figure 3.3.1.2).

Combined Russian and Norwegian data (229 stations in total) (Figure 3.3.1.1), covering the entire area surveyed in the Barents Sea in 2019, provided an estimated average zooplankton biomass of 7.9 (SD 6.3) $\text{g dry-weight m}^{-2}$, which is the arithmetic average for all stations shown in Figure 3.3.1.1. This estimate is not directly comparable with that for 2018 due to the above-mentioned differing sampling coverage in the eastern region in 2018 versus 2019. In the Russian sector, average biomass for the area covered in 2019 was 7.5 (SD 6.1) $\text{g dry-weight m}^{-2}$. This value is based on 58 observations, and

also not directly comparable to the 2018 estimate for the same reason as described above.

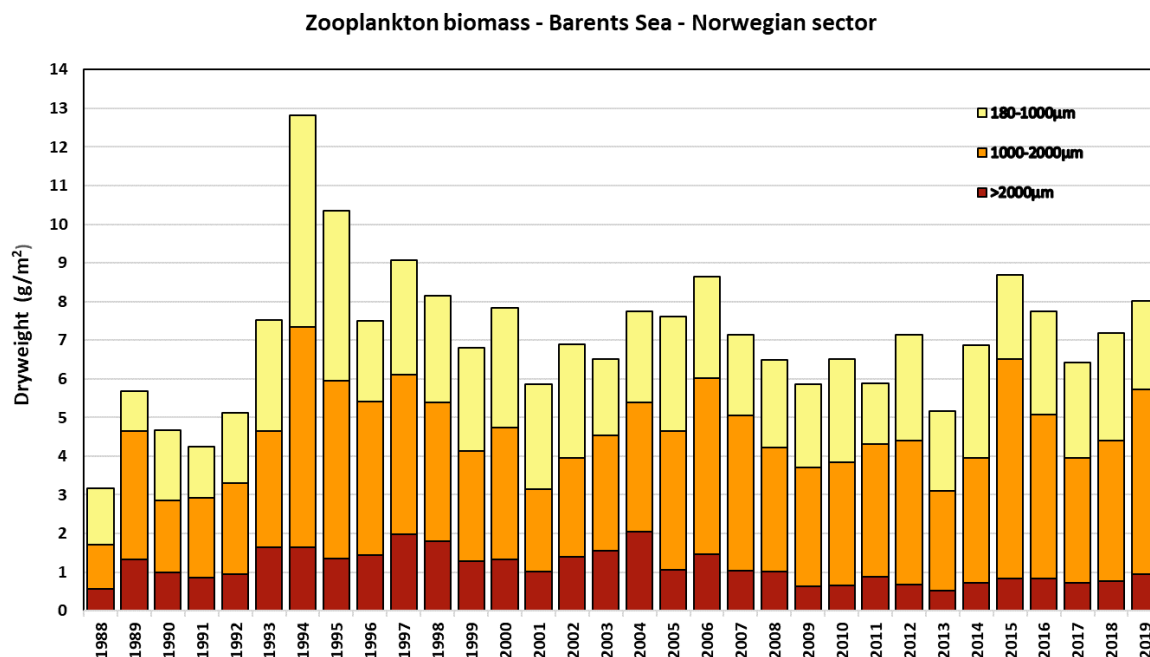


Figure 3.3.1.2. Time-series of average mesozooplankton biomass from surface to sea floor (dry-weight, g m⁻²) for western and central Barents Sea (Norwegian sector) during the autumn BESS (1988–2018). Data are shown for three size-fractions; 0.18–1 mm (yellow), 1–2 mm (orange), and >2 mm (red) based on wet-sieving.

Zooplankton biomass varies between years and is believed to be partly controlled by predation pressure, e.g. from capelin. However, the annual impact of predation varies geographically. Predation from other planktivorous pelagic fish (herring, polar cod, and blue whiting) and pelagic juvenile demersal fish species (cod, haddock, saithe, and red-fish), and larger plankton forms (e.g. chaetognaths, krill, and amphipods) can also impact meso-zooplankton in the Barents Sea. In addition, processes such as advective transport of plankton from the Norwegian Sea into the Barents Sea, primary production, and local production of zooplankton are likely to contribute to the variability of zooplankton biomass. As mentioned above, methodological factors such as differing spatial survey coverage also contribute to the variability of biomass estimates between years. For a more direct comparison of interannual trends, that is less influenced by variable spatial coverages, time-series of biomass estimates for specific sub-areas of the Barents Sea are provided in the following section).

Mesozooplankton biomass in subareas of the Barents Sea

By Hein Rune Skjoldal and Padmini Dalpadado

Zooplankton biomass data for 2019 have been calculated as average values for each of 12 subareas or polygons. Time-series of biomass estimates for these subareas for the 1989-2016 period were described in a background document (2018 WGIBAR Report, Annex 4). Time-series estimates for four Atlantic water subareas (Bear Island Trench,

South-West, Thor Iversen Bank, and Hopen Deep), two central subareas (Central Bank and Great Bank), and two subareas in the eastern Barents Sea (South-East Basin and North-East) are shown in Figure 3.3.1.3.

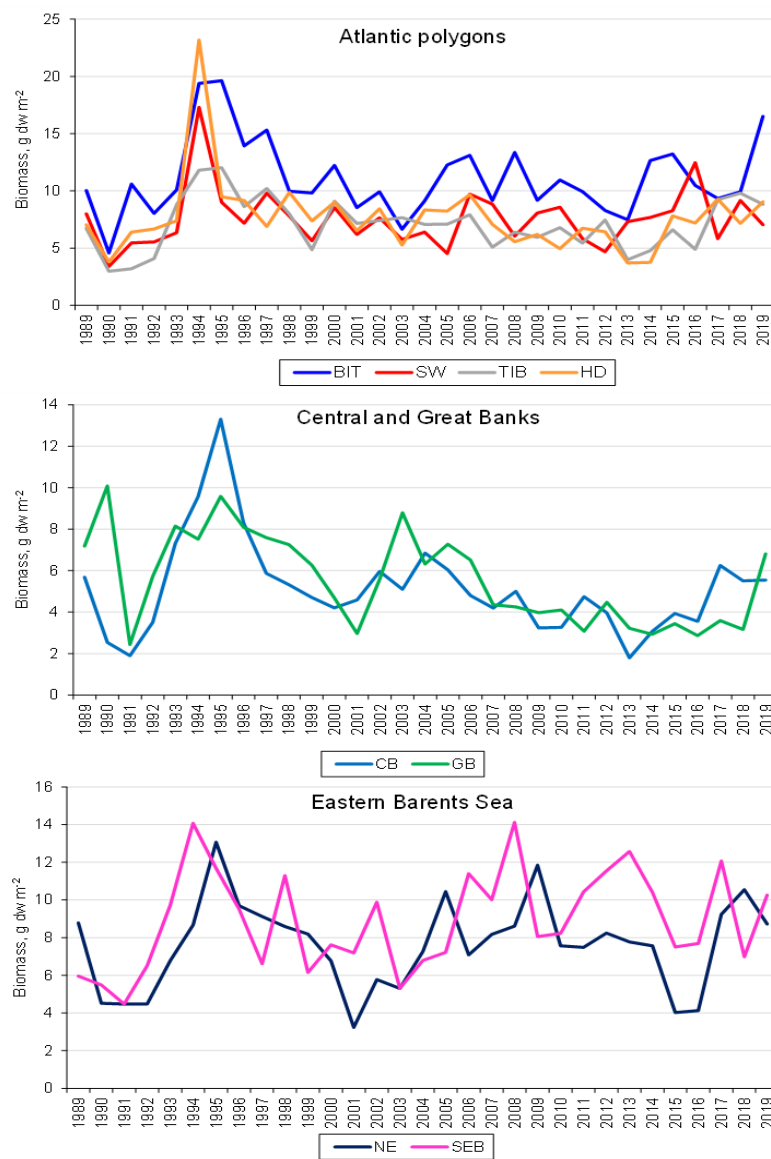


Figure 3.3.1.3. Time-series for mean zooplankton biomass (g dw m⁻²) for stations within subareas of the Barents Sea (see WGIBAR 2018 Report, Annex 4) based on autumn survey data for the 1989-2019 period. Upper panel – four subareas in the southwestern Barents Sea covered mainly with Atlantic water: Bear Island Trench (BIT); South-West (SW); Hopen Deep (HD); and Thor Iversen Bank (TIB). Middle panel – two subareas in the central Barents Sea with colder and partly Arctic water conditions: Central Bank (CB) and Great Bank (GB). Lower panel – two subareas in the eastern Barents Sea: Southeast Basin (SEB) and North East (NE). Results represent total biomass collected with WP2 or Juday plankton nets.

Biomass estimates in the ‘Atlantic’ subareas have fluctuated between 5 to 10 g dw m⁻² since about year 2000, with generally higher values for the Bear Island Trench. In this subarea, the biomass showed a marked increase to 16.5 g dw m⁻² in 2019. The biomass of the Hopen Deep (HD) and Thor Iversen Bank (TIB) subareas have shown an increase from low values of about 4 g dw m⁻² in 2013-14 to about 9 g dw m⁻² in 2019. It should be noted that sampling variance is high, with coefficient of variation (CV = SD/mean)

of about 0.5 for mean values per subarea (see WGIBAR 2018 report, Annex 4). This translates into confidence intervals (95%) of ± 20 -25% around the mean for n observations of 16–25 (which is the typical number of stations within a subarea).

Biomass estimates at Central Bank and Great Bank showed declining trends since the 1990s to minimum values around 2013 (Figure 3.3.1.3 - Middle). The biomass at these two subareas have subsequently increased, with a marked jump from 2018 to a relatively high value (6.8 g dw m^{-2}) for the GB in 2019. The zooplankton biomass in the eastern polygons, South-East Basin and North-East, has shown fluctuations with no clear trends in the last 10 years. The biomass values were relatively high in 2019, around 9 - 10 g dw m^{-2} for both polygons.

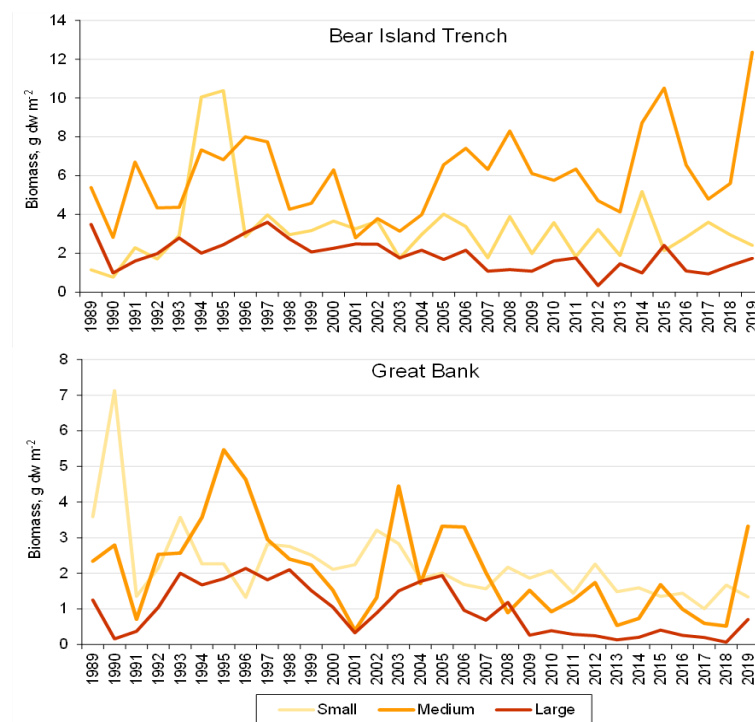


Figure 3.3.1.4. Zooplankton biomass ($\text{g dry-weight m}^{-2}$) in three size fractions (small $<1 \text{ mm}$, medium $1\text{--}2 \text{ mm}$, and large $>2 \text{ mm}$) for Bear Island Trough (upper panel) and Great Bank (lower panel) subareas for the 1989-2019 period. Note: Size fractions are based on screen mesh size, not size of individual zooplankton.

Size composition of mesozooplankton is shown in Figure 3.3.1.4 for two subareas: Bear Island Trench - a region of Atlantic water inflow; and Great Bank. These two subareas have had different temporal development. Bear Island Trench has had a more consistent pattern, with relatively high biomass of the medium size fraction since 2005. This fraction contains older stages of *Calanus* spp. which dominate mesozooplankton biomass in the Barents Sea (Aarflot et al. 2017). The increase in total biomass in 2019 reflected an increase of the medium size fraction. The recent situation likely reflects high influx of *Calanus finmarchicus* with Atlantic inflow to the Barents Sea, possibly related to a second generation within a single spawning season under warmer climate conditions (Skjoldal et al., unpublished manuscript).

Decline in biomass for Great Bank has been associated with a shift in dominance from the medium size fraction to the small fraction over the last decade. During this same period, the large size fraction declined to a very low level. The decline and shift from large to small zooplankton could reflect a combination of warming and predation from capelin (Dalpadado et al., unpublished manuscript). The Great Bank used to be part of the domain for the dominant Arctic species *Calanus glacialis* (Melle and Skjoldal, 1998) and has traditionally been a core feeding area for capelin. The increase in biomass for the Great Bank subarea in 2019 was due to an increase of the medium size fraction.

Figure 3.3.1.5 shows a comparison of long-term average estimates of zooplankton biomass (1989–2016) for each subarea together with estimates for 2019 and the previous year 2018. The 2019 biomass was considerably higher than the long-term average for the Bear Island Trench (by >50 %), Thor Iversen Bank, Hopen Deep, and Great Bank subareas. The biomass in 2019 was also higher than in 2018 for these subareas, except Thor Iversen Bank.

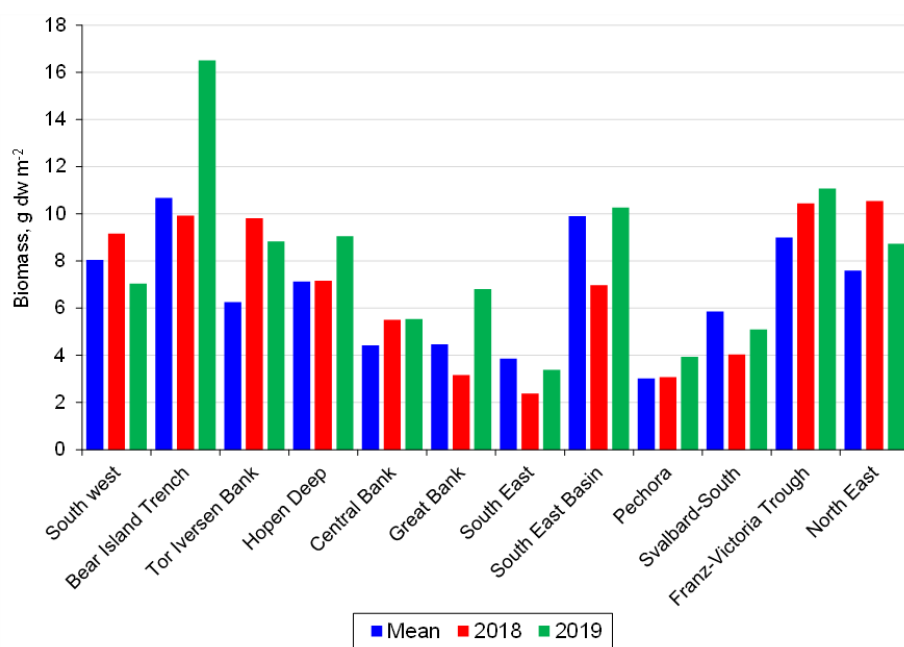


Figure 3.3.1.5. Average zooplankton biomass (g dry-weight m⁻²) for twelve subareas of the Barents Sea, comparing long-term averages for the 1989–2016 period with average values for stations sampled in 2018 and 2019.

Mesozooplankton species-composition along the Fugløy - Bear Island and the Kola transects

By Irina Prokopchuk, Espen Bagøien, Jon Rønning, Padmini Dalpadado and Valentina Nesterova

The Fugløy - Bear Island (FB) transect, spanning the western entrance to the Barents Sea, is generally monitored by IMR 5-6 timer per year, covering the different seasons. Up to eight stations with fixed positions are sampled during each coverage, although the number may vary depending on weather conditions. Zooplankton samples collected each year during the 1995–2019 period from four fixed locations at different latitudes (70.30°N, 72.00°N, 73.30°N, and 74.00°N) and representing different water masses (Coastal, Atlantic, and mixed Atlantic/Arctic) have been analysed

taxonomically. Average annual abundance for each of the species *C. finmarchicus*, *C. glacialis* and *C. hyperboreus* is estimated by pooling the four stations throughout the seasonal cycle and summing up the copepodite stages I-VI (Figure 3.3.1.6, left). The arcto-boreal species *C. finmarchicus* is, by far, the most common of these three species, and displays some interannual variation in abundance. *C. finmarchicus* tends to be most abundant at the three southernmost stations. A particularly high abundance was recorded during 2010 along most of the transect, except at the northernmost station. After registering very low abundances at all stations in 2013, *C. finmarchicus* has generally been abundant along most of the transect during the last 6 years (2014–2019).

The Arctic species *C. glacialis* has typically been most abundant at the two northernmost stations, representing Atlantic and mixed Atlantic-Arctic waters, respectively. This species also shows some interannual variation in abundance, particularly in the late nineteen-nineties (Figure 3.3.1.6, left). Abundance of *C. glacialis* along the FB transect has decreased since the initial years of this time-series (1995–1998), with very low abundance recorded in 2005, 2008, and during the 2012–2014 and 2017–2018 periods. The abundance of the large and Arctic species, *C. hyperboreus*, along the FB transect has been low relative to the abundance of *C. finmarchicus*, but generally also compared to *C. glacialis* throughout the study period. Few individuals of this species were observed during 2008–2010, 2013, and 2016. The FB time-series of *C. hyperboreus* abundance shows a clear interannual variability, and the abundances were not low in 2018 and 2019 (Figure 3.3.1.6, left).

Calanus helgolandicus, a more southerly species, is observed regularly at the Fugløya-Bear Island transect, particularly during the December-February period (Dalpadado *et al.*, 2012).

Even in winter, the abundance of *C. helgolandicus* along the FB transect seldom surpasses a few hundred individuals per square meter. In spring and summer, this species is more or less absent at the entrance to the Barents Sea. In recent years, *C. helgolandicus* has become more abundant in the North Sea, and it is also observed in the Norwegian Sea off mid-Norway, particularly in autumn (Continuous Plankton Recorder data, Espen Strand, IMR, pers. comm.). *C. helgolandicus* is similar in appearance to *C. finmarchicus* and taxonomic separation of these two species is time-consuming. Hence, the IMR-routine is to examine a limited number of individuals belonging to the later stages of the *C. finmarchicus/helgolandicus* assemblage – up to 20 copepodites of stage V and up to 20 adult females – to establish the species-proportions in each FB sample. Our FB time-series provides no evidence of an increase over the years, neither of the proportion or absolute abundance of *C. helgolandicus* at the entrance to the Barents Sea.

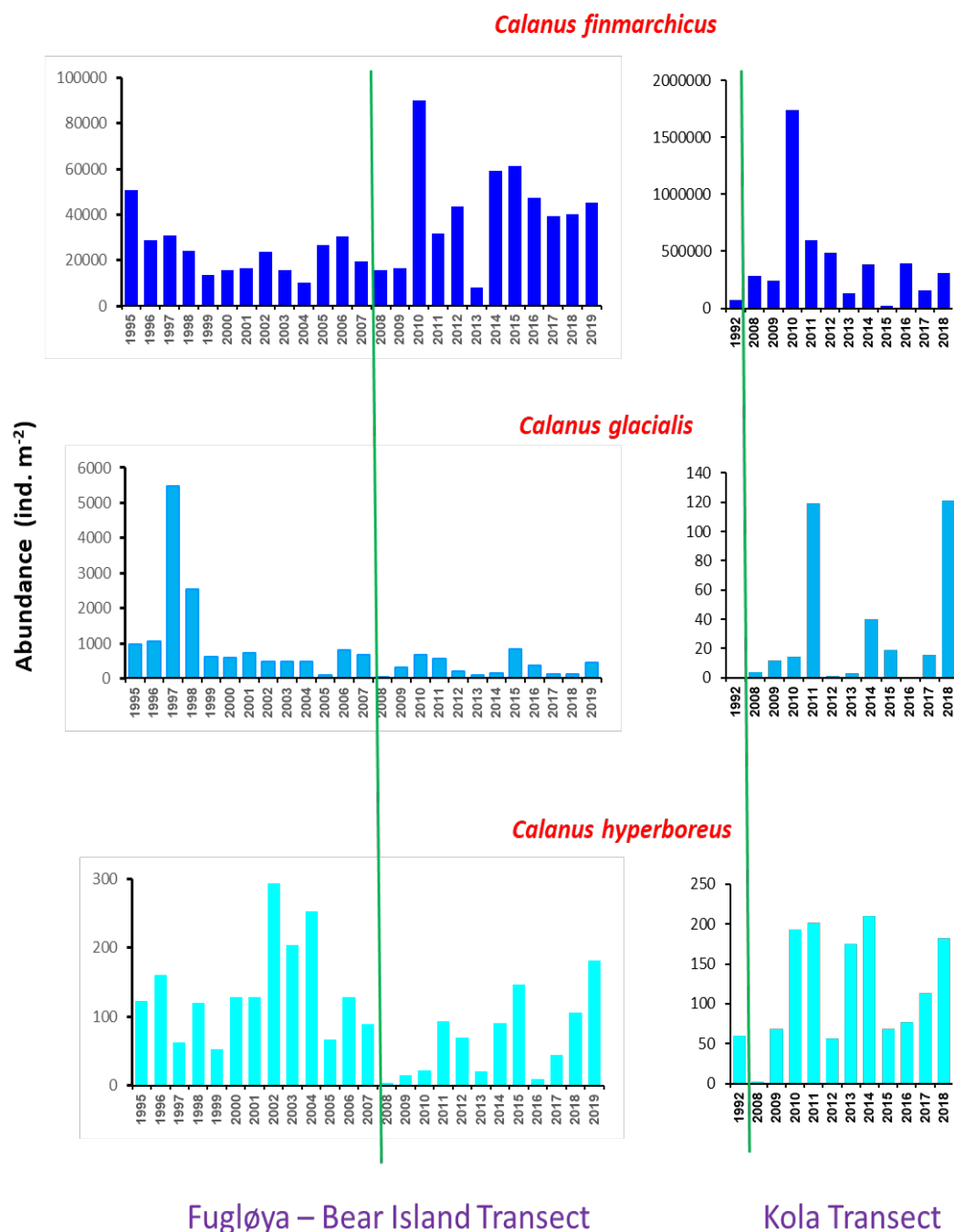


Figure 3.3.1.6. Time series of abundances (ind. m⁻²) of *Calanus finmarchicus*, *C. glacialis*, and *C. hyperboreus* along the Fugløy-Bjørnøya (1995-2020) (left) and Kola (1992, 2008-2018) (right) transects. For the FB transect, each bar generally represents the annual average for 4 stations and 5–6 coverages per year. For the Kola transect the data show early-summer abundances. Note strongly differing scales for abundances between the two transects and the species. The right-hand sides from the vertical green lines show the same years for the two transects.

Russian (PINRO) investigations along the Kola section in June 2018 showed copepods as the dominant group of zooplankton at that time, comprising on average 64% in abundance and 85% in biomass, and *Calanus finmarchicus* as the dominant species. Average abundance of *C. finmarchicus* in 2018 was 308 309 ind. m⁻², almost twice the 2017 value, but lower than for 2016 and long-term average (Figure 3.3.1.6, right). The highest abundance of *C. finmarchicus* was observed at the most southerly station of the

section at 69°30'N and further north at 72°30'N, while its lowest abundance was observed at 70°00'N. In the *C. finmarchicus* population, individuals at all life stages were present: CIII-CIV stages dominated at the southern stations, and CI-CIV individuals were represented at the northern stations.

Average abundance of the arctic species *C. glacialis* in 2018 was 121 ind. m⁻², which is 7.6 times higher than the 2017 estimate, and 4.2 times higher than the long-term average (Figure 3.3.1.6, right). *C. glacialis* mainly occurred from 73°00' N and northwards; only copepodites CV were observed for this species.

Average abundance of the arctic species *C. hyperboreus*, the largest *Calanus* species in the Barents Sea, was higher in 2018 than in 2017 (182 and 113 ind. m⁻², respectively) and exceeded the long-term average (117 ind. m⁻²) (Figure 3.3.1.6, right). A gradual increase in *C. hyperboreus* abundance has been observed since 2015. The highest abundance of this species was observed northwards from 73°00' N, and the population was represented by copepodites CIV-CV.

Species composition from the autumn ecosystem cruise

PINRO investigations of mesozooplankton conducted by the BESS during August-September 2018 showed that in the Russian part, copepods dominated both in terms of abundance (86.7%) and biomass (63.2%) (Fig. 3.3.1.7). Total zooplankton abundance in the southern (south of ca. 75°N) Barents Sea was lower than in the northern part (north of ca. 75°N) of the sea (1 324 and 2 012 ind. m⁻³, respectively). Total zooplankton biomass was higher in the northern than the southern Barents Sea (243.5 and 134.0 mg m⁻³, respectively). However, the results from the southern Barents Sea are not quite comparable with previous years as the number of stations in the southern part of the sea in 2018 was very low (only 9 stations).

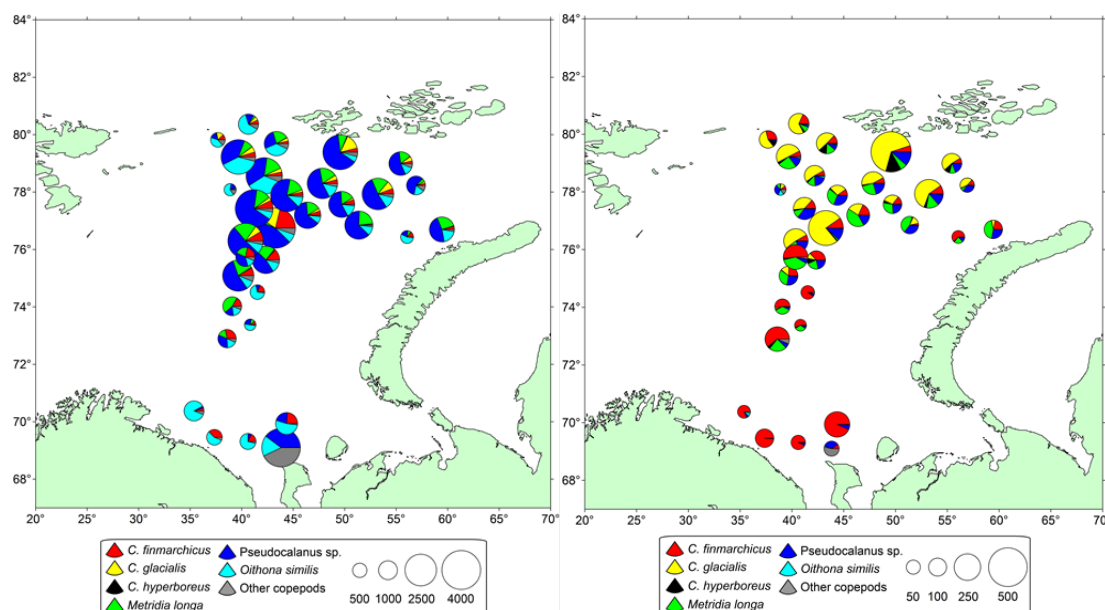


Figure 3.3.1.7. Abundance (ind. m⁻³) (left) and biomass (mg wet-weight m⁻³) (right) of the most numerous copepod species (surface to sea floor) in the Barents Sea (based on PINRO samples from the BESS during August-September 2018)

In the southern Barents Sea, total zooplankton abundance and biomass in 2018 had decreased slightly (by factor 1.1) compared to 2017. Copepods dominated both abundance and biomass (78.5 and 65.9%, respectively). Among other groups, the most important were chaetognaths comprising 25.5% of total zooplankton biomass. Their abundance had increased by a factor of 3.0 and the biomass increased by factor of 2.0 compared to 2017. Considering species composition of copepods, the small *Oithona similis* and *Pseudocalanus* sp. and the larger *C. finmarchicus* were the most abundant (48.6, 17.2 and 17.5% of total copepod abundance, respectively), and the large *Metridia longa* comprised 8.0% (Figure 3.3.1.7). However, in terms of copepod biomass, *C. finmarchicus* (70.7%), *M. longa* (10.2%), and *Pseudocalanus* sp. (8.1%) were the most important species, while *O. similis* comprised only 2.1% (Figure 3.3.1.7). In 2018, abundance of *Pseudocalanus* sp. and *M. longa* had increased compared to 2017, while abundance of other important copepods had decreased. Biomass of the main copepods (with the exception of *Pseudocalanus* sp.) had also decreased in 2018.

In the northern Barents Sea, total zooplankton abundance and biomass in 2018 increased by factors of 1.4 and 1.3, respectively, in comparison to 2017. The main increase of abundance and biomass was observed in the populations of copepods and chaetognaths. Copepods were the most abundant (90.0%) zooplankton group. Regarding total zooplankton biomass, copepods also represented the most important group (63.1%) during 2018, while chaetognaths, pteropods and hydrozoans comprised 24.5, 4.3 and 4.2%, respectively. In the northern Barents Sea, the small copepods *Pseudocalanus* sp. and *O. similis* and the larger *M. longa* contributed 45.6, 22.4 and 14.4%, respectively; while, *C. finmarchicus*, and *C. glacialis* contributed only 7.2 and 5.0% to total copepod numbers, respectively (Figure 3.3.1.7). Total copepod biomass consisted mainly of *C. glacialis* (36.9%), *M. longa* (20.4%), *C. finmarchicus* (17.5%) and *Pseudocalanus* sp. (18.6%). Abundance of *C. finmarchicus*, *C. glacialis*, and *M. longa* have been increasing since 2015, and *Pseudocalanus* sp. since 2016. At the same time, abundance of *O. similis* have been decreasing since 2016. The same trends were observed in biomass of these copepod species. The most prominent increases in both abundance and biomass were observed for *M. longa* in 2017-2018.

3.3.2 Macroplankton biomass and distribution

Krill

Krill (euphausiids) represent the most important group of macrozooplankton in the Barents Sea, followed by hyperiid amphipods. Krill play a significant role in the Barents Sea ecosystem, facilitating transport of energy between different trophic levels. There are mainly four species of krill in the Barents Sea; *Thysanoessa inermis* primarily associated with the Atlantic boreal western and central regions, whereas the neritic *Thysanoessa raschii* mainly occurs in the southeastern Barents Sea. These two species can reach 30 mm in length. *Meganytiphanes norvegica*, the largest species (up to 45 mm) is mainly restricted to typical Atlantic waters. The smallest of the species, the oceanic *Thysanoessa longicaudata* (up to 18 mm), is associated with the inflowing Atlantic water.

Winter distribution and abundance

By Ksenia Zaytseva (PINRO), Valentina Nesterova (PINRO), Andrey Dolgov (PINRO)

Figures by Ksenia Zaytseva (PINRO) and Irina Prokopchuk (PINRO)

The PINRO long-term data series on euphausiids was initiated in 1959 and stopped in 2016 (Figure 3.3.2.1). In 2017, only a part of this survey was conducted; results from only one cruise covering the southern part of the Barents Sea were presented in the previous WGIBAR Report. In November-December 2019, the survey was conducted in western and north-western areas only and the samples are being processed now. These data are not comparable with the previous years.

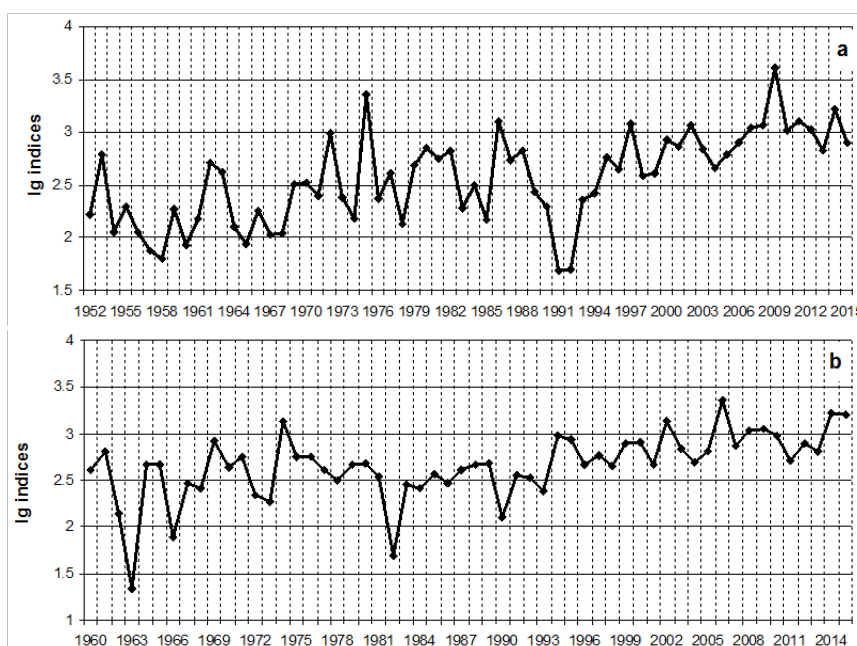


Figure 3.3.2.1. Abundance-indices of euphausiids (\log_{10} of number of individuals per 1000 m^3) in the near-bottom layer of the Barents Sea based on data from the Russian winter survey during October-December for the 1959-2015 period. Based on trawl-attached plankton net catches from the bottom layer in: a) Southern Barents Sea; and b) Northwestern Barents Sea. Note that these data-series were stopped in 2016 but are presented here to show the general trends since the early 1950s and 1960s.

Euphausiids were collected in the southern Barents Sea during the Russian-Norwegian winter survey (February-March 2019) with the trawl-attached plankton net (Figure 3.3.2.2). Euphausiid sampling in this survey was initiated in 2015 onboard a Russian research vessel, but different areas were covered in different years. These results are very preliminary, and comparison with previous years requires caution. Results indicate that in 2019, distribution of euphausiids in the southern Barents Sea was similar to 2018. Average abundance of euphausiids in all areas (866 ind. 1000 m^3) was lower than in 2015 and 2018 (1255 and 1214 ind. 1000 m^3), but higher than in 2016 (561 ind. 1000 m^3). In 2019 the average abundance of euphausiids in the central and coastal areas decreased considerably compared to 2018, was similar in the western areas but increased considerably in the eastern areas. As during previous years (2015-2018), euphausiid concentrations were formed mainly by local species (*T. inermis* and *T. raschii*) and Atlantic species (*M. norvegica* and *T. longicaudata*). It should be noted that

one more warmwater species *Nematoscellis megalops* has occurred in the coastal, western and central areas since 2003. The abundance of this species started to increase since 2012 (up to 1-3% of total euphausiids abundance), and in 2019 their average abundance consisted of 0.3%. Probably it was related to intensive inflow of Atlantic waters from the Norwegian Sea.

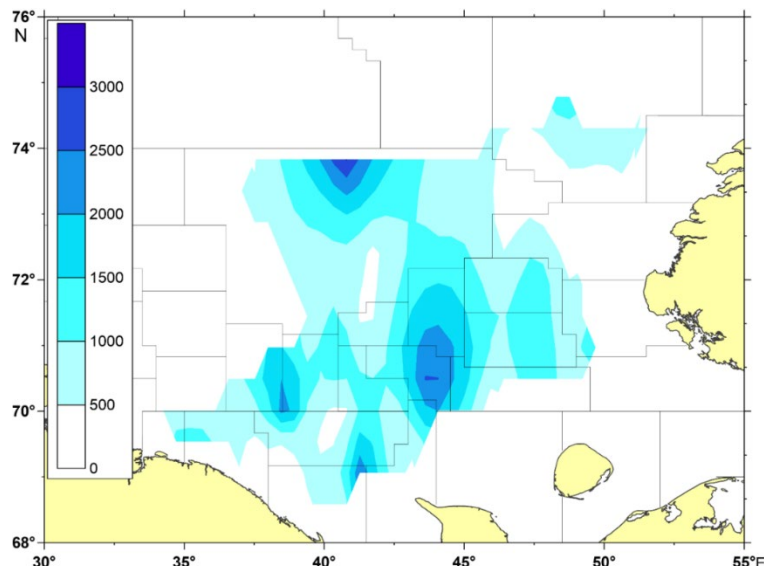


Figure 3.3.2.2. Distribution of euphausiids (abundance, ind. 1000 m⁻³) in the near-bottom layer of the Barents Sea based on data from the Russian-Norwegian winter survey during February-March 2019.

Summer-autumn distribution and biomass

By Tatyana Prokhorova (PINRO), Elena Eriksen (IMR) and Irina Prokopchuk (PINRO)

Figures by Pavel Krivosheya (PINRO), Tatyana Prokhorova (PINRO) and Irina Prokopchuk (PINRO)

In 2019, krill (euphausiids) were caught by standard pelagic «Harstad» trawl and 39% of all samples were identified to species level. The data here reported on krill represent bycatches from trawling on the 0-group fish.

In 2019, krill were widely distributed in the BESS area (Figure 3.3.2.3). The biomass values in the report are given as grams of wet weight per square m (g m⁻²). Larger catches (more than 50 g m⁻²) were made around Svalbard/Spitsbergen and in the western and southeastern Barents Sea. About one third of the stations during the survey in 2019 were sampled during night (Table 3.3.2.1). The total krill biomass was estimated on basis of night catches only. During the night, most of the krill migrate to upper layers to feed and are therefore more accessible for the trawl. Both the day and night catches in 2019 (means of 8.2 g m⁻² and 18.5 g m⁻² respectively) were higher than the long-term means (2.5 g m⁻² and 8.0 g m⁻² respectively).

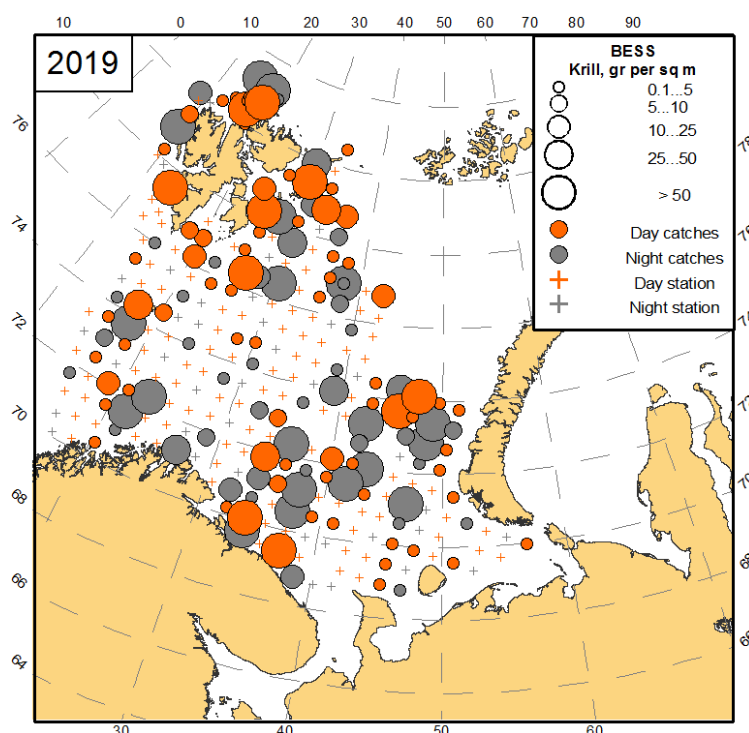


Figure 3.3.2.3. Krill distribution (biomass, g wet-weight m^{-2}), based on pelagic trawl stations covering the upper water layers (0-60 m), in the Barents Sea in August-October 2019.

Species identification of euphausiids took place on the Norwegian vessels only. *M. norvegica* and *T. inermis* were widely observed in the Norwegian samples, while *T. longicaudata* were mostly observed in the western areas (Figure 3.3.2.4).

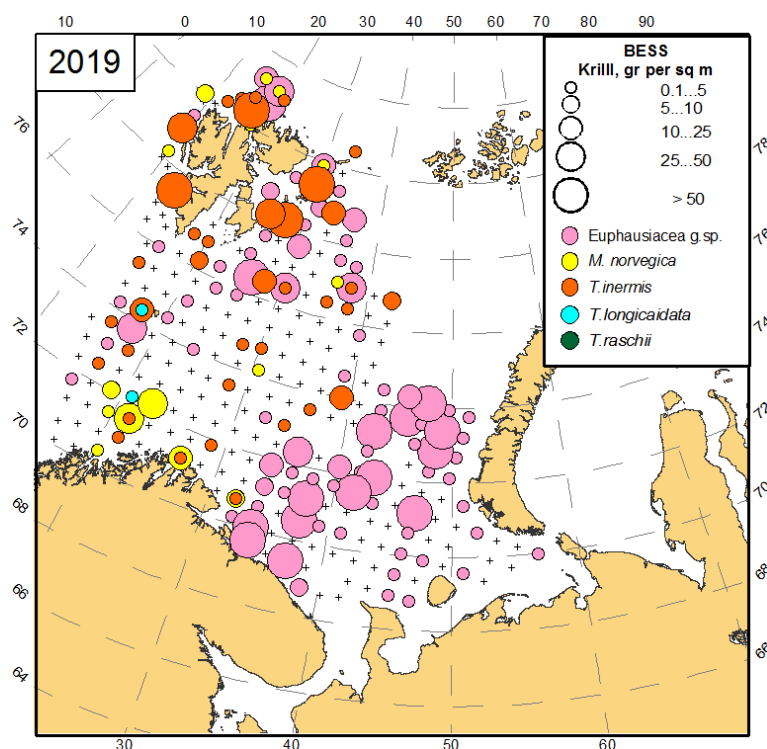


Figure 3.3.2.4. Krill species distribution (biomass, g wet-weight m^{-2}), based on trawl stations covering the upper water layers (0-60 m), in the Barents Sea in August-October 2019.

During the survey, length measurements of krill onboard the Norwegian vessels were made. Length distribution of two common species (*M. norvegica* and *T. inermis*) is shown in Figure 3.3.2.5. The length of *M. norvegica* varied from 10 to 46 mm (with an average of 30.1 mm), and *T. inermis* from 13 to 33 mm (with an average of 22 mm).

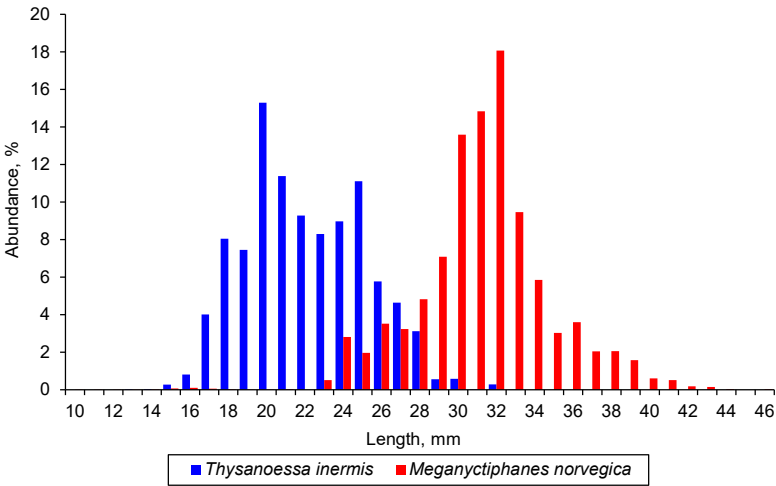


Figure 3.3.2.5 Length distribution of *T. inermis* and *M. norvegica* from catches with standard pelagic trawl in the upper layers (0-60 m) of the Barents Sea in August-October 2019.

In 2019, the total biomass of krill was estimated as 22.3 million tonnes for the whole Barents Sea. It is the highest biomass since 2011, and much higher than long-term mean of 9.3 million tonnes (Fig. 3.3.2.6).

Table 3.3.2.1 Day and night total catches (g m⁻²) of krill taken by the pelagic trawl in the upper water layers (0-60 m).

Year	Day			Night		
	N	Mean g m ⁻²	Std Dev	N	Mean g m ⁻²	Std Dev
1980	237	1.49	11.38	90	4.86	23.96
1981	214	1.19	9.14	83	7.95	21.53
1982	192	0.18	1.19	69	6.29	22.57
1983	203	0.32	2.76	76	0.39	1.91
1984	217	0.15	1.64	66	1.72	9.17
1985	217	0.07	0.54	75	0.80	4.42
1986	229	3.03	11.70	76	11.90	37.82
1987	200	4.90	22.44	88	3.82	13.08
1988	207	2.69	30.16	81	11.84	55.84
1989	296	1.99	8.45	129	3.71	13.01
1990	283	0.11	0.76	115	1.18	6.32
1991	284	0.03	0.33	124	7.03	25.11
1992	229	0.11	1.18	77	0.92	2.92
1993	194	1.21	6.69	79	2.23	7.36
1994	175	3.01	10.23	72	7.27	18.78
1995	166	4.86	18.86	80	9.13	34.46
1996	282	4.34	26.62	118	9.32	21.53
1997	102	4.12	22.71	167	3.58	12.94
1998	176	2.24	16.00	185	5.68	23.95
1999	140	1.50	9.64	90	4.64	13.09
2000	202	1.52	9.53	67	3.54	11.49
2001	212	0.07	0.63	66	5.77	19.60

2003	203	1.26	9.54	74	2.84	11.23
2004	229	0.34	2.94	80	6.49	22.47
2005	314	3.50	30.53	86	9.02	24.78
2006	227	1.23	6.66	103	9.66	31.54
2007	192	1.79	10.93	112	9.04	39.29
2008	199	0.11	1.02	77	16.92	43.57
2009	241	0.42	2.56	131	10.29	25.02
2010	198	1.76	13.00	105	14.98	43.35
2011	212	0.13	0.69	95	19.46	77.70
2012	243	4.00	12.35	84	11.48	34.21
2013	222	0.11	0.88	83	13.23	42.16
2014	196	4.16	27.85	98	4.85	27.36
2015	199	9.70	54.43	97	14.22	44.61
2016	122	16.56	54.81	78	13.48	19.66
2017	146	0.57	2.60	85	15.35	42.54
2019*	179	8.20	35.04	97	18.51	43.17
1980-2019	210	2.45		94	7.98	

* – 2018 is not included due to the poor coverage

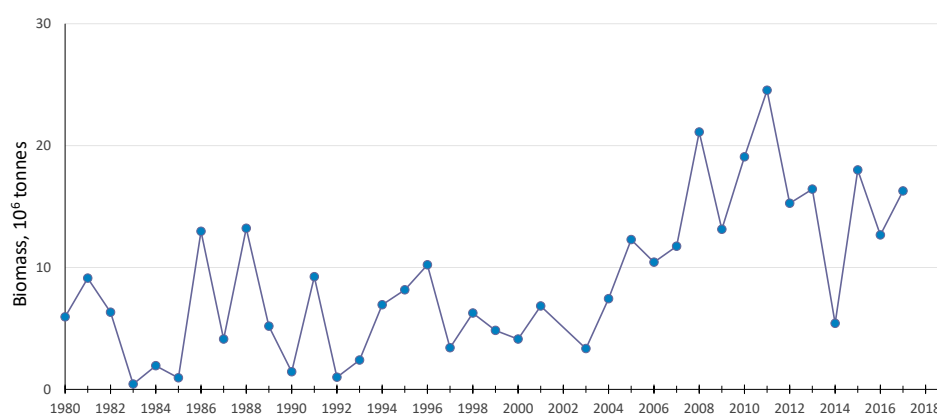


Figure 3.3.2.6. Krill biomass (wet-weight, million tonnes) estimated for upper layers of the whole Barents Sea during 1980-2019, based on night catches with standard pelagic «Harstad» trawls covering the upper water layers (0-60 m)

Amphipods (mainly hyperiids)

By Tatyana Prokhorova, Elena Eriksen and Irina Prokopchuk

Figures by Pavel Krivosheya, Tatyana Prokhorova and Irina Prokopchuk

The data here reported on pelagic amphipods represent bycatches from trawling on the 0-group fish, using the standard pelagic «Harstad» trawl in the 60-0 m layer in autumn. During 2012 and 2013, amphipods were absent from pelagic trawl catches, while in 2014 some limited catches were taken north of Svalbard/Spitsbergen. Several large catches were made east and north of Svalbard/Spitsbergen during 2015-2017. In 2018, amphipods were caught east of the Svalbard/Spitsbergen Archipelago. In 2019, amphipods were found mainly in the northern part of surveyed area (Figure 3.3.2.7). The largest catches were dominated by Arctic *Themisto libellula*, and made north and east of Svalbard/Spitsbergen (Figures 3.3.2.7 and 3.3.2.8).

In 2019, the mean day-time catches were higher than the night-time catches (1.1 g m⁻² and 0.8 g m⁻², respectively), and the same was the case for the maximum catches (39.8

g m⁻² during day and 17.0 g m⁻² during night). This year, the estimated amphipod biomass for the upper 60 m of the whole Barents Sea was high (1.23 million tonnes), and about twice as high as in 2015-2016 (close to 570 thousand tonnes) and more than 20 times higher than in 2017. The higher biomasses in 2019 were most likely related to lower temperatures in the northern area, which was covered by Arctic water masses (close to 0°C and below).

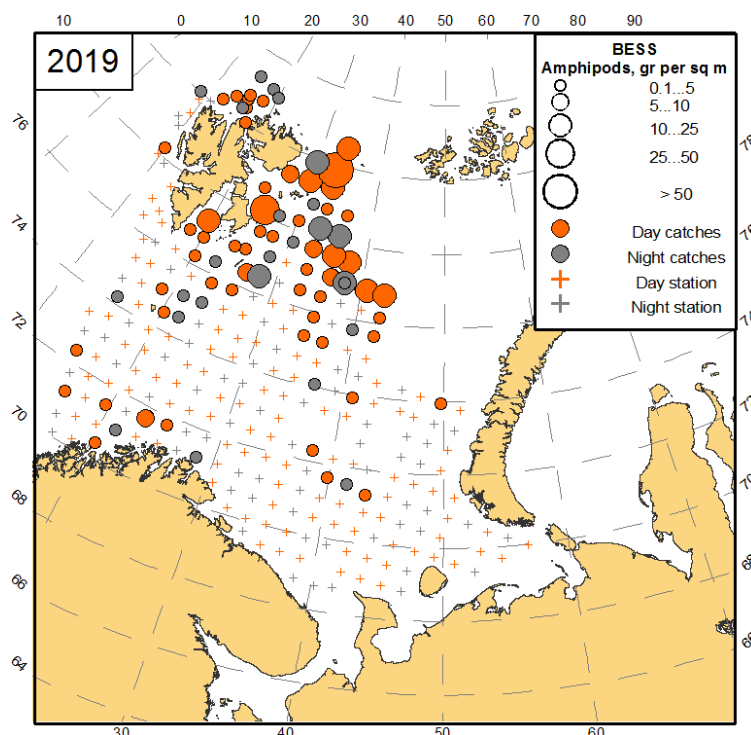


Figure 3.3.2.7 Amphipods distribution (biomass, g wet-weight m⁻²), based on standard pelagic «Harstad» trawls covering the upper layers (0-60 m) of the Barents Sea in August-October 2019.

T. libellula dominated in the catches, while only two catches of *Themisto abyssorum* were taken during the survey. In addition, to *Themisto* sp., low catches of *Hyperia galba*, which associates with jellyfish, were found in the northern part of the central area, where jellyfish were abundant.

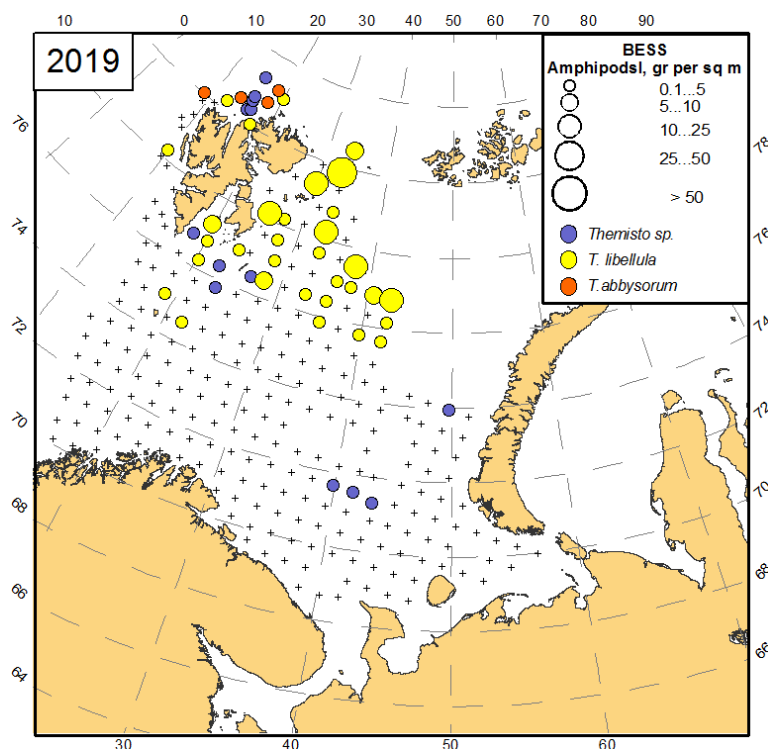


Figure 3.3.2.8. Distribution of amphipods of genus *Themisto* (biomass, g wet-weight m^{-2}), based on standard pelagic «Harstad» trawls covering the upper layers (0-60 m) of the Barents Sea in August-October 2019.

The length of the most common and abundant *T. libellula* varied from 11.0 to 39.0 mm with an average length of 20.0 mm (Figure 3.3.2.9).

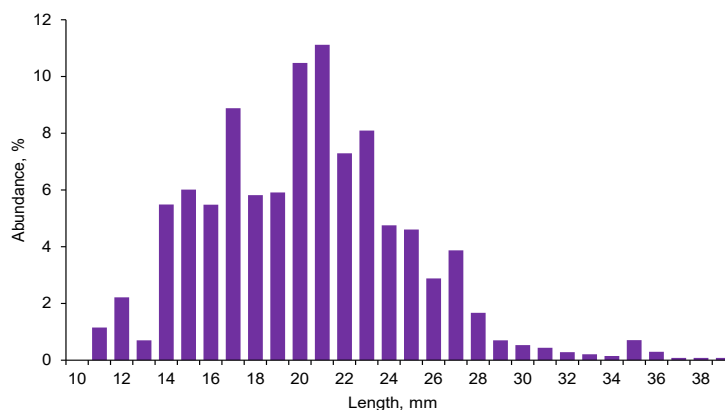


Figure 3.3.2.9 Length distribution of *T. libellula* from catches with standard pelagic trawl in the upper layers (0-60 m) of the Barents Sea in August-October 2019.

Jellyfish

By Elena Eriksen

The estimated biomass of gelatinous zooplankton here presented represents bycatches from trawling on the 0-group fish, using the standard pelagic «Harstad» trawl in the 60-0 m layer in autumn during BESS. The biomass of gelatinous zooplankton for the entire Barents Sea was not estimated for 2018 due to an incomplete spatial coverage that year and has not yet been possible for 2019 for logistical reasons. Therefore, we here only

present the time series on estimated biomass for the Barents Sea as a whole for the years 1980-2017 (Fig. 3.3.2.10).

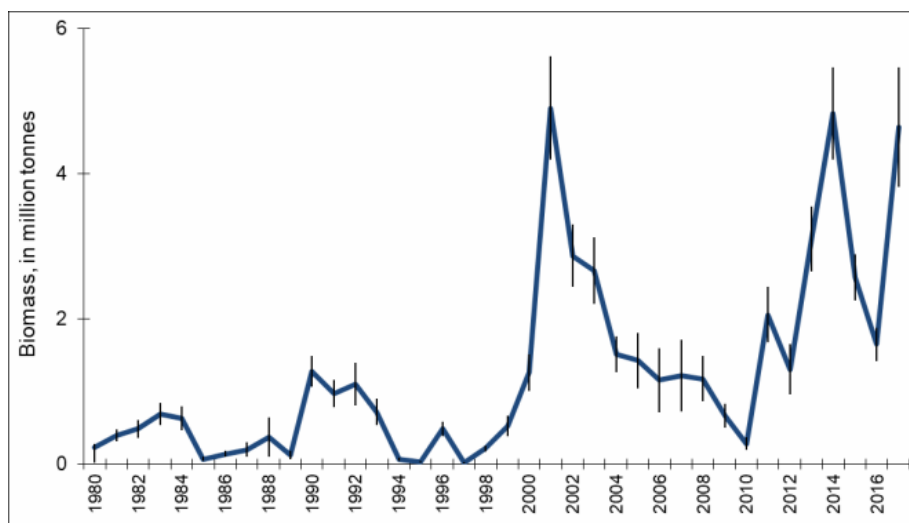


Figure 3.3.2.10. Estimated total biomass of the jellyfish, mainly constituting *Cyanea capillata*, in the BESS sampling area during August-October for the 1980-2017 period. Based on catches by Harstad trawl in the upper 0-60 m layer - 95% confidence interval indicated by grey lines.

3.4 Benthos and shellfish

3.4.1 Benthos

By N.A. Strelkova (PINRO), L.L. Jorgensen (IMR)

Benthos is an essential component of the marine ecosystems. It can be stable in time, characterizing the local situation, and is useful to explain ecosystem dynamics in retrospect. It is also dynamic and shows pulses of new species distribution, such as the snow crab and the king crab, and changes in migrating benthic species (predatory and scavenger species such as sea stars, amphipods and snails with or without sea anemones). The changes in community structure and composition reflect natural and anthropogenic factors. There are more than 3000 species of benthic invertebrates registered in the Barents Sea (Sirenko, 2001), but here we only present the megafaunal component of the benthos collected by trawl and registered (species, abundance and biomass) during the Barents Sea Ecosystem Survey (BESS). This includes mainly large bodied animals with long lifespans. This investigation was first initiated in 2005 resulting in a short timeline compared to investigations related to plankton and fish. Accordingly, interpretation of long-term trends for megabenthic data must be pursued with caution.

Benthos collection. Benthos, collected with the standard demersal trawl gear during the BESS, have been registered annually by benthic taxonomic specialists since 2005 onboard Russian vessels; annual surveys have been conducted during 2007–2013 and 2015–2016 onboard Norwegian vessels. Species identification has been to the lowest possible taxonomic level. In cases where there were no specialist available onboard (2007–2008 in northern Barents Sea in the Norwegian sector), the benthos were identified to major benthic group. Work is ongoing between IMR and PINRO specialists to

standardize and improve species identification, as well as the catchability of benthos between different trawls and vessels. Several articles have been published based on the resulting megabenthic data (Anisimova et al., 2011; Ljubin et al., 2011; Jørgensen et al., 2015; Jørgensen et al., 2016; Zimina et al., 2015; Degen et al., 2016; Johannesen et al., 2016; Lacharité et al., 2016; Jørgensen, 2017; Jørgensen et al., 2017; Jørgensen et al., 2019).

Megafauna description. The distribution of large benthos groups shows that Porifera (mainly species within the Geodiidae) dominate the biomass in the west, while Echinodermata (mainly brittle stars) dominate in the central and northern part of the sea. In the Northeast, Cnidaria (where the biomass is mainly made up by species such as the sea pen *Umbellula encrinus*) dominates together with Echinodermata, while Crustacea dominates together with the Echinodermata in the Southeast (Figure 3.4.1.1).

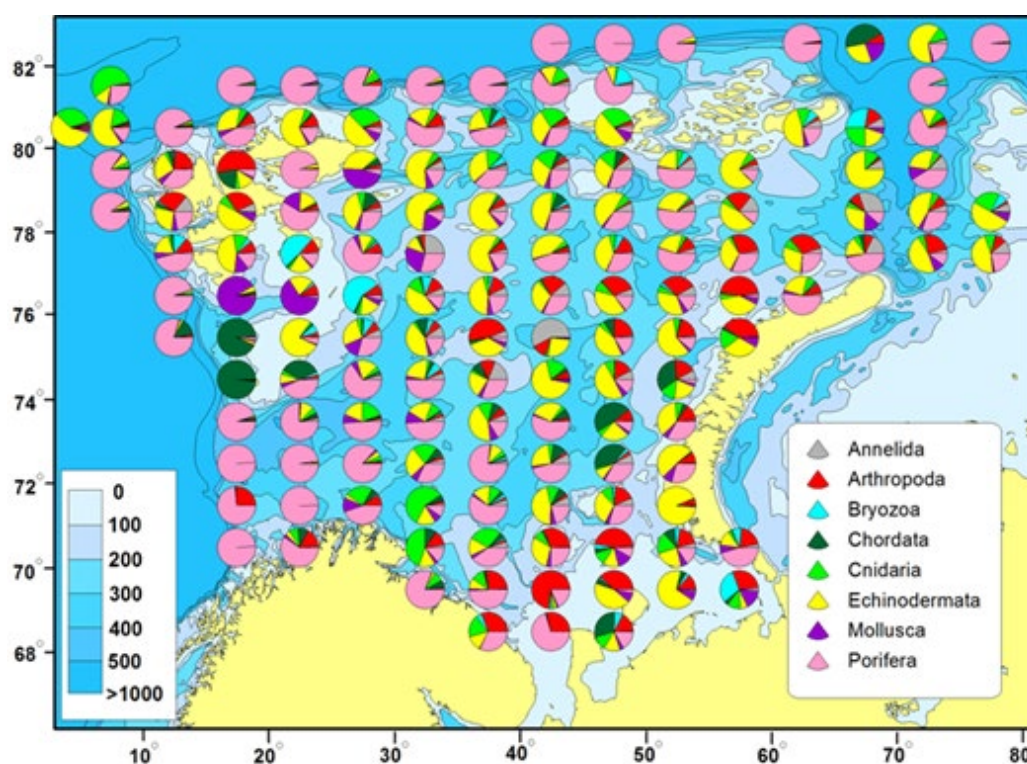


Figure 3.4.1.1 The biomass distribution of the main benthic groups per area integrated as the mean for the period 2012-2017.

Statistical analyses of monitoring data show that there are four distinct zones of benthos in the Barents Sea (Jørgensen *et al.*, 2015, fig. 3.4.1.2). These four zones are characterized with temperate species in the southwestern zone, cold-water species in the eastern zone, arctic species in the northern and north-eastern zone, and an area in the eastern Barents Sea where the snow crab, a new non-indigenous large benthic species, are expanding. The period with warmer water entering the Barents Sea has led to migration eastwards and northwards of temperate species and groups (Jørgensen *et al.*, 2015). The retreating ice front opens for new areas for human impact as well as imposing changes in the planktonic production and annual cycles, with possible impact on the benthic zones.

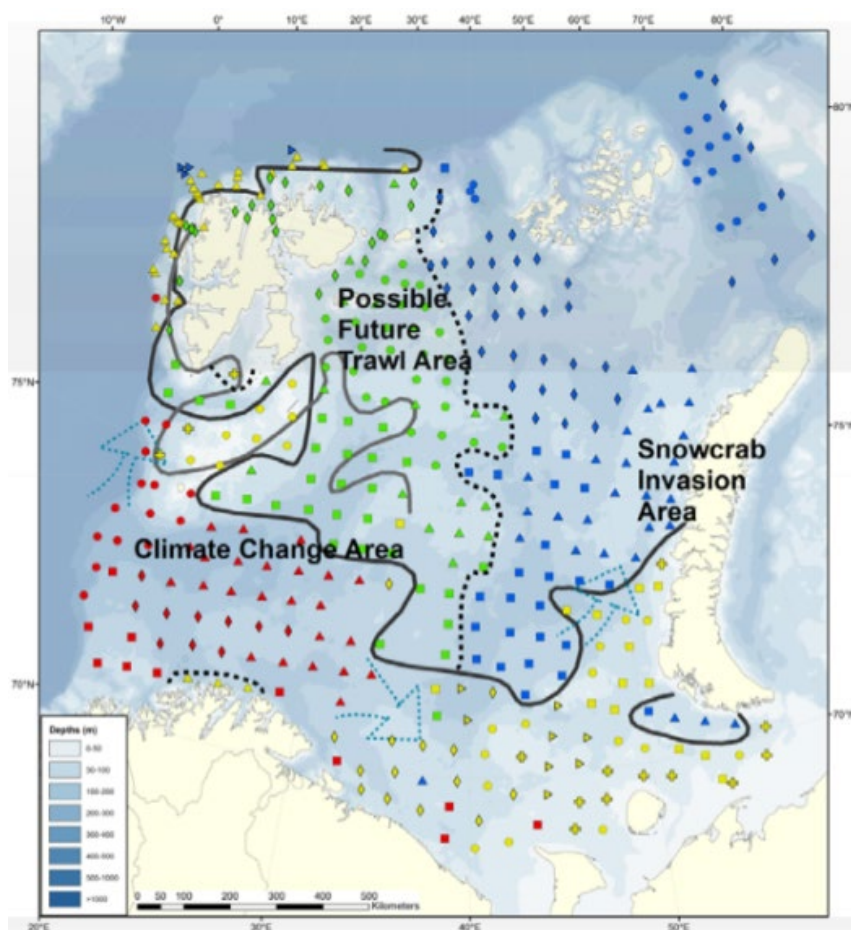


Figure 3.4.1.2 The baseline map of the Barents Sea mega-benthic zones in 2011, based on fauna similarity (see Jørgensen *et al.*, 2015 for methodology, results and discussion) with the northern (green and blue) and southern (yellow and red) region where the black full line is illustrating the “benthic polar front” in 2011. The grey full line is the approximately oceanographic Polar Front. Dotted line: Is partly illustrating a west-east division. Red: South West subregion (SW) Yellow: Southeast, banks and Svalbard coast (SEW). Green: North West and Svalbard fjords (NW). Blue: North East (NE). Source: IMR.

Jørgensen *et al.* (2019) show a recent increase in community mean temperature ranks ($P=0.0011$), indicating an increased importance of species with affinity for warmer waters and a reduced importance of cold-water species. Commercial fish stocks expands northward (Fossheim *et al.*, 2015) while and the snow crab expands toward the western part of the Barents Sea, thereby simultaneously increasing the exposure of both large immobile species to trawling and of small prey species to crab predation. Overall, we have found a high-level of vulnerability toward temperature increase, bottom trawling and snow-crab predation in the northwestern Barents Sea, because this might lead to alterations in community structure and diversity.

The status of megabenthos in 2019

The area covered in 2019 are given in figure 3.4.1.3. Ten Russian and Norwegian experts were involved in the megabenthos by-catch processing across the four BESS vessels. The main results are given in table 3.4.1.1 while the megabenthos distribution are given in figure 3.4.1.3

Table 3.4.1.1. The main characteristics of the megabenthic by-catches during BESS 2018 and 2019

Characteristics Year	Values	
	2018	2019
Number of stations	217	305
Total number of taxa / species	574 / 404	621/427
Number of taxa per station; min-max / average ± standard error	5-95 / 39.0±1.1	1-100 / 36.57±1.06
Number of individual per station; min-max / average ± standard error	11-50221 / 3966±485	5-78760 / 3310±380
Biomass per station (kg); min-max / average ± standard error	0.055-6897 / 91.08±36.40	0.184-1938 / 44.20±7.82

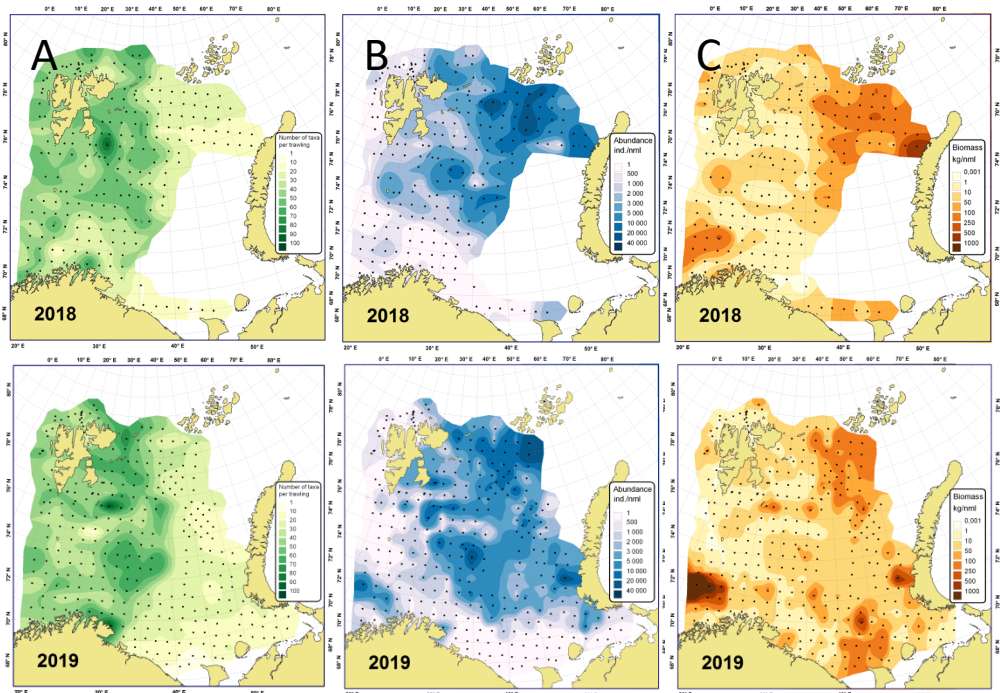


Figure 3.4.1.3. The A) number of taxa, B) number of individuals and, C) biomass per nautical mile (nml) according to BESS 2018 and 2019

The results of 2019 showed a high number of taxa (fig. 3.4.1.3 A) in the western part of the sea (Norwegian area of the survey) and low number in the east (Russian area of the survey). This might include a low level of taxonomical processing of the by-catches in the Russian vessel “Vilnus” due to the lack of benthic experts onboard. The general distribution of abundance and biomass are resemble the distribution in 2018. The abundance (fig. 3.4.1.3 B) showed high numbers of individuals in the northeast and middle part of the sea, including coastal waters of the Novaya Zemlya archipelago. But in the south and along the slope in the west the abundance was low. The biomass (fig. 3.4.1.3 C) were high in the northeast, in the southeast (near Novaya Zemlya coast, Kanin peninsula and in North-Kanin Bank), and particularly in the southwest.

Long-term trends in distribution of the megabenthic biomass.

Spatial distribution. The monitoring time-series of the megabenthos biomass distribution shows relative stable large-scale patterns, with high biomass particularly in the southwest; biomass is also stable in the northeast, but more variable. In the

central Barents Sea, biomass has a high level of spatial and temporal variability which is difficult to characterize due to the relatively short data time-series (Fig. 3.4.1.4).

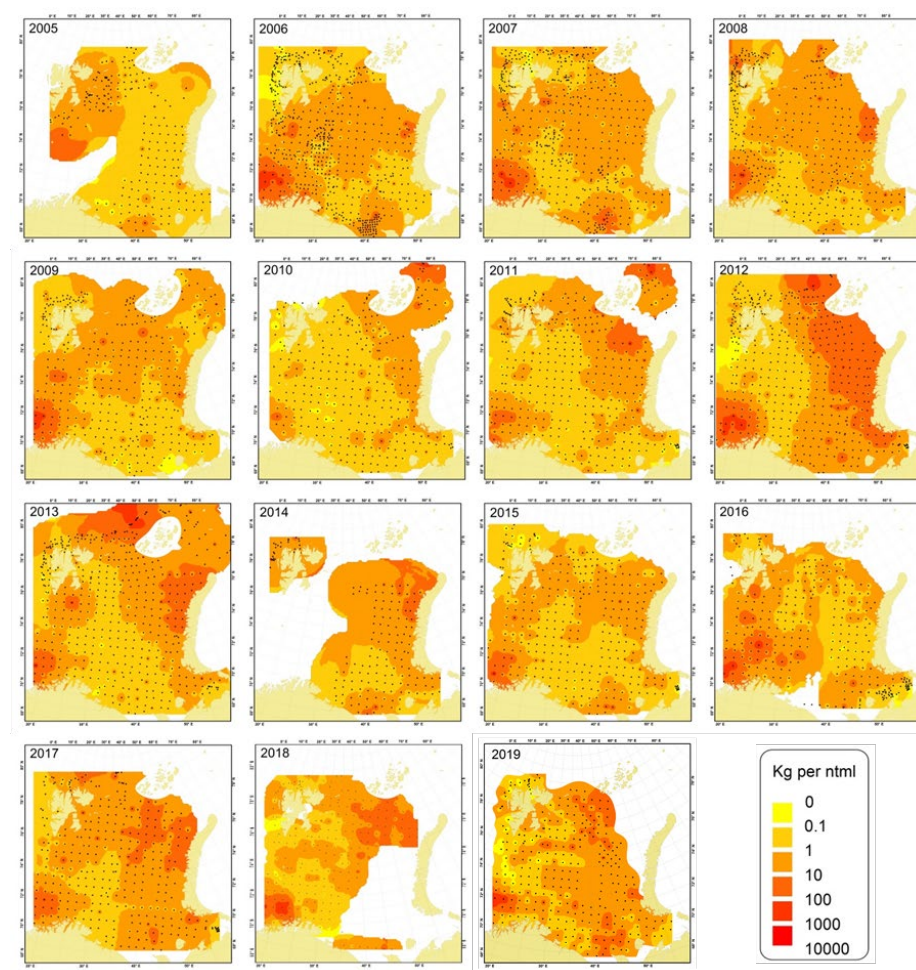


Figure 3.4.1.4 Distribution of the megabenthos biomass (excluding *Pandalus borealis*) in the Barents Sea from 2005 to 2019.

Figure 3.4.1.4. also illustrates the deficiency and fault in the megabenthos assessment for several years. In 2005, 2014 and 2018 there were a lack of station coverage in the Norwegian or Russian areas. In 2019, the north-eastern part of the sea was incompletely covered. In 2014, 2015, 2016 and 2019 the Loop-hole area was not sampled because a commercial snow crab fishery. In 2012 and probably 2017 the biomass was overestimated in the Russian zone due to technical issues with the trawl tuning. Such lack of coverage and non-standardised processing should be taken into account when analyzing the megabenthic time series.

Inter-annual fluctuation of the mean megabenthos biomass.

To estimate long-term dynamics of the megabenthos, inter-annual changes of the mean biomass were calculated for the total Barents Sea and separated for the four sectors – northeast, northwest, southeast and southwest part of the sea (Fig. 3.4.1.5 A, B, ICES, 2018, 2019).

In 2018, the eastern part of the Barents Sea was only partly covered (Fig. 3.4.1.4). This made it impossible to estimate the annual biomass-trend for the “total Barents Sea” (Fig. 3.4.1.5 A) and for the “eastern part” of the Barents Sea (Fig. 3.4.1.5 D). But the data from the western part of the sea shows moderate increase of the megabenthic biomass in 2019 comparing to 2018 (Fig. 3.4.1.5.C).

The fourteen years of monitoring shown a moderate linear positive trend of increasing megabenthic biomass for the “Total Barents Sea” (Fig. 3.4.1.5 B). At the same time, interannual biomass fluctuations show positive correlation ($r = 0.59$ for “total”) with the water temperature on the Kola Sections (0-200 m layer, st. 3-7, Fig. 3.4.1.5 A) with a time lag of 7 years (except NW) (Table 3.4.1.2).

Table 3.4.1.2. Correlation (r) between water temperature on the Kola Section (average annual water temperature in the layer 0-200 m in the st. 3-7) and mean biomass for the Barents Sea within 68-80° N and 15-62° E (Total) and its four sectors (NW – 74-80° N, 15-40° E; NE – 74-80° N, 40-62° E; SW – 68-74° N, 15-40° E; SE – 68-74° N, 40-62° E) when shifting back temperature time-series from 1 to 10 years

Shift backward, year	Total	NW	NE	SW	SE
0	0,152	0,319	-0,142	0,350	0,024
1	0,699	0,180	0,684	0,574	0,359
2	0,453	0,351	0,315	0,157	0,477
3	-0,031	0,089	-0,140	-0,134	0,067
4	0,025	0,008	0,099	-0,003	0,003
5	0,390	0,039	0,390	0,238	0,147
6	-0,105	-0,472	0,030	-0,029	0,141
7	0,587	-0,112	0,580	0,461	0,507
8	-0,006	-0,092	0,204	-0,124	-0,229
9	0,023	-0,014	0,125	0,005	-0,088
10	0,149	0,157	0,098	0,215	0,103

Similar response to change of environmental conditions was documented for the Barents Sea macrobenthos, but with a delay in approximately four years (Lubina et al., 2012, 2016; Denisenko, 2013). Difference in duration of the time-lag between macro- (grab's) and mega- (trawl's) benthos is caused by different mean size and longevity of the lifespan of these size groups of benthic organisms.

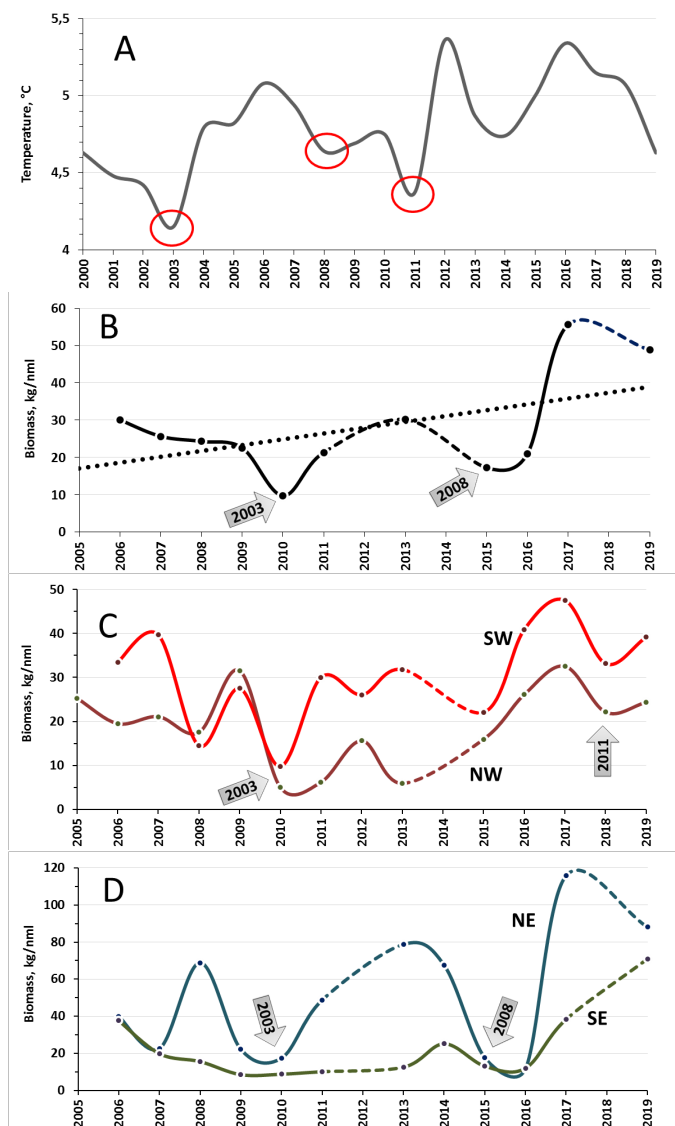


Figure 3.4.1.5 Variations of the average annual temperature in the water layer 0-200 m in the 3-7 stations of the Kola Section (A) (<http://www.pinro.ru>) and the inter-annual fluctuation of the mean megabenthos biomass in total Barents Sea (B) and in its western (C) and eastern (D) sections. "Total" – Barents Sea within 68-80° N, 15-62° E, "NE" – north-eastern sector (74-80° N, 40-62° E), "NW" – north-western sector (74-80° N, 15-40° E), "SE" – south-eastern sector (68-74° N, 40-62° E), "SW" – south-western sector (68-74° N, 15-40° E). Biomass of *Pandalus borealis* and all catches more than 1t are excluded. Red circles in the plot A show cold years which could cause decrease of the biomass in 2010, 2015 and probably in 2018 (are shown by grey arrows). The dotted line in the plot B is linear trend

References

- Anisimova N.A., Iørgensen L.L., Liubin P., Manushin I. 2011. Benthos. In "The Barents Sea Ecosystem Resources and Management. Half a century of Russian-Norwegian Cooperation". Ed by T. Jakobsen, V. Ozhigin. Tapir Academic Press, Trondheim Norway. Pp 121-159.
- Degen R., Iørgensen L., Liubin P., Ellingsen I., Pehlke H., Brev T (2016). Patterns and drivers of megabenthic secondary production on the Barents Sea shelf, Marine Ecology Progress Series, 546: 1-16. doi: 10.3354/meps11662
- Denisenko S.G. 2013. Biodiversity and bioresources of macrozoobenthos in the Barents Sea. Structure and long-term changes. Saint Petersburg: Nauka. 284 pp. (In Russian).
- Fossheim, M., Primicerio, R., Johannesen, E., Ingvaldsen, R. B., Aschan, M. M., & Dolgov, A. V. (2015). Recent warming leads to a rapid borealization of fish communities in the Arctic. *Nature Climate Change*, 5(7), 673-677.

- Impact of trawl fishery on benthic ecosystems of the Barents Sea and opportunities to reduce negative consequences. Ed. by S.G.Denisenko & K.A.Zgurovsky. Murmansk, WWF, 2013. 55 pp.
- ICES 2018. Interim Report of the Working Group on the Integrated Assessments of the Barents Sea (WGIBAR). WGIBAR 2018 REPORT 9-12 March 2018. Tromsø, Norway. ICES CM 2018/IEASG:04/ 210 pp. <http://ices.dk/sites/pub/Publication%20Reports/Expert%20Group%20Report/IEASG/2018/WGIBAR/WGIBAR%202018.pdf> (дата обращения 06.11.2019).
- ICES 2019. The Working Group on the Integrated Assessments of the Barents Sea (WGIBAR). ICES Scientific Reports, volume 1, issue 42, 157 pp. <http://doi.org/10.17895/ices.pub.5536> (дата обращения 06.11.2019).
- Iohannesen E., Iørgensen L.L., Fossheim M., Primicerio R., Greenacre M., Liubin P.A., Dolgov A.V., Ingvaldsen R.B., Anisimova N.A., Manushin, I.E. 2016. Consistent large-scale patterns in community structure of benthos and fish in the Barents Sea. Polar Biology DOI 10.1007/s00300-016-1946-6.
- Iørgensen L.L., Liubin P., Skioldal H.R., Ingvaldsen R.B., Anisimova N., Manushin I. (2015). Distribution of benthic megafauna in the Barents Sea: baseline for an ecosystem approach to management. ICES Journal of Marine Science: 72 (2): 595-613
- Iørgensen L.L., Planque B., Thangstad T.H., Certain G 2016. Vulnerability of megabenthic species to trawling in the Barents Sea. ICES Journal of Marine Science, 73: i84-i97. DOI: 10.1093/icesjms/fsv107.
- Iørgensen (2017) Trawl and temperature pressure on Barents benthos. FEATURE ARTICLE – ICES, 11 July 2017.
- Iørgensen, L.L., Archambault P., Blicher M., Denisenko N., Guðmundsson G., Iken K., Rov V., Sørensen J., Anisimova N., Behe C., Bluhm B.A., Denisenko S., Denisenko N., Metcalf V., Olafsdóttir S., Schiøtte T., Tendal O., Ravelo A.M., Kedra M., Piepenburg D. (2017) "Benthos" In: CAFF. State of the Arctic Marine Biodiversity Report. Conservation of Arctic Flora and Fauna, Akurevri Iceland.
- Iørgensen L.L., Primicerio R., Ingvaldsen R.B., Fossheim M., Strelkova N.A., Thangstad T.H., Zakharov D.V. (2019). Impact of multiple stressors on sea bed fauna in a warming Arctic. Marine Ecology Progress Series, 608: 1-12.
- Lacharité M., Iørgensen L.L., Metaxas A., Lien V.S., Skioldal H.R. 2016. Delimiting oceanographic provinces to determine drivers of spatial mesoscale patterns in offshore shelf benthic megafauna: a case study in the Barents Sea. Progress in Oceanography 146: 187-198
- Lyubin P.A., Anisimova N.A., Iørgensen L.L., Manushin I.E., Prokhorova T.A., Zakharov D.V., Zhuravleva N.E., Golikov A.V., Morov A.R. 2010. Megabenthos of the Barents Sea. Nature of the shelf and the European Arctic. Complex investigation of the Svalbard archipelago nature. Issue 10. Proceedings of the International scientific conference (Murmansk, 27-30 October 2010). Moscow: GEOS, 2010, pp. 192-200. (in Russian).
- Lyubin, P. A., Anisimova, A. A., and Manushin, I. E. 2011. Long-term effects on benthos of the use of bottom fishing gears. In: The Barents Sea: Ecosystem, Resources and Management: Half a Century of Russian-Norwegian Cooperation, Ed. By T. Jakobsen, and V. K. Ozhigin. Fagbokforlaget, Bergen, Norway. pp. 768-775.
- Lyubina O.S., Frolova E.A., Dikaeva D.R. (2012). Current zoobenthos monitoring at the Kola Transect in the Barents Sea. Berichte zur Polarforschung, 640: 177-189.
- Lyubina O.S., Strelkova (Anisimova) N.A., Lyubin P.A., Frolova E.A., Dikaeva D.R., Zimina O.L., Akhmetchina O.Yu., Manushin I.E., Nekhaev I.O., Frolov A.A., Zakharov D.V., Garbul E.A., Vvaznikova V.S. 2016. Modern quantitative distribution of zoobenthos along the transect Kola Section / Transactions of the Kola Science Centre. Series 3 Oceanology. 2/2016 (36): 64-91 (In Russian).
- Sirenko B.I. 2001. Introduction. In List of species of free-living invertebrates of Eurasian Arctic Seas and adjacent waters. Ed by Sirenko B.I. Explorations of the fauna of the seas, 51(59). St.-Petersburg: 3-8.
- Zimina O.L., Lyubin P.A., Iørgensen L.L., Zakharov D.V., Lyubina O.S. 2015. Decapod Crustaceans of the Barents Sea and adjacent waters: species composition and peculiarities of distribution. Arthropoda Selecta 24(3): 417-428 (In Russian).

3.4.2 State of selected benthic species

By D.V. Zakharov (PINRO) and Ann Merethe Hjelset (IMR)

Snow crab

The snow crab (*Chionoecetes opilio*) is a non-indigenous species in the Barents Sea and was first recorded in 1996 on the Goose Bank area (Strelkova, 2016). It is not known whether it is introduced by accident or if it has expanded its distribution area. Preliminary results show that the latter is the most probable explanation. The establishing of the snow crab in the Barents Sea is believed to have occurred during 1993–1996.

Regular annual monitoring of the snow crab population began with BESS in 2004. This survey is, currently, the most important source of information on snow crab population status.

Assessments of snow crab dynamics based on BESS data (Table 3.4.2.1 and Figures 3.4.2.1 and 3.4.2.2) indicate that in the Barents Sea the snow crab population is still developing (spreading, population increase).

Table 3.4.2.1 Characteristics of the snow crab catches during BESS 2005-2018

Year	Total number of station	Number of station with snow crab	Total numbers, ind.	Total biomass, kg	Mean abundance, ind./nm	Mean biomass, kg/nm
2005	649	10	14	2.5	1	0.3
2006	550	28	68	11	3	0.5
2007	608	55	133	18	3	0.4
2008	452	76	668	69	11	1.2
2009	387	61	276	36	6	0.8
2010	331	56	437	22	10	0.5
2011	401	78	6 219	154	99	2.4
2012	455	116	37 072	1 169	395	12.6
2013	493	131	20 357	1 205	210	12.7
2014	304	78	12 871	658	206	10.5
2015	335	89	4 245	378	57	5.2
2016	317	84	2 156	137	26	1.9
2017	376	159	25 878	1422	147	10.0
2018	217	61	19 494	846	393	16.7

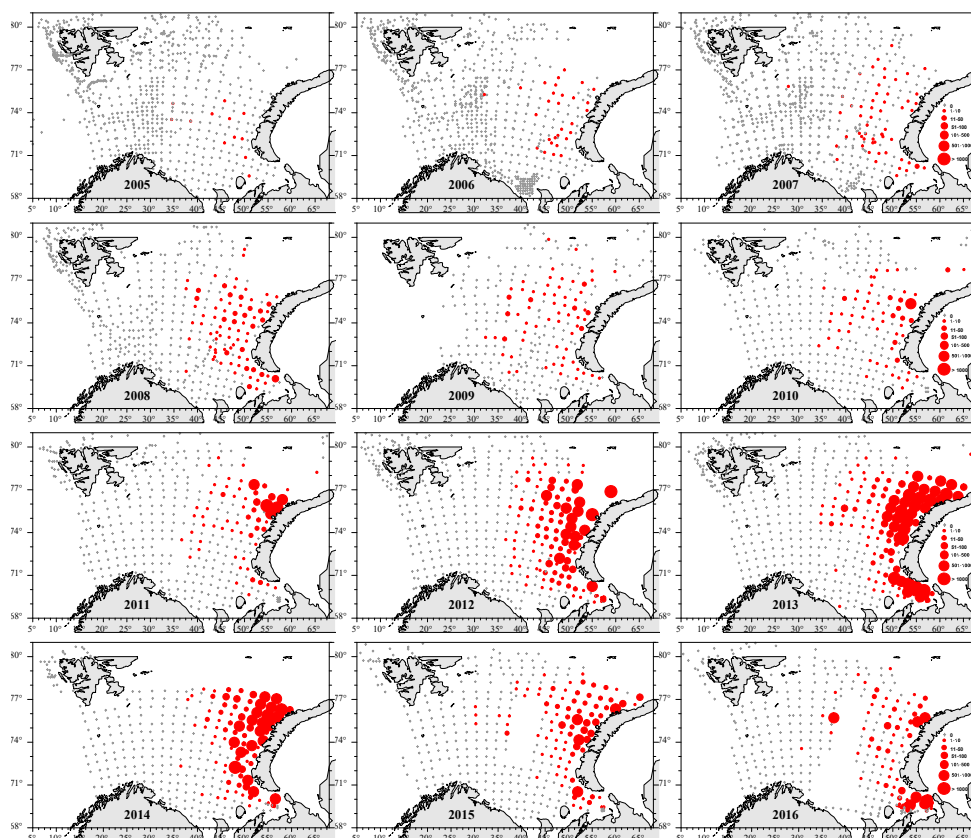


Figure 3.4.2.1. The temporal distribution of the snow crab population in the Barents Sea (number of individuals/nm) according to BESS 2005-2016

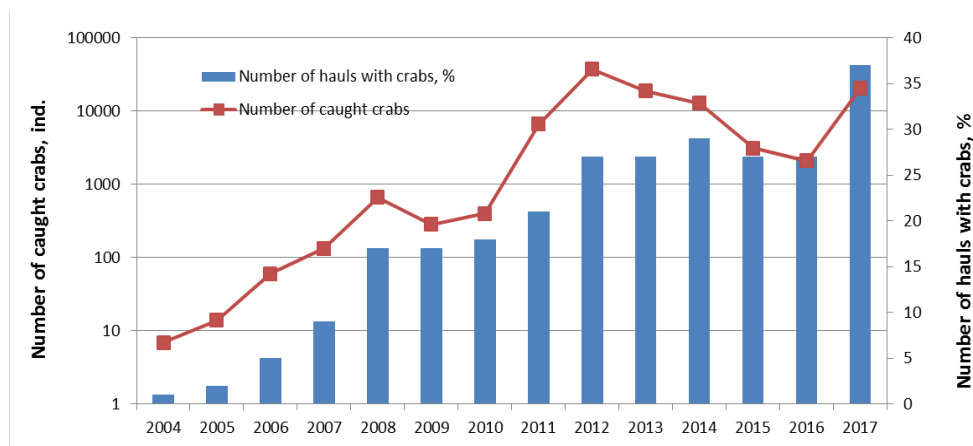


Figure 3.4.2.2. The dynamic of the snow crab population in the Barents Sea given as the total number of crabs (blue bars) and the number of trawl hauls with crabs (red line) during the BESS 2004–2017.

In 2018, as in previous years, the densest aggregations of snow crabs (more than 1000 ind/nml) were concentrated in the central part of the Barents Sea in the Loophole area and near Novaya Zemlya archipelago within the Russian Economic Zone. In 2017, the snow crab was for the first time recorded at Svalbard. One record was made in Storfjorden at 162 m depth (two immature males with 47 mm and 48 mm carapace widths); the other was northwest of Svalbard archipelago at 506 m depth (juvenile male 14 mm carapace width) (fig. 3.4.2.3).

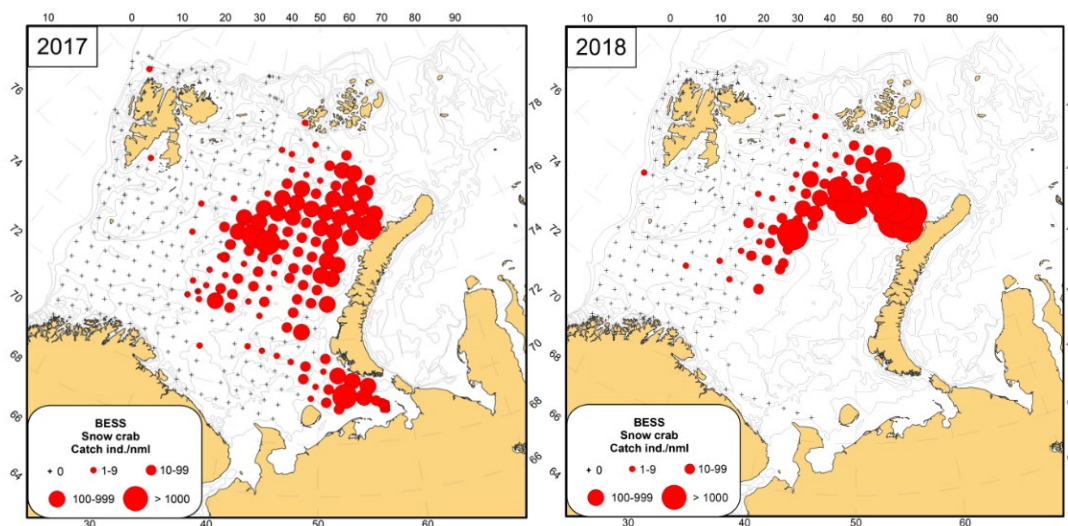


Figure 3.4.2.3 Distribution of the snow crab (*Chionoecetes opilio*) in the Barents Sea in August-October 2017-2018 (BESS data)

Studies of snow crab population size structure indicate that abundant generations appear periodically, and that this affects the overall population dynamics in the Barents Sea. During the ecosystem survey period, abundant generations were recorded with 3 years' interval - in 2009, 2012, and 2015–2016 (fig. 3.4.2.4, Bakanev & Pavlov 2016).

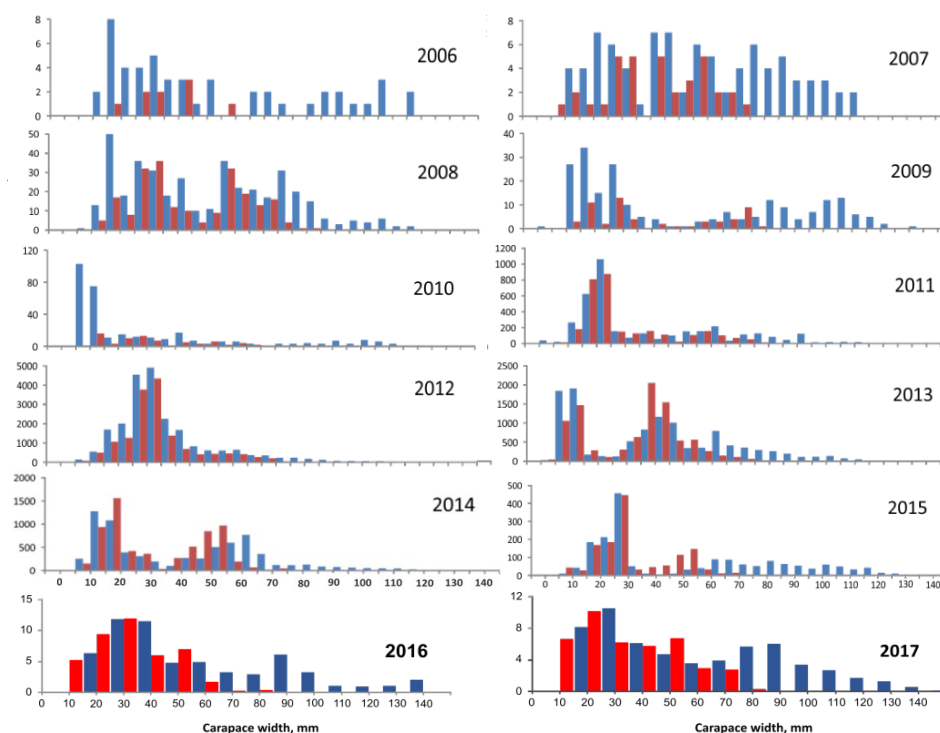


Figure 3.4.2.4 The sex and size structure of the snow crab population from 2006–2017 (Bakanev & Pavlov 2016, with editions). On vertical axes: 2006–2015 – number of individuals; 2016–2017 – abundance, %.

Compared with previous year, the mean abundance of snow crab, standardized to nautical mile, has increased 2.7 times while biomass 1.2 times only. It can be results of

preferential increasing of juvenile part of population that is agreeing with size structure of the crab catches in 2018 (Fig. 3.4.2.5).

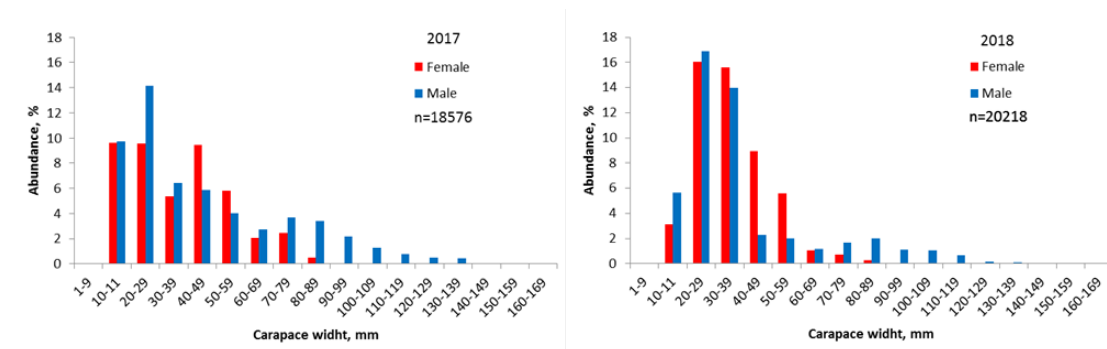


Figure 3.4.2.5. Size structure of the snow crab population in the Barents Sea in 2017 and in the north part of the sea in 2018

Since 2003, snow crabs in the eastern part of the Barents Sea, have been recorded in stomachs of bottom fish species (cod, haddock, catfish, American dub, and starry ray).

In recent years, snow crabs have become one of the most important prey species for cod. In 2011–2012 it made up about 2% of the cod stomachs examined, in 2013–2014 it made up 4–7%, and in 2015–2016 it made up 5–6%. All size categories of snow crab (up to 120 mm carapace width) are eaten by cod. Cod feeding on snow crabs was most intensive (up to a quarter of total stomach content) during autumn at Novaya Zemlya, Great Bank, Central Banks.

Northern shrimp

Northern shrimp (*Pandalus borealis*) is common and widely distributed in the Barents Sea above the deep (250-350 m) muddy flats of the Barents Sea and in temperatures between 1 - 2°C (Fig. 3.4.2.6).

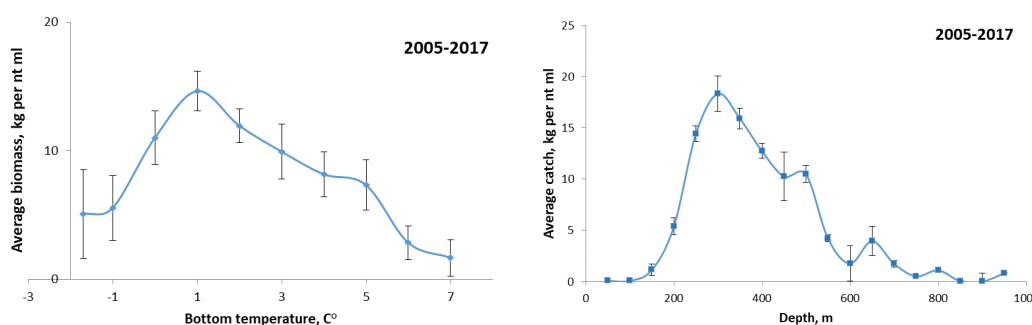


Figure 3.4.2.6. Mean biomass (kg per nt ml) per bottom temperature (C°) and and depth (m) in the Barents Sea during BESS 2005-2017 (Zakharov 2019)

During the 2018 BESS survey, it was recorded at 160 of the 2018 trawl stations with a biomass that varied from a few grams to 128.9 kg per nautical mile, with an average catch of 10.2 ± 1.4 kg/nml across 218 station. The densest concentrations of shrimp were registered in central Barents Sea, around Spitsbergen, and in Franz Victoria Trough (fig. 3.4.2.7).

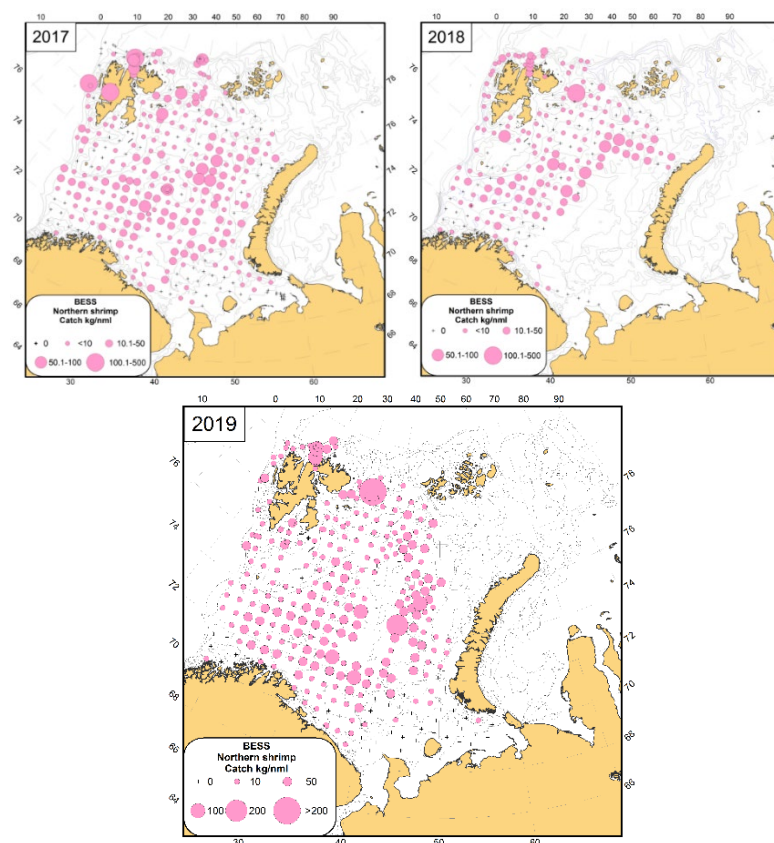


Figure 3.4.2.7. Distribution of the Northern shrimp (*Pandalus borealis*) in the Barents Sea, August–October 2017, 2018 and 2019.

During the BESS 2006–2018 average catches of the shrimp varied from 4 to 11 kg (Figure 3.4.2.8), all stayed stable around the average level. The increase of biomass in 2017–2018 may be connected with the investigations in northeastern where large biomasses of shrimp were recorded.

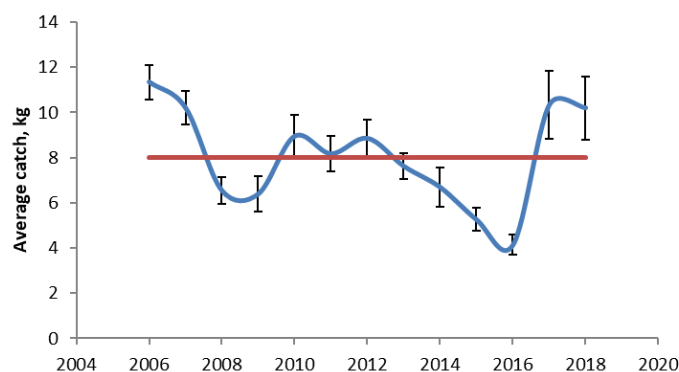


Figure 3.4.2.8. Mean catches of the Northern shrimp (*Pandalus borealis*) in the Barents Sea during the BESS 2006–2018. The red line shows mean value over the all years (Zakharov, 2019)

Biological analyses of the northern shrimp population in the eastern part of the BESS were conducted in 2018 by Russian scientists. Similar to 2017, the bulk of the population consisted of younger individuals: males of 12–27 mm carapace length; and females of 17–30 mm carapace length (fig. 3.4.2.9).

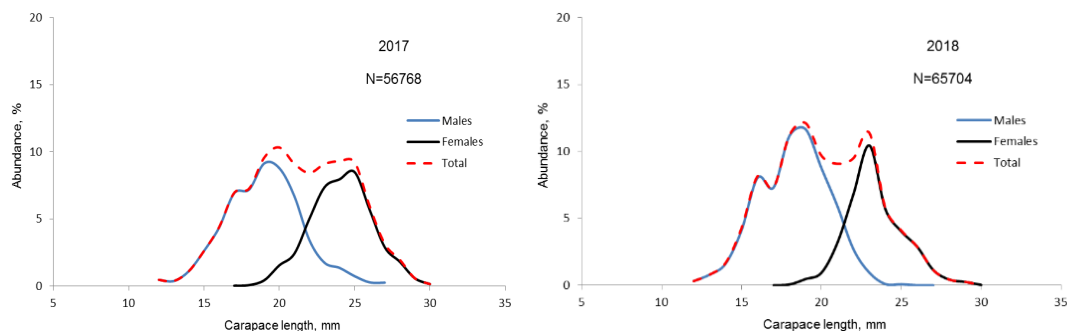


Figure 3.4.2.9 Size and sex structure of catches of the Northern shrimp (*Pandalus borealis*) in the eastern Barents Sea, August–October 2017–2018 (Zakharov, 2019)

In the western survey area, as in the eastern part of the Barents Sea, smaller shrimp (males 11–23 mm carapace length, and females 18–28 mm carapace length) were most abundant; comprising up 64% of catches (fig. 3.4.2.10)

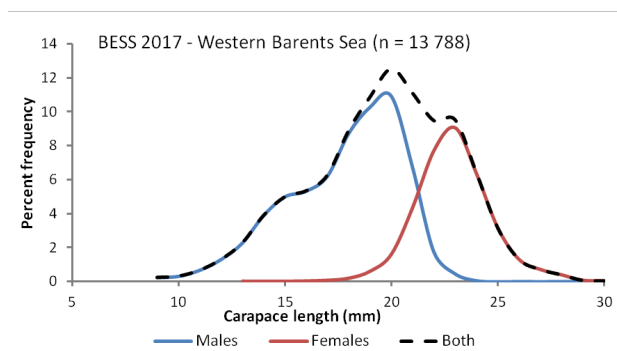


Figure 3.4.2.10. Size and sex structure of catches of the Northern shrimp (*Pandalus borealis*) in the western Barents Sea, August–October 2017

References:

- Paylov V.A., Bakanev S.V., Snow crab State of biological resources of the Barents and the White seas and the North Atlantic in 2016, 2017
 Zakharov D.V. Shrimp State of biological resources of the Barents and the White seas and the North Atlantic in 2018, 40-41, 2019

3.5 Pelagic fish

By D. Prozorkevich (PINRO), E.Eriksen (IMR), B.Bogstad (IMR), T.Prokhorova (PINRO)

3.5.1 Total biomass

Zero-group fish are important consumers of plankton and are prey for other predators, and, therefore, are important for transfer of energy between trophic levels in the ecosystem. Estimated total biomass of 0-group fish species (cod, haddock, herring, capelin, polar cod, and redfish) varied from a low of 165 thousand tonnes in 2001 to a peak of 3.4 million tonnes in 2004 with a long-term average of 1.7 million tonnes (1993–2017) (Figure 3.5.1.1). Biomass was dominated by cod and haddock, and mostly distributed in central and northern-central parts of the Barents Sea. In 2018 and 2019, the biomass of 0-group fish was not estimated.

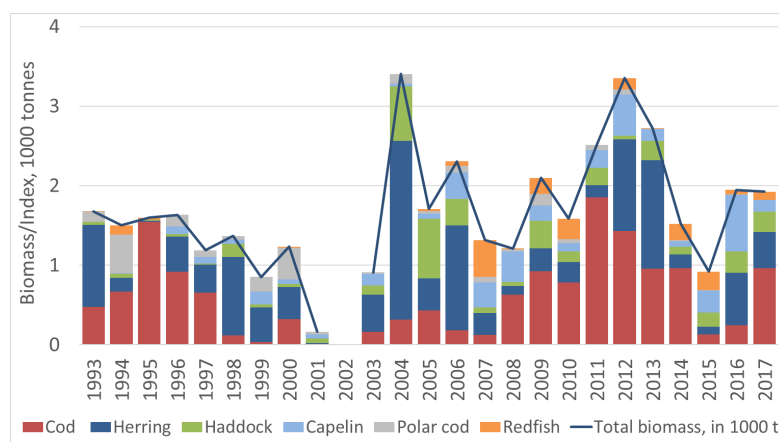


Figure 3.5.1.1. Biomass of 0-group fish species in the Barents Sea, August–October 1993–2017.

Abundance estimates and mean length were calculated for the new 15 subareas (Fig. 3.5.1.2) by MatLab software for period 1980–2018 and that summarized for the entire Barents Sea. This was done due to the use of new software and new strata system (ICES 2019-WGIBAR). The «new» 0-group indices are very close to those calculated before by other software (SAS, MS Access and etc.). Abundance estimates and fish length, presented in the report, takes into account capture efficiency of the trawl (Dingsør 2005, Eriksen et al. 2009). For calculation indices in 2019 using StoX software (Johnsen et al. 2019). These indices were not checked for comparability with previous calculations. Thus, the 2019 indexes are preliminary and will be verified later.

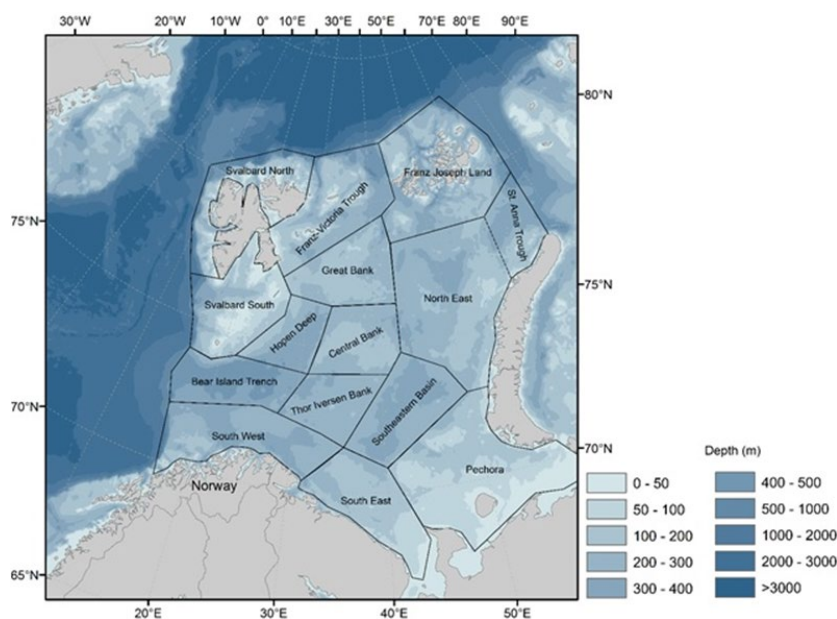


Figure 3.5.1.2. Map showing subdivision of the Barents Sea into 15 subareas (regions) used to calculate estimates of 0-group abundance and fish length based on the BESS (more description in ICES 2018).

Capelin, young herring, and polar cod constitute the bulk of pelagic fish biomass in the Barents Sea. During some years (e.g., 2004–2007 and 2015–2016), blue whiting (*Micromesistius poutassou*) also had relatively high biomass in the western Barents Sea (east of the continental slope). Total biomass of the main pelagic species during 1986–2019 fluctuated between 0.5 and 9 million tonnes; largely driven by fluctuations in the

capelin stock. During 2017-2018, the cumulative biomass of capelin, herring, polar cod, and blue whiting was close to the long-term average (Figure 3.5.1.3). In 2019, the total biomass of pelagic fish in the Barents Sea is below 2 million tons, this is less than the long-term mean and at its lowest level over the past 23 years.

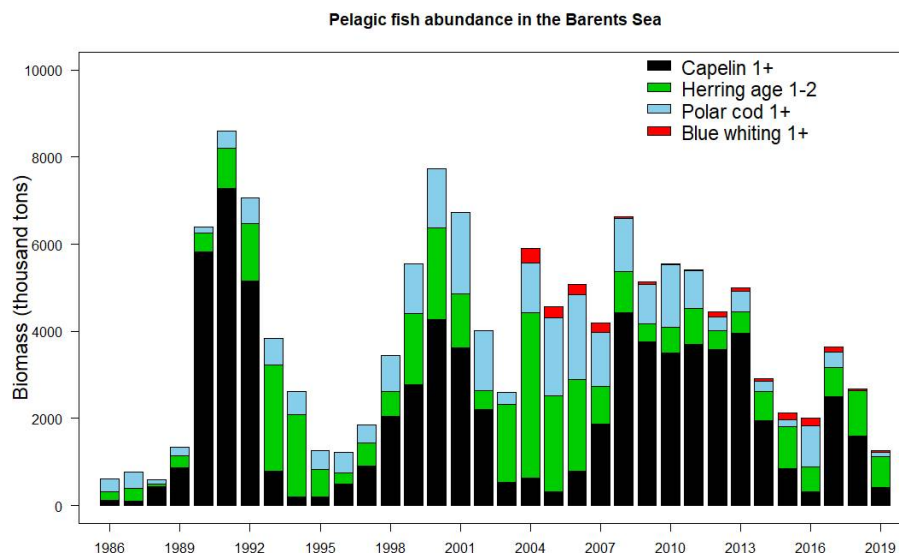


Figure 3.5.1.3. Total biomass of pelagic fish component (excluding 0-group) in the Barents Sea in 1986-2019.

3.5.2 Capelin

Young-of-the-year

Estimated abundance of 0-group capelin varied from 2082 million individuals in 1993 to 1 251 469 million individuals in 2008 with an average of 397 222 million individuals for the 1980-2019 period (Figure 3.5.2.1). In 2019, the total abundance index for 0-group capelin was estimated in 564,080 million individuals which is above the long-term average.

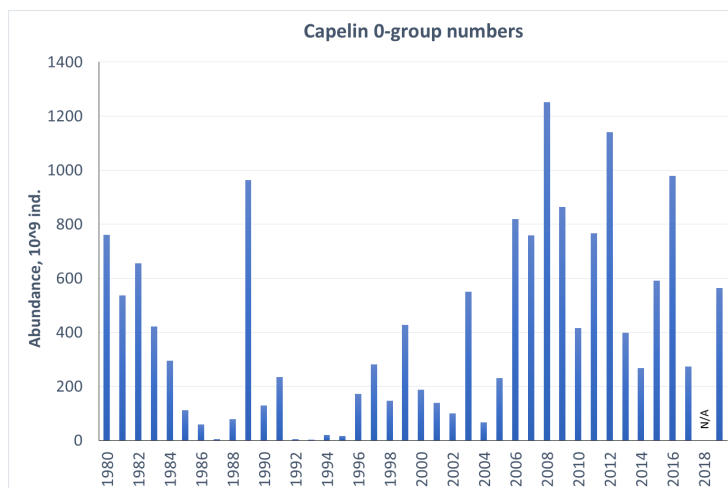


Figure 3.5.2.1. 0-group capelin abundance estimates and fluctuation 1980-2019. Note that estimates were calculated for the new 15 subareas in the Barents Sea for the period of 1980-2018 in MatLab (ICES 2018), while for 2019 using StoX (Johnsen et al. 2019).

In 2019, the spatial indices were estimated for the all main regions. The highest numbers of capelin were found in the Hopen Deep and Thor Iversen Bank area (west-central) and South East area (south-central Barents Sea). High local densities of 0-group capelin were also found to west and north of Svalbard (Spitsbergen) and near to Norwegian coast, however with relative low average numbers for these regions (figure 3.5.2.2).

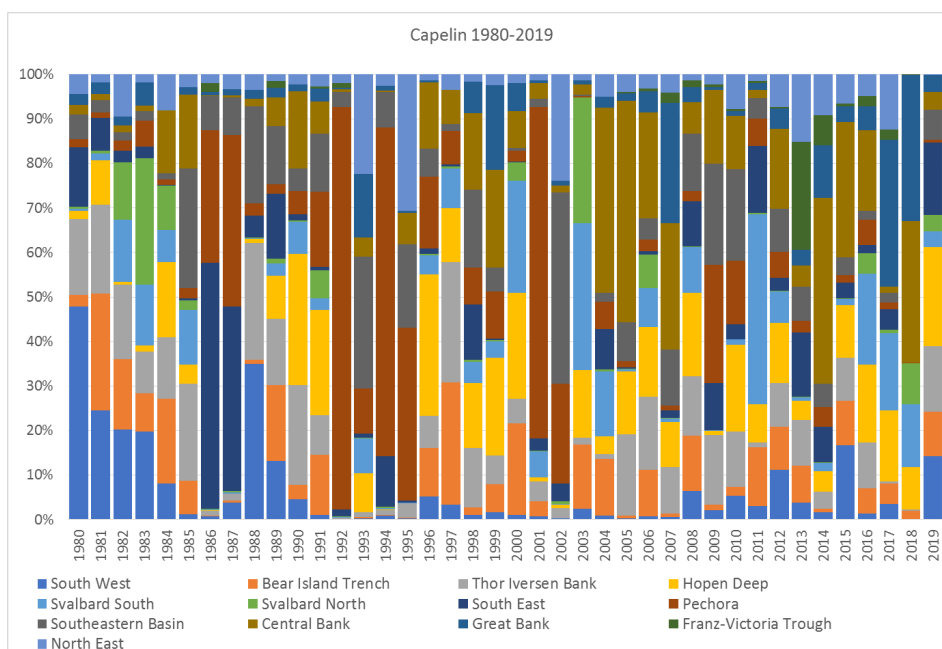


Figure 3.5.2.2. Percentage of 0-group capelin abundance in the 15 regions of the Barents Sea 1980-2019. Note that estimates were calculated for the new 15 subareas in the Barents Sea for the period of 1980-2018 in MatLab (ICES 2018 WGIBAR), while for 2019 using StoX (Johansen et al. 2019).

2019-year class dominated by fish of 4.5 - 5.5 cm length. The largest capelin (with an average close to 6 cm) were observed to the north-eastern boarder of their distribution in the Franz-Viktoria Land and North East areas, while smallest capelin (with an

average length of 5.1 cm) were found close to the coast in the South West and South East areas.

Distribution of 0-group capelin has varied during the last four decades. The total area of distribution was smallest during the 1990s, has been largest during the current decade, and associated with the occurrence or non-occurrence of strong year classes (Figure 3.5.2.3) Capelin have expanded distribution in the southeastern and northeastern direction (Eriksen et al. 2017).

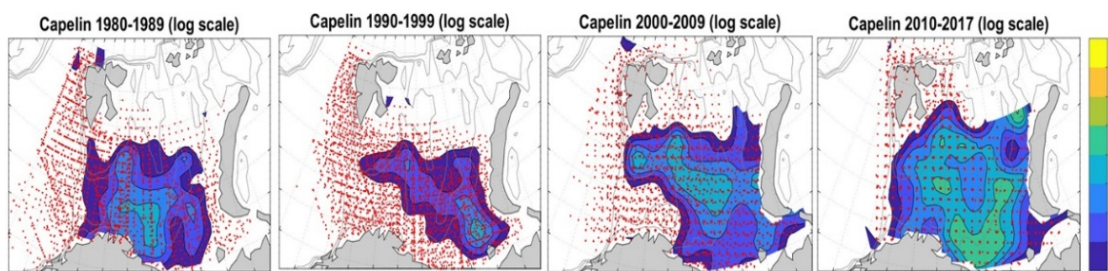


Figure 3.5.2.3. Distribution of 0-group capelin abundance in the Barents Sea during the 1980s, 1990s, 2000s, and 2010s. Abundance was log-transformed (natural logarithms) before mapping. Fish density varied from low (blue) to high (yellow). Red dots indicated sampling locations.

Adult capelin

Sampling the main area of capelin distribution during 2019 was timely and well covered. To north from Spitsbergen (81°N) capelin was distributed outside survey area, but probably insignificant amounts of fish were outside the survey area. Thus, capelin stock assessment in 2019 was well done and comparable to last year. The geographic distribution of capelin density is shown in Figure 3.5.2.4. Capelin distribution area in 2019 was significantly smaller compared to 2018, the main concentrations were found close to the coast east of Edge Island between 77° and 78°N, and on the eastern part of Great Bank at similar latitude. Very little capelin was found in the east and to the north. In all regions, capelin concentrations were significantly lower than in 2018.

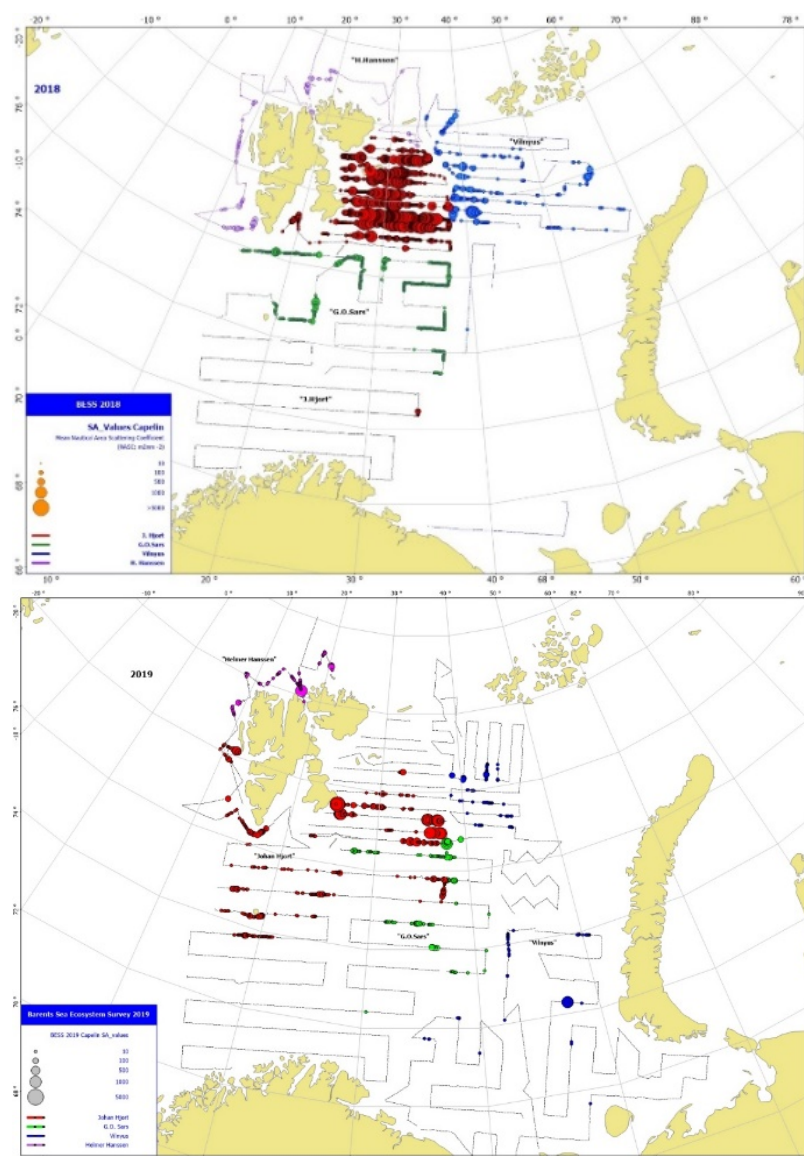


Figure 3.5.2.4. Geographic distribution of capelin in 2018 (left) and 2019 (right). Circle size corresponds to SA (area back-scattering coefficient) values per nautical mile.

Average length of capelin in 2019 was 12.63 cm; average weight was 11.8 g, it is very close to values 2018. For age 1 capelin, no evident trends in length and weight were observed (Figure 3.5.2.5). For age 2 and 3 capelin, average fish weight and length were higher compared to 2017. In general, all biological characteristics of capelin were at the average long-term level. This is most clearly observed in age 2 fish (Figure 3.5.2.5). Usually this age group forms a large component of total stock and reflects general trends in condition of the capelin stock.

Dynamics of changing average weight-at-age reflect capelin feeding conditions during the summer-autumn period. These conditions are determined not only by the stock size, but also by the state of the plankton community in the Barents Sea. It is evident that in 2019 the capelin food base (zooplankton abundance and species composition) was stable.

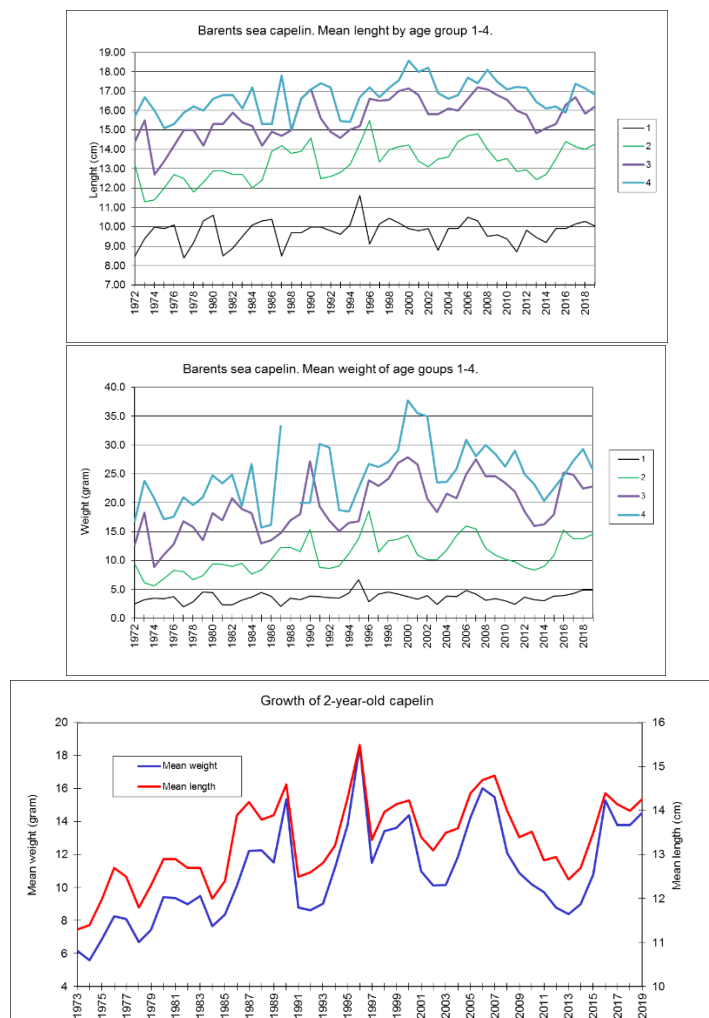


Figure 3.5.2.5. Biological characteristics of capelin during August-September (1973-2019).

The total capelin stock was estimated to be approximately 0.41 million tonnes in 2019, which is significant below the long-term average (2.95 million tonnes) and represents a 75% decrease from 2018. About 73% (0.3 million tonnes) of the 2019 stock was above 14 cm in length and considered to be maturing (Figure 3.5.2.5).

Age 3 capelin (2016-year class) amount only 3.3% of total stock by number; the 2017-year class (age 2) made up 26.5% of the stock by number. The recruiting age 1 (2018 year class) was estimated at 17.46 billion individuals, this age group is dominated the stock composition by number ($\approx 50\%$), but this is far below the long-term average value, lowest since 1995 and close to the minimum for the historical observation period. Thus, in 2019, the stock of Barents Sea capelin is at its lowest level since the period of collapse 2003-2005 (Figures 3.5.2.6, 3.5.2.7).

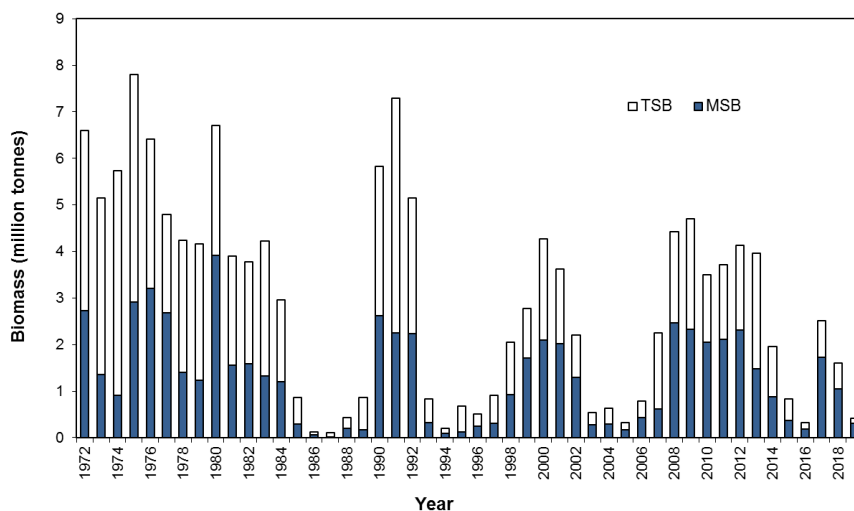


Figure 3.5.2.6. Capelin biomass based on 1972–2019 acoustic survey data: maturing stock biomass (MSB) and total stock biomass (TSB).

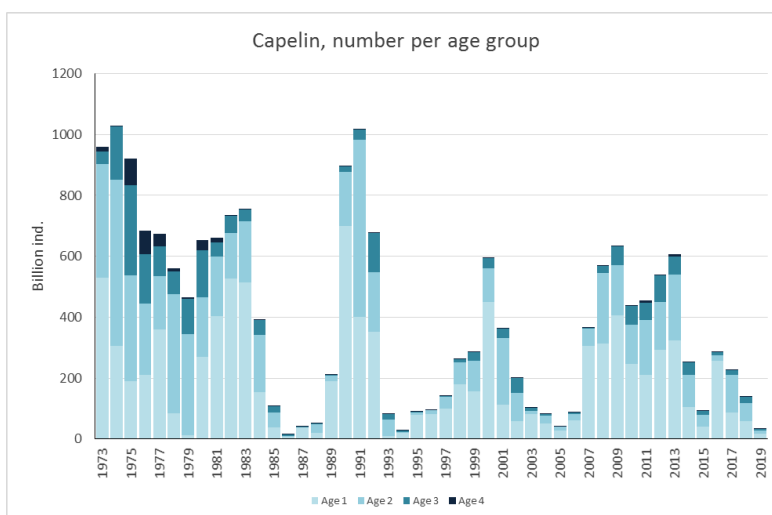


Figure 3.5.2.7. Capelin stock age composition (age 1-4) during 1972–2019. (Note: age 5 and older was removed due to negligible numbers in the total stock).

Due to significant spawning mortality, the natural mortality of capelin can be estimated indirectly only. Since fishing mortality for ages 1 and 2 is absent or very small, it can be assumed that total mortality for age groups is natural. Figure 3.5.2.8 shown natural mortality (M) calculated as the decrease from age 1 to age 2 in the autumn survey. In some years were a negative mortality values obtained. It is most likely the consequence of underestimation of age 1 fish in the survey.

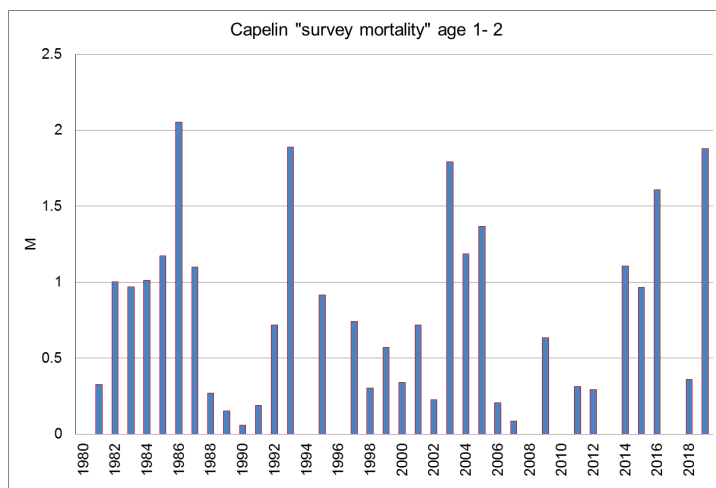


Figure 3.5.2.8. Capelin natural mortality from age 1 to age 2, estimates based on acoustic survey data. (Negative mortality has been removed).

Spatial distribution of capelin in the Barents Sea depends on environmental and stock conditions, primarily: position of the ice edge; distribution of zooplankton; and capelin stock size and structure. In years with a large stock, capelin is distributed widely. Juvenile capelin are distributed further south than adults. During the 1972-1979 period, the capelin stock was large and widely distributed. During 1980-1989, the stock decreased, and distribution was more southward. Since the 2000s, capelin began movement north- and eastwards. During 2010-2017, the stock was in good condition and moved significantly northward into ice-free waters (Figure 3.5.2.8). This represented a shift northward an average of 60-80 nautical miles further than observed in the 1970s. During 2018-2019, capelin stock size has decreased; the area of distribution has decreased as well (Figure 3.5.2.9). In general, during periods of warming in the Barents Sea, capelin move further north and north-eastward to find feeding grounds with high plankton biomass. However, at low stock levels, capelin have adequate food availability, and temperature does not appear to be a key factor driving northward expansion.

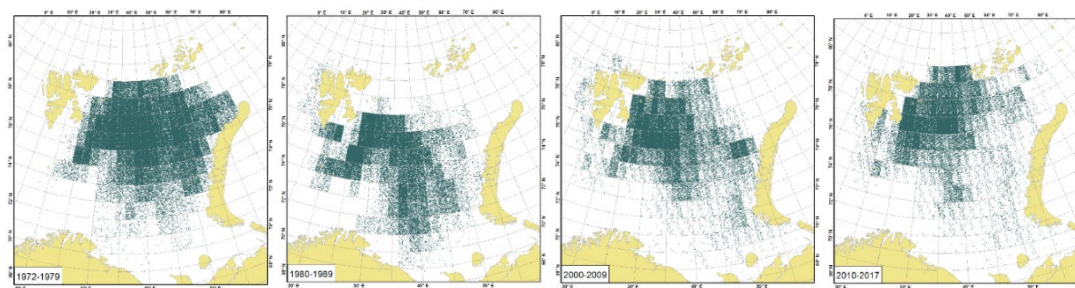


Figure 3.5.2.9a. Estimated capelin biomass during August-September by decade (1970s, 1980s, 1990s, 2000s, and 2010s). Biomasses presented for World Meteorological Organization (WMO) squares system of geocodes which divide areas into latitude-longitude grids (1° latitude by 2° longitude). One dot is equal to 500 tonnes.

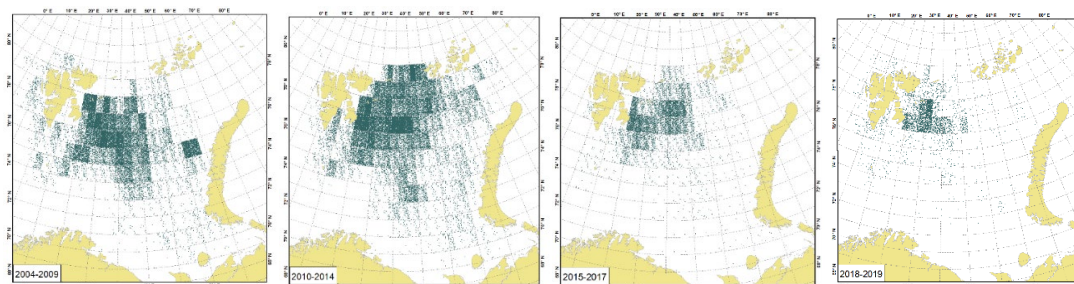


Figure 3.5.12b. Estimated capelin biomass during August-September for recent periods of high temperature condition and cod stock size. Note that cod abundance peaked in 2013 and that temperature decreased in 2018-2019. Time periods are further broken down into sub-periods (2004-2009, 2010-2014 and 2015-2017 and 2018-2019). Biomass is presented for WMO squares. One dot is equal to 500 tonnes.

3.5.3 Herring

Young-of-the-year

Estimated abundance of 0-group herring varied from 93 million individuals in 1986 to 940,773 million individuals in 2004 with a long-term average of 188,586 million individuals for the 1980-2019 period (Figure 3.5.3.1). Low total abundance of 0-group herring (17,245 million individuals) was estimated in 2019, which was significantly lower than the long-term level and the lowest in last 18 years.

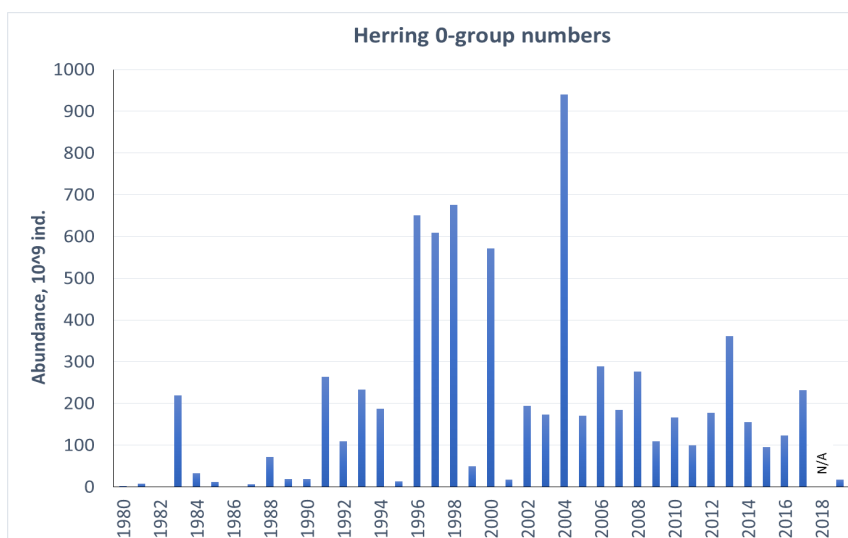


Figure 3.5.3.1. 0-group herring abundance estimates and fluctuation 1980-2019. Note that estimates were calculated for the new 15 subareas in the Barents Sea for the period of 1980-2018 in MatLab (ICES 2018 WGIBAR), while for 2019 using StoX (Johnsen et al. 2019).

In 2019, distribution of 0-group was covered well. The spatial indices were estimated for the all regions. Herring were distributed in the central, north western and south-central Barents Sea. Very few herring were found in the southeastern part of the Barents Sea. Most of 0-group herring were found in the west-central areas: Bear island Trench and Thor Iversen Bank (Figure 3.5.3.2).

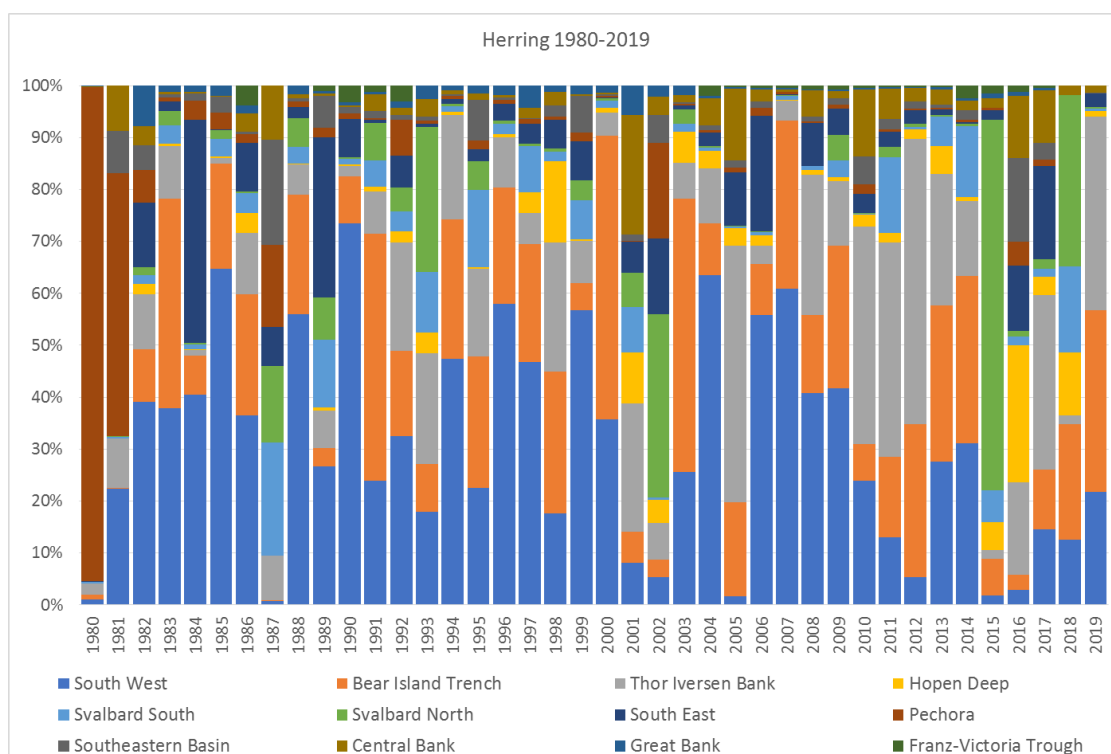


Figure 3.5.3.2. Percentage of 0-group herring abundance in the 15 regions of the Barents Sea 1980-2019. Note that estimates were calculated for the new 15 subareas in the Barents Sea for the period of 1980-2018 in MatLab (ICES 2018), while for 2019 using StoX (Johansen et al. 2019).

Spatial distribution of 0-group herring varied over the last four decades, was most limited during the 1980s and has increased since that time. Extent of the area occupied was associated with the occurrence or lack of occurrence of strong year classes (Figure 3.5.3.3). Higher densities of herring have been observed in the northwestern areas during the last decade than during the previous three decades.

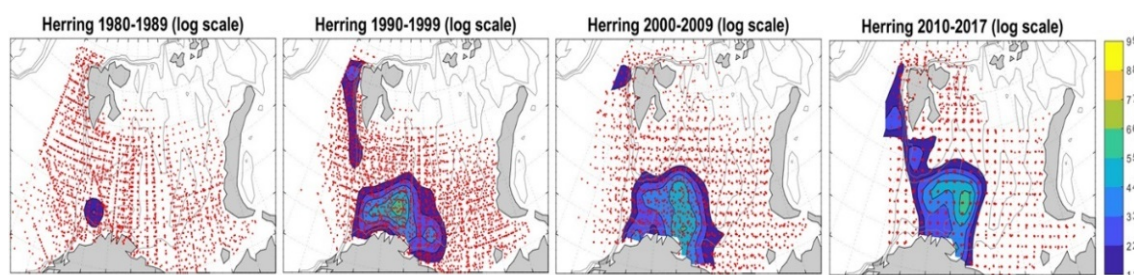


Figure 3.5.3.3. Distribution of 0-group herring abundance in the Barents Sea during 1980s, 1990s, 2000s, and 2010s. Abundance estimates were log-transformed (natural logarithms) before mapping. Fish density varied from low (blue) to high (yellow). Red dots indicate sampling locations.

Herring age 1-2

During 2013–2017, abundance of young herring in the Barents Sea was relatively stable. It increased from 2017 to 2018 mainly due to contribution of the strong 2016-year class, and then decreased again in 2019. Figure 3.5.3.4 shows herring distribution in 2019 with highest amounts in the south-west and south-eastern parts of the Barents Sea. Figure 3.5.3.4 shows biomass estimates of age 1 and 2 herring combined in the Barents Sea based on the last ICES assessment for age 2+ herring, assuming $M=0.9$ for age 1.

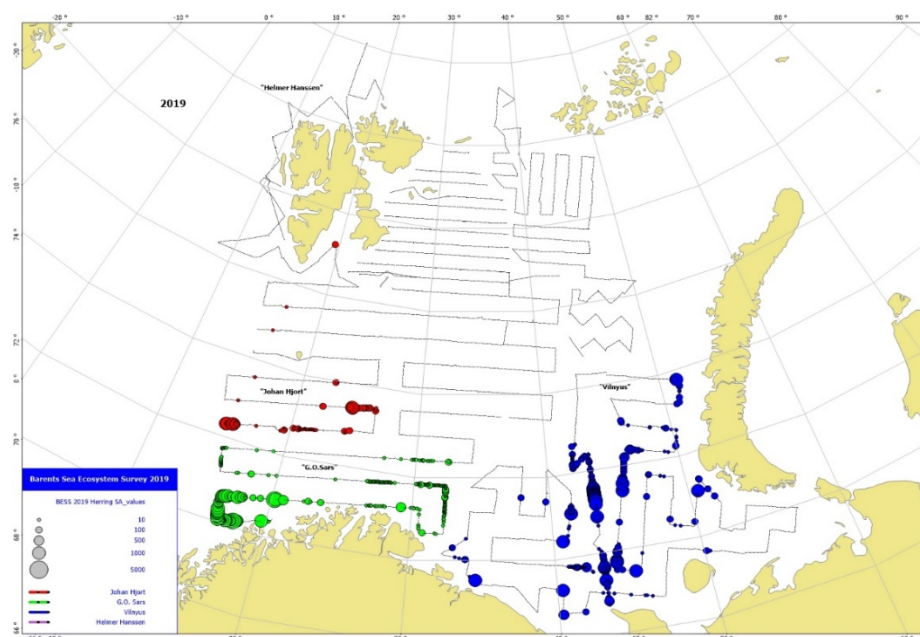


Figure 3.5.3.4. Estimated distribution of herring, August-October 2019. Circle sizes correspond to S_A (area back-scattering coefficient) averaged over 1 nautical mile.

It should be noted that in the herring surveys in the Barents Sea in 2019 age 3 herring dominated. Neither the abundance of age 1-2 as shown in Figure 3.5.3.5 nor the abundance estimates from the surveys (June survey and BESS) carried out on young herring give a coherent picture. The estimates from the assessment depend heavily on the assumption of M and also it varies between years whether or not also age 3 herring is present in the Barents Sea. On the other hand, there are not survey data for all years and they are often inconsistent between years (e.g. the abundance of the 2016-year class was approximately the same both at age 1, 2 and 3). Thus, an analysis to determine a time series for young herring abundance in the Barents Sea, taking all data sources into account, should be given high priority.

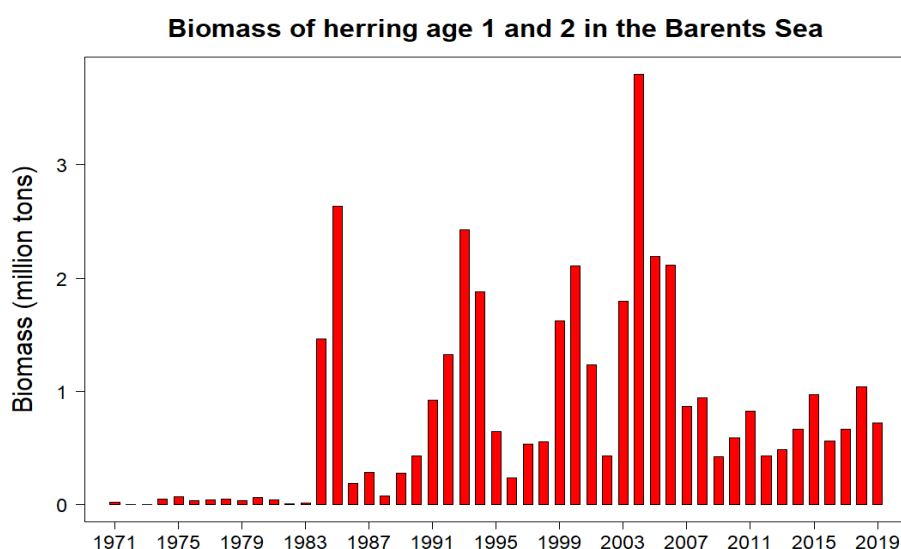


Figure 3.5.3.5. Estimated biomass of Norwegian Spring Spawning herring Age 1 and 2 in the Barents Sea – based on Working Group on Widely Distributed Stocks (WGWIDE) VPA estimates (ICES 2019b).

3.5.4 Polar cod

Polar cod is an Arctic species with a circumpolar distribution. Historically, the world's largest population of this species has been observed in the Barents Sea. In recent years, there have been significant changes in the stock size and distribution of polar cod.

Young of the year

Estimated abundance of 0-group polar cod varied from 519 million in 1995 to 2488460 million individuals in 1994 with a long-term average of 438,152 million individuals for the 1980-2019 period (Figure 3.5.4.1). In 2019, a low abundance for 0-group polar cod was observed within the standard survey area.

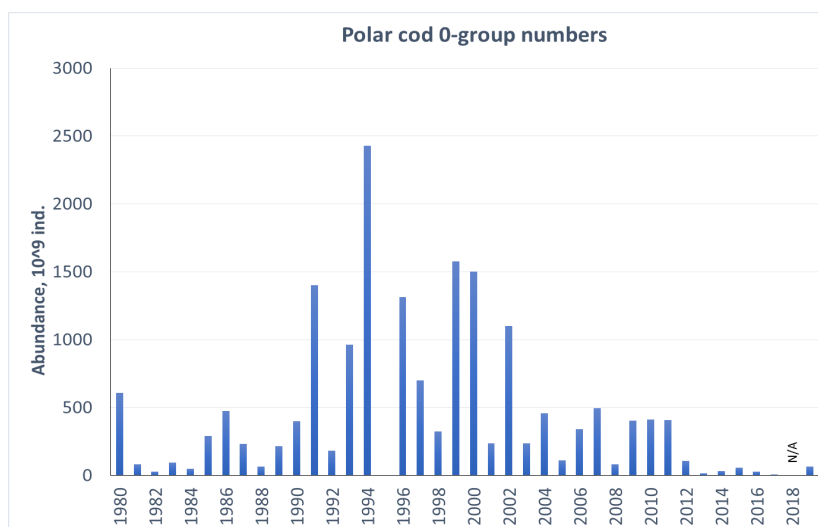


Figure 3.5.4.1. 0-group polar cod abundance estimates and fluctuation 1980-2019. Note that estimates were calculated for the new 15 subareas in the Barents Sea for the period of 1980-2018 in MatLab (ICES 2018), while for 2019 using StoX (Johansen et al. 2019).

In 2019, the distribution area of 0-group polar cod increased significantly compared to previous years. Polar cod were widely distributed with denser concentration south of the Svalbard (Spitsbergen) and south of Novaya Zemlya. In 2019, the spatial indices were estimated for the all regions. The highest abundance was observed in the Svalbard South and Svalbard North regions (Figure 3.5.4.2).

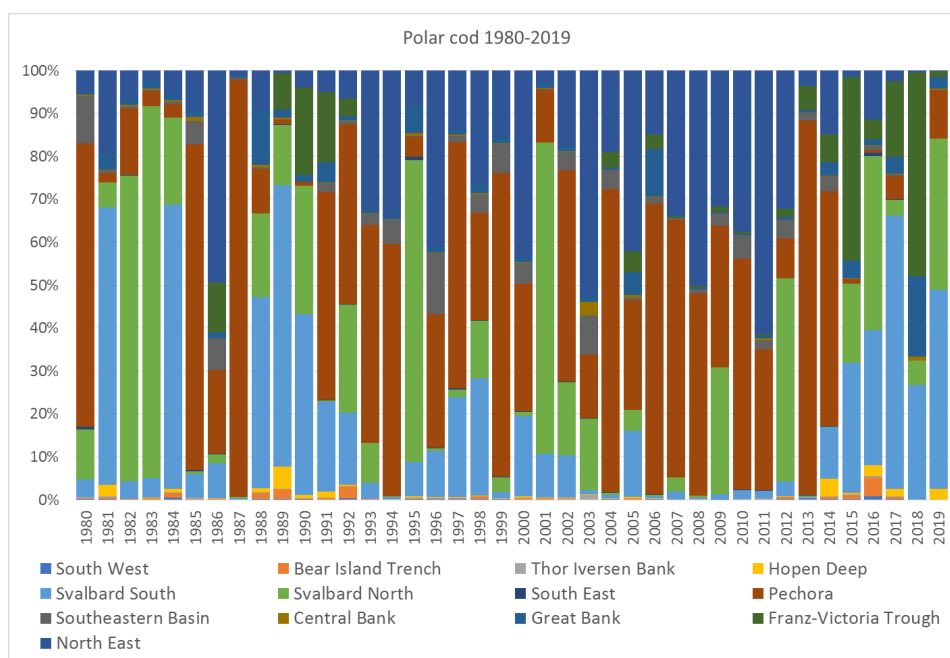


Figure 3.5.4.2. Percentage of 0-group polar cod abundance in the 15 regions of the Barents Sea 1980-2019. Note that estimates were calculated for the new 15 subareas in the Barents Sea for the period of 1980-2018 in MatLab (ICES 2018), while for 2019 using StoX (Johnsen et al. 2019).

Since 2015, the proportion of 0-group polar cod in the southeast of the Barents Sea (Pechora region) has been decreasing (Figure 3.5.4.2.). Low abundance of 0-group cod in the traditional core area, the Pechora Sea, most likely due to redistribution of spawning sites out of the Barents Sea and into the western part of Kara Sea. This is indirectly confirmed by 2019 studies in the Kara Sea, where a significant amount of the 0-group polar cod were found.

The distribution of 0-group polar cod varied over the last four decades, and was largest during the 1990s and 2000s. Size of area occupied was associated with the occurrence or non-occurrence of strong year classes from the Pechora Sea, in the southeastern corner of the Barents Sea (Figure 3.5.4.3.).

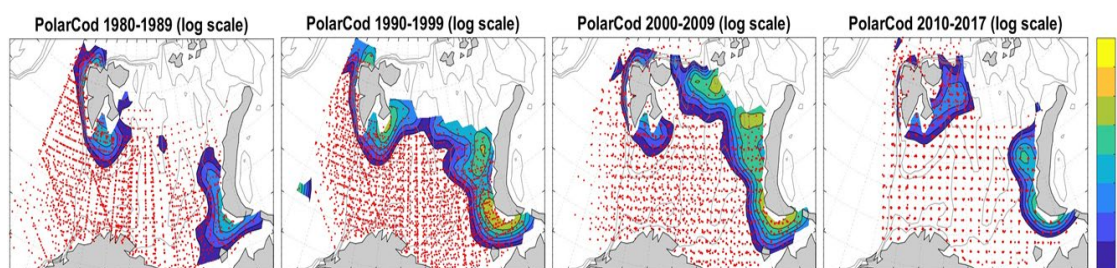


Figure 3.5.4.3. Distribution of 0-group polar cod abundance in the Barents Sea during the 1980s, 1990s, 2000s, and 2010s. Abundance estimates were log-transformed (natural logarithms) before mapping. Fish density varied from low (blue) to high (yellow). Red dots indicated sampling locations.

Adult polar cod

In 2019, the area of polar cod distribution was covered partly. The BESS survey area has been regularly decreasing in recent years, especially in the north-eastern part.

Probably, polar cod distributed north-east Barents Sea, outside the surveyed area, as significant concentrations were found on the border of the survey area (Figure 3.5.4.4). Main concentration of polar cod were found in the same places as previous years, around Franz Josef bank. Small, isolated concentrations were also recorded to south and to north of Svalbard (Spitsbergen). In all areas, the density of polar cod was low.

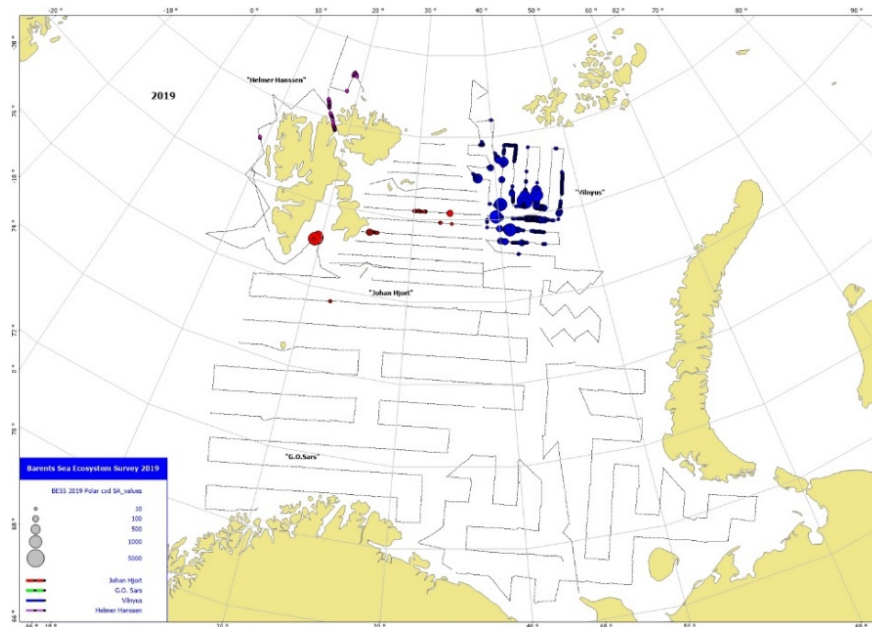


Figure 3.5.4.4. Estimated distribution of polar cod during August–October 2019. Circle size corresponds to SA (area back-scattering coefficient) values per nautical mile.

The total stock was estimated to be 87.2 thousand tonnes, which likely does not reflect the actual stock size. Thus, there is no reliable new information about polar cod stock abundance in 2019. Polar cod density in 2019 in the distribution area was slightly higher than in 2018. Anyway, the polar cod stock inside the Barents Sea border remains at a low level. From 2012 total abundance and biomass of polar cod in the Barents Sea has decreased significantly. Only one year-class of 2015 gave a short-term increase the polar cod stock in 2016 (Figure 3.5.4.5), then the stock quickly decreased again. The issue of the situation with stocks of polar cod in the Barents Sea and adjacent areas remains open. Such a decrease in the polar cod stock may be the result of increased natural mortality due to increased consumption by cod. Assuming that a significant part of the polar cod stock migrated outside the Barents Sea, why did some of the polar cod remain in the Barents Sea? It is obviously that polar cod populations of the Barents and Kara Seas are related. However, how mutual populations interchange going on is not yet clear. To solve this problem, it is necessary to carry out a complete study of the Barents Sea, especially the northeastern regions which are not covered annually.

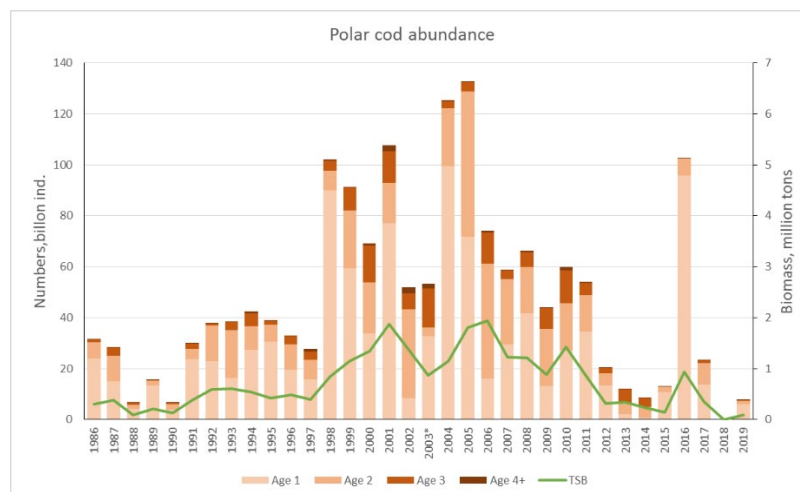


Figure 3.5.4.5. Total abundance in billions (coloured bars / left axis) and biomass in millions of tonnes (green line / right axis) of polar cod in the Barents Sea (acoustic survey and BESS data) collected August-September during the 1986–2019 period. (2003 values based on VPA due to poor survey coverage. A reliable estimate is not available for 2018).

3.5.5 Blue whiting

Acoustic estimates for the proportion of the blue whiting stock present in the Barents Sea have been made since 2004. In 2017, the BESS data time-series were recalculated using a newer target strength equation (Pedersen *et al.*, 2011), and a standardized area. The revised estimates were on average about one third of previous estimates. During 2004–2007, estimated biomass of blue whiting in the Barents Sea was >200 000 tonnes (Figure 3.5.5.1) but decreased abruptly in 2008 and remained low until 2012. In 2012 and 2013 the strong 2011-year class contributed to an observed increased abundance of blue whiting and in 2015 and 2016 the even stronger 2014-year class contributed largely to the total estimated biomasses >150 000 tons in 2015 and 2016 (Figure 3.5.5.1). With strong year classes the young blue whiting are abundant along the shelf break to the Norwegian Sea and partly distribute into the Barents Sea (Figure 3.5.5.2). In 2018 and 2019 the blue whiting abundance in the Barents Sea was very low, and dominated by older fish.

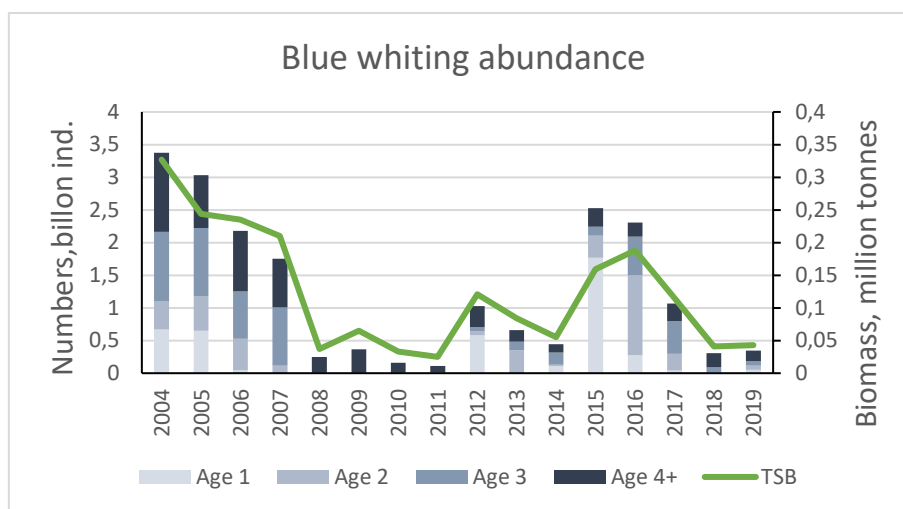


Figure 3.5.5.1. Total abundance in billions (coloured bars / left axis) and biomass in millions of tonnes (gray line / right axis) of blue whiting in the Barents Sea (BESS data revised in 2017) collected August–September during the 2004–2019 period.

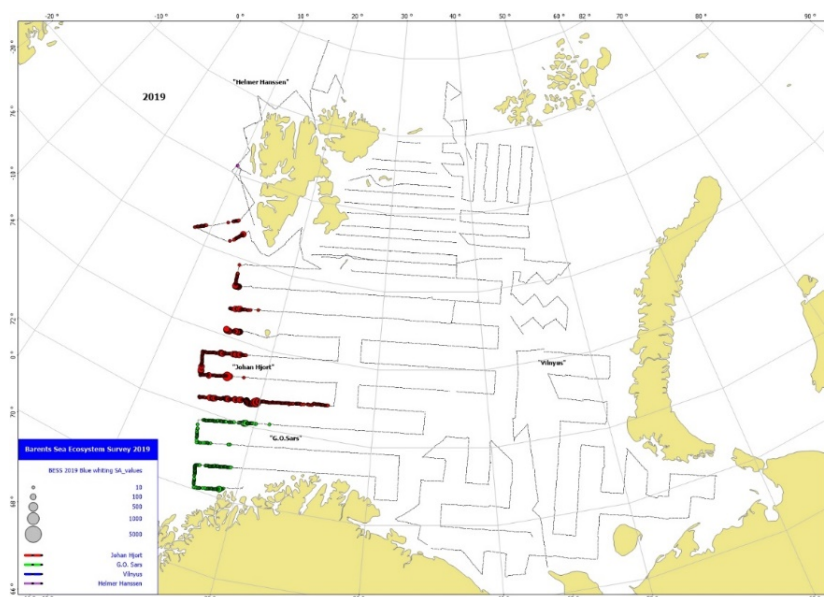


Figure 3.5.5.2. Estimated distribution of blue whiting during August–October 2019. Circle size corresponds to S_a (area back-scattering coefficient) averaged over 1 nautical mile.

References:

- Dingsør, G. E. 2005. Estimating abundance indices from the international 0-group survey in the Barents Sea. *Fisheries Research* 72(2-3):205-218.
- Eriksen, E., Prozorkevich, D. V. and Dingsør, G. E. 2009. An evaluation of 0-group indices of Barents Sea Fish stocks. *The Open Fish Science Journal*, 2:6-14.
- Eriksen, E., Skioldal, H.R., Gjosæter, H. and Primicerio R. 2017. Spatial and temporal changes in the Barents Sea pelagic compartment during the recent warming. *Progress in Oceanography* 151: 206-226, <http://dx.doi.org/10.1016/j.pocean.2016.12.009>
- ICES 2019a. Arctic Fisheries Working Group (AFWG). ICES Scientific Reports. 1:30. 930 pp. <http://doi.org/10.17895/ices.pub.5292>
- ICES 2019b. Working Group on Widely Distributed Stocks (WGWIDE). ICES Scientific Reports. 1:36. 948 pp. <http://doi.org/10.17895/ices.pub.5574>
- Iohansen, E., Totland, A., Skålevik, Å., Holmin, A. I., Dingsør, G. E., Fuglebakk, E., & Handegard, N. O. (2019). StoX: An open source software for marine survey analyses. *Methods in Ecology and Evolution*, 10 :1523 – 1528. <https://doi.org/10.1111/2041-210X.13250>
- Pedersen, G., Godø, O. R., Ona, E., and Macaulay, G. I. 2011. A revised target strength–length estimate for blue whiting (*Micromesistius poutassou*): implications for biomass estimates. – *ICES Journal of Marine Science*, 68: 2222–2228.

3.6 Demersal fish

B. Bogstad (IMR), D. Prozorkevich (PINRO), E. Eriksen (IMR), T. Prokhorova (PINRO), A. Russkikh (PINRO), A. Filin (PINRO) and P. Krivosheya (PINRO)

Most Barents Sea fish species are demersal (Dolgov *et al.*, 2011); this fish community consists of about 70–90 regularly occurring species, which have been classified into zoogeographic groups. Approximately 25% are either Arctic or mainly Arctic species. The commercial species are boreal or mainly boreal species (Andriashev and Chernova, 1995), except for Greenland halibut (*Reinhardtius hippoglossoides*) that is classified as either Arcto-boreal (Mecklenburg *et al.*, 2013) or mainly Arctic (Andriashev and Chernova, 1995).

Distribution maps based on Barents Sea Ecosystem Survey (BESS) data for cod, haddock, long rough dab, Greenland halibut, redfish, and six other demersal fish species can be found at: http://www.imr.no/tokt/okosystemtokt_i_barentshavet/utbredelseskart/en.

Abundance estimates are available for commercial species that are assessed routinely at the ICES AFWG. Figure 3.6.1 shows such biomass estimates for cod, haddock, and saithe (*Pollachius virens*) calculated in 2019. Saithe occurs mainly along the Norwegian coast and along the southern coast of the Barents Sea; few occur farther offshore in the Barents Sea itself. Total biomass of these three species peaked in 2010–2013 and has declined since; but remains above the long-term average for the time series dating back to 1960. Greenland halibut and deepwater redfish (*Sebastes mentella*) are important commercial species with large parts of their distribution within the Barents Sea. Time-series of biomass estimates for deepwater redfish and Greenland halibut are much shorter than those for haddock, cod, and saithe. Other than these main commercial stocks, long rough dab is the demersal stock with the highest biomass. Overall, cod is the dominant demersal species.

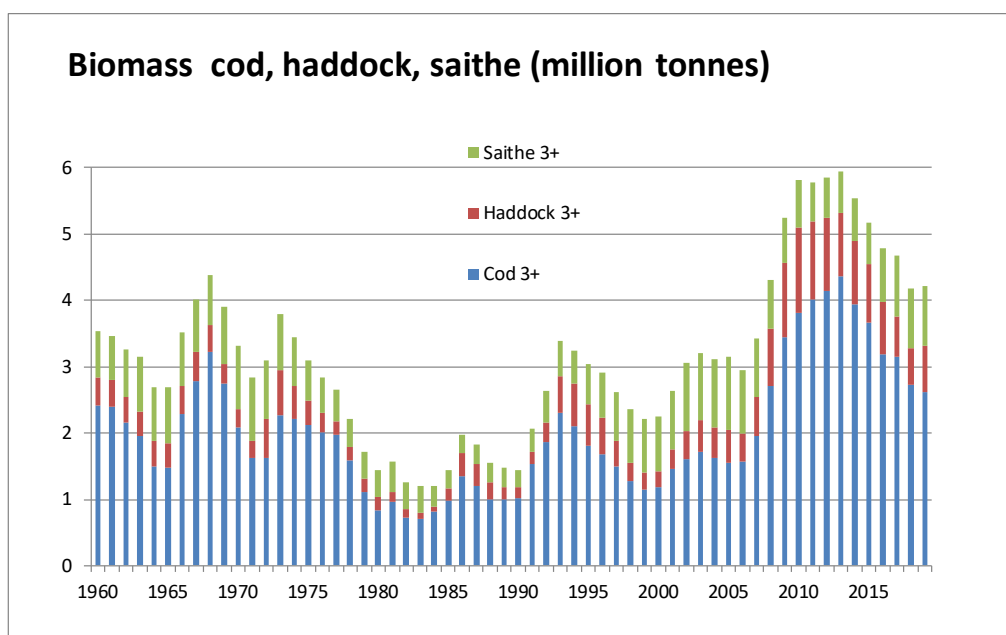


Figure 3.6.1 Biomass estimates for cod, haddock, and saithe during the 1960–2019 period from AFWG 2019 (ICES 2019a). Note: saithe is only partly distributed in the Barents Sea.

3.6.1 Cod

Young-of-the-year

Estimated abundance of 0-group cod varied from 325 million in 1981 to 614,744 million individuals in 2014 with a long-term average of 139,460 million individuals for the 1980-2019 period (Figure 3.6.2). In 2018, the total abundance index for 0-group cod was not estimated due to lack of coverage. In 2019, the total abundance index for 0-group cod was 23,404 million individuals.

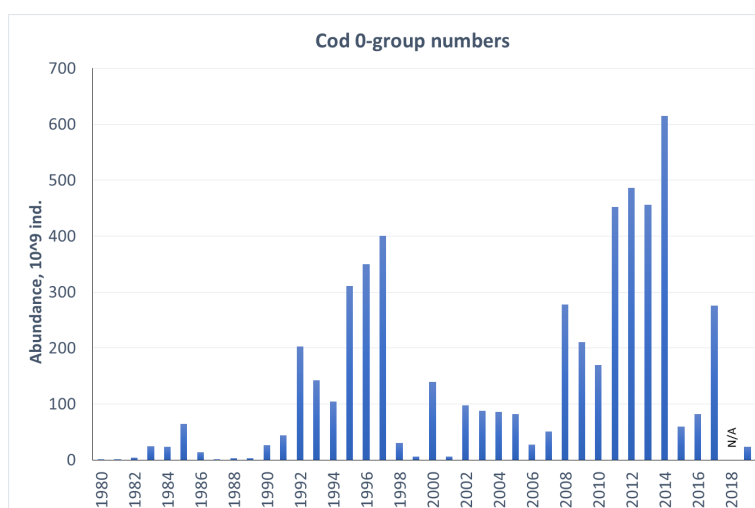


Figure 3.6.2. 0-group cod abundance estimates and fluctuation 1980-2019. Note that estimates were calculated for the new 15 subareas in the Barents Sea for the period of 1980-2018 in MatLab (ICES 2018), while for 2019 estimates were calculated using StoX (Johansen et al. 2019).

In 2019, the distribution of 0-group cod in the Barents Sea was covered well and abundance indices were estimated. The abundance index of 2019 year class is well

below the long-term mean, and thus may be characterized as weak. 0-group cod were widely distributed on the surveyed area, except northern and south-eastern areas.

The main dense concentrations were found in the South West area (Figure 3.6.3.). In 2019, 0-group cod was dominated by fish of 5 - 7.5 cm length. The largest cod (with an average length of 8.0 cm) were observed in the Central Bank, Svalbard South and Svalbard North areas, while smallest cod (with an average length of 5.1 cm) were found in the North East.

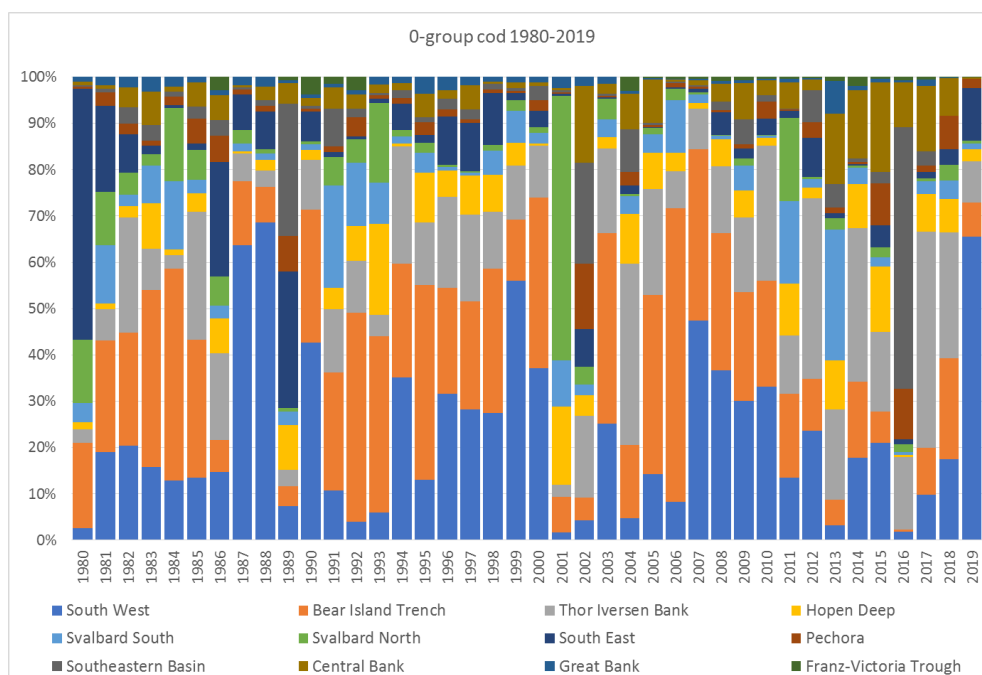


Figure 3.6.3. Percentage of 0-group cod abundance distributed by different regions of the Barents Sea during the 1980-2019. Note that estimates were calculated for the new 15 subareas in the Barents Sea for the period 1980-2018 in MatLab (ICES 2018 WGIBAR), while for 2019 using StoX (Johnsen et al. 2019).

Cod one year old and older

The northeast Arctic cod stock is currently in good condition, with high total stock size, and high spawning-stock biomass (Figure 3.6.4). Strong 2004- and 2005-year classes were estimated as average at age 3 (Figure 3.6.5). 0-group abundance has been very high in the beginning of the last decade (2011–2014); but this has not resulted in strong year classes, as seen from the updated stock-recruitment plot shown in Figure 3.6.6.

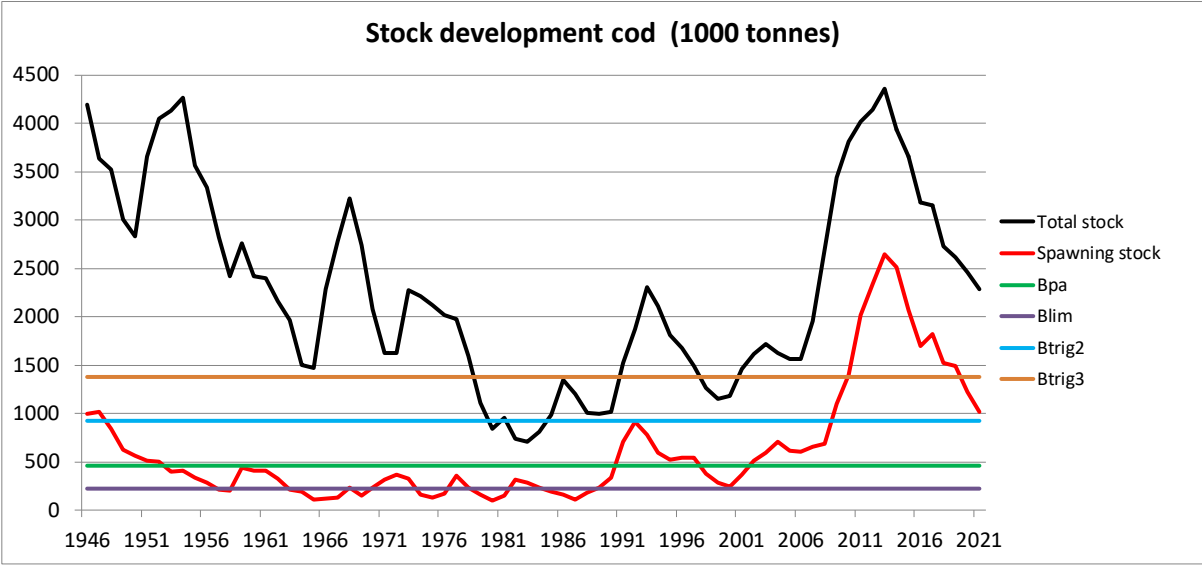


Figure 3.6.4. Cod total stock and spawning stock biomass during the 1946-2019 period, including forecast for 2020-2021. From AFWG (ICES 2019a).

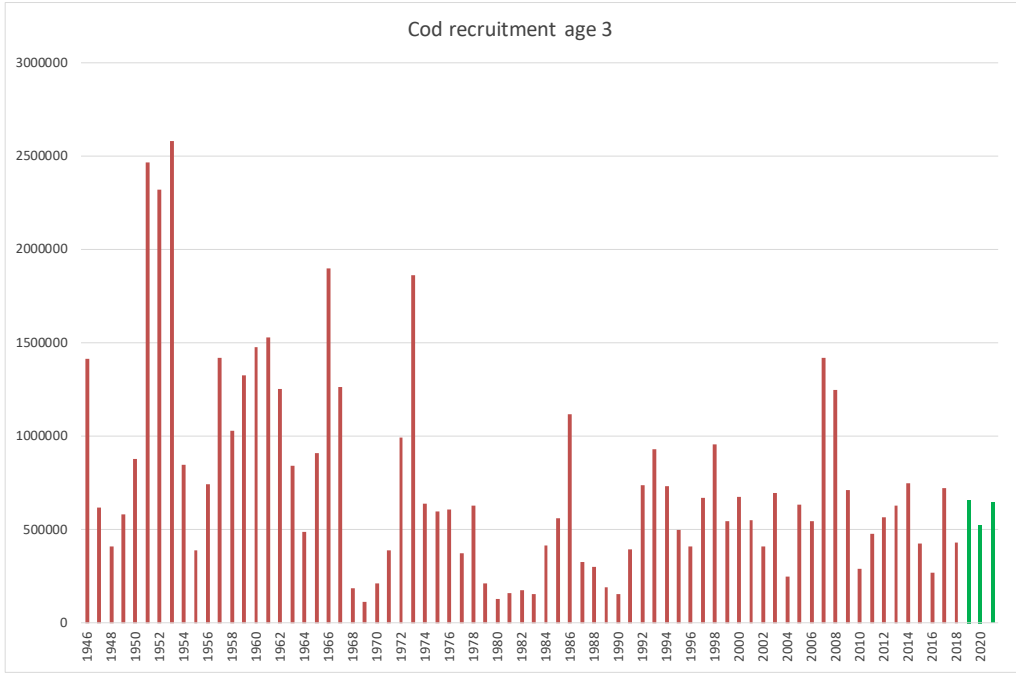


Figure 3.6.5. Cod recruitment at age 3 during the 1950-2018 period and forecast for 2019-2021 (ICES 2019).

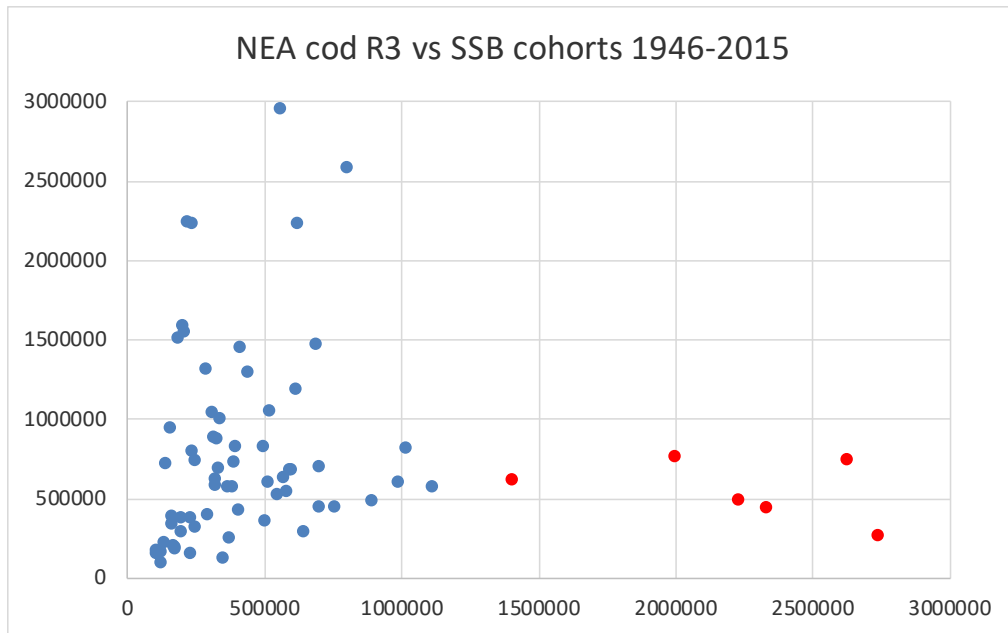


Figure 3.6.6 Spawning stock-recruitment plot for cod cohorts 1946-2015. Cohorts 2010-2015 shown as red dots.

Strong 2004- and 2005-year classes have, together with a low fishing mortality, led to rebuilding of the cod stock's age structure to that observed in the late 1940s (Figure 3.6.7).

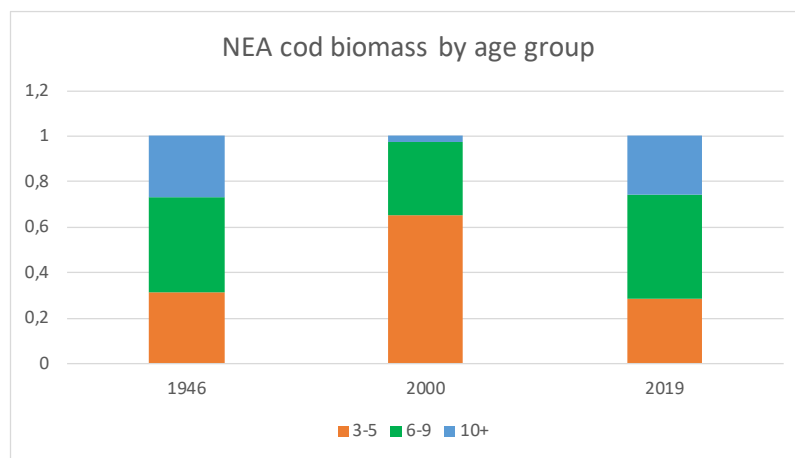


Figure 3.6.7. Age composition of the cod stock (biomass) in 1946, 2000 and 2019. From stock assessment in ICES 2019.

Cod expanded the area occupied during the period, as seen from the average distribution for three periods (2004-2009, 2010-2014, and 2015-2019, Figure 3.6.8). Higher catches of cod were distributed over larger area during the 2004-2009 period, while distribution was limited in the north and northeast Barents Sea. During the 2010-2014 period, higher catches of cod were observed mainly in the north and southeast, while their distribution extended northward and slightly north-eastward. Occupation of larger areas and redistribution of higher catches was most likely influenced by record high stock sizes, dominated by larger and older fish. During the 2015-2019 period, smaller catches of cod were taken in the northern and eastern areas compared

to the 2010-2014 period, and the northern limit of the distribution in the area between Spitsbergen and Frans Josef Land was shifted southwards from 2017 to 2019. Since 2004, ice free areas have generally increased in the northern Barents Sea, increasing areas of suitable habitat for cod and allowing record high production. However, a notable decrease in ice-free areas was observed in the winter survey 2019 compared to previous winter surveys, and preliminary reports from the 2020 winter survey indicate a further decrease in 2020.

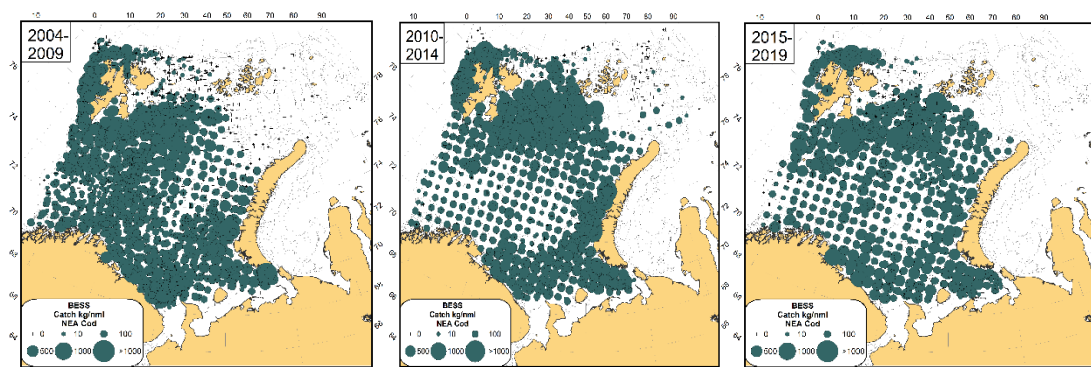


Figure 3.6.8. Distribution of cod catches (kg/nm) during August-September; averaged over 3 periods (2004-2009, 2010-2014, and 2015-2019).

Figure 3.6.9 shows the distribution of cod ≥ 50 cm based on data from the winter survey (January-March during 2008, 2011, and 2019). Note: the survey area was extended northwards in 2014 and coverage is often limited by ice conditions. Cod distribution observed during this survey increased throughout the period, but it is unknown when cod began to inhabit areas north of Bear Island and west of Svalbard during winter.

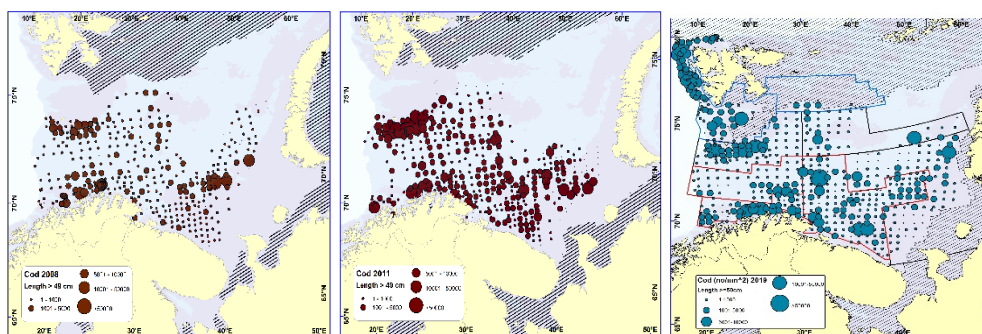


Figure 3.6.9. Distribution of cod ≥ 50 cm during winter 2008, 2011, and 2019.

3.6.2 NEA haddock

Young-of-the-year

Estimated abundance of 0-group haddock varied from 696 million in 1989 to 98,745 million individuals in 2005 with a long-term average of 13,440 million individuals for the 1980-2019 period (Figure 3.6.11). In 2019, the total abundance estimates for 0-group haddock were 892 million, that it is one of the lowest values observed in the time series. Thus the 2019-year class may be characterized as very weak.

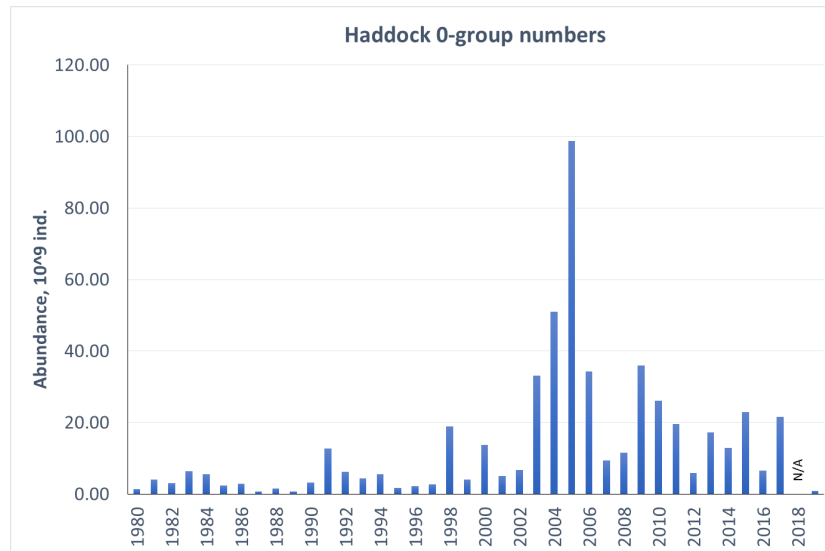


Figure 3.6.11. 0-group haddock abundance estimates and fluctuation in 1980-2019. Note that estimates were calculated for the new 15 subareas in the Barents Sea for the period 1980-2018 in MatLab (ICES 2018 WGIBAR), while for 2019 estimates were calculated using StoX (Johnsen et al. 2019).

In 2019, 0-group haddock in the Barents Sea was covered well, and spatial indices were estimated for all regions. 0-group haddock were distributed mainly in western regions (Svalbard South and Bear Island Trench, Figure 3.6.12). Haddock length varied from 2.5 to 13.5 cm, while the length distribution was dominated by haddock of 8.5-10.5 cm length. The smallest haddock were found in South West, while the largest was found in the Great Bank area.

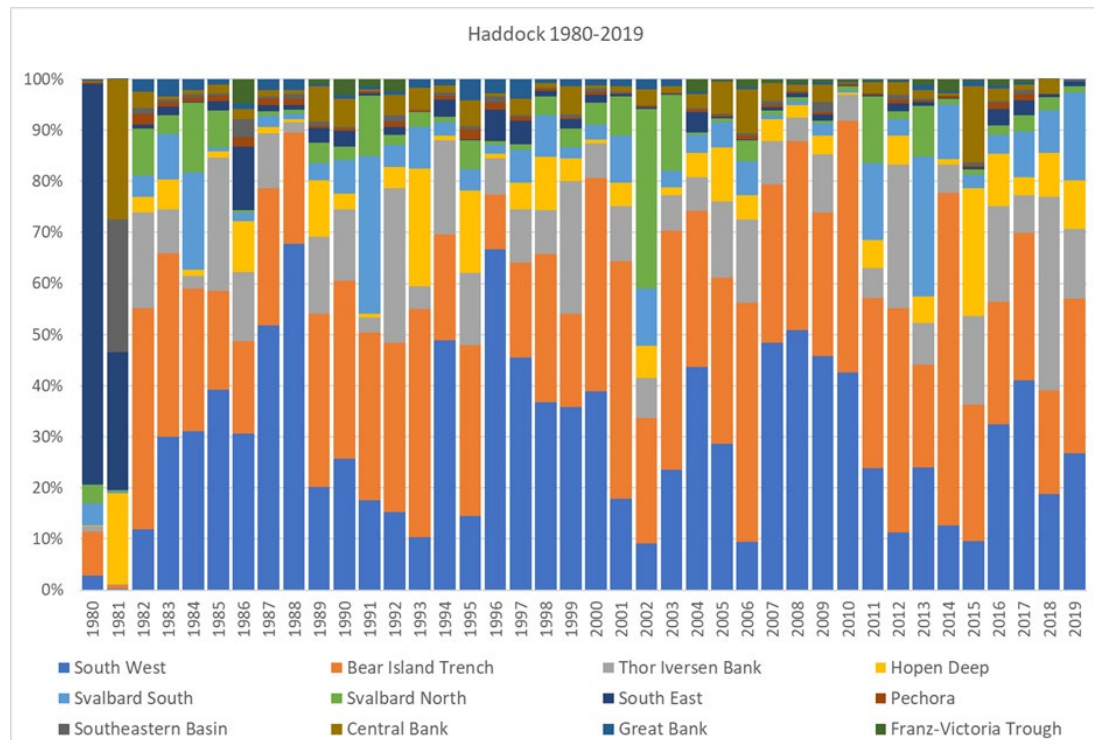


Figure 3.6.12. Percentage of 0-group haddock abundance distributed by different regions of the Barents Sea during 1980-2019. Note that estimates were calculated for the new 15 subareas in the Barents Sea for the period 1980-2018 in MatLab (ICES 2018 WGIBAR), while for 2019 the estimates using StoX (Johnsen et al. 2019).

Haddock one year old and older

The Northeast Arctic haddock stock reached record high levels in 2009–2013, due to very strong 2004–2006-year classes. Subsequent recruitment has normalized; the stock remains at a relatively high level but has declined in recent years. Forecasts based on survey indices indicate that the abundant 2016- and 2017-year classes may increase stock size rapidly in future years if survival is good. (Figures 3.6.13 and 3.6.14). The large spawning stock did not, until 2016, result in strong year classes (Figure 3.6.15).

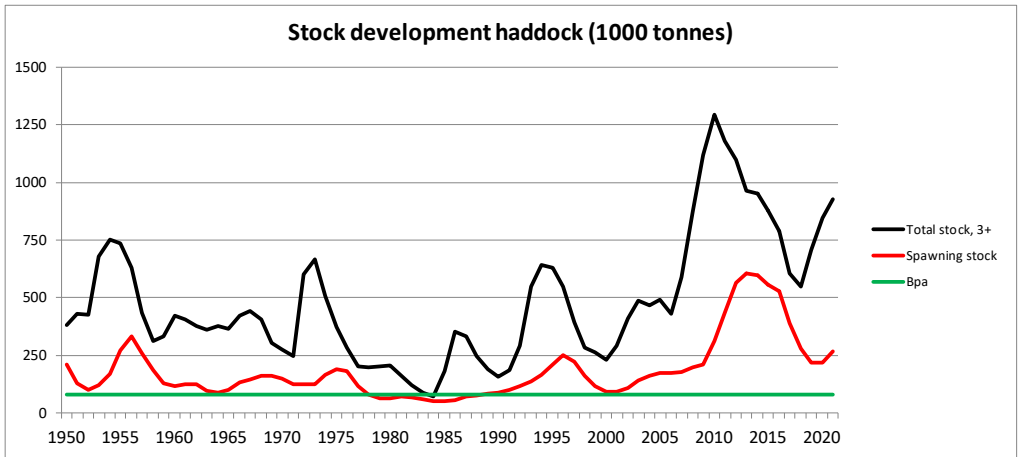


Figure 3.6.13. Haddock total stock and spawning stock development during the 1950-2019 period and forecast for 2020-2021 from AFWG (ICES 2019a).

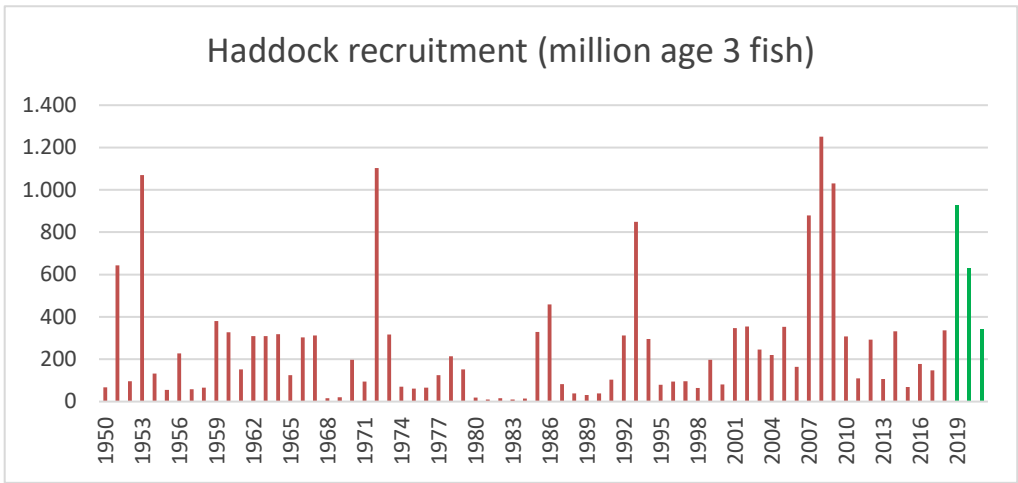


Figure 3.6.14 Recruitment of haddock during the 1950-2018 period (red) and forecast for 2019-2021 (green) from AFWG (ICES 2019a).

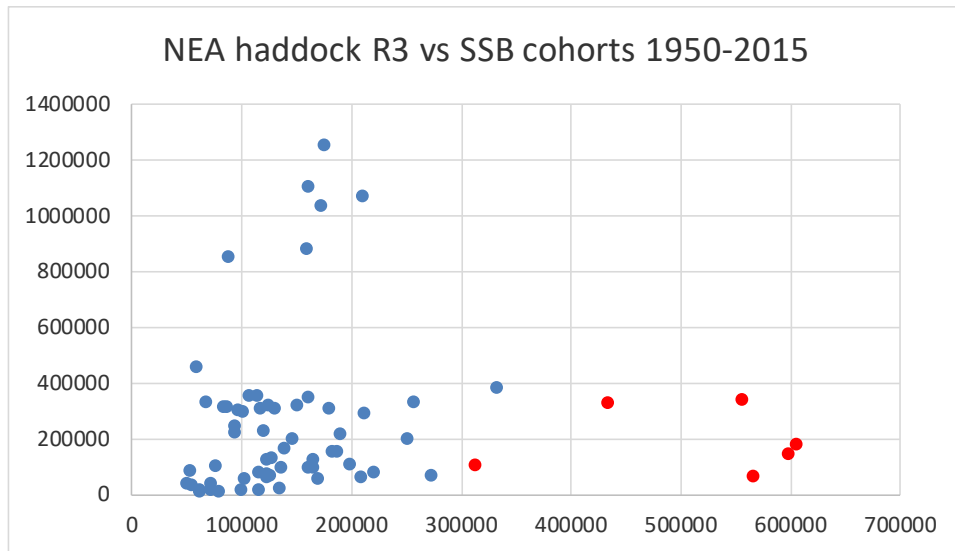


Figure 3.6.15. Spawning stock-recruitment plot for haddock cohorts 1950-2015. Cohorts 2010-2015 shown as red dots.

Occurrence of the very strong 2004-2006-year classes led to higher catches in the western and coastal areas. During the last two periods (2010-2014 and 2015-2019) haddock was distributed in the same areas but in much lower amounts (Figure 3.6.16).

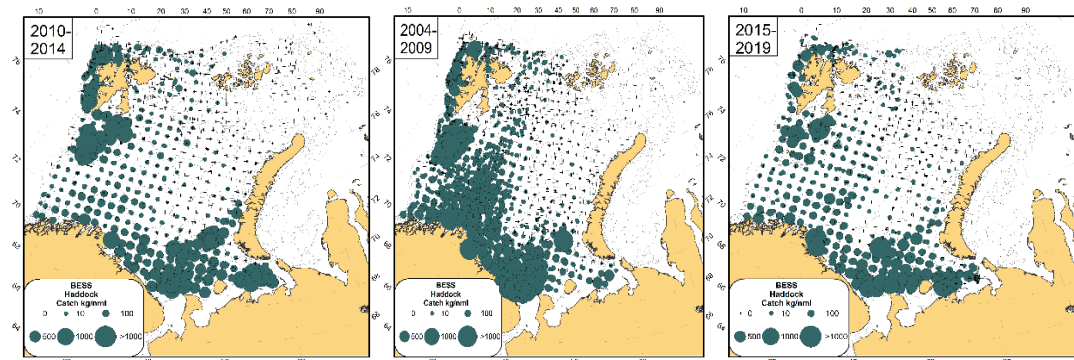


Figure 3.6.16. Distribution of haddock catches (kg/nm) during August-September averaged over 3 periods (2004-2009, 2010-2014, and 2015-2019).

Figure 3.6.17 shows the distribution of haddock ≥ 50 cm based on winter survey data (January-March) from 2008, 2011, and 2019. Note that the survey area was extended northwards in 2014 and that coverage often is limited by ice extent. Haddock distribution observed during this survey increased during this period, but when haddock began to inhabit areas north of Bear Island and west of Svalbard during winter is unknown.

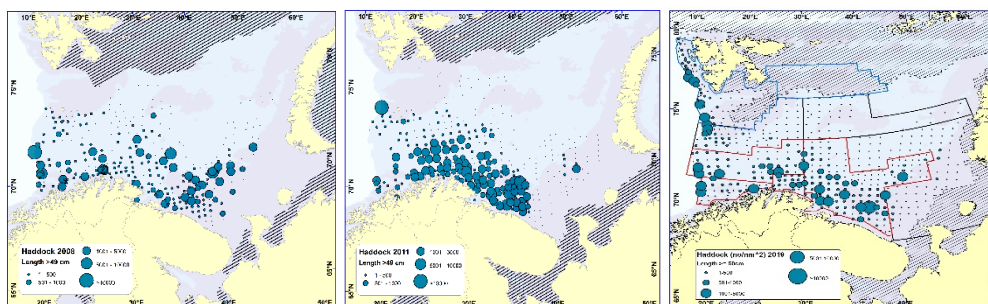


Figure 3.6.17. Distribution of haddock larger than 50 cm during winter 2008, 2011, and 2019.

3.6.3 Long rough dab

Young of the year

No abundance index for 0-group fish is available for 2018 due to a lack of survey coverage. Figure 3.6.18 shows the time series for the 1980-2017 period.

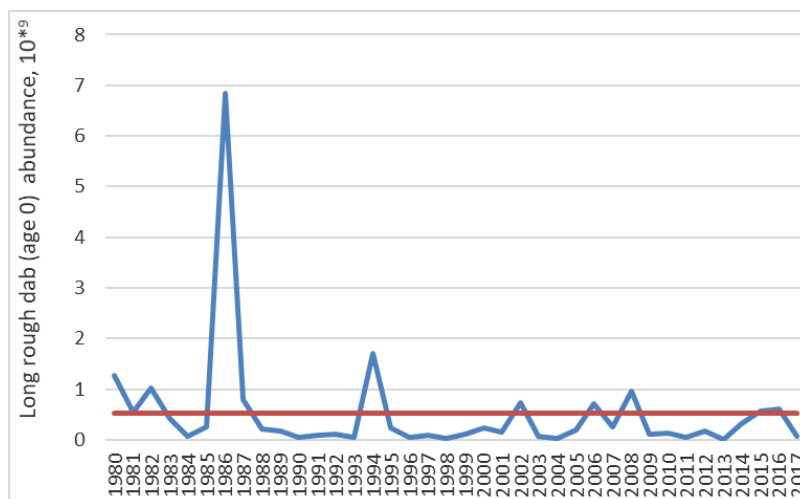


Figure 3.6.18. 0-group long rough dab abundance in the Barents Sea during the 1980-2017 period corrected for trawl efficiency. Red line shows the long-term average; the blue line indicates fluctuating abundance.

Older long rough dab

Older long rough dab (age 1+) are widely distributed in the Barents Sea. Long rough dab abundance estimates based on results from the BESS time-series (August–September) have been relatively stable during the current decade. Many small fish were observed in trawl catches especially in eastern areas during the 2015-2017 BESS. The 2018 index was not calculated due to limited survey coverage in the eastern region of the Barents Sea and in 2019 index estimated abundance somewhat above mean for period 2004-2017. (Figure 3.6.19).

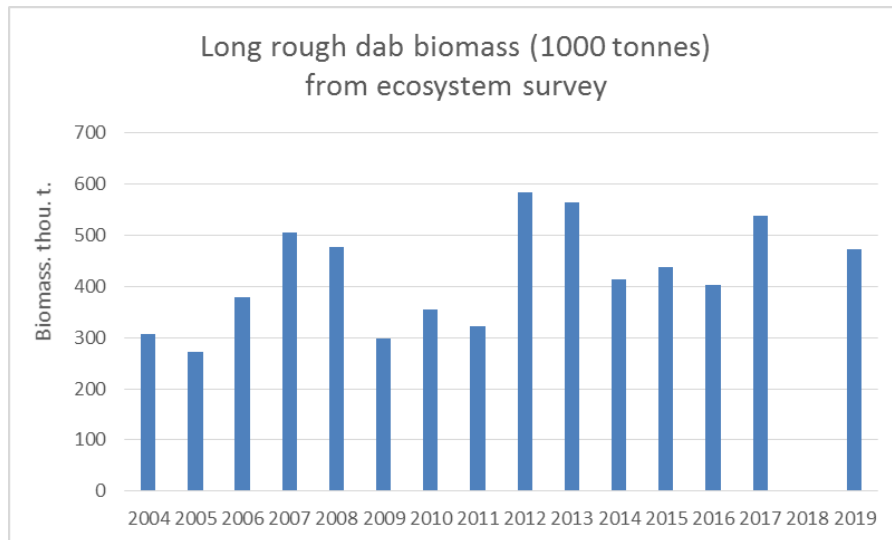


Figure 3.6.19. Stock biomass of long rough dab based on BESS data during the 2004–2019 period, calculated using bottom-trawl estimated swept area.

Previously during the Russian Autumn-Winter Survey (October-December) major concentrations of long rough dab in the central, northern, and eastern areas were found.

The catch-per-unit-effort index (CPUE) from this survey was calculated as number of specimens caught per 1 hour of trawling. For period 1982–2015 the index ranged from 30 to 120, amounting to 90 specimens per 1 hour of trawling on average.

In 2017 values twice as high as the long-term average were found as the survey was performed in a limited area where the main concentration of young long rough dab occurred. Excluding areas with low fish concentrations in calculations can lead to overestimates in this index (Figure 3.6.20). It is difficult to track trends with this index, because in 2016 and in 2018–2019 the survey was not performed.

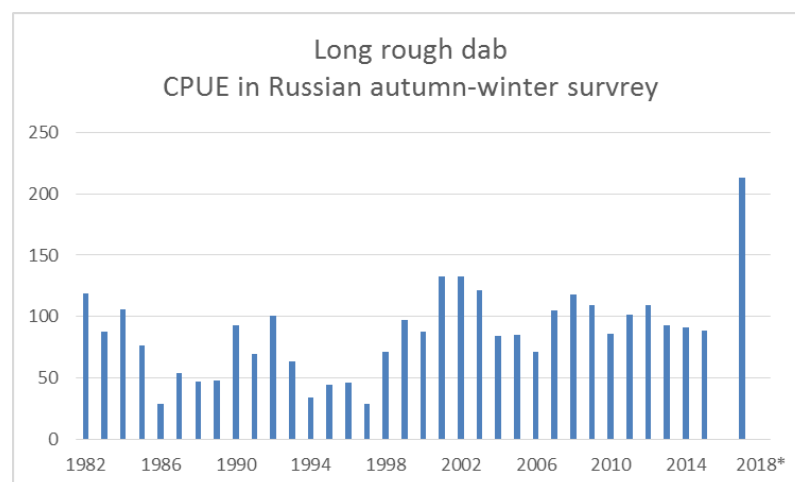


Figure 3.6.20. Estimated of long rough dab from the Russian Autumn-Winter Survey (October-December) during the 1982–2019 period. No survey coverage in 2016 and 2018–2019 and limited survey coverage in 2017.

3.6.4 Greenland halibut

Young of the year

The 2018 index for 0-group fish is not available due to lack of survey coverage.

Older Greenland halibut

The adult component of the stock was, as usual, mainly distributed outside the ecosystem survey area, i.e. on the slope. The abundance on the slope has decreased in recent years (Fig 3.6.21). In recent years, however, an increasing number of large Greenland halibut has been captured in deeper waters of the area surveyed by the BESS (Figure 3.6.22). Northern and north-eastern areas of the Barents Sea serve as nursery grounds for the stock. Greenland halibut are also relatively abundant in deep channels running between the shallowest fishing banks.

The fishable component of the stock (length ≥ 45 cm) increased from 1992 to 2012 and has remained stable since that time (Figure 3.6.23). The harvest rate has been low and relatively stable since 1992.

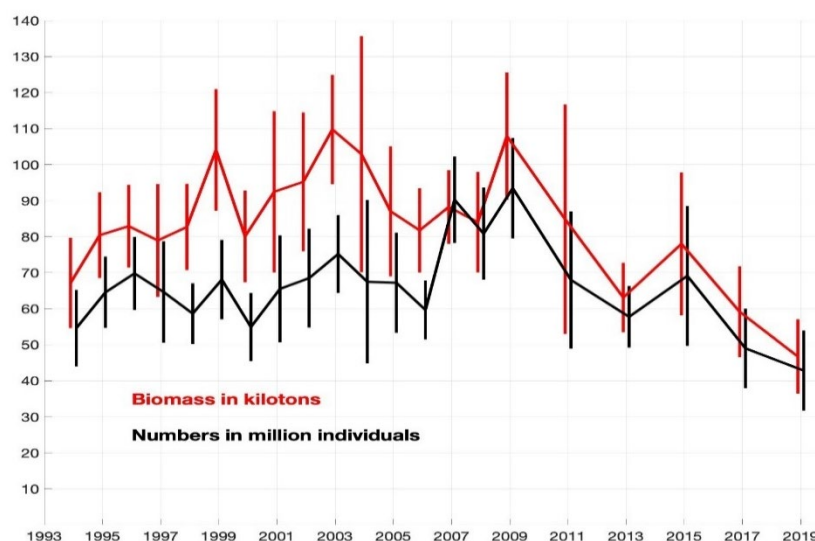


Figure 3.6.21. Biomass index for Greenland halibut from Norwegian slope survey; 2014 excluded due to poor area coverage (update of ICES 2019a fig 8.7)

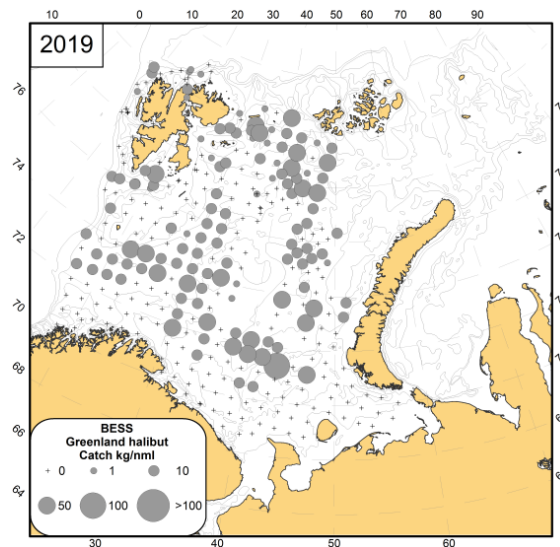


Figure 3.6.22 Greenland halibut distribution (specimens/nautical mile) during August–September 2019 based on the BESS data.

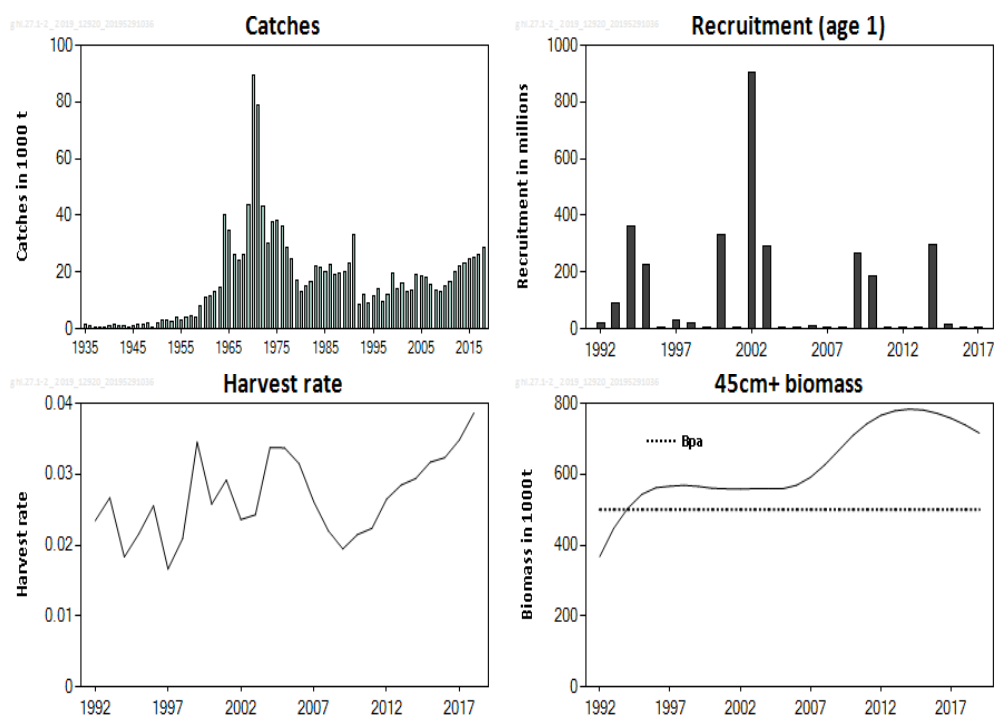


Figure 3.6.23. Northeast Arctic Greenland halibut: catches, recruitment, harvest rate and biomass of 45+ cm Greenland halibut as estimated by the GADGET model during the 1992–2018 period (ICES 2019a).

3.6.5 Beaked (deepwater) redfish (*S. mentella*)

Young-of-the-year

Estimated abundance of 0-group deepwater redfish varied from 9 million individuals in 2001 to 191,145 million in 2007 with an average of 53,355 million individuals for the 1980–2019 period (Figure 3.6.24). In 2019, the total abundance index for 0-group

deepwater redfish were 91,065 million individuals, which is higher than the long-term mean. Thus the 2019-year class may be characterized as close to strong.

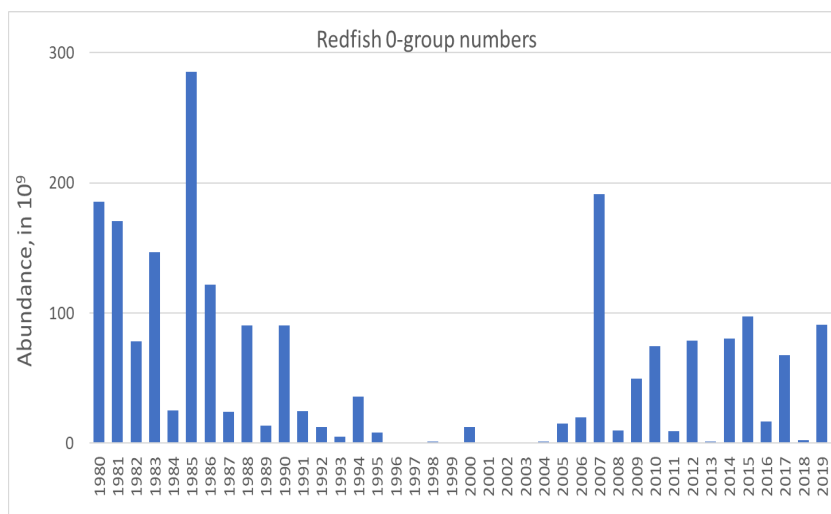


Figure 3.6.24. 0-group deepwater redfish abundance (corrected for trawl efficiency) in the Barents Sea during 1980-2019. Note that estimates were calculated for the new 15 subareas in the Barents Sea for the period 1980-2018 in MatLab (ICES 2018 WGIBAR), while for 2019 they were calculated using StoX (Johnsen et al. 2019).

In 2019, 0-group deepwater redfish were distributed mainly in regions of Svalbard (Svalbard South and Bear Island Trench, Figure 3.6.25). The deepwater redfish were 3.9 cm long (on average). The largest fish with average length 4.6 cm were observed in Svalbard North, while smallest with an average of 2.1 cm in the South West.

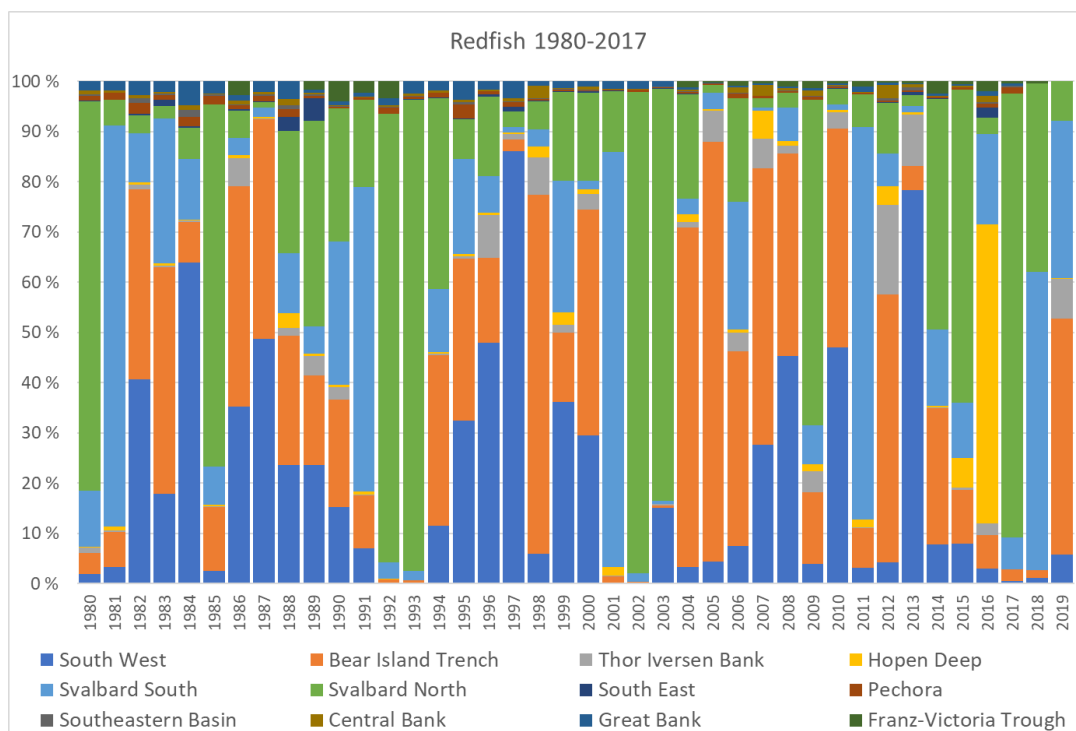
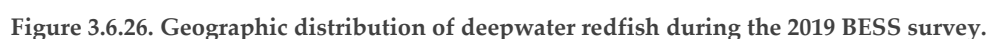


Figure 3.6.25. Percentage of 0-group deepwater redfish abundance in the Barents Sea during 1980-2019. Note that estimates were calculated for the new 15 subareas in the Barents Sea for the period 1980-2018 in MatLab (ICES 2018 WGIBAR), while for 2019 they were calculated using StoX (Johansen et al. 2019).

In 2019, deepwater redfish were widely distributed in the Barents Sea. During the BESS and the winter survey, the largest concentrations were observed, as usual, in western and north western parts of the Barents Sea. Biomass was higher during 2013–2019 than in preceding years. Geographic distribution of deepwater redfish during the 2019 BESS is shown in Figure 3.6.26. The area of coverage for redfish during BESS 2019 was complete in the north and east. Most of the adult fish are observed in the Norwegian Sea. Stock development trends from the latest ICES AFWG assessment are shown in Figure 3.6.27. During the last decade the deepwater redfish total stock biomass has remained relatively stable around 1 million tonnes. From 1992 to 2002, there was an increase in the total stock, then, from 2003 to 2011, its stabilization, and in 2012-2018 - further growth, which has slowed in the last 3 years. Spawning stock increased in the period from 1992 to 2007, then it declined until 2013. Over the past 5 years, the biomass of spawning stock has stabilized. The decrease in spawning stock was due to poor year-classes of 1996-2003. Year classes of 2011-2016 were estimated as below average, but above the poor year-classes of 1996-2003.



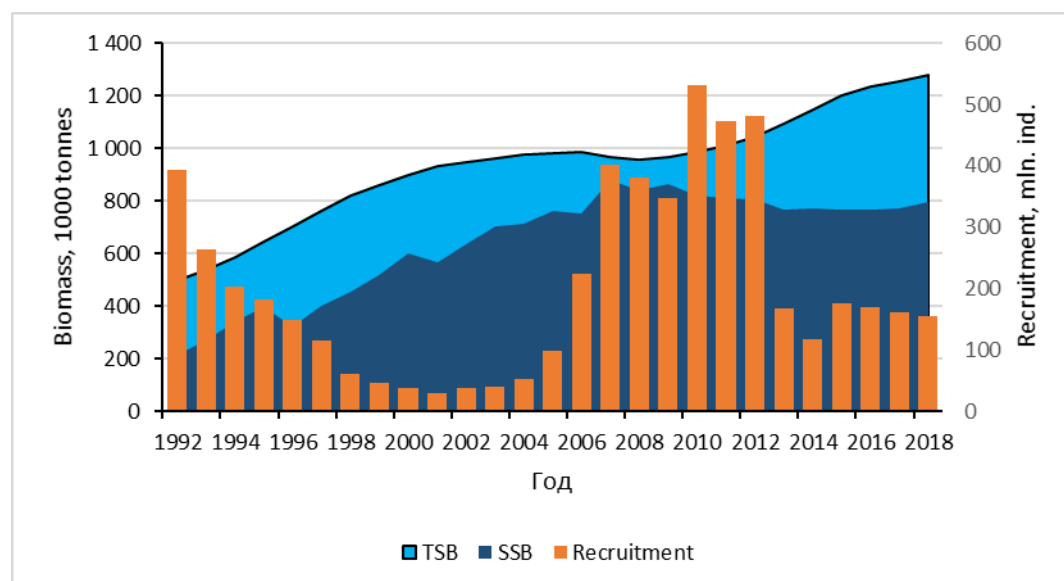


Figure 3.6.27. Results from a statistical catch-at-age model showing trends in total stock biomass (TSB) (1000 tonnes), spawning-stock biomass (SSB, 1000 tonnes) and recruitment-at-age 2 (individuals) during the 1992–2018 period for beaked redfish in ICES Subareas 1 and 2 (ICES, 2019a).

References

- Andrivashev, A.P. and Chernova, N.V. 1995. Annotated list of fish-like vertebrates and fishes of the Arctic Seas and adjacent waters. *Journal of Ichthyology*, 34: 435-456.
- Dolgov, A.V., Johannesen, E., and Høines, Å. 2011. Main species and ecological importance. In *The Barents Sea Ecosystem Resources and Management. Half a century of Russian-Norwegian Cooperation*. Pp 193-200. Ed by T. Jakobsen, V. Ozhigin. Tapir Academic Press, Trondheim Norway.
- ICES 2019a. Arctic Fisheries Working Group (AFWG). ICES Scientific Reports. 1:30. 930 pp. <http://doi.org/10.17895/ices.pub.5292>
- Johnsen, E., Totland, A., Skålevik, Å., Holmin, A. I., Dingsør, G. E., Fuglebakk, E., & Handegard, N. O. (2019). StoX: An open source software for marine survey analyses. *Methods in Ecology and Evolution*, 10 :1523 – 1528. <https://doi.org/10.1111/2041-210X.13250>
- Mecklenburg, C.W., I. Bvrkiedal, I.S. Christiansen, O.V. Karamushko, A. Lvnghammar and P. R. Møller. 2013. List of marine fishes of the arctic region annotated with common names and zoogeographic characterizations. *Conservation of Arctic Flora and Fauna*, Akureyri, Iceland

3.7 Zoogeographical groups of non-commercial species

By E. Johannesen (IMR), T. Prokhorova (PINRO) and B. Husson (IMR)

Non-commercial demersal fish species were grouped according to their biogeography to assess their relative abundance, trends and suitable habitats. Abundance of Arctic species seems to have increased in 2019 compared to the two previous years. This is probably due to high catches of Liparids. Zoogeographic grouping is consistent with their suitable habitats. Temperature is a major driver of the suitable habitats

During the 2019 Barents Sea Ecosystem Survey (BESS) 90 fish species from 28 families were recorded in pelagic and bottom trawl catches, some taxa were recorded at genus or family level only (Prokhorova et al 2020). The species were grouped into seven zoogeographic group (Widely Distributed, South Boreal, Boreal, Mainly Boreal, Arctic-Boreal, Mainly Arctic and Arctic) defined in Andriashev and Chernova (1995). In the following only bottom trawl catches of non-commercial fishes were used. Both demersal (including benthopelagic) and pelagic (neritopelagic, epipelagic, bathypelagic) species were included.

The survey coverage at BESS in 2018 was poor (Prokhorova et al 2019) so we cannot easily compare the abundance and distribution of zoogeographical groups in 2019 with 2018, but we can compare with 2017 (Prokhorova et al 2018a, Prokhorova et al 2020). There seems to be an increase in the abundance (medium and maximum catches in bottom trawls) in Arctic and Mainly Arctic species in 2019 (Figure 3.7.1). The increase in arctic fishes in 2019 is mostly due very high catches of *Liparis fabricii*. This is consistent with the observed increase in 0-group liparids observed in the 2017 survey (Prokhorova et al 2018b).

A paper is submitted to Fisheries Oceanography estimating the potential suitable habitats of the 33 most abundant fish species of Barents Sea using bottom trawl data from the ecosystem survey (2004-2017). It relies on the modelling of a high quantile (99th) of the biomass distribution of each of the 33 species in response to 10 potential predictors: bottom and surface temperatures and salinities, ice coverage, depth of the surface mixing layer, chlorophyll a concentrations and temporally fixed environmental conditions like sediment, slope and depth. The method identifies habitat variables that limit the fish distributions. The same analysis was run on the zoogeographic groups (species pooled, the common species excluded, see figures 3.7.2-3.7.7.

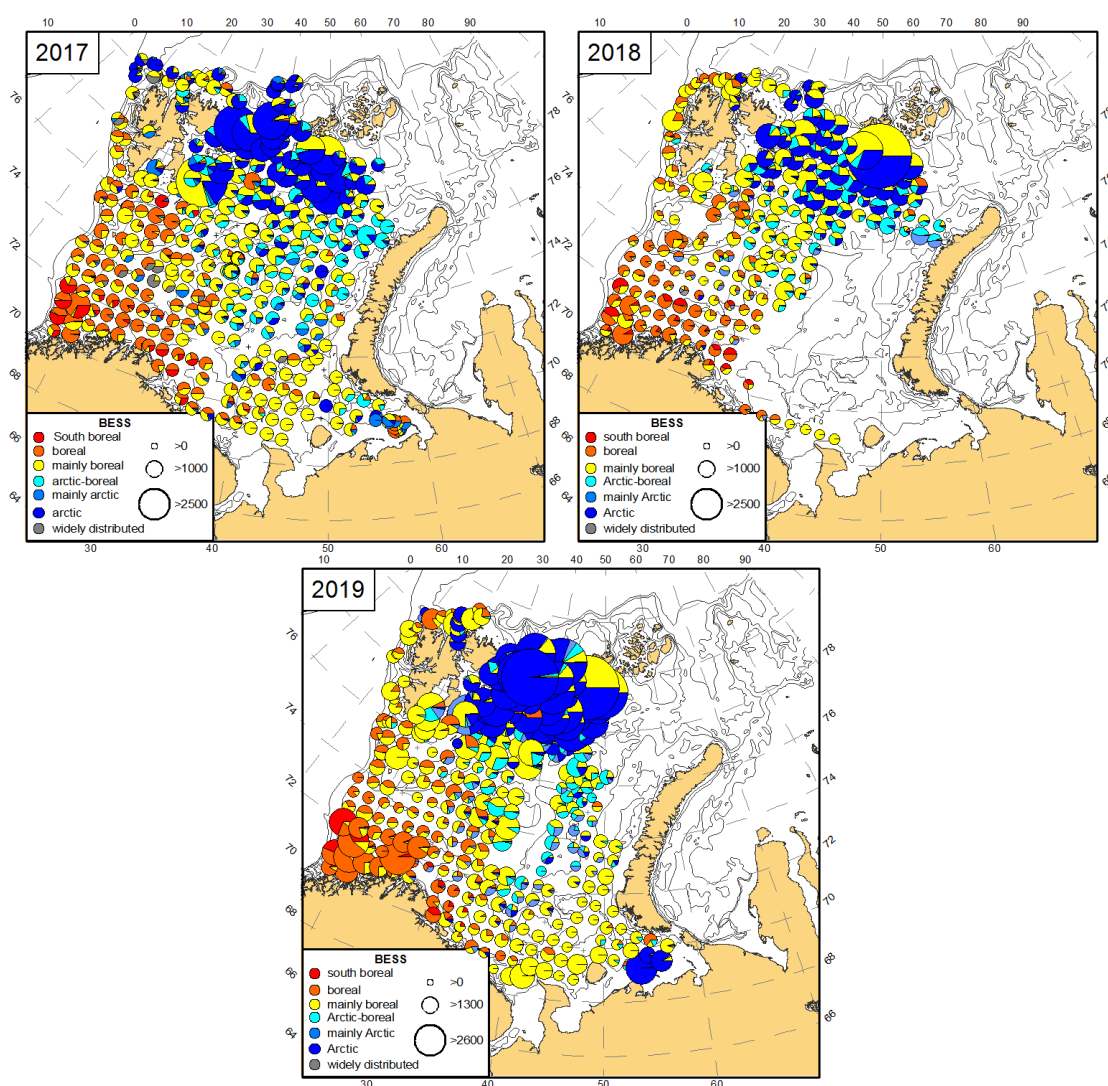


Figure 3.7.1. Distribution of non-commercial fish species from zoogeographic groups during the ecosystem survey 2017-2020. The size of circle corresponds to abundance (individuals per nautical mile, only bottom trawl stations were used, both pelagic and demersal species are included). Taken from survey reports (Prokhorova et al 2018a, Prokhorova et al 2019, Prokhorova et al 2020).

What we designated as «arctic» are species from north and east limited in the south west by bottom temperature and salinity (Figure 3.7.2).

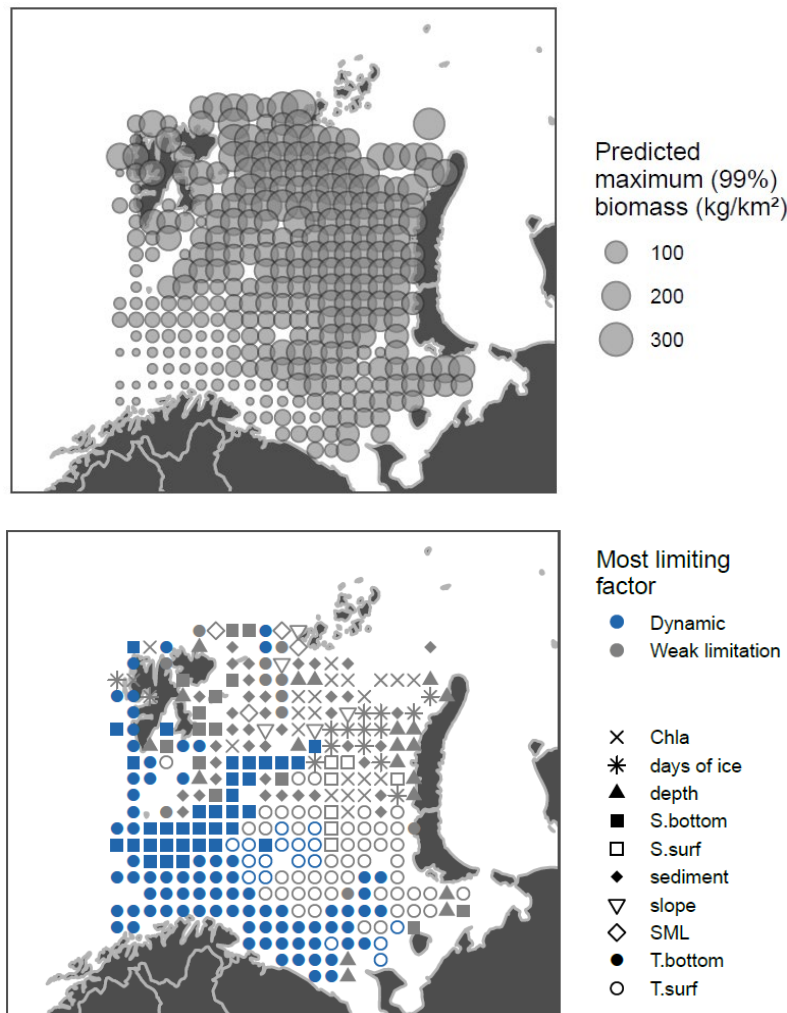


Figure 3.7.2. Arctic fishes (*Amblyraja hyperborea*, *Aspidophoroides olrikii*, *Careproctus* spp., *Eumicrotremus derjugini*, *Gaidropsarus argentatus*, *Liparis fabricii*, *Liparis tunicatus*, *Lycenchelys kolthoffi*, *Lycenchelys muraena*, *Lycodes adolfi*, *Lycodes eudipleurostictus*, *Lycodes frigidus*, *Lycodes luetkenii*, *Lycodes pallidus*, *Lycodes polaris*, *Lycodes reticulatus*, *Lycodes rossi*, *Lycodes seminudus*, *Lycodes squamiventer*, *Lycodon flagellicauda*, *Paraliparis bathybius*, *Rhodichthys regina*, *Triglops nybelini*) data from ecosystem survey 2013. Top: max predicted abundance, bottom: symbols show limiting habitat factors: green if they are temporally fixed (sediment, depth, slope), blue if they are temporally dynamic (all other parameters), grey if they are only weakly limiting (predicted maximum biomass $\geq 25\%$ of the species-predictor QGAM model maximum).

What we designated as «Mainly-arctic» are: Species mainly from north limited in the south by ice and surface temperature and sensitive to shallow depth (Figure 3.7.2).

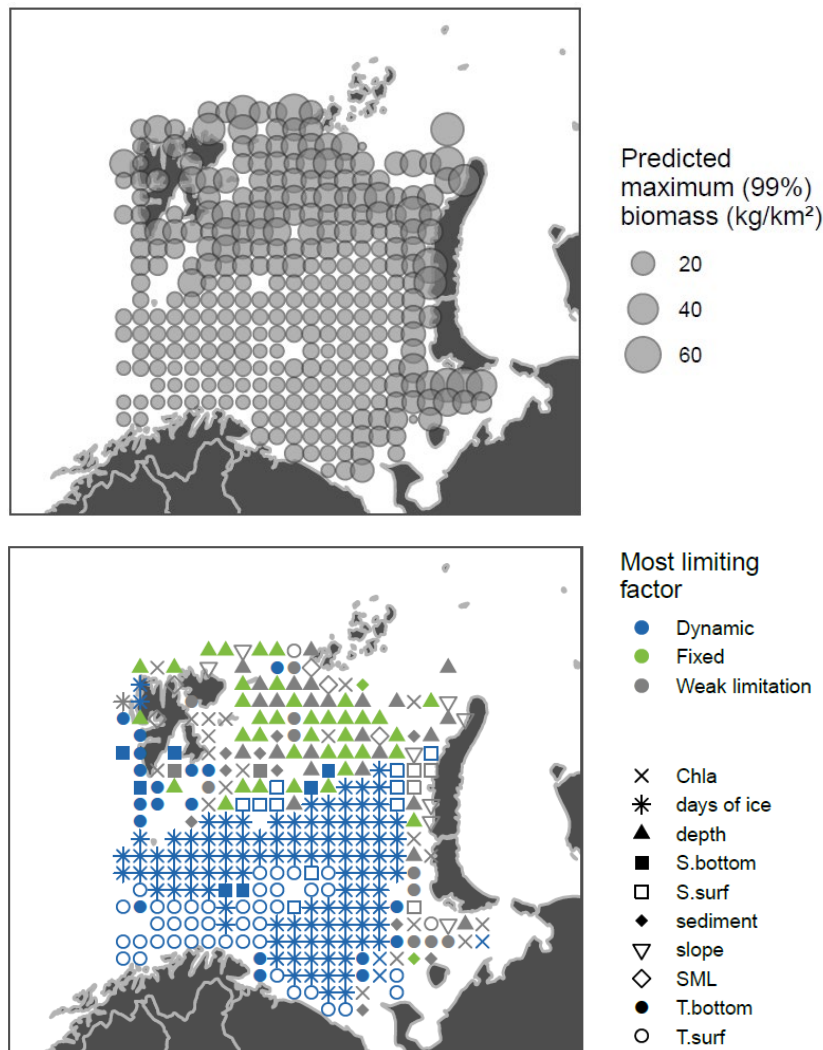


Figure 3.7.3. Mainly Arctic fishes (*Cottunculus microps*, *Eumicrotremus spinosus*, *Gymnocanthus tricuspis*, *Liparis bathyarcticus*) data from ecosystem survey 2013. Top: max predicted abundance, bottom: symbols show limiting habitat factors: green if they are temporally fixed (sediment, depth, slope), blue if they are temporally dynamic (all other parameters), grey if they are only weakly limiting (predicted maximum biomass $\geq 25\%$ of the species-predictor QGAM model maximum).

What we designated as « arctic-boreal » are: Species from north and east limited in the south west by temperature (Figure 3.7.4). The difference with the Arctic group may be a question of depth preferences.

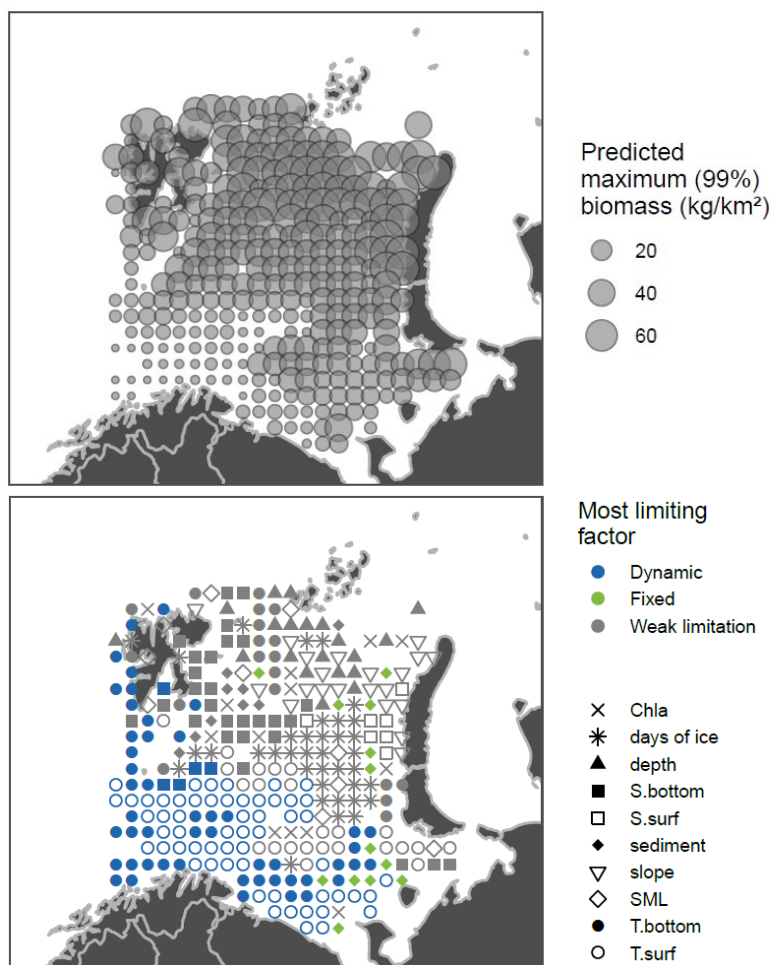


Figure 3.7.4. Arctic boreal fishes (*Leptagonus decagonus*, *Triglops pingelii*) data from ecosystem survey 2013. Top: max predicted abundance, bottom: symbols show limiting habitat factors: green if they are temporally fixed (sediment, depth, slope), blue if they are temporally dynamic (all other parameters), grey if they are only weakly limiting (predicted maximum biomass $\geq 25\%$ of the species-predictor QGAM model maximum).

What we designated as « mainly boreal » are: Widespread species not really limited by the environmental conditions in the Barents Sea

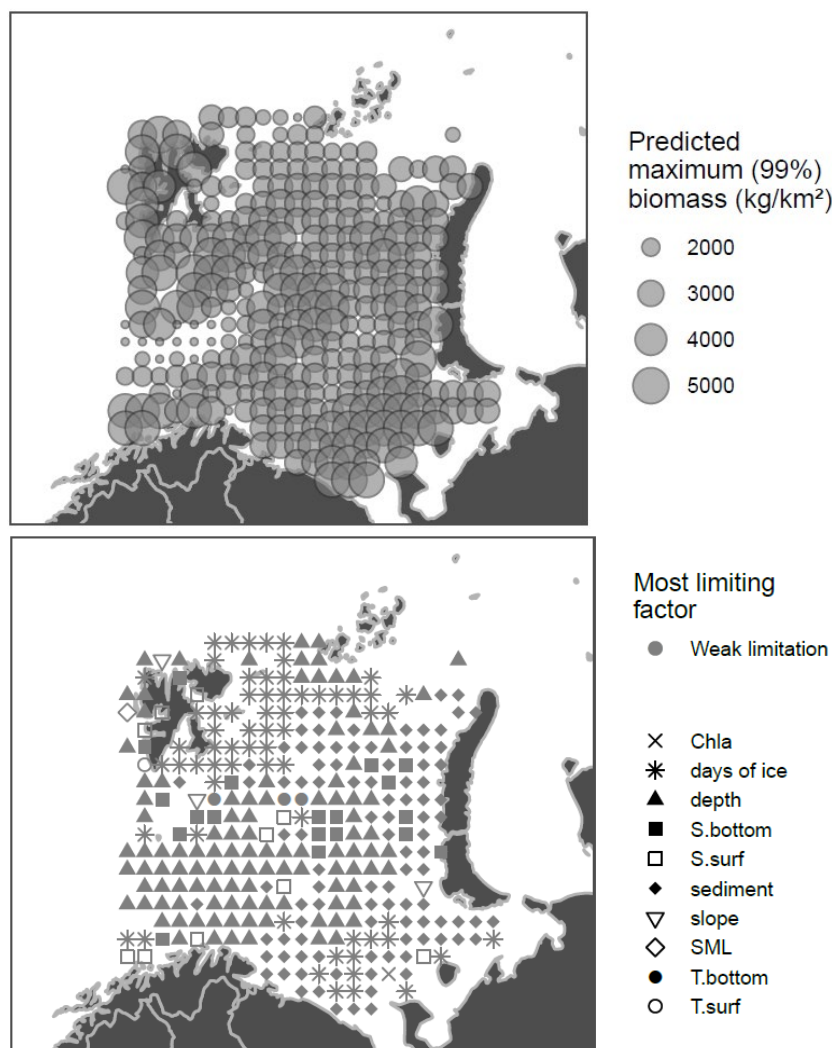


Figure 3.7.5. Mainly boreal fishes (*Amblyraja radiata*, *Anarhichas denticulatus*, *Anarhichas lupus*, *Anarhichas minor*, *Arctodiellus atlanticus*, *Bathyraja spinicauda*, *Brosme brosme*, *Cyclopterus lumpus*, *Glyptocephalus cynoglossus*, *Hippoglossoides platessoides*, *Hippoglossus hippoglossus*, *Leptoclinus maculatus*, *Lethenteron camtschaticum*, *Limanda limanda*, *Lumpenus lampretaeformis*, *Lycodes esmarkii*, *Lycodes gracilis*, *Myoxocephalus scorpius*, *Pleuronectes platessa*, *Pollachius virens*, *Rajella fyllae*) data from ecosystem survey 2013. Top: max predicted abundance, bottom: symbols show limiting habitat factors: green if they are temporally fixed (sediment, depth, slope), blue if they are temporally dynamic (all other parameters), grey if they are only weakly limiting (predicted maximum biomass $\geq 25\%$ of the species-predictor QGAM model maximum).

What we designated as «boreal» are: Species from the south limited in the north by temperature and that avoid depth (Figure 3.7.6).

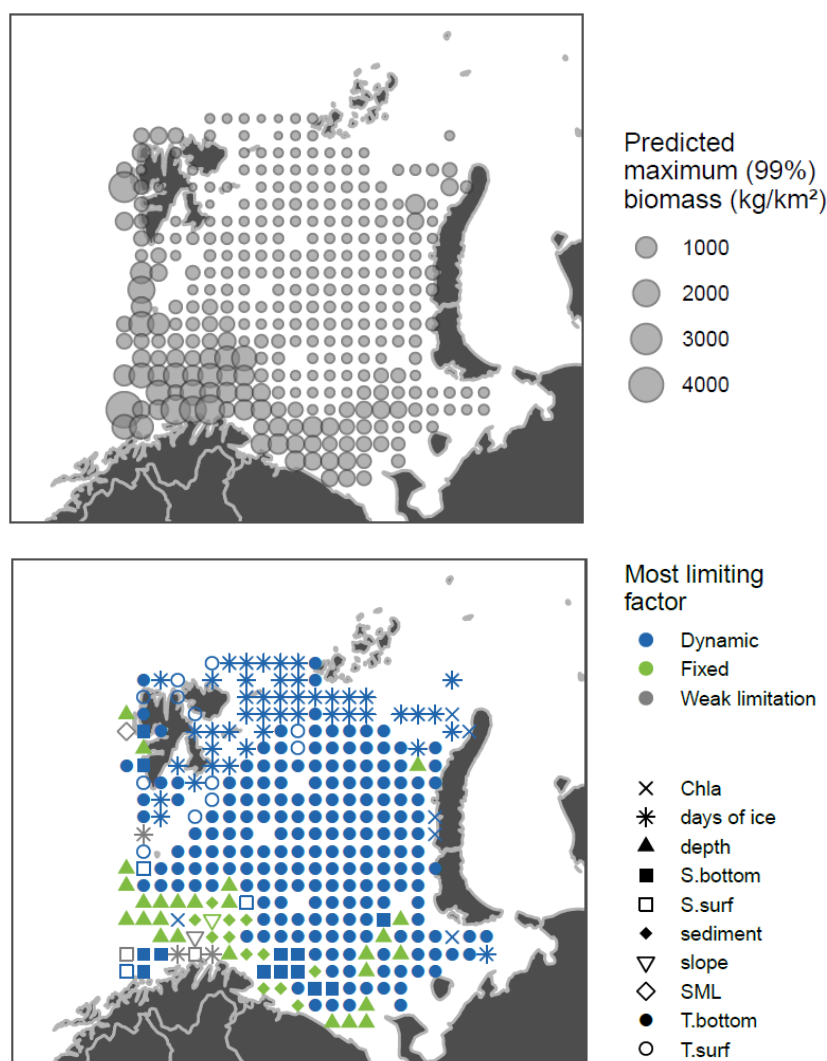


Figure 3.7.6. Boreal fishes (*Anisarchus medius*, *Argentina silus*, *Chimaera monstrosa*, *Enchelyopus cimbrius*, *Liparis liparis*, *Lycenchelys sarsii*, *Macrourus berglax*, *Microstomus kitt*, *Molva molva*, *Pollachius pollachius*, *Rajella lintea*, *Sebastes viviparus*, *Triglops murrayi*, *Trisopterus esmarkii*, *Phrynorhombus norvegicus*) data from ecosystem survey 2013. Top: max predicted abundance, bottom: symbols show limiting habitat factors: green if they are temporally fixed (sediment, depth, slope), blue if they are temporally dynamic (all other parameters), grey if they are only weakly limiting (predicted maximum biomass $\geq 25\%$ of the species-predictor QGAM model maximum).

What we designated as «south-boreal» are: Species from the south limited in the north by temperature and that avoid depth (Figure 3.7.7). These species appear to have very similar suitable habitats as the boreal species (Figure 3.7.7).

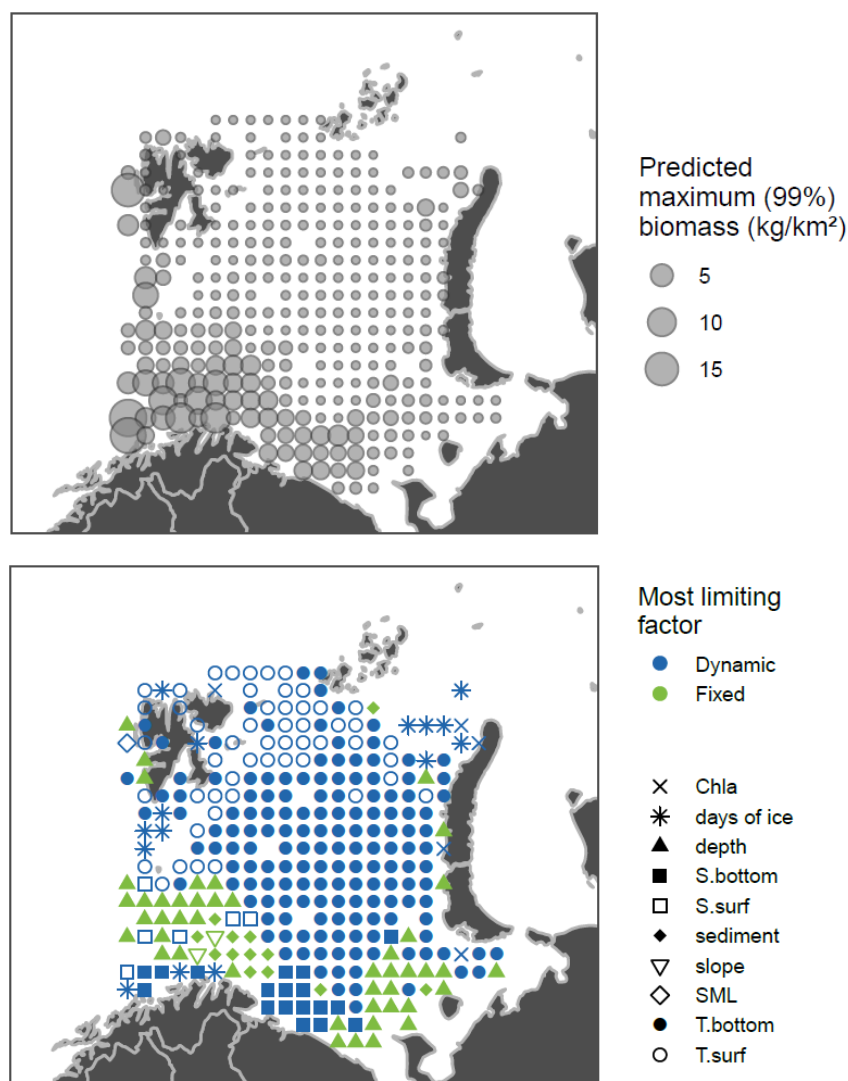


Figure 3.7.7. South boreal fishes (*Gadiculus argenteus*, *Lophius piscatorius*, *Merlangius merlangus*, *Merluccius merluccius*, *Phycis blennoides*) data from ecosystem survey 2013. Top: max predicted abundance, bottom: symbols show limiting habitat factors: green if they are temporally fixed (sediment, depth, slope), blue if they are temporally dynamic (all other parameters), grey if they are only weakly limiting (predicted maximum biomass \geq 25% of the species-predictor QGAM model maximum).

To sum up, there seem to be an increase in abundance of Arctic species in 2019 compared to the years after 2013. Some very high catches of *Liparis fabricii* is mainly responsible for this increase.

References

- Andrivashev, A.P. and Chernova, N.V. 1995. Annotated list of fish-like vertebrates and fishes of the Arctic Seas and adjacent waters. *Journal of Ichthyology*, 34: 435-456.
- Husson B., Certain G., Filin A., Planque B. submitted to *Fisheries Oceanography*, Suitable habitats of fish species in the Barents Sea
- Prokhorova T., Johannesen E., Dolgov A. and Wienerroither R. 2018a. Zoogeographic groups. In: Survey report from the joint Norwegian/Russian ecosystem survey in the Barents Sea and adjacent waters, August-October 2017. Prozorkevich, D., Johansen G.O., and van der Meeren, G.I. 2018 (Eds.) IMR/PINRO Joint Report Series, No. 2/2018
- Prokhorova T., Eriksen E., and Dolgov A. 2018b. Fish biodiversity in the pelagic component In: Survey report from the joint Norwegian/Russian ecosystem survey in the Barents Sea and adjacent waters, August-October 2017. Prozorkevich, D., Johansen G.O., and van der Meeren, G.I. 2018 (Eds.) IMR/PINRO Joint Report Series, No. 2/2018
- Prokhorova T., Johannesen E., Dolgov A. and Wienerroither R. 2019. Zoogeographic Survey

report from the joint Norwegian/Russian ecosystem survey in the Barents Sea and adjacent waters, August-October 2018 (ed by van der Meeren, G.I and Prozorkevich D.). IMR/PINRO Joint Report Series, No. 2/2019.

Prokhorova T., Iohannesen E., Dolgov A. and Wienerroither R. 2020. Zoogeographic groups. In: Survey report from the joint Norwegian/Russian ecosystem survey in the Barents Sea and adjacent waters, August-October 2018 (ed by van der Meeren, G.I and Prozorkevich D.). IMR/PINRO Joint Report Series, No. x/2020

3.8 Marine mammals and sea birds

3.8.1 Marine mammals

By Nils Øien and Roman Klepikovskiy

The summer abundance of minke whales in the Barents Sea has recently increased from a stable level of about 40,000 animals to more than 70,000 animals. Also, humpback whales have increased their summer abundance in the Barents Sea from a low level prior to year 2000 to about 4,000 animals thereafter. The other cetacean populations have remained stable in numbers. In 2019, 2686 individuals of ten species of marine mammals were sighted during the Barents Sea Ecosystem Survey (BESS) in August-October 2019, as well as an additional 64 individuals which were not identified to species. The baleen whales had a more aggregated and southerly distribution than in previous years with main occurrence in the Bear Island area and west and north of Hopen, and south of 78°N. This may have been caused by the reduced capelin abundance.

During the Barents Sea ecosystem survey in August-October 2019 marine mammal observers were onboard all vessels. In total, 2686 individuals of 10 species of marine mammals were observed and an additional 64 individuals were not identified to species. The observations are presented in Table 3.8.1.1 and distributions in the Figures 3.8.1.1 (toothed whales) and 3.8.1.2 (baleen whales).

As in previous years, the white-beaked dolphin (*Lagenorhynchus albirostris*) was the most common species with nearly 60% of all individual registrations. This species was widely distributed in the survey area. Apparently, most records of this species coincide with the distributions of herring, capelin, polar cod, juvenile cod and other fishes in the research area.

Besides the white-beaked dolphins, sperm whales (*Physeter macrocephalus*), harbour porpoises (*Phocoena phocoena*) and killer whales (*Orcinus orca*) were represented among the toothed whales. Sperm whales were observed in deep waters along the continental slope but also within the Barents Sea proper west of 29° E. The harbor porpoises were observed in the southern parts of the Barents Sea, including coastal areas. A notable observation was made of a group of 6 killer whales in the northern Barents Sea at 79°45'N-41°33'E.

Table 3.8.1.1. Numbers of marine mammal individuals observed from the R/V “Johan Hjort”, “G.O. Sars”, “Helmer Hansen” and “Vilnyus” during BESS 2019.

Order/suborder	Name of species	Total	%
<i>Cetacea/ Baleen whales</i>	Fin whale	205	7.5
	Humpback whale	266	9.7
	Minke whale	241	8.8
	Unidentified large whale	51	1.9
<i>Cetacea/ Toothed whales</i>	White-beaked dolphin	1593	57.9
	Harbour porpoise	15	0.5
	Killer whale	10	0.4
	Sperm whale	13	0.5
	Unidentified dolphin	8	0.3
<i>Pinnipedia</i>	Harp seal	338	12.3
	Walrus	3	0.1
	Bearded seal	2	0.1
	Unidentified seal	5	0.2
Total sum		2750	100

The baleen whale species minke (*Balaenoptera acutorostrata*), humpback (*Megaptera novaeangliae*) and fin (*Balaenoptera physalus*) whales were abundant in the Barents Sea, and 25% of all the animals belonged to them. These species were often found together in aggregations. In 2019, unlike in previous years, baleen whales were observed mainly south of 78°N due to low concentrations of capelin in the north.

Minke whales are widely distributed in the Barents Sea. In 2019 minke whales were recorded in large numbers in the area between Bear island and the Norwegian coast, in the southeastern Barents Sea and north of Hopen and the Great Bank. In 2018 their highest concentrations were further north and they were seen in reduced numbers both compared to the previous year 2017 and the following year 2019. In 2019 the densest concentrations of minke whales in northern and eastern areas overlapped with capelin, polar cod and herring aggregations.

In 2019 the humpback whales were recorded in considerable numbers in the area around Bear Island, west of Hopen Island and in the northern Barents Sea. This was different from the 2018 pattern when the humpbacks were concentrated in the northern area. The change was probably caused by the low concentrations of capelin in the north.

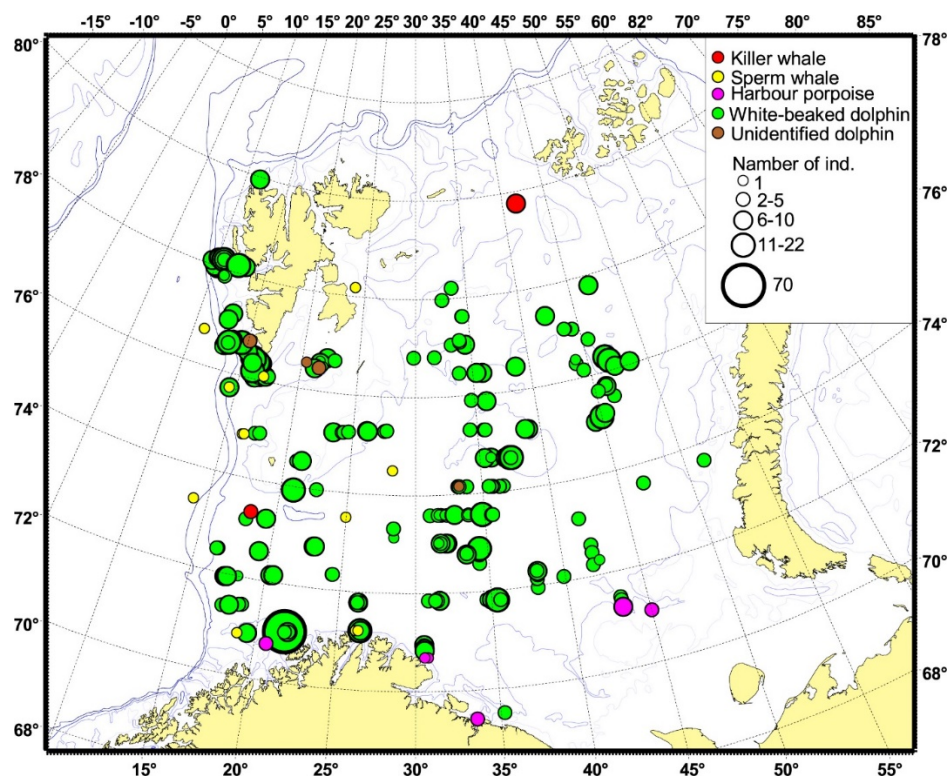


Figure 3.8.1.1. Distribution of toothed whales in August-October 2019.

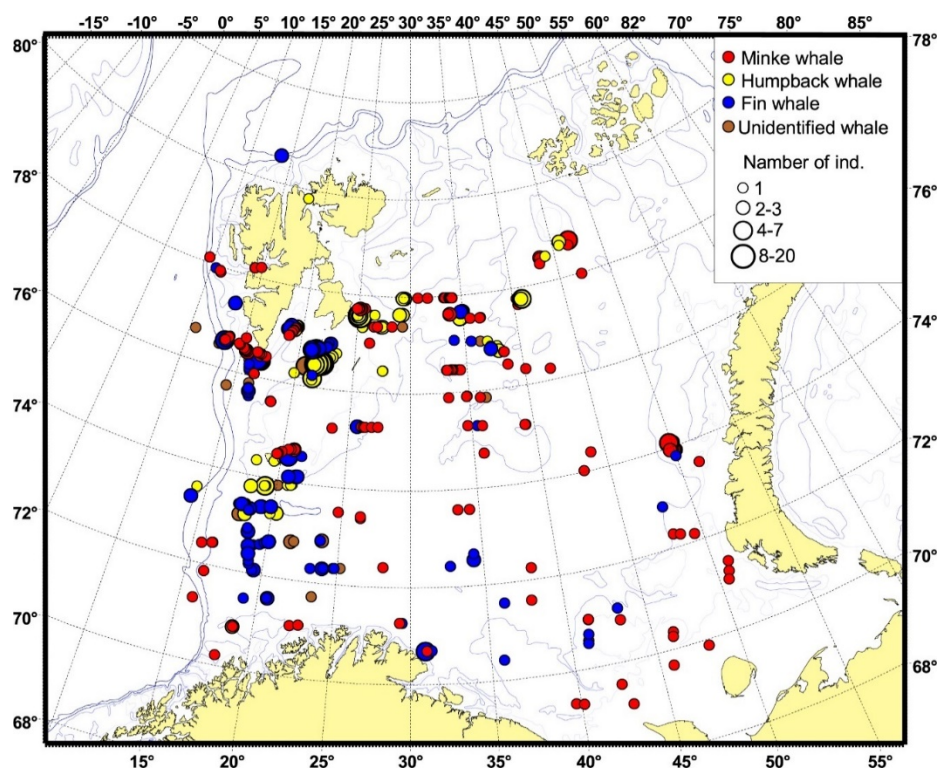


Figure 3.8.1.2. Distribution of baleen whales in August-October 2019.

In 2019, fin whales showed an apparent increase in abundance and were more numerous in association with the continental slope southwards from Spitsbergen and around Bear Island than in 2018.

No blue whales (*Balaenoptera musculus*) were recorded during the ecosystem survey in 2019.

Pinniped species recorded during the joint ecosystem survey were harp seal (*Phoca groenlandica*), bearded seal (*Erignathus barbatus*) and walrus (*Odobenus rosmarus*). The main concentrations of harp seals were found north of 80°N in the area of newly formed ice. Walrus and bearded seals were also observed north of 80°N. Polar bears (*Ursus maritimus*) were not observed during the ecosystem survey.

Since the late 1980ies Norway has conducted visual sighting surveys in the Northeast Atlantic with minke whales as target species to estimate summer abundance of this species and other cetacean species. The surveys have been run as mosaic coverages of the total survey area over six-year periods. In the Barents Sea the species most often observed during these surveys have been the minke whale, followed by white-beaked dolphins, harbour porpoises, humpback whales and fin whales. The impression is that minke whales are abundant in the northern and eastern areas during the summer. Harbour porpoises are mostly observed in the southern parts of the area and we know that they are associated with the coastal areas along Kola and the fjord systems. Humpback whales are mainly sighted in the northwest and associated with the capelin distribution. The white-beaked dolphins are observed in the southern and central parts of the survey area, especially over the Sentralbanken. From these surveys a series of abundance estimates can be compiled to illustrate the status over a time period of nearly 30 years. Over the period from about 1995 to 2015 the summer abundance of minke whales has been quite stable but has recently shown a considerable increase to the present 73,000 animals (Figure 3.8.1.3). Also, humpback whales have shown a large increase in summer abundance in the Barents Sea from very low numbers prior to year 2000 to around 4,000 animals afterwards. Other cetacean species have shown relatively stable abundances within the Barents Sea over the survey period.

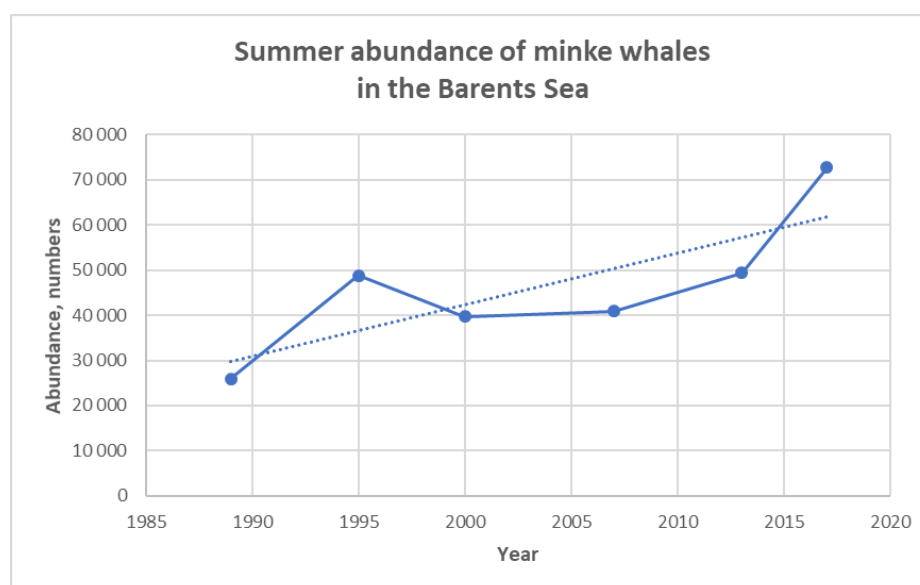


Figure 3.8.1.3. Summer abundance of minke whales in the Barents Sea over the past nearly 30 years.

Marine mammal frequency of occurrence

By Roman Klepikovskiy

The Barents Sea is a productive ecosystem and an important feeding ground for marine mammals during summer and autumn. During the joint Norwegian-Russian ecosystem (BESS), marine mammals have been observed visually from the vessels by experts. Frequency of occurrence (FO, number of observations, not number of observed marine mammals) were estimated based on the BESS for the period 2004-2019 and shown in Fig 3.8.1.4. Three peaks of FO of marine mammals were observed in 2007, 2010 and 2017-2019. Note, that marine mammal observers were not at all vessels in the western part (2004, 2005, 2008, 2009 and 2014), and lack of full coverage in the eastern parts of the Barents Sea in 2016 and 2018 may influence the result.

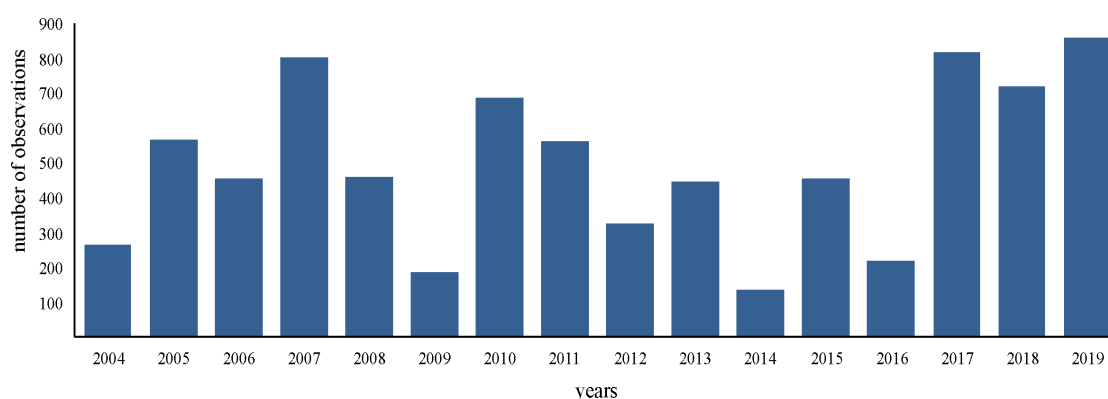


Figure 3.8.1.4 Frequency of occurrence of marine mammals' (number of observations) in the Barents Sea, during BESS in 2004-2019.

The BESS cover open sea and thus 90% of observations of all marine mammals' observations belongs to *Cetacea*. The most frequently occurring species during the August-September were white-beaked dolphin (*Lagenorhynchus albirostris*), minke whale (*Balaenoptera acutorostrata*), fin whale (*Balaenoptera physalus*) and humpback whale (*Megaptera novaeangliae*) (Figure. 3.8.1.5).

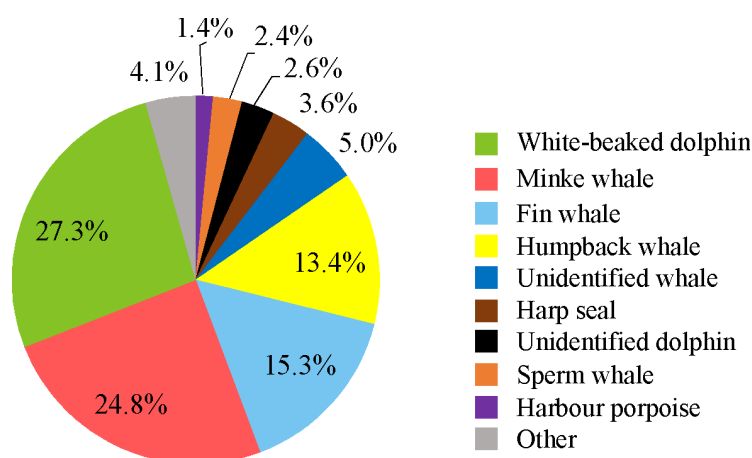


Figure 3.8.1.5 Species composition of marine mammals' observations, and their proportion in the Barents Sea, during BESS in 2004-2019.

The Barents Sea were divided in to four (western, Svalbard or Spitsbergen, south-eastern and north-eastern) regions (Fig. 3.8.1.6) and FO's were calculated for each region.

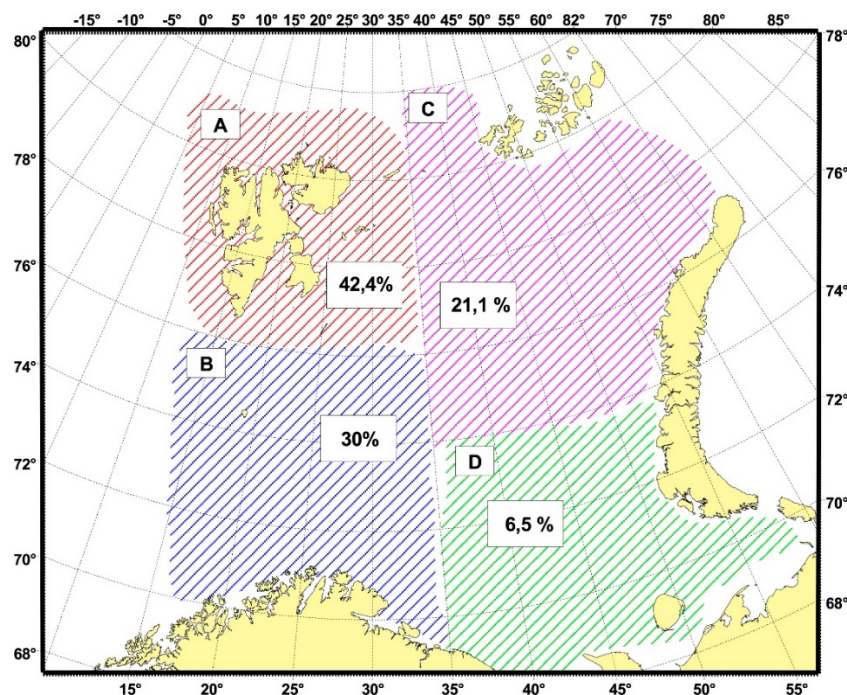


Figure 3.8.1.6 – Frequency of occurrence of marine mammals (%) in the four regions in Barents Sea during BESS in 2004-2019: A – Svalbard/Spitsbergen, B – Western, C – North-eastern, D – South-eastern.

A. The Svalbard area is located between 76°N and 82°N and between 5 °E and 35 °E. The highest frequency of occurrence of marine mammals (42.4% of all observations) were observed in the area. Additionally, the highest number of species (14) were also observed in the area. This area, especially east of Svalbard is a main capelin area. Capelin are an important prey for many of marine mammals and overlap between highest numbers of observations and species and main mature capelin observations most likely link to important feeding ground (first of all capelin, but also euphausiids). Most frequently observed in the area were representatives of baleen whales (*Mysticeti*): minke whale, fin whale and humpback whale (Figure 3.8.1.7 A).

B. The western area is located between 76 °N and the Norwegian and Russian coasts and between 5 °E and 35 °E. In this area, one third part of all observation were observed. 13 species of marine mammals (next highest number of species) were observed in the area, among them were white-beaked dolphin, minke whale, fin whale, sperm whale (*Physeter macrocephalus*), humpback whale (Figure 3.8.1.7 B). The western area is also productive area with highest concentrations of euphausiids and juveniles' fish such as haddock, cod, herring, redfish and capelin. Immature capelin and herring also observed here.

C. The north-eastern area is located between 74 °N and 82°N and between 35 °E and 70 °E. The numbers of marine mammals observed here were less than in two other areas and consisted 21.1% of all observations. Totally, 11 species were observed here

such as white-beaked dolphin, minke whale, humpback whale, fin whale, and harp seal (*Pagophilus groenlandicus*) (Figure 3.8.1.7 C). This area are dominated by polar cod, cod and capelin. Polar cod is an important prey for harp seals and a decrease of polar cod abundance since 2012 can therefore impact feeding conditions negatively.

D. The south-eastern area is located between 74 N the Russian coast and between 35 °E and 70 °E. During BESS, the lowest numbers of marine mammals' observations 6.5% of all observations) were observed in the area. However, 10 different species were recorded, and most frequent were white-beaked dolphin, minke whale, harbour porpoise (*Phocoena phocoena*) and fin whale (Figure 3.8.1.7 D). This area dominated by polar cod, cod and herring.

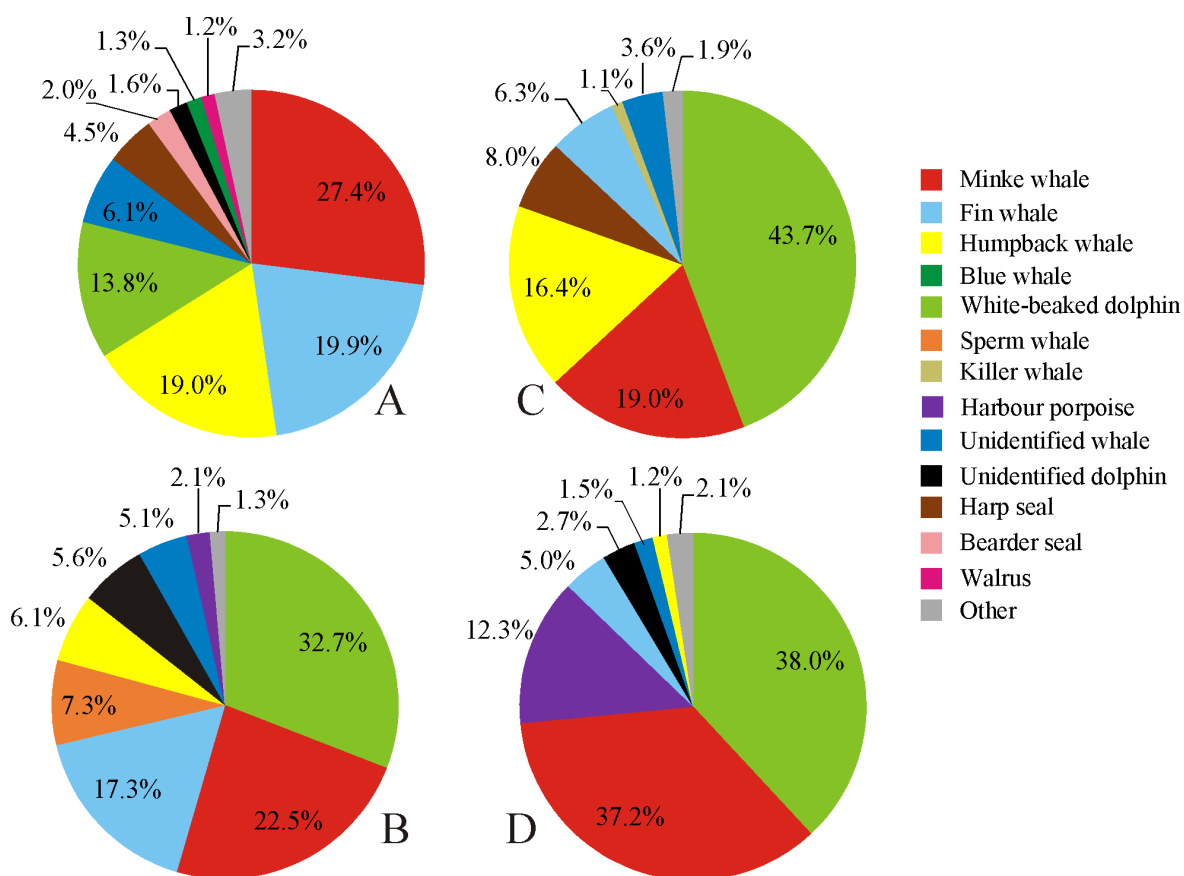


Figure 3.8.1.7. Frequency of occurrence of marine mammals and species composition (%) in different areas (A - Svalbard, B - Western, C - Northeastern, D - Southeast) in the Barents Sea during BESS in 2004-2019.

Figure 3.8.1.8 shown frequency of occurrence of marine mammals in these four areas in different years. More often marine mammals visited Svalbard areas compared to other areas, and number of observations increased from 2004 to 2019. During last three years marine mammals were observed more than 400 times in the Svalbard area. Next highest visited area was western area, or most likely transfer corridor for some whales. Highest numbers of observations were observed during 2005-2007, 2010 and 2019. area. The frequency of occurrence and species composition varied between these four areas of the Barents Sea. The Svalbard, inhabiting by capelin, polar cod and macroplankton such as euphausiids and amphipods, were visited more frequently and by higher

number of species, and thus had highest predation pressure. The western area, inhabiting by 0-group fishes and macroplankton, experienced next highest predation pressure, but this differ between years.

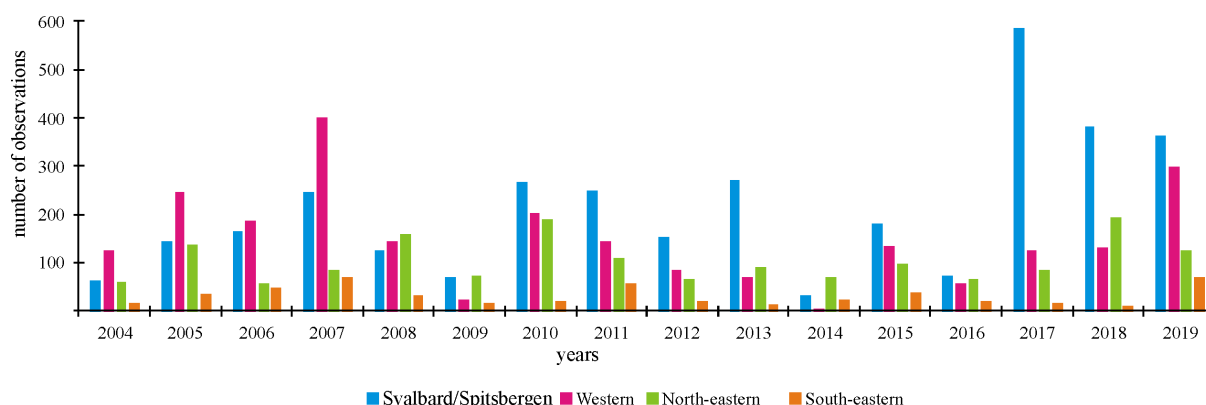


Figure 3.8.1.8 Frequency of occurrence of marine mammals in four areas of the Barents Sea during 2004-2019.

3.8.2 Sea birds

By Per Fauchald (NINA)

About six million pairs from 36 seabird species breed regularly in the Barents Sea (Barrett et al. (2002), Table 3.8.2.1). Allowing for immature birds and non-breeders, the total number of seabirds in the area during spring and summer is about 20 million individuals. 90% of the birds belong to only 5 species: Brünnich's guillemot, little auk, Atlantic puffin, northern fulmar and black-legged kittiwake. The distribution of colonies is shown in Figure 3.8.2.1. Colonies in the high-Arctic archipelago are dominated by little auks, Brünnich's guillemots and kittiwakes. These birds utilize the intense secondary production that follows the retreating sea ice. Little auks feed mainly on lipid rich *Calanus* species, amphipods and krill while Brünnich's guillemots and black-legged kittiwakes feed on polar cod, capelin, amphipods and krill. The seabird communities, as well as their diet change markedly south of the polar front. In the Atlantic part of the Barents Sea, the seabirds depend more heavily fish, including fish larvae, capelin, I-group herring and sandeels. The shift in diet is accompanied by a shift in species composition. In the south, Brünnich's guillemots are replaced its sibling species, the common guillemot. Large colonies of Atlantic puffins that largely sustain on the drift of fish larvae along the Norwegian coast, are found in the southwestern areas.

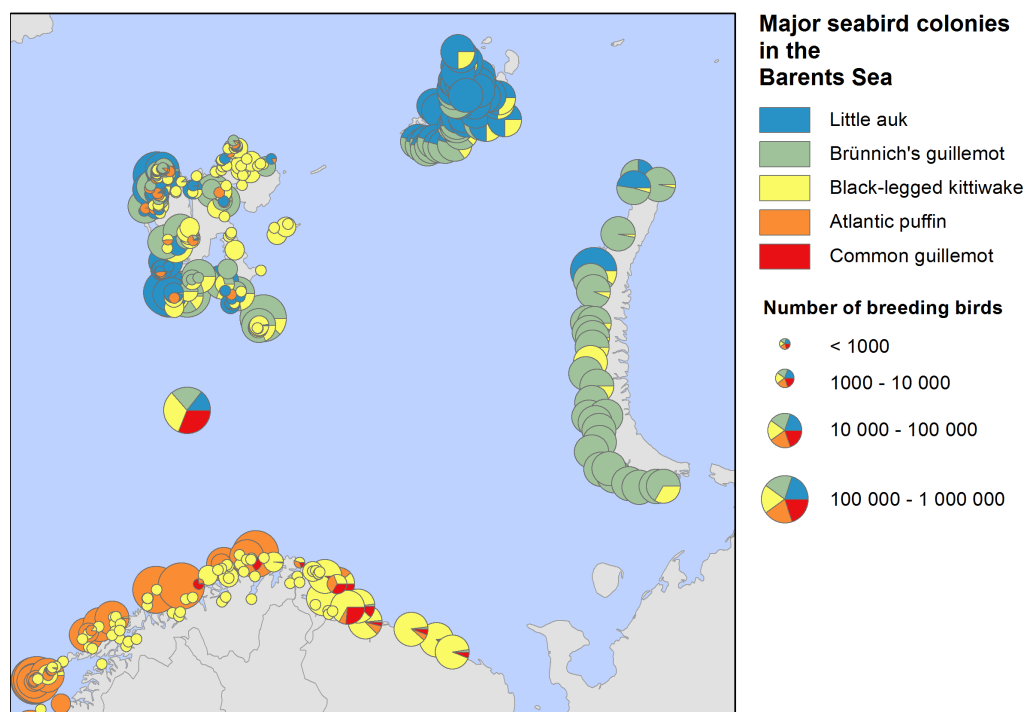


Figure 3.8.2.1. Major seabird colonies in the Barents Sea. Data compiled from SEAPOP (www.seapop.no), Fauchald et al. (2015), Anker-Nilssen et al. 2000 and The Seabird Colony Registry of the Barents and White Seas.

Table 3.8.2.1. Seabirds in the Barents Sea sorted by breeding population size in decreasing number. Breeding pairs are from Strøm et al. (2009). Observations on BESS 2019 are the observations from Norwegian and Russian vessels during the ecosystem survey in 2019.

Species name	Scientific name	Breeding pairs	Observations on BESS 2019
Brünnich's guillemot	<i>Uria lomvia</i>	1 250 000	6 904
Little auk	<i>Alle alle</i>	>1 010 000	20 365
Atlantic puffin	<i>Fratercula arctica</i>	910 000	1 362
Northern fulmar	<i>Fulmarus glacialis</i>	500 000-1 000 000	53 864
Black-legged kittiwake	<i>Rissa tridactyla</i>	682 000	17 546
Common eider	<i>Somateria mollissima</i>	157 000-159 000	0
Herring gull	<i>Larus argentatus</i>	122 600	2 150
Common guillemot	<i>Uria aalge</i>	104 000	359
Arctic tern	<i>Sterna paradisaea</i>	65 000	20
Black guillemot	<i>Cepphus grylle</i>	58 000	173
Great black-backed gull	<i>Larus marinus</i>	22 930	331
Razorbill	<i>Alca torda</i>	19 600	23
Mew gull	<i>Larus canus</i>	14 200	0
Glaucous gull	<i>Larus hyperboreus</i>	9 000-15 000	914
Great cormorant	<i>Phalacrocorax carbo</i>	11 570	7
European shag	<i>Phalacrocorax aristotelis</i>	6 350-6 400	1
European storm-petrel	<i>Hydrobates pelagicus</i>	1 000-10 000	0
Lesser Black-backed gull	<i>Larus fuscus</i>	3 500	5
Ivory gull	<i>Pagophila eburnea</i>	2 200-3 750	333
Northern gannet	<i>Morus bassanus</i>	1 900-2 150	58
Arctic skua	<i>Stercorarius parasiticus</i>	1 150	139
King eider	<i>Somateria spectabilis</i>	1 000	1
Common tern	<i>Sterna hirundo</i>	>1 000	0
Heuglin's Gull	<i>Larus heuglini</i>	600-1 100	513
Great skua	<i>Stercorarius skua</i>	540-1 100	82
Leach's storm petrel	<i>Oceanodroma leucorhoa</i>	100-1 000	0
Steller's eider	<i>Polysticta stelleri</i>	10-100	0
Sabine's gull	<i>Xema sabini</i>	1-10	1
Great northern diver	<i>Gavia immer</i>	0-3	2
Long-tailed duck	<i>Clangula hyemalis</i>	?	0
Black scoter	<i>Melanitta nigra</i>	?	0
Velvet scoter	<i>Melanitta fusca</i>	?	0
Red-breasted merganser	<i>Mergus serrator</i>	?	0
Black-throated loon	<i>Gavia arctica</i>	?	1
Long-tailed skua	<i>Stercorarius longicaudus</i>	?	30
Pomarine skua	<i>Stercorarius pomarinus</i>	?	650
Sooty shearwater	<i>Puffinus griseus</i>	0	7
Ross's gull	<i>Rhodostethia rosea</i>	0	0

Population monitoring in Norway and Svalbard has revealed a marked downward trend for several important seabird species the last 30 years, including puffin, Brünnich's guillemot and kittiwake (Figure 3.8.2.2). The population of common guillemot was decimated in the 1980s mainly due to a collapse in the capelin stock combined with low abundance of alternative prey. The population has increased steadily since then. The status and trends of the large populations of seabirds in the Eastern Barents Sea is less known.

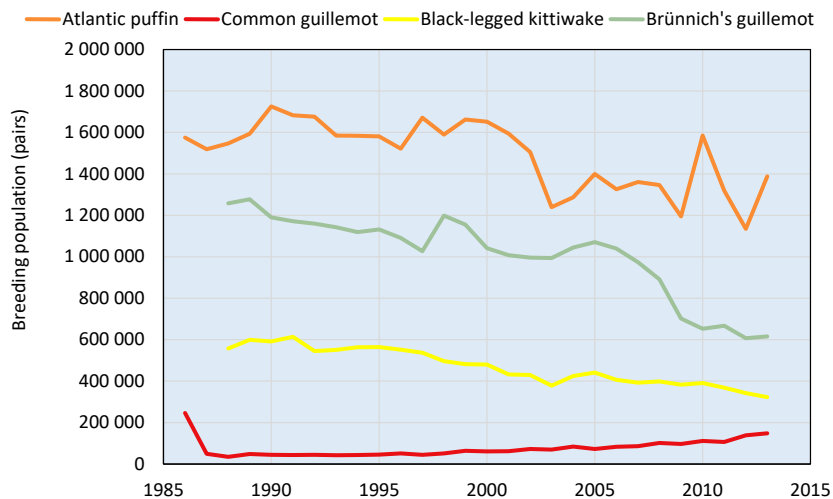


Figure 3.8.2.2: Size and trends of puffin, guillemots and kittiwake populations in the Western Barents Sea (Norway and Svalbard incl. Bjørnøya). Data from Fauchald et al. (2015).

In addition of being an important breeding area for seabirds, data from recent tracking studies (Fauchald et al. 2019) show that the Barents Sea is an important feeding area for seabirds in early autumn. Accordingly, the number of pelagic seabirds reaches a maximum of approximately 10 million individuals in August, just after breeding (Figure 3.8.2.3). This peak is mainly due to Atlantic puffins, Northern fulmars, common guillemots and black-legged kittiwakes migrating from colonies around the Norwegian Sea in to the Barents Sea to feed. This period, from August to September, is also the period when the auk species moult and become flightless for several weeks. After the feeding period, large parts of the populations of Atlantic puffin, Brünnich's guillemot, black-legged kittiwakes, Northern fulmar and little auks leave the Barents Sea. Thus, the number of birds reaches a minimum in the darkest period from December to January with about 5 million birds (Figure 3.8.2.3). In general, populations from the western colonies leave the Barents Sea earlier (September-October) and return later (March-April) than birds from the eastern colonies, and a larger proportion of the eastern populations tend to stay in the Barents Sea throughout the winter. Migrating birds overwinter in large ocean areas in the northwest and north-central part of the North Atlantic, including the coastal areas off southern and western Greenland, around Iceland, in the Denmark Strait and in the Irminger and Labrador Seas. Common guillemots from Bjørnøya, Murman and Finnmark stay in the southern Barents Sea throughout the non-breeding period. The seabirds return gradually to the colonies and adjacent areas in early spring from February to April.

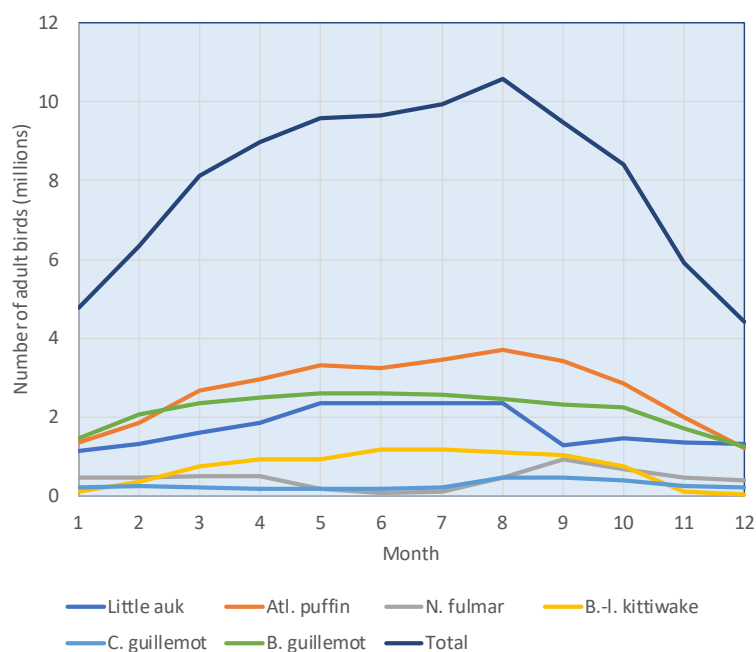


Figure 3.8.2.3: Estimated number of adult breeding seabirds present in the Barents Sea area during the annual cycle. Estimates are based on population size and year-round tracking of different populations by the SEATRACK program (see Fauchald et al. 2019).

Broadly, the spatial distribution of seabirds during the ecosystem survey in September reflects the climatic gradient from a boreal Atlantic climate with common guillemots, puffins, herring and black-backed gull in the south and west, to an Arctic climate with little auks, Brünnich's guillemots and kittiwakes in the north and east (Figure 3.8.2.4). Seabirds have been surveyed uninterruptedly on Norwegian vessels in the western part of the Barents Sea since 2004, however, the first years did not cover the northern areas. Based on the minimum annual survey extent from 2009 on onward, the abundance (Figure 3.8.2.5) of different species and the centre of gravity of the spatial distribution (Figure 3.8.2.6) was calculated for each year.

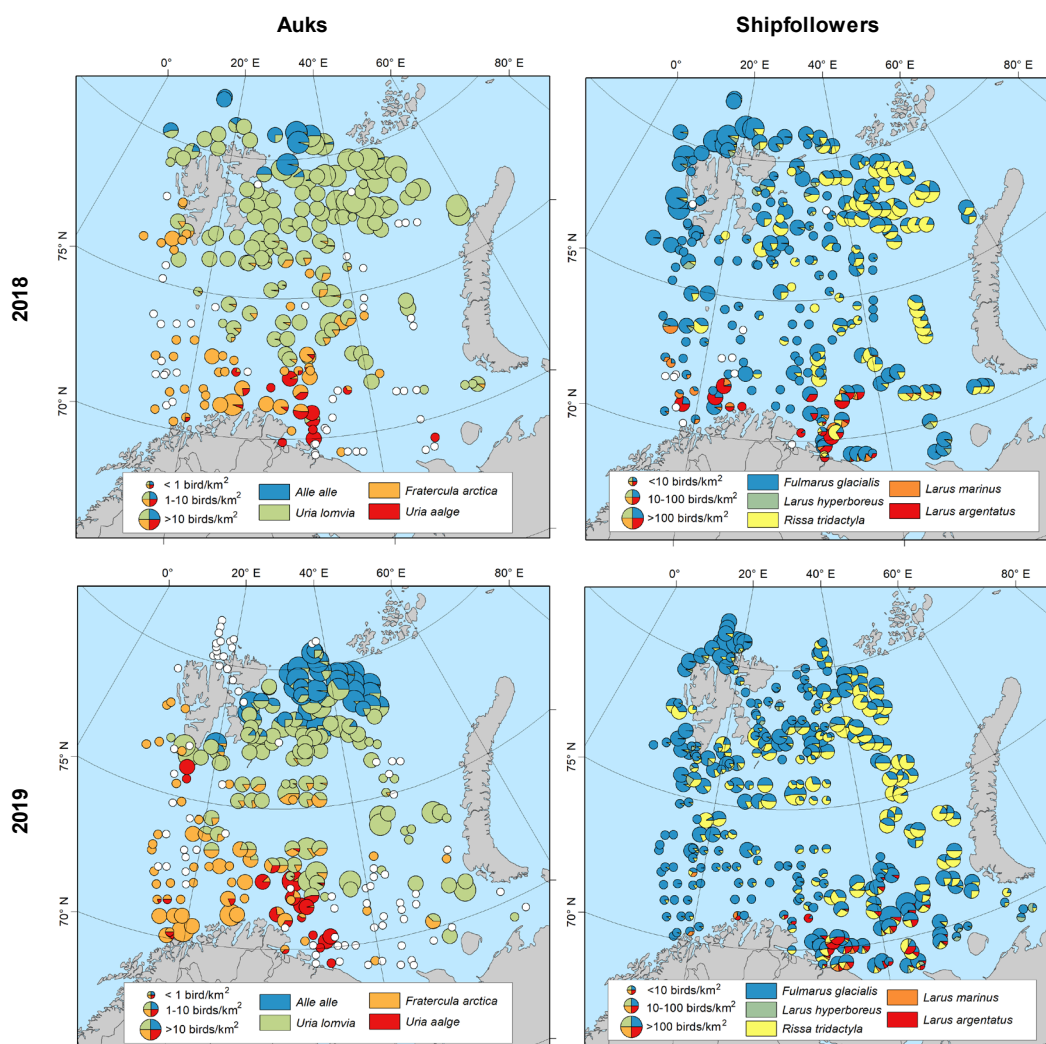


Figure 3.8.2.4. Density of seabirds during the Barents Sea ecosystem surveys in 2018 (top) and 2019 (bottom). Left panel is the distribution of auks (little auk, Brünnich's guillemot, Atlantic puffin and common guillemot). Right panel is the distribution of shipfollowers (Northern fulmar, glaucous gull, black-legged kittiwake, black-backed gull and herring gull).

Abundance estimates indicate relatively large fluctuations in the number of seabirds at-sea (Figure 3.8.2.5). Northern fulmar, black-legged kittiwake and herring gull have decreased significantly in abundance the last ten years. These changes do not necessarily reflect the observed population trends from the colonies (cf. Figure 3.8.2.2) since the at-sea abundances also are influenced by annual differences in migration pattern. Note that the ship-followers are attracted to the ship from the surrounding areas and individual birds are therefore likely to be counted several times. Accordingly, the estimated numbers of ship-followers are probably grossly over-estimated. Analyses of the centres of gravity show a northward displacement for several species the last ten years (Fig. 3.8.2.6). The centres of gravity of little auks, Brünnich's guillemot, glaucous gull, black-legged kittiwake, northern fulmar and black-backed gull have moved from 150 to 500 km northward from 2008 to 2019, suggesting that seabirds have been displaced toward the north following a period of warming. Although longer time series might be warranted, this result could be an early

signal of a “borealization” (Fossheim et al. 2015) of the seabird communities in the Barents Sea.

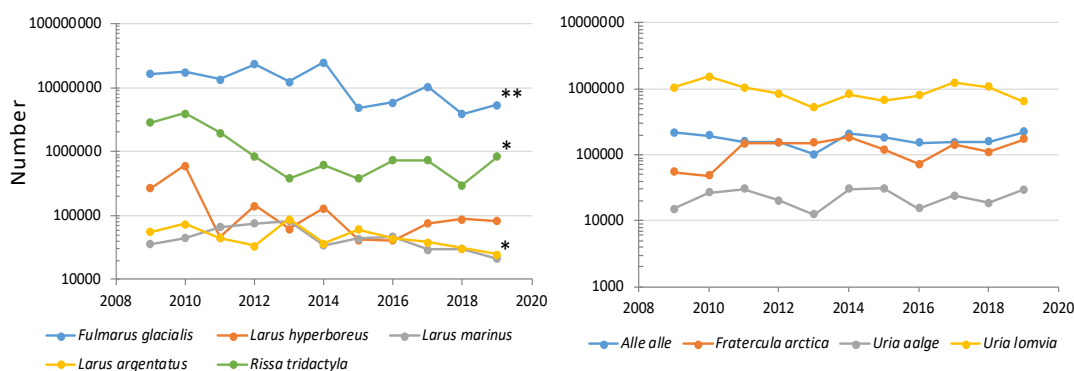


Figure 3.8.2.5. Abundance of auks (left) and shipfollowers (right) in the Western Barents Sea during the ecosystem surveys 2009-2019. Note that the numbers of ship-followers are probably systematically over-estimated. Asterisks indicate significant negative trends in the abundance estimates (* $P < 0.05$, ** $P < 0.001$).

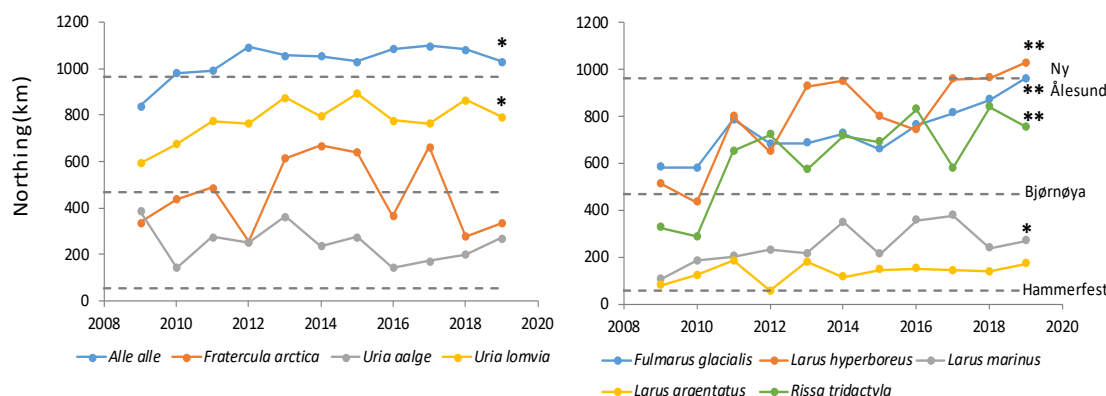


Figure 3.8.2.6. Centre of gravity in the north direction of the distribution of auks (left) and shipfollowers (right) in the Western Barents Sea during the ecosystem surveys 2009-2019. Hatched lines indicate the positions of Hammerfest (Norwegian coast), Bjørnøya and Ny Ålesund (Spitsbergen). Asterisks indicate significant positive linear trends in the position of the centre of gravity (* $P < 0.05$, ** $P < 0.001$).

References

- Anker-Nilssen, T., Bakken, V., Strøm, H., Golovkin, A.N., Bianki, V.V. and Tatarinkova, I.P. 2000. The Status of Marine Birds Breeding in the Barents Sea Region. Norsk Polarinstitutt Rapportserie. 113. 213 pp.
- Barrett, R.T., Anker-Nilssen, T., Gabrielsen, G.W. and Chapdelaine, G. 2002. Food consumption by seabirds in Norwegian waters. - ICES Journal of Marine Science, 59: 43-57.
- Fauchald, P., Zirvanov, S. V., Strøm, H. and Barrett, R. T. 2011. Seabirds of the Barents Sea. Pages 373-394 in Jakobsen T, Ozhigin VK (Eds) The Barents Sea. Ecosystem, Resources, Management. Tapir Academic Press, Trondheim, Norway.
- Fauchald, P., Anker-Nilssen, T., Barrett, R., Bustnes, I. O., Bårdsen, B. I., Christensen-Dalsgaard, S., Descamps, S., Engen, S., Erikstad, K. E., Hanssen, S. A., Lorentsen, S.-H., Moe, B., Reiertsen, T., Strøm, H. and Svstad, G. H. (2015). The status and trends of seabirds breeding in Norway and Svalbard. NINA report 1151: 84 pp.
- Fauchald, P., Tarroux, A., Bråthen, V. S., Descamps, S., Ekker, M., Helgason, H. H., Merkel, B., Moe, B., Åström, I. and Strøm, H. (2019). Arctic-breeding seabirds' hotspots in space and time -a methodological framework for year-round modelling of abundance and environmental niche using light-logger data. NINA Report 1657: 85pp.
- Fossheim M, Primicerio R, Iohannesen E, Ingvaldsen RB, Aschan M and Dolgov AV. 2015. Recent warming leads to a rapid borealization of fish communities in the Arctic. Nature Climate Change 5, 673–677.
- Strøm, H., Gavrilov, M.V., Krasnov, I.V. and Svstad, G.H. 2009. Seabirds. In Joint Norwegian-Russian Environmental Status 2008 Report on the Barents Sea Ecosystem. Part II – Complete report, pp. 67-73. Ed. by J.E.

Stiansen, O. Korneev, O. Titov, P. Arneberg, A. Filin, J.R. Hansen, Å. Høines and S. Marasaev. IMR/PINRO Joint Report Series, 3/2009.

3.9 Anthropogenic impact

3.9.1 Fisheries

The commercial fisheries in the Barents Sea Ecoregion target few stocks. The largest pelagic fishery targets capelin using midwater trawl. The largest demersal fisheries target cod, haddock, and other gadoids; predominantly using trawls, gillnets, longlines, and handlines. The crustacean fisheries target deep-sea prawn, red king crab, and snow crab. Most catches of crabs are from coastal areas. Harp seals and minke whales are also hunted in the region.

Fisheries overview in the Barents Sea is available on <https://www.ices.dk/sites/pub/Publication%20Reports/Advice/2019/2019/FisheriesOverviewBarentsSea2019.pdf>

3.9.2 Catches of shellfish

By D.V. Zakharov (PINRO)

Northern shrimp (*Pandalus borealis*)

Norwegian and Russian vessels harvest northern shrimp over the stock's entire area of distribution in the Barents Sea. Vessels from other nations are restricted to trawling shrimp only in the Svalbard zone and the Loophole — a piece of international waters surrounded by the EEZs of Norway and Russia. No overall TAC has been set for northern shrimp, and the fishery is regulated through effort control, licensing, and a partial TAC in the Russian zone only. The regulated minimum mesh size is 35 mm. Bycatch is constrained by mandatory sorting grids, and by temporary closures in areas with high bycatch of juvenile cod, haddock, Greenland halibut, redfish, and shrimp (<15 mm carapace length or <6 cm total length). Catches have varied between 19 000 and 128 000 tonnes per year since 1977. Since the mid-1990s, a major restructuring of the fleet toward fewer and larger vessels has taken place. Since 1995, average engine size of a shrimp vessel in ICES Divisions 1 and 2 increased from 1000 HP (horsepower) to more than 6000 HP in the early 2010s, and the number of fishing vessels has declined markedly. Overall catch decreased from approximately 83 000 tonnes since 2000, reflecting reduced economic profitability in the fishery. After a low of about 20 000 tonnes in 2013, catches again began to increase and reached about 34 000 tonnes in 2015, but decreased to 30 000 tonnes in 2016 and 2017 before increasing considerably to about 55 000 t in 2018. The 2018-2019 stock assessment indicated that the stock has been fished sustainably and has remained well above precautionary reference limits throughout the history of the fishery. Accordingly, ICES used the MSY-approach to advice a 2020 TAC of 150 000 metric tonnes (ICES 2018).

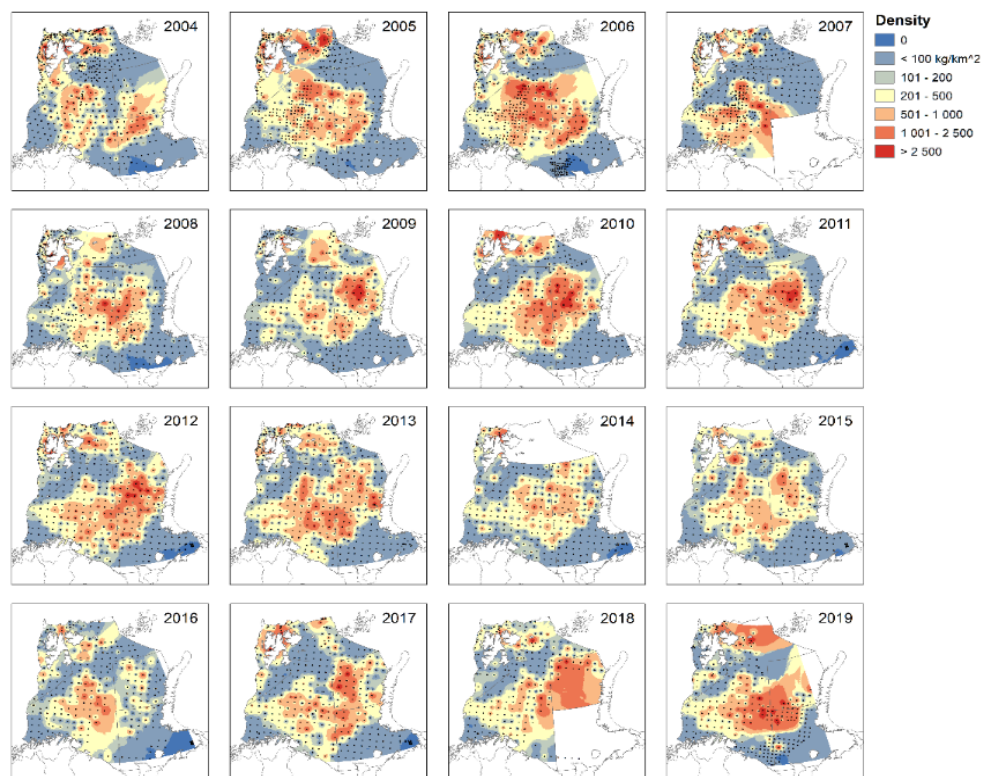


Figure 3.9.2.1. Shrimp density by year from inverse distance weighted interpolation between trawl stations (black dots) for the BESS data.

Geographical distribution of the stock in 2009–2019 was more easterly compared to previous years (Fig. 3.9.2.1). As results, catch levels from some of the more traditional western fishing grounds have declined. Recent reports indicate lower catch rates than would be expected given the overall good stock condition. This may be related to operation costs for a relatively small fleet to move away from more traditional fishing grounds, and to find new grounds with commercially viable shrimp concentrations.

Fisheries for northern shrimp in the Barents Sea and waters adjacent to Spitsbergen Archipelago have been carried out since the 1950s. The largest catches were recorded in the mid-1980s (more than 120 000 tonnes) and during 1990–1991, 2000 (approximately 80 000 tonnes). Since 2005, total annual catch of northern shrimp in this area have remained at the 20 000- 40 000 thousand tonnes level (Fig. 3.9.2.2) after 2018 total catch is rapidly grow mainly by Russian fishery.

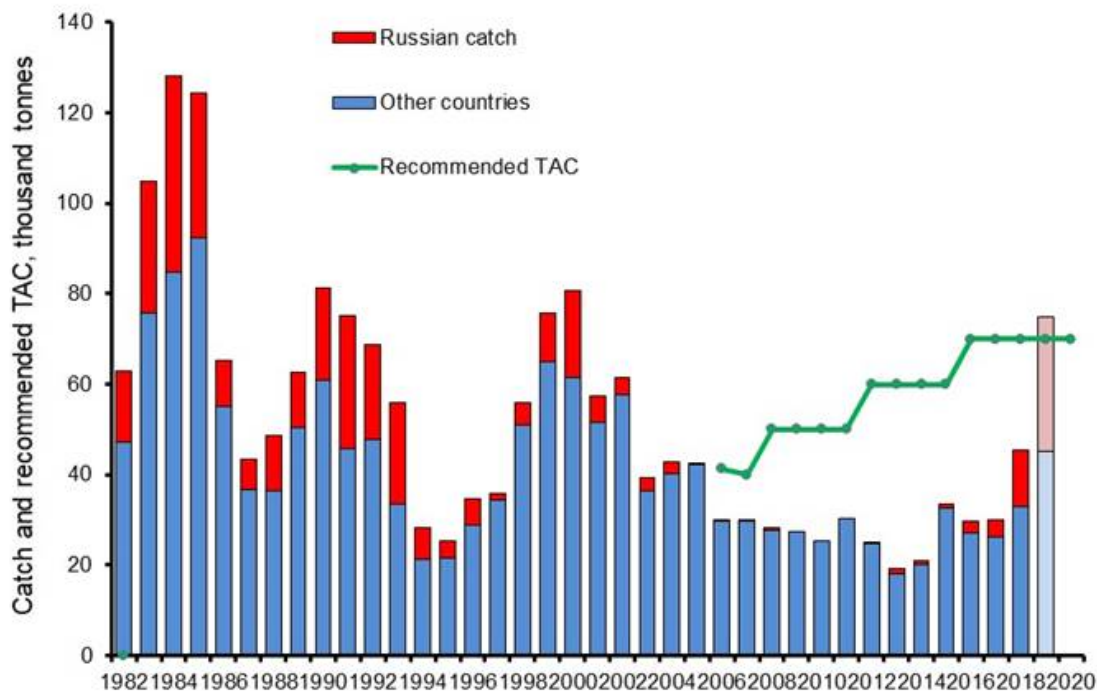


Figure 3.9.2.2 Catch and recommended TAC of the northern shrimp in the Barents Sea and waters around Spitsbergen archipelago in 1982–2019 (Zakharov, 2019)

Trawl surveys of northern shrimp stocks have been carried out in the Barents Sea since 1982. During the 2005–2019 period, the stock was relatively stable.

Red king crab (*Paralithodes camtschaticus*)

Red king crab is managed separately in the NEZ and REZ.

The commercial fishery for red king crab in the Russian Economic Zone of the Barents Sea has been carried out since 2004. Russian Fisheries Regulations stipulate that males with carapace width greater than or equal to 150 mm can only be caught using traps.

Heavy exploitation of the stock during 2005–2006 led to a decrease in the commercial component of the red king crab population, and reduced productivity in the fishery. In 2011, decreased fishery pressure prompted population growth, and subsequent stabilization of the commercial stock. Total catch also increased in subsequent years (Fig. 3.9.2.3); in 2016, total catch of red king crabs in Russian Economic Zone was 8.3 thousand tonnes.

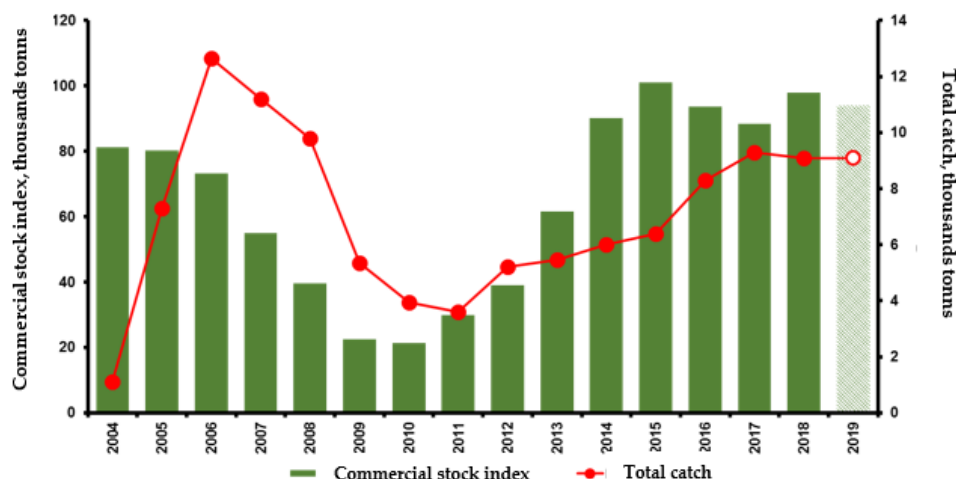


Figure 3.9.2.3. Commercial stock index and the total catch of the red king crab in the Russian Economic Zone of the Barents Sea in 2006–2016 (Bakanev and Stesko, 2019). Data of 2019 is a forecast

One of the most detailed trap surveys to assess distribution of the red king crab commercial stock was conducted in 2013. Results from this survey indicated the densest concentrations of commercial sized male crabs (more than 1000 ind./km²) was recorded on Rybachya Bank and Kildinskaya Bank, in the eastern part of Murmansk Rise, and in the southern part of North Kanin Bank. In other parts of this area, the abundance of commercial sized males varied from 100 to 500 ind./km² (Fig. 3.9.2.4). Subsequently, aggregations of fishable crabs shifted eastward to the western part of the Kanin-Kolguev Shallow. The most eastern extent of red king crab distribution was recorded in 2015 and 2017. Two adult individuals (male and female with clutch) in eastern Pechora Sea near Vaygach Island, and the southwestern coast of Novaya Zemlya Archipelago. This change in distribution could be caused by both migrations to find new food resources and climatic warming.

In 2016, ten Russian vessels fished red king crabs in the eastern Barents Sea, the Murmansk Rise, and Kanin Bank using rectangular and trapezoidal traps. The largest catches were obtained at southeastern Murmansk Rise outside the 12-mile coastal zone. In 2018, the commercial stock index for red king crab was 94 thousand tonnes (Bakanev and Stesko, 2019).

The Norwegian fishery for the red king crab (RKC) is subjected to two different management regimes; a vessel quota fishery in the quota regulated area (QRA) and a free fishery with a discard ban in the free fishing area (FFA) (See Sundet & Hoel 2016, for detailed information).

The Norwegian fishery for the RKC have taken place since 1994, but the commercial fishery started in 2002. In 2008 there was a dramatic change in the management of this fishery with the introduction of an annual vessel quota in tons, minimum legal-size restrictions fishery for both male and female crabs on 130 mm carapace length and trap limits of 30 traps among other things. Since then, the annual total quotas (TAC) has varied between 900 and 2000 tons (Table 3.9.2.1). Number of participating vessels have

increased since then and were close to 600 in 2018 (figure 5). This fishery is strictly monitored and the landings each year were always identical to or close the annual TAC (Table 3.9.2.1).

The fishery in the FFA has varied much between years and has mainly taken place in western Finnmark, close to the western border of the QRA (Figure 3.9.2.4).

Table 3.9.2.1. Recommended TAC, fixed TAC and landings of male and female red king crabs from the Norwegian quota regulated area during 2009 – 2018.

Year	Comments	Recommended quota	Fixed quota	Landed male crabs (tons)	Landed female crabs (tons)
2009	Recommended harvest rate – 50% of legal stock	600 t	1185 t	1 395	54
2010	New models applied – options for quota: 0 – 2600 t	0 ¹⁾	900 t	832	36
2011	Quota-options for different MLS; 120 – 137 mm	900 – 1800 t	1100 t	1267	35
2012		500 t	900 t	1090	32
2013		900 t	1000 t	946	24
2014		1000 t	1000 t	1283	31
2015		1250 t	1040 t	1211	33
2016		2000 t	2000 t	2202	60
2017		1500 t	2000 t ²⁾	1688	115
2018		1250 t	1750	1508**)	128**)

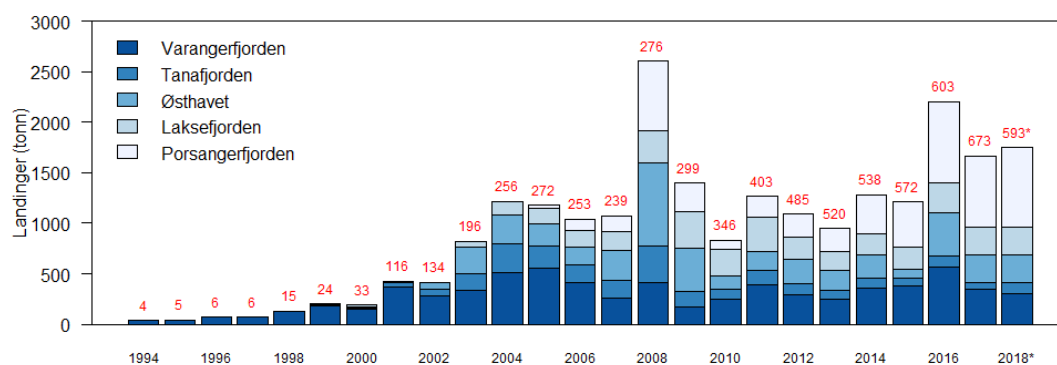


Figure 3.9.2.4. Landings of male red king crabs in Norwegian quota regulated area divided on different areas during 1994 – 2018. Number of participating vessels are shown in red numbers on top of columns each year.

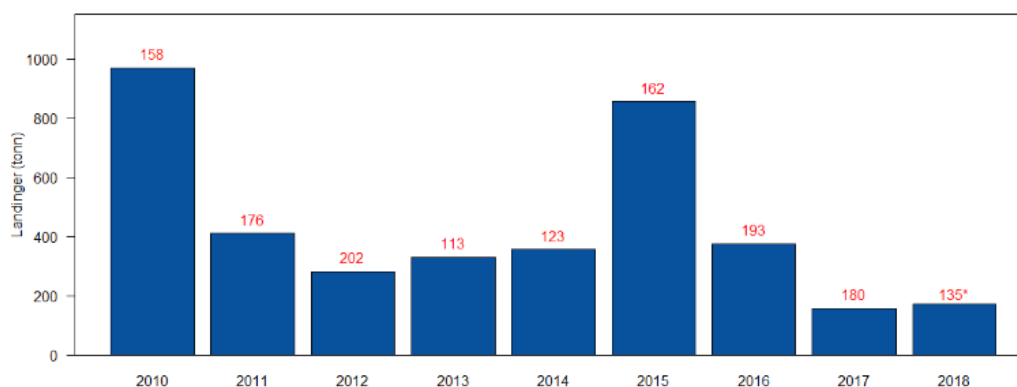


Figure 3.9.2.5. Landings of red king crab from the Norwegian free fishing area west of 26° E. Number of participating vessels are shown in red numbers on top of columns each year.

Snow crab (*Chionoecetes opilio*)

The fishery for snow crab in the Barents Sea commenced in 2012. The harvest increased rapidly and in addition to the Norwegian fleet also EU boats and Russian fishermen participate in the fishery from 2013, which was unregulated and most of the fishery went on in international waters, the Loophole.

Russian vessels fished crabs in this area until 2016. In 2016, Russian vessels started fishing snow crabs in Russian waters (Fig. 3.9.2.6). In 2017, the Russian fishery for snow crabs was conducted only within the Russian EEZ.

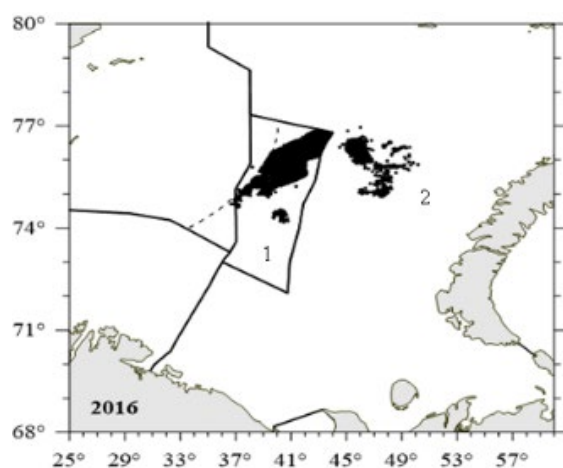


Figure 3.9.2.6. Russian fishery for the snow crab location in the Barents Sea in the Loophole (international waters) in 2013–2016 (1) and national waters from 2016 (2) (Bakanov and Pavlov, 2017)

Russian vessels mainly use conical traps for the snow crab fishery. Statistics for the Russian snow crab fishery in the Barents Sea during 2013–2016 are shown in Table 2.

Table 3.9.2.2. Russian fishery statistics for the snow crabs in the Barents Sea during 2013–2016 (Bakanov, Pavlov, 2019)

Year	Number of vessels	Total fishery days	Numbers of traps, th.	Total catch, tonnes
International waters (Loop Hole)				
2013	2	22	2,4*	62.0
2014	12	1 153	788.7	4 104.2
2015	20	3 119	2894.7	8 894.6
2016	18	2 576	2687.5	6 486.7
Russian waters				
2016	5	178	91.7	1 499.9

During the 2013–2016 period of unregulated fishing in Loophole, the total international catch of snow crabs exceeded 55 thousand tonnes. During 2015–2016, average daily catch declined by 10–20% from the 2014 estimate (Bakanov and Pavlov, 2017).

Decreased fishery productivity (Fig. 3.9.2.7) indicated significant overfishing of the Barents Sea snow crab stock.

In July 2015, Norway and Russia agreed upon the designation of the snow crab as a sedentary species. This decision changed the status from a water column species to a continental shelf resource (Joint Norwegian-Russian Fisheries Commission, 2015). The

snow crab stock in the Loophole area then shifted from being in international waters to become Russian and Norwegian property on their continental shelves. So 85% belongs to the Russian continental shelf and the last rest of 15% belongs to the Norwegian continental shelf.

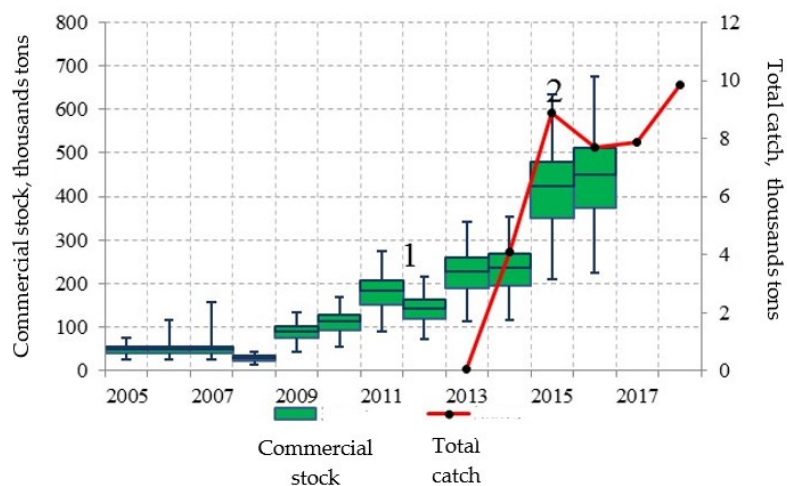


Figure 3.9.2.7. Biomass of commercial stock of snow crab in the Barents Sea in 2005-2017 and its forecast for 2018; catch of snow crab in the Barents Sea in 2014-2017 and expected catch in 2018 (Bakanev and Pavlov, 2019).

The snow crab fishery conducted by Norwegian vessels started in 2012 and 2.5 tones was landed. The next years, the number of boats and the catches increased. Since then the number of participating vessels has increased and the fishing area used was centered in the Barents Sea, including the Loophole and the Svalbard Fisheries Protection Zone (Figure 3.9.2.8).

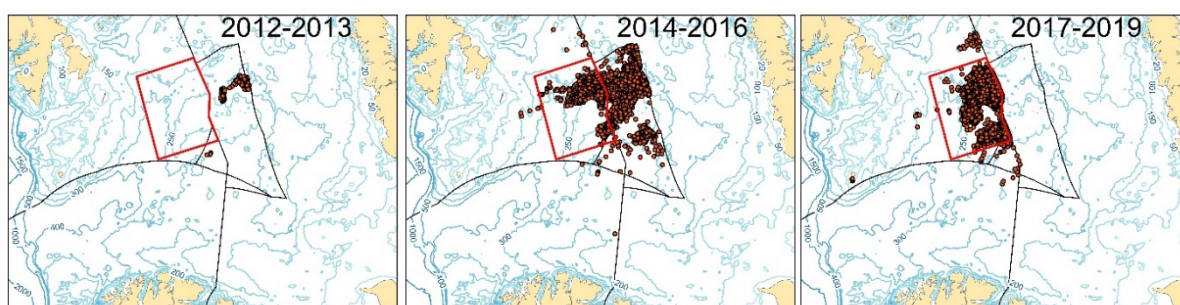


Figure 3.9.2.8. Fisheries activity in the Barents Sea by Norwegian vessels in three periods, 2012-2013, 2014-2016 and 2017-2019.

Norway introduced a TAC for the first time in 2017 and it was set to 4000 tones and have been stable for 2018 and 2019. Even though the TAC has been on 4000 tones, the landings has been around 3000 tones the last two years (Table 3).

Table 3 Recommended quota, fixed quota and landings of snow crab from the Norwegian snow crab fishery in 2012 – 2019.

Year	Recommended quota	Quota (tonnes)	Landings (tonnes)
2012			2.5
2013			189
2014			1 800
2015			3 482
2016			5 290
2017	3 600 – 4 500	4 000	3 153
2018	4 000 – 5 500	4 000	2 804
2019	3 500 – 5 000	4 000	4 038

References

- Sundet, I.H. and Hoel, A.H. 2016. The Norwegian management of an introduced species: the Arctic red king crab fishery. *Marine Policy*, 72: 278-284. DOI: 10.1016/j.mar.pol.2016.04.041
- Bakanev S.V., Stesko A.V. Red king crab State of biological resources of the Barents and the White seas and the North Atlantic in 2018, 43-44, 2019
- Pavlov V.A., Bakanev S.V., Snow crab State of biological resources of the Barents and the White seas and the North Atlantic in 2018, 44-45, 2017
- Pavlov V.A., Bakanev S.V., Snow crab State of biological resources of the Barents and the White seas and the North Atlantic in 2016, 2017
- Zakharov D.V. Shrimp State of biological resources of the Barents and the White seas and the North Atlantic in 2018, 40-41, 2019

3.9.3 Whaling and seal hunting

By Nils Øien (IMR)

Common minke whale (*Balaenoptera acutorostrata*)

Management of the minke whale is based on the Revised Management Procedure (RMP) developed by the Scientific Committee of the International Whaling Commission. Inputs to this procedure are catch statistics and absolute abundance estimates. The present quotas are based on abundance estimates from survey data collected in 1989, 1995, 1996–2001, 2002–2007, and 2008–2013. For the areas available for exploitation by Norwegian whalers, the most recent estimates (2008–2013) are 89 600 animals in the Northeastern stock, and 11 000 animals in the Jan Mayen area. The present (2016–2021) RMP quota of 880 animals annually - 710 in the Northeastern Atlantic and 170 in the Jan Mayen area - is considered precautionary, conservative, and protective for the minke whale population in the Northeast Atlantic. At present only Norway utilizes this quota. The total catch in 2019 was 429 minke whales.

Harp seals (*Pagophilus groenlandicus*)

Northeast Atlantic stocks of harp seals are assessed every second year by the ICES Working Group on Harp and Hooded Seals (WGHARP). The assessments are based on modelling, which provides ICES with enough information to give advice on both status and catch potential of the stocks. The applied population model estimates current total population size, incorporating historical catch data, estimates of pup production and historical values of reproductive rates. Modelled abundance is projected into the future to provide an estimate of future population size for which statistical uncertainty is provided for various sets of catch options. Russian aerial surveys of White Sea harp seal pup production conducted during the period 1998–2013 indicate a severe reduction in pup production after 2003. This could be due to changes in fecundity and/or changes in survival. The Barents Sea/White Sea population of harp

seals is now considered data poor (available data for stock assessment older than 5 years). The population model provided a poor fit to pup production survey data; primarily due to the abrupt reduction after 2003. Nevertheless, the ICES WGHARP decided to continue to use the model which estimated a total 2019 abundance of 1,497,190 (95% C.I. 1,292,939-1,701,440) seals. The modelled total population indicates that the abundance decreased from its highest level in 1946 to the early 1960s, where after an increase has prevailed. Current level is 74% of the 1946 level. ICES recommended that removals be restricted to the estimated sustainable equilibrium level of 10 090 age 1+ animals, or an equivalent number of pups (where one 1+ seal is balanced by 2 pups), per year, and this was supported by the Joint Norwegian-Russian Fisheries Commission. The catches from the White Sea harp seal population are however at a very low level; in 2019 the total catch was 602 animals, which is only 6% of the sustainable catch level.

3.9.4 Fishing activity

By Gro van der Meeren (IMR) and Alexey Russkikh (PINRO)

Fishing activity in the Barents Sea is tracked by the Vessel Monitoring System (VMS). Figures 3.9.4.1 and 3.9.4.2 show fishing activity in 2017-2019 based on Russian and Norwegian data. VMS data offer valuable information about temporal and spatial changes in fishing activity. The most widespread gear used in the Barents Sea is bottom trawl; but longlines, gillnets, Danish seines, and handlines are also used in demersal fisheries. Pelagic fisheries use purse-seines and pelagic trawls. The shrimp fishery used special bottom trawls.

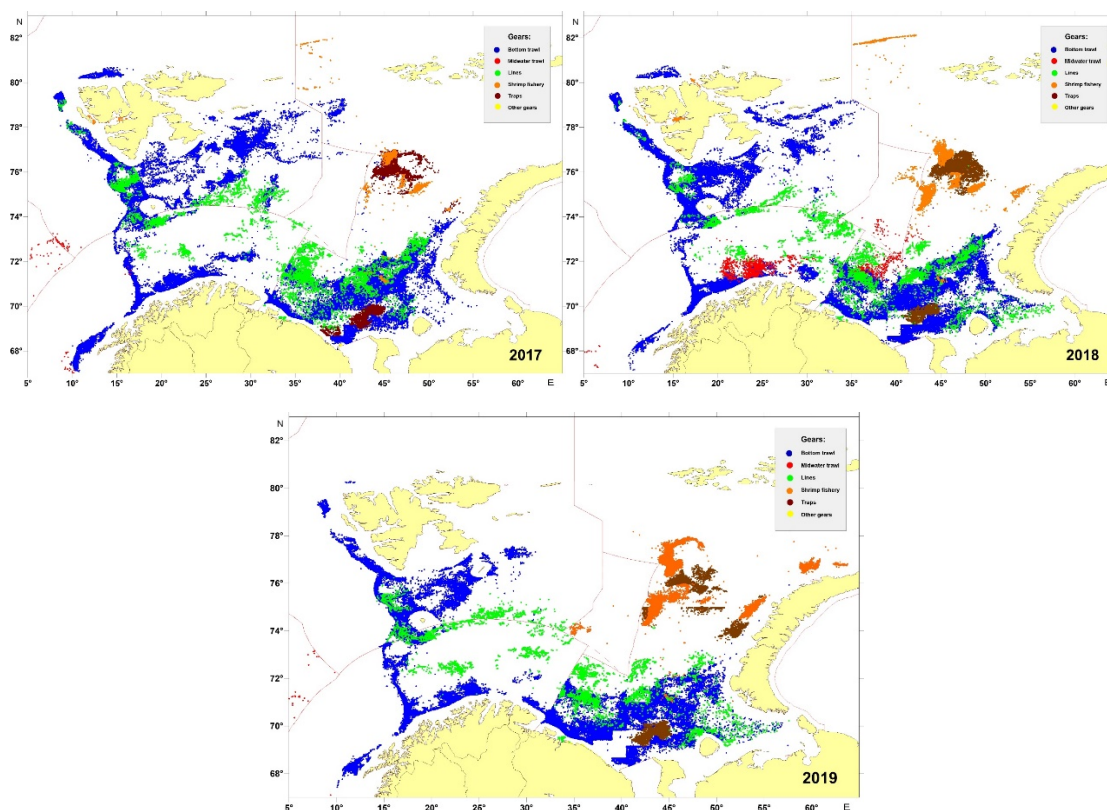


Figure 3.9.4.1. Location of Russian and foreign fishing activity from commercial fleets and fishing vessels used for research purposes in 2017-2019 as reported (VMS) to Russian authorities. These are VMS data linked with logbook data (source: PINRO Fishery statistics database).

From 2011 onwards, minimum mesh size for bottom-trawl fisheries for cod and haddock is 130 mm for the entire Barents Sea; previously the minimum mesh size was 135 mm in the Norwegian EEZ and 125 mm in the Russian EEZ. It is still mandatory to use sorting grids. Minimum legal catch size was harmonized at the same time: for cod from 47 cm (Norway) and 42 cm (Russia) to 44 cm for all, and for haddock from 44 cm (Norway) and 39 cm (Russia) to 40 cm for all.

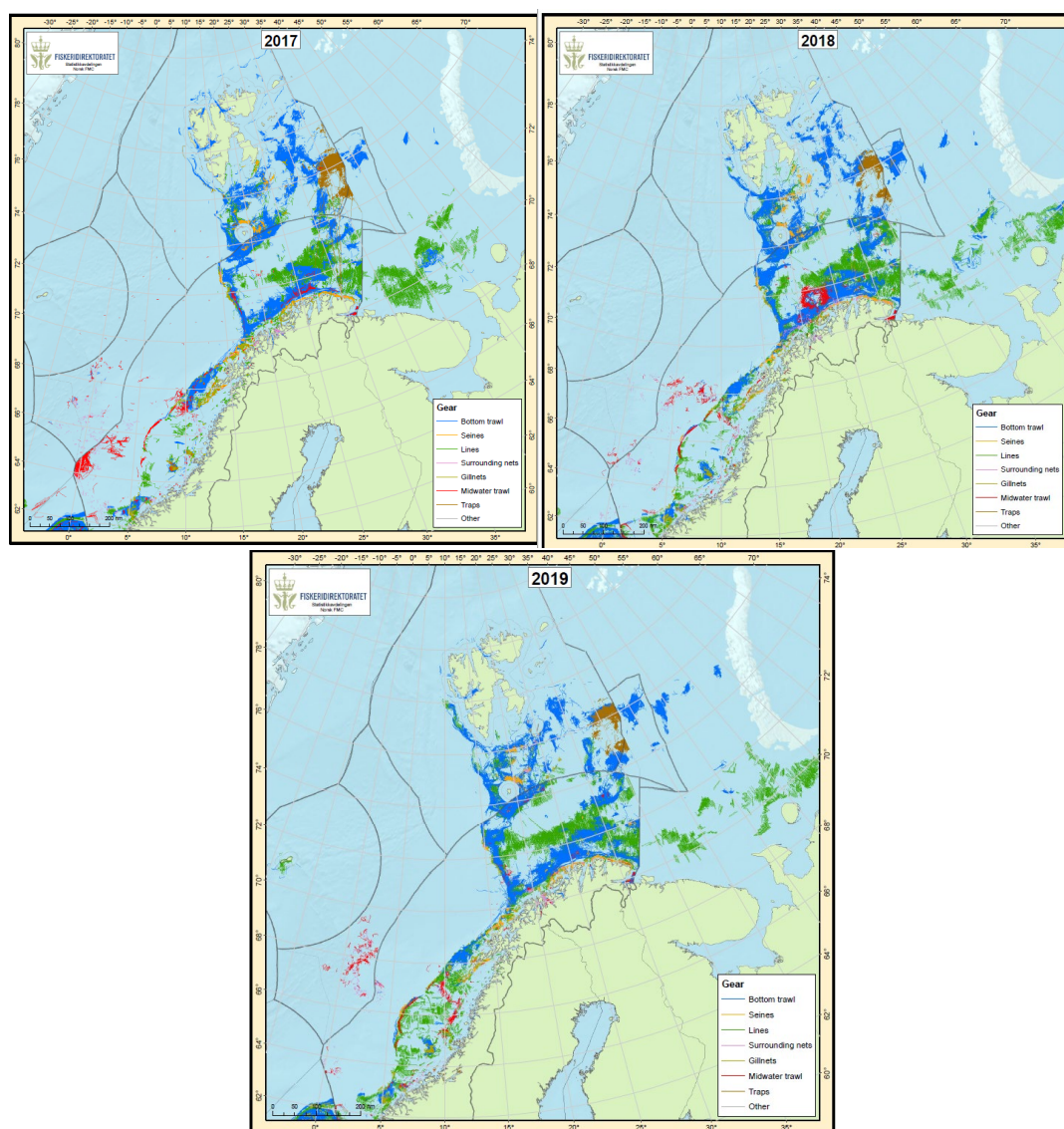


Figure 3.9.4.2 Location of Norwegian and foreign fishing activity from commercial fleets (larger than 15 m) and fishing vessels used for research purposes in 2017-2019 as reported (VMS) to Norwegian authorities. These are VMS data linked with logbook data. Surrounding nets = Danish seine (source: Norwegian Directorate of Fisheries). Fishery tracking (not AIS) linked to landing

3.9.5 Discards

Fisheries overview in the Barents Sea, including discards is available on https://www.ices.dk/sites/pub/Publication%20Reports/Advice/2019/2019/FisheriesOverviewBarentsSea_2019.pdf

3.9.6 Shipping activity

By Gro van der Meeren (IMR)

Shipping statistics include both fishing vessels and other. The vessels excluding fishing vessels, cover less distance than in other ocean regions, but the traffic is increasing every year (Figure 3.9.6.1).

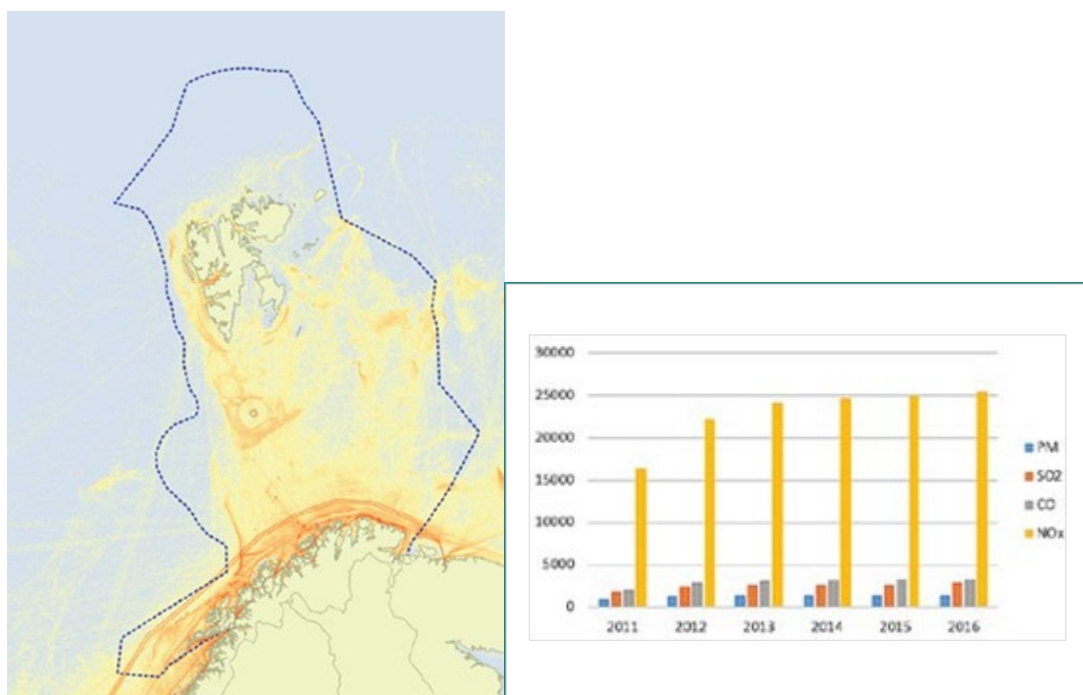


Figure 3.9.6.1. Left: Shipping through the year from July 2016 to June 2017. Right: Release (Tonnes) to air of particles (PM), SO₂, CO, NO_x.

With less ice and longer season for passable conditions for navigating the Northeast passage between the Atlantic and Pacific Oceans, more tourist cruises and increased petroleum-related activities, the traffic is expected to increase.

The impacts, linked to ordinary release of wastes and pollutants due to normal cruising, also include risk of introducing alien species, underwater noise and illegal release of pollutants. Release of pollutants from ordinary cruising may be countered by improved technology and fuel, reducing the environmental footprints even when the traffic increases (ref)(tabs). The shipping lanes between the Barents Sea and the North Atlantic is the main route for most of the ship traffic. This should allow for improved surveillance and reduced risk for major pollutions due to accidents, as vessels shipping dangerous goods, like oil or gas, are closely monitored.

Distance sailed, Barents Sea and Lofoten 2018 from vessel categories 2012-2018 (Nm)

Year	2012	2013	2014	2015	2016	2017	2018
Bulk carriers	590 332	608 545	583 707	554 578	514 287	602 810	575 064
Chemical tankers	309 312	320 480	250 433	287 059	285 924	342 781	369 669
Container ships	8 582	3 402	3 973	8 571	2 313	4 040	6 154
Crude oil tankers	54 414	82 083	101 406	128 172	187 295	233 629	228 828
Cruise ships	214 650	216 720	238 901	231 937	232 851	267 439	326 818
Fishing vessels	4 542 729	4 306 748	4 395 898	4 727 184	4 899 288	4 505 003	4 549 010
Gas tankers	65 940	59 962	65 906	77 337	75 580	75 036	235 650
General cargo ships	1 291 668	1 178 548	1 220 460	1 290 867	1 406 426	1 390 914	1 379 872
Offshore supply ships	173 208	232 442	265 727	188 606	192 403	224 427	189 278
Oil product tankers	176 096	136 987	110 924	96 799	119 074	99 822	159 070
Other activities	953 798	1 008 632	1 271 034	1 106 212	1 054 342	1 189 138	1 029 672
Other service offshore vessels	81 501	93 199	134 328	68 172	32 759	57 347	33 438
Passenger ships	1 197 541	1 210 504	1 299 703	1 439 125	1 572 041	1 575 047	1 603 535
Refrigerated cargo ships	277 648	273 220	299 969	269 730	284 966	280 214	279 943
Ro-Ro cargo ships	45 149	46 249	39 366	41 475	25 217	32 598	36 126
Sum	9 982 565	9 777 720	10 281 736	10 515 823	10 884 766	10 880 243	11 002 127

Release from vessels, Barents Sea and Lofoten 2018 from vessel categories (tons)

Vessel type	CO ₂	CO	NO _x	SO ₂	PM
Bulk carriers	146 958	340	3 458	558	316
Chemical tankers	86 030	198	1 895	280	163
Container ships	1 451	3	23	2	1
Crude oil tankers	99 904	229	2 251	502	189
Cruise ships	114 768	254	2 287	418	179
Fishing vessels	431 593	1 006	6 037	245	163
Gas tankers	245 423	562	5 600	1 290	485
General cargo ships	126 267	294	2 020	173	56
Offshore supply ships	79 557	171	1 076	46	33
Oil product tankers	17 841	41	329	41	22
Other activities	124 024	273	1 710	94	49
Other service offshore vessels	9 719	20	132	7	4
Passenger ships	214 632	463	3 776	490	275
Refrigerated cargo ships	40 815	89	545	54	16
Ro-Ro cargo ships	5 732	13	93	9	3
Total sum	1 744 713	3 958	31 232	4 209	1 955

3.9.7 Oil and gas

By Gro van der Meeren (IMR)

It is increased activities for searching, test drilling and developing the oil- and gas production in the Barents Sea. In recent years the search for valuable locations has increased and moved further eastward (Figures 3.9.7.1-3.9.7.4).

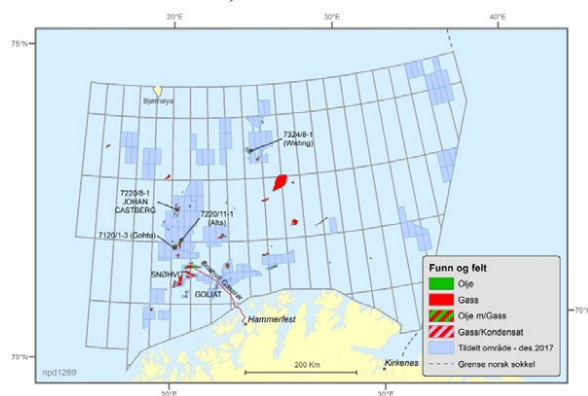


Figure 3.9.7.1. Active fields for oil- and gas exploitation in the Norwegian EEZ, by December 2017. (source The Norwegian Petroleum Directorate)

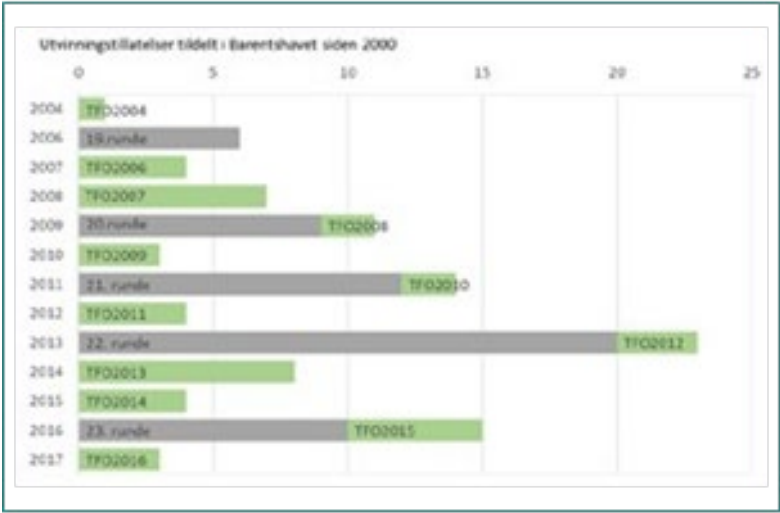


Figure 3.9.7.2. Licenses approved by year 2000 to 2017 for the Norwegian EEZ. (source The Norwegian Petroleum Directorate)

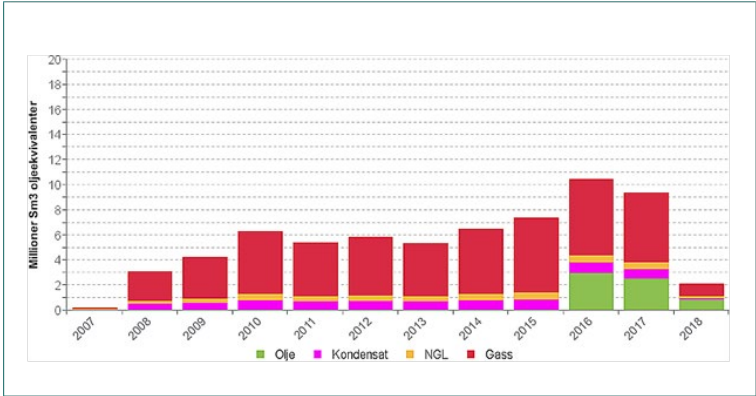


Figure 3.9.7.3. Annual production from the Barents Sea petroleum fields, from 2007 to 2018. (source The Norwegian Petroleum Directorate)

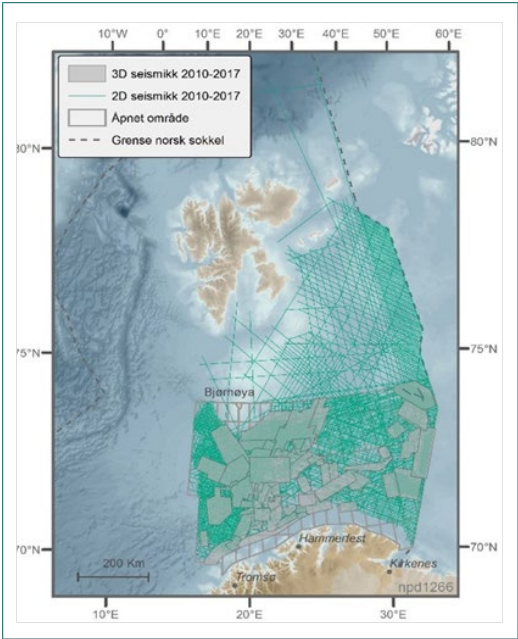


Figure 3.9.7.4. Seismic activities in the Norwegian EEZ from 2010 to 2017.

Seismic activities are known to evoke fear reaction in fish and some marine mammals. Minke whales and harbour porpoises react on distances from 600 to 1000 m away. Some fish species flee the area while other turn passive and stop feeding. Any long-lasting effects are not known.

3.9.8 Marine litter

Anthropogenic litter were observed at every fourth (pelagic) and every second (bottom) station, and plastic dominated among all observations. Amounts of plastic and other litter are relatively low in comparison to other sea areas.

T. Prokhorova (PINRO), B.E. Grøsvik (IMR) and P. Krivosheya (PINRO)

Due to poor coverage of the Russian Zone by BESS in 2018 it is impossible to compare distribution of litter and some parameters, for example average weight of litter in trawl, between 2019 and 2018.

Plastic dominated among anthropogenic litter on the sea surface in 2019 (59% of observations, Fig. 3.9.8.1). The maximum surface observation of plastic litter was 0.331 m³, with an average of 0.014 m³. Wood was recorded in 39% of the observations. The maximum surface observation of wood was 2.8 m³, with the average of 0.4 m³. Metal, paper and rubber was observed singularly.

Fishery related litter was recorded in 15.3% of plastic litter observations at the surface (Figure 3.9.8.2). Fishery related litter was represented by ropes and floats/buoys.

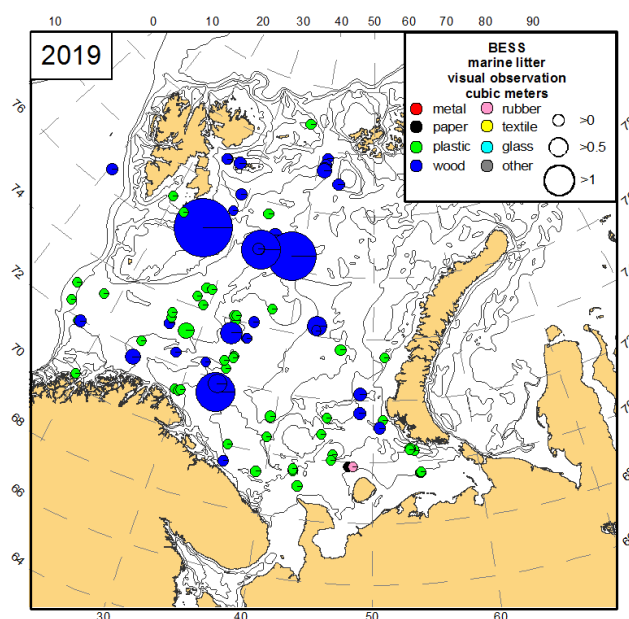


Figure 3.9.8.1 Type of observed anthropogenic litter (m³) at the surface in the BESS 2019 Taken from the 2019 BESS survey report (Prokhorova and Grøsvik 2020).

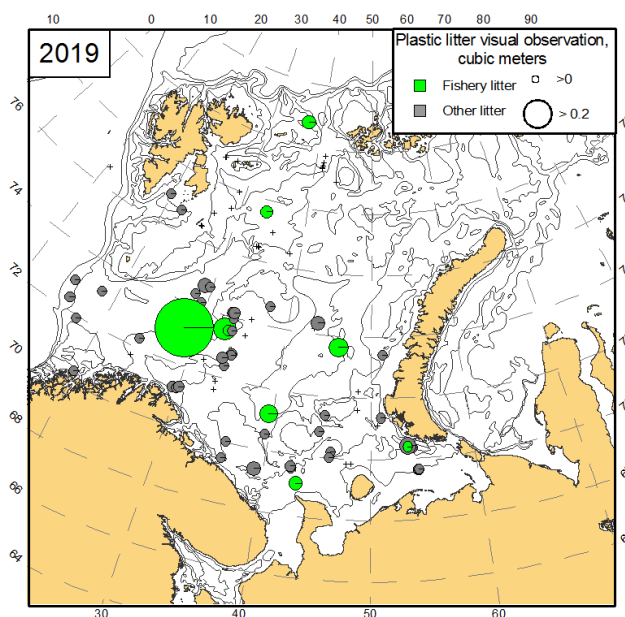


Figure 3.9.8.2 Litter observations of plastic at the surface indicated as fishery related and other litter in the BESS 2019 (crosses – occurrences of anthropogenic litter).

Anthropogenic litter was observed in 25.8% of the pelagic trawl stations (Fig. 3.9.8.3). The number of litter recordings from both pelagic and bottom stations increased in the period since these recordings started (2010) to 2018. In 2010, 6.6% of pelagic trawls contained litter, 2.9 % in 2011 and 24.2 % in 2018 (ICES, 2019). Plastic dominated among all anthropogenic matter in pelagic trawls. Frequency of occurrence of plastic in pelagic trawls was approximately the same in all years. Thus, plastic was recorded in 96.5% of the stations with observed litter in 2019, in 94.7 % in the period of 2010-2013 and 95.6% in the period of 2014-2018 (ICES, 2019). The weight of plastic litter from pelagic trawls varied from 0.1 g to 23 kg with an average of 0.03 kg (except the single maximum catch of 23 kg). Other types of litter (wood, textile, paper and metal) were observed singularly. The maximum catch of litter by pelagic trawl was 10.5 kg per nm, with an average of 0.037 kg per nm.

Litter was observed throughout the survey in the bottom trawl catches (43.8% of the bottom trawl stations) (Fig. 3.9.8.3). Plastic also dominated the litter content from the bottom trawls (82.3% of stations with observed litter in 2019 compared with 81 % of stations in the period of 2010-2013 and 88.7 % in the period of 2014-2018) (ICES. 2019). The weight of plastic litter in bottom trawls was from 0.1 g to 11.3 kg with an average of 0.04 g (except the single maximum catch of 11.3 kg). Wood was registered in bycatch in shallow waters in the south-eastern part of the Barents Sea, also in the northern part of the survey area (24.8 % of stations with observed litter). In 2019 more wood litter was observed than in previous periods (11.3% in 2010-2013 and 19% in 2014-2018) (ICES. 2019). Textile, paper, metal, rubber and glass were observed among the bottom trawl catches sporadically. The maximum catch of litter by bottom trawl was 21.0 kg per nm, with an average of 0.17 kg per nm.

Litter from fishery was a significant part of plastic litter both in the pelagic and bottom trawls (63.4 % and 41.1 % respectively) (Figure 3.9.8.4).

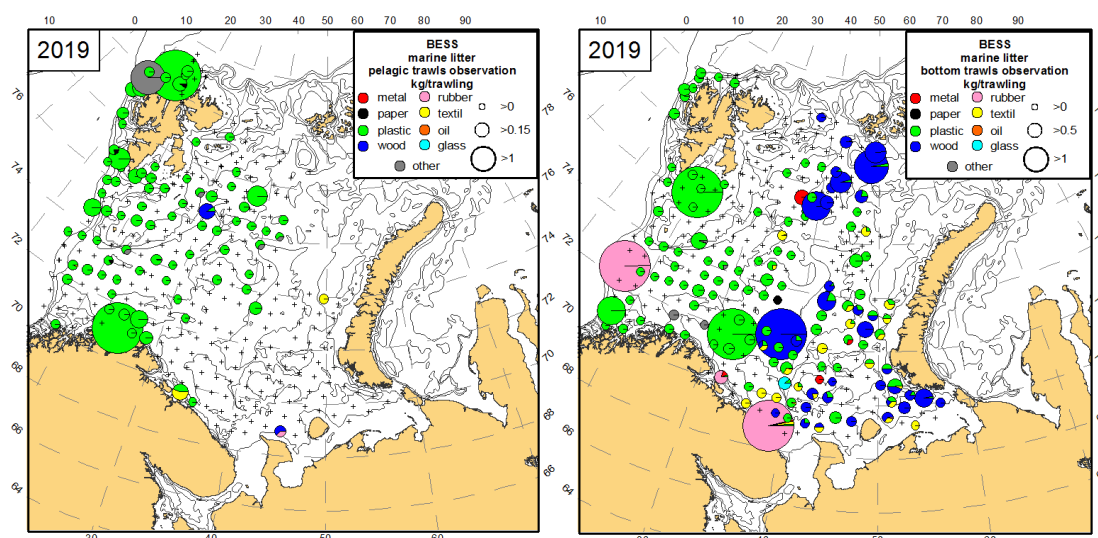


Figure 3.9.8.3 Type of anthropogenic litter collected in the pelagic trawls (left) and bottom trawls (right). Size of circles indicate weight in the range of >0, >150g or > 1000 g for pelagic trawls or in the range of >0, >0.5 g or > 1000 g for bottom trawls. Crosses indicate trawl stations. Taken from the 2019 BESS survey report (Prokhorova and Grøsvik 2020).

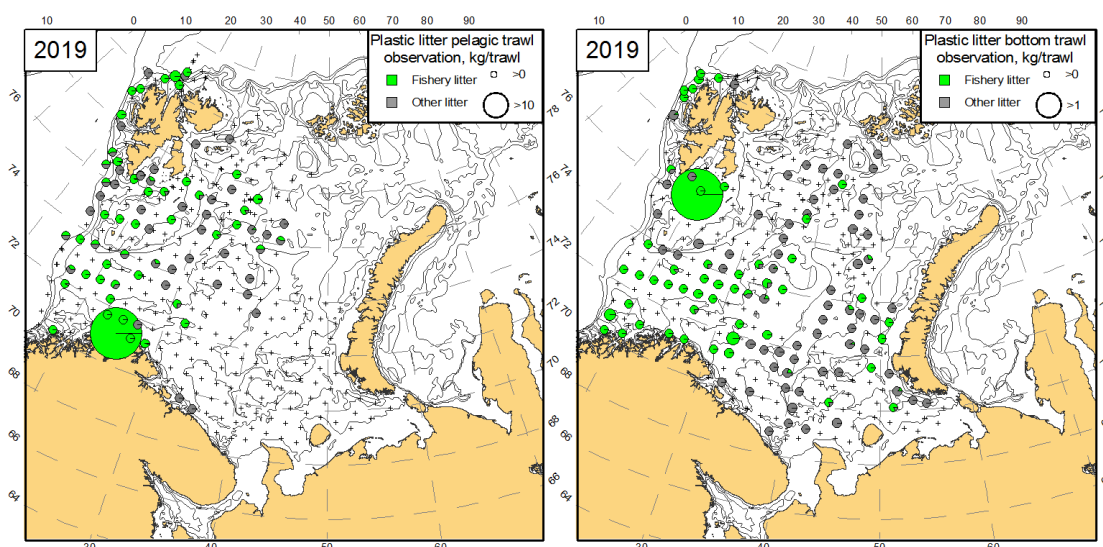


Figure 3.9.8.4 Fishery plastic proportion among the plastic litter collected in the pelagic (to the left) and bottom trawls (to the right) in the BESS 2019 (crosses – trawl stations).

References

ICES. 2019. The Working Group on the Integrated Assessments of the Barents Sea (WGIBAR). ICES Scientific Reports. 1:42. 157 pp. <http://doi.org/10.17895/ices.pub.5536>

3.9.9 Contaminants in marine organisms

By Sylvia Frantzen (IMR)

Levels of contaminants in fish from the Barents Sea are in general relatively low and below EU and Norway's maximum levels set for food safety. For most substances, concentrations are stable or slightly decreasing.

Monitoring programs

IMR conducts regular monitoring of chemical contaminants in biota through two different programs. 1) A three-year monitoring program designed to monitor the level of pollution in the Barents Sea, and 2) An annual monitoring program with focus on seafood safety and pollution level in indicator species.

In program 1, levels of certain organic contaminants (PCB, chlorinated pesticides and PBDEs) are analysed mainly in liver of fish. The exact species sampled varies from year to year, but some species have been sampled repeatedly in three year cycles and temporal data exist for Greenland halibut, long rough dab, haddock, capelin, polar cod, saithe (*Pollachius virens*), herring, cod and golden redfish. The sampling programme is designed to monitor pollution levels over time. Samples are mainly taken on the ecosystem cruise in summer/early fall.

In program 2, levels of metals including As, Cd, Hg and Pb are analysed in fillet and liver of Atlantic cod, whole capelin and polar cod as well as whole and peeled boiled northern shrimp (*Pandalus borealis*). Levels of organic pollutants (POPs) are analysed in liver of cod, whole capelin and polar cod and whole boiled shrimp, and a few samples of cod fillet have also been analysed. The POPs include dioxins and dioxin-like PCBs, non-dioxinlike PCBs (PCB6, PCB7), organochlorine pesticides, brominated flame retardants (PBDEs, HBCD and TBBP-A), per- and polyfluoralkyl substances (PFAS) and PAHs. The monitoring program is designed to document levels of contaminants with regards to food safety, while also gaining information on pollution levels by analysing indicator organisms representing varying trophic levels and niches. Samples are mainly taken on the winter cruise in January-March.

In addition to these regular monitoring programs, samples of several species have been taken in the Barents Sea and analysed. Some are sampled and analysed on a regular basis and as a part of special surveys. Contaminants in saithe and Greenland halibut are monitored annually. Species where we collected data on contaminants for special surveys include redfish species (*Sebastes norvegicus* and *S. mentella*, (Nilsen et al. 2020), tusk (*Brosme brosme*), haddock and wolffish (Atlantic, spotted and jelly; *Anarhichas* spp.) and snow crab (Frantzen and Maage 2016) as well as red king crab from coastal areas (Julshamn et al. 2015).

In both program 1 and 2, where temporal data exist, samples are not taken at fixed positions or at fixed fish size, so temporal trends must be interpreted with caution. The positions sampled during 2006-2019 for program 2 are shown in figures 3.9.9.1-3.9.9.4.

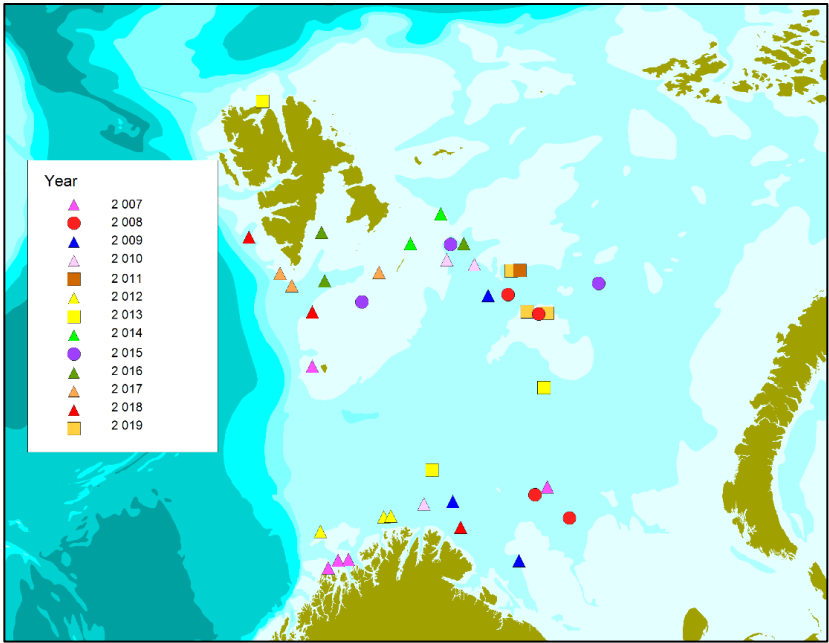


Figure 3.9.9.1 Positions in the Barents Sea where capelin (*Mallotus villosus*) was sampled for program 2 during 2007-2019. The colour and shape of the points indicate sampling year.

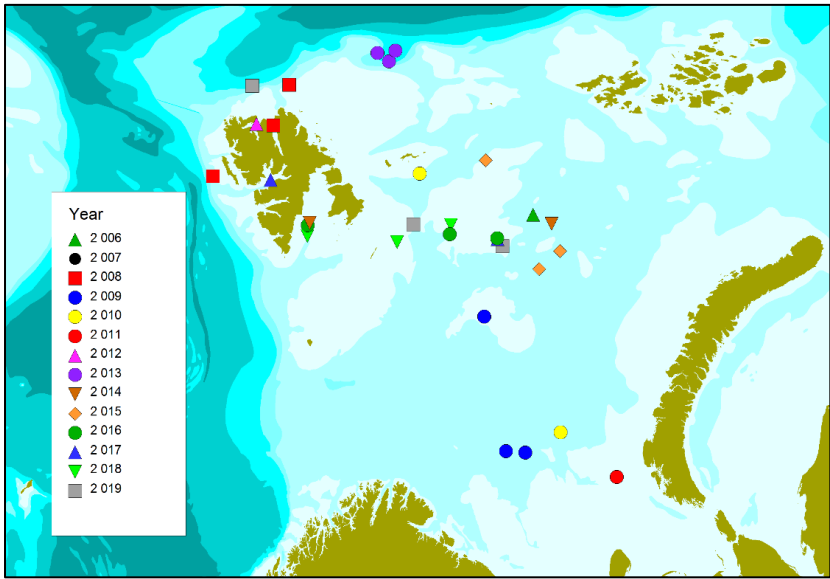


Figure 3.9.9.2 Positions in the Barents Sea where polar cod (*Boreogadus saida*) was sampled for program 2 during 2006-2019. The colour and shape of the points indicate sampling year.

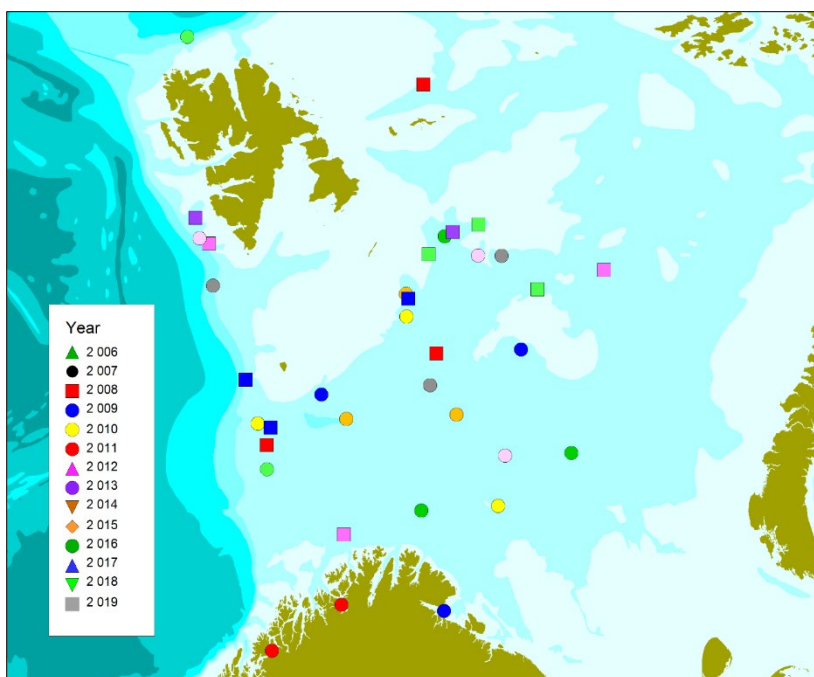


Figure 3.9.9.3 Positions in the Barents Sea where northern shrimp (*Pandalus borealis*) was sampled for program 2 during 2006-2019. The colour and shape of the points indicate sampling year.

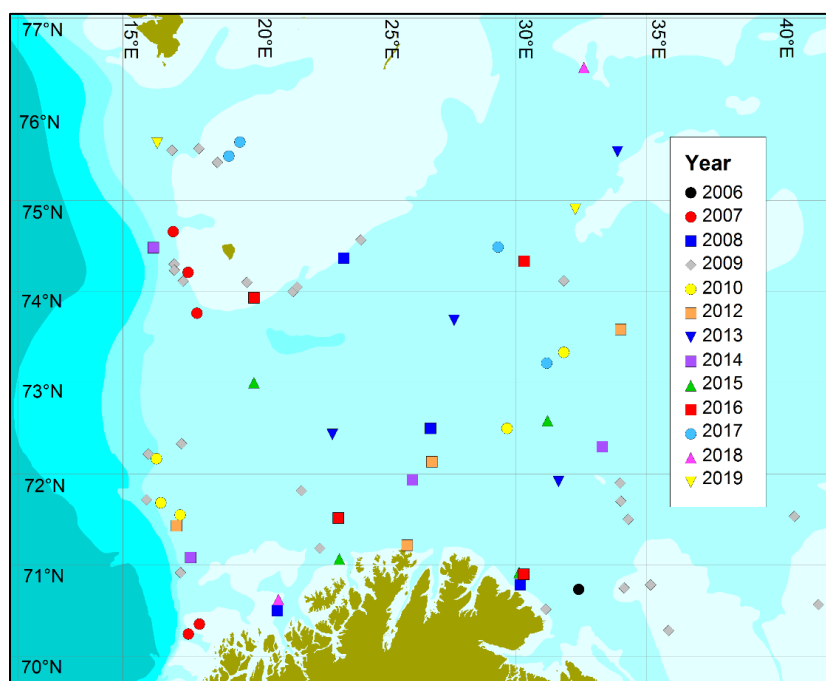


Figure 3.9.9.4 Areas in the Barents Sea where cod (*Gadus morhua*) was sampled for program 2 during 2006-2019. The colour and shape of the points indicate sampling year.

Analyses are performed with accredited analytical methods according to ISO 17025.

Levels of contaminants with focus on food safety

In general, levels of contaminants in fillet of fish from the Barents Sea are very low and below EU and Norway's maximum levels for food safety for substances where these exist (Hg, Cd, Pb, sum dioxins and dioxin-like PCBs and sum PCB6) (Figure 3.9.9.5).

Mercury is the contaminant that is most often of concern for food safety, especially with regard to muscle of lean fish. The levels of mercury in muscle of fish from the Barents Sea are generally lower than in other (Norwegian) sea areas. The highest concentrations are found in Greenland halibut, tusk and Atlantic wolffish, and the lowest concentrations are found in some of the most commercially important species such as cod, saithe and haddock (Figure 3.9.9.5). Beaked redfish had somewhat higher level of mercury than golden redfish. The varying levels of mercury are probably at least partly due to the different species' trophic level, as methylmercury is a typically biomagnifying contaminant. Other factors that can lead to between-species variation in mercury levels are for instance age, growth rate and geographical area.

Arsenic levels in some of the fish species were relatively high (Figure 3.9.9.5). The arsenic present in fish muscle is in general arsenobetain, which has very low toxicity. The most toxic species of arsenic is inorganic arsenic (EFSA 2009). A large number of fish samples from Norwegian sea areas were previously analysed for total and inorganic arsenic, and even those with very high total arsenic concentrations had very low levels of inorganic arsenic (Julshamn et al. 2012). In Norway and EU, there is no maximum level for arsenic, while Russia has a maximum level of 5 mg/kg, which some of the fish species exceeded (Figure 3.9.9.5). Differences between species in arsenic level may at least in part be related to their diet, where a more benthic diet seems to lead to higher arsenic levels than a predominantly pelagic diet (Neff 1997).

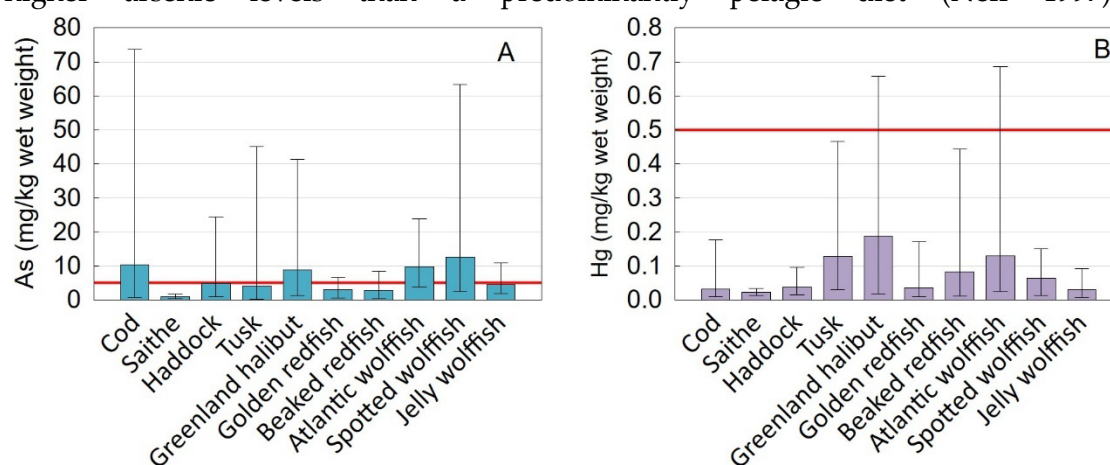


Figure 3.9.9.5 Concentrations of A) Arsenic (As, mg/kg wet weight) and B) mercury (Hg, mg/kg wet weight) in muscle of cod (2018-2019, N=98), saithe (2018-2019, N = 75), haddock (2014, N=40), tusk (2014, N=160), Greenland halibut (2018, N= 52), golden redfish (2018, N = 50), beaked redfish (2018, N = 249), Atlantic wolffish (2014, N=29), spotted wolffish (2014, N=27) and jelly wolffish (2014, N=12). Mean, minimum and maximum values are shown. Red lines indicate maximum allowable levels set for food safety.

The levels in muscle of the lipid soluble persistent organic pollutants dioxins and dioxin-like PCBs and sum PCB6 were higher in Greenland halibut, redfishes and wolffishes than in other fish species (Figure 3.9.9.6). The different levels of these substances in fillet are probably related to the different fat contents of the different fish species, since Greenland halibut is a fatty fish (fat content ca. 10g/100g), redfish and wolffish species are semi-fatty, while cod, saithe and haddock are typically lean fish

species with fat contents lower than 1 g/100 g. Lean fish species primarily store their fat and fat soluble organic contaminants in the liver, where the concentrations of these substances may get very high as can be seen in figure 3.9.9.9. The EU and Norway have established special maximum levels applying to dioxins and dioxin-like PCBs and sum PCB6 in liver, which are set much higher than for fillet. In some areas, these higher maximum levels are exceeded. This is normally not a great food safety issue, as fish liver is not generally consumed in large amounts. However, to protect the most vulnerable parts of the population (i.e. foetuses and young children) against dioxin and dioxin-like PCB toxicity, the Norwegian Food Safety Authority has issued a warning for children and pregnant and breastfeeding women, against eating fish liver (https://www.matportalen.no/matvaregrupper/tema/fisk_og_skalldyr/barn_gravide_og_ammende_bor_ikke_spise_rognleverpostei).

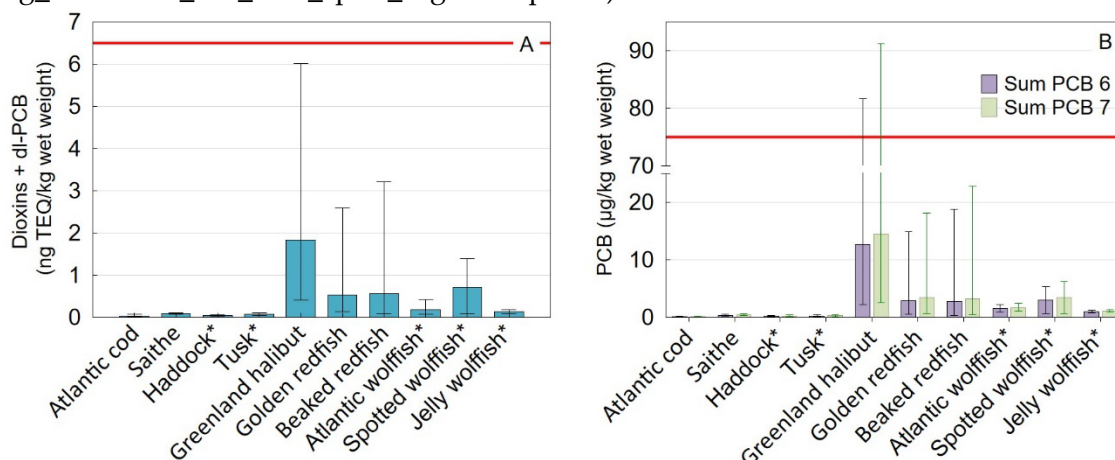


Figure 3.9.9.6 Concentrations of A) Sum of dioxins and dioxin-like (dl-) PCBs (ng TEQ/kg weight) and B) sum PCB6 sum PCB7 (µg/kg wet weight) in muscle of cod (2018-2019, N=20), saithe (2019, N=5), haddock (2014, N=7*), tusk (2014+2016; N=10*), Greenland halibut (2018-2019, N= 74), golden redfish (2018, N=49), beaked redfish (2018, N = 347), Atlantic wolffish (2014, N=6*), spotted wolffish (2014, N=4*) and jelly wolffish (2014, N=2*). Mean, minimum and maximum values are shown. Red lines indicate maximum allowable levels set for food safety in EU and Norway. For non-dioxinlike PCBs, maximum level in EU and Norway applies to the sum PCB6. * Composite samples analysed.

Concentrations of some heavy metals in muscle tissue of the crustaceans red king crab, snow crab and shrimp, are shown in Figure 3.9.9.7. Levels of mercury and cadmium were very low and well below maximum levels set for food safety in EU and Norway (Figure 3.9.9.7A, B). The level of cadmium was considerably higher in shrimp than in both crab species. Cadmium is a heavy metal that accumulates in the hepatopancreas of crustaceans, and shrimp analysed whole have relatively high cadmium concentrations which in many cases exceed the maximum level. However, since shrimps are usually peeled before being consumed this is not considered a food safety issue. Pure muscle tissue in general has very low cadmium levels. Still, cadmium levels in shrimp from the Barents Sea are higher than the levels in shrimp sampled in Norwegian sea areas further south. This corresponds well with findings from other studies of increasing cadmium levels in crustaceans from south to north (Wiech et al. 2020; Zauke et al. 1996, Zauke and Schmalenbach 2006). It likely has natural causes. However, a good explanation has so far not been found.

Levels of arsenic in the snow crab and shrimp were very high (Figure 3.9.9.7C). Again, this is most likely arsenobetain, which is known as a non-toxic substance. Analysis of inorganic arsenic in red king crab has shown that inorganic arsenic contributes a very small part (<0.4%) of the total arsenic concentrations (Julshamn et al. 2015).

The levels of dioxins and PCBs were very low in the crustacean muscle tissue (Figure 3.9.9.8), which is also very lean with mean fat contents in the area of 0.5-2.2 g/100 g (Seafood data). The concentrations of both sum dioxins and dioxin-like PCBs and sum PCB6 were far below the maximum levels set for food safety in EU and Norway.

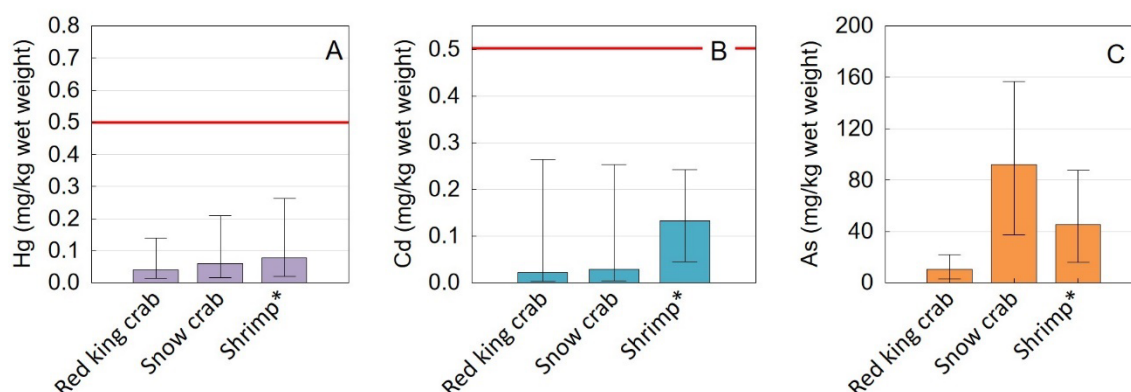


Figure 3.9.9.7 Concentrations of A) mercury (Hg, mg/kg wet weight), B) cadmium (Cd, mg/kg wet weight) and C) arsenic (As, mg/kg wet weight) in muscle of red king crab (*Paralithodes camtchaticus*, 2012), snow crab (*Chionoecetes opilio*, 2014 + 2016) and shrimp (*Pandalus borealis*, boiled, 2015-2019). Mean, minimum and maximum values are shown. Red lines indicate maximum allowable levels set for food safety. *Composite samples.

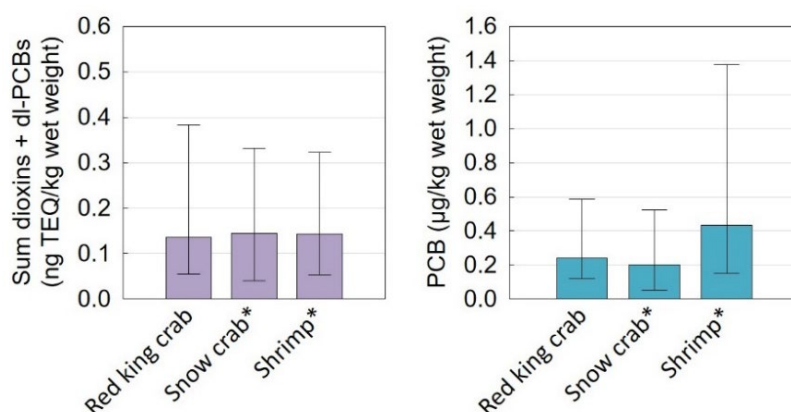


Figure 3.9.9.8 Concentrations of A) sum of dioxins and dioxin-like (dl-) PCBs (ng TEQ/kg weight) and B) sum PCB6 (µg/kg wet weight) in composite muscle samples of red king crab (2012, N = 29), snow crab (2014, N = 9*) and shrimp (2015-2019, N=15* cooked and peeled). Mean, minimum and maximum values are shown. *Composite samples analysed.

Levels of contaminants with focus on pollution level and environmental effects

Figures 3.9.9.9 and 3.9.9.10 show concentrations of selected lipid soluble organic contaminants (Dioxins+dioxin-like PCBs, PCB7) in liver of different fish species from the Barents Sea. Tusk liver had among the highest levels of both dioxins and dioxin-like PCBs and PCB7. Haddock had the highest mean concentration of dioxins and dioxin-like PCBs, while PCB7 was not very high. The results shown for haddock for

dioxins and dioxinlike PCBs and for PCB7 are from different projects, and the differences could be due to differences in sampling area. The species where we have the most data from other areas for comparison, is cod. The mean levels of dioxins and dioxinlike PCBs and PCB7 in liver of cod from the Barents Sea were much lower than in liver of cod from the North Sea, which in 2016 were 20.6 ng TEQ/kg and 162 µg/kg, respectively (miljostatus.no). It has also been shown that the levels of contaminants in tusk and saithe from the Barents Sea in general are lower than in the same species from the Norwegian Sea and the North Sea (Frantzen and Maage 2016; Nilsen et al. 2013a, Nilsen et al. 2013b). It must be kept in mind that the different species in Figure 3.9.9.9 and Figure 3.9.9.10 were taken in different years (see figure legends), and this may also affect the observed differences between the species. Herring liver was only analysed for PCB7 in program 1, and herring had the lowest mean concentration of PCB7 of all the different species, followed by Greenland halibut. Since herring and Greenland halibut are fatty fish species, they store much of their lipids and lipid soluble pollutants in their fillet, explaining the low concentrations in their liver. In contrast, the species with the highest concentrations of these substances in liver are lean fish species, which store all surplus lipids in their liver.

Brominated flame retardants (PBDEs) show almost same pattern of between-species variation as dioxins and dioxin-like PCBs and non-dioxin like PCBs (Figure 3.9.9.11). This is probably because the same factors control the between-species variations for the lipid soluble brominated compounds as the dioxins and PCBs. Also for PBDEs, concentrations in the Barents Sea are lower than in the North Sea for species where we have comparable data from the North Sea. Concentrations of chlorinated pesticides such as DDTs and HCB in fish liver vary between species in much the same way, and results are not shown here.

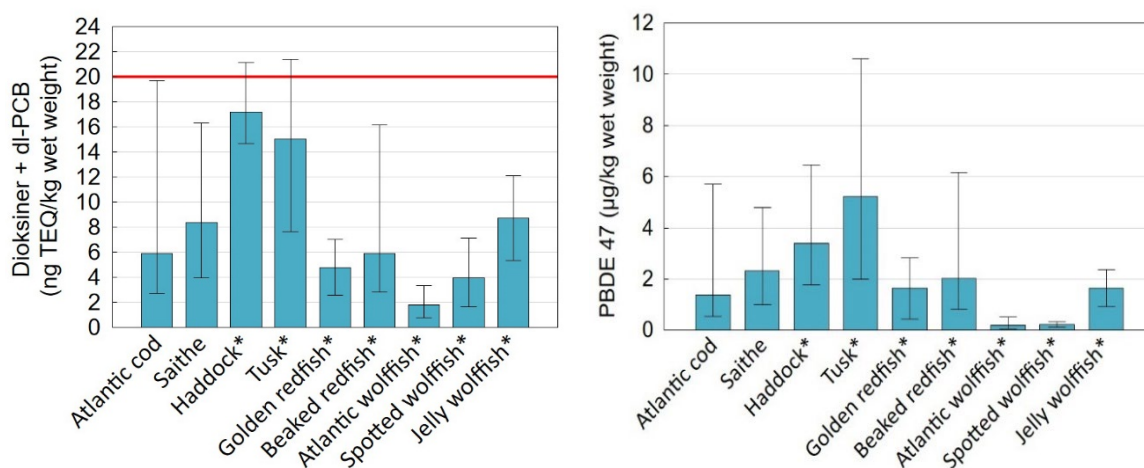


Figure 3.9.9.9 Concentration of sum of dioxins and dioxin-like (dl-) PCBs (ng TEQ/kg weight) in liver of cod (2018-2019, N=92), saithe (2018-2019, N=75), haddock (2014, N=8*), tusk (2014; N=9*), golden redfish (2018, N=2*), beaked redfish (2018, N = 14*), Atlantic wolffish (2014, N=6*), spotted wolffish (2014, N=4*) and jelly wolffish (2014, N=2*). Mean, minimum and maximum values are shown. Red lines indicate maximum allowable levels set for food safety in EU and Norway. For non-dioxinlike PCBs, maximum level in EU and Norway applies to the sum PCB6. * Composite samples analysed.

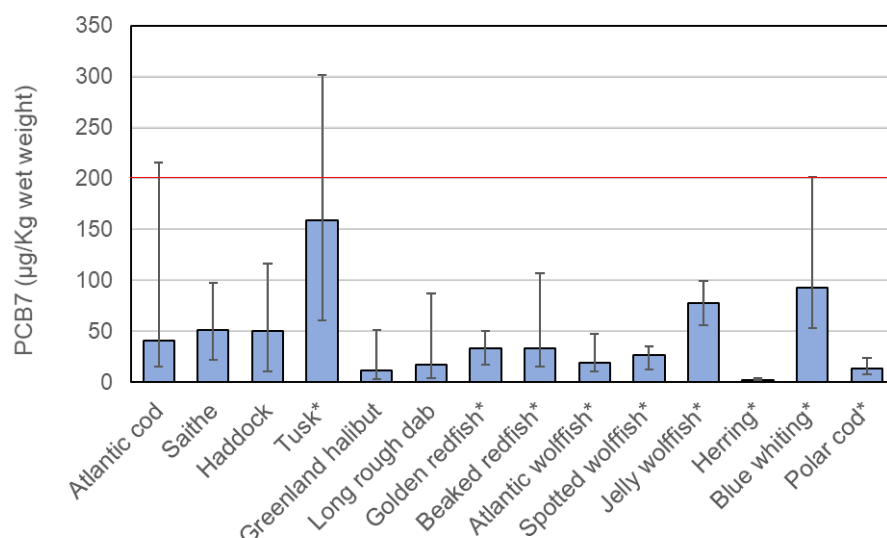


Figure 3.9.9.10 Concentrations of the sum PCB7 (µg/kg wet weight) in liver of cod (2018-2019, N=92), saithe (2018-2019, N=75), haddock (2015, N = 49), tusk (2014; N=9*), Greenland halibut (2015, N = 50), long rough dab (2015, N = 43), golden redfish (2018, N=2*), beaked redfish (2018, N = 14*), Atlantic wolffish (2014, N=6*), spotted wolffish (2014, N=4*), jelly wolffish (2014, N=2*), herring (2015, N = 10*), blue whiting (2015, N = 10*) and polar cod (2015, N = 5*). Mean, minimum and maximum values are shown. Red line indicates maximum level applying to fish liver in EU and Norway. * Composite samples analysed.

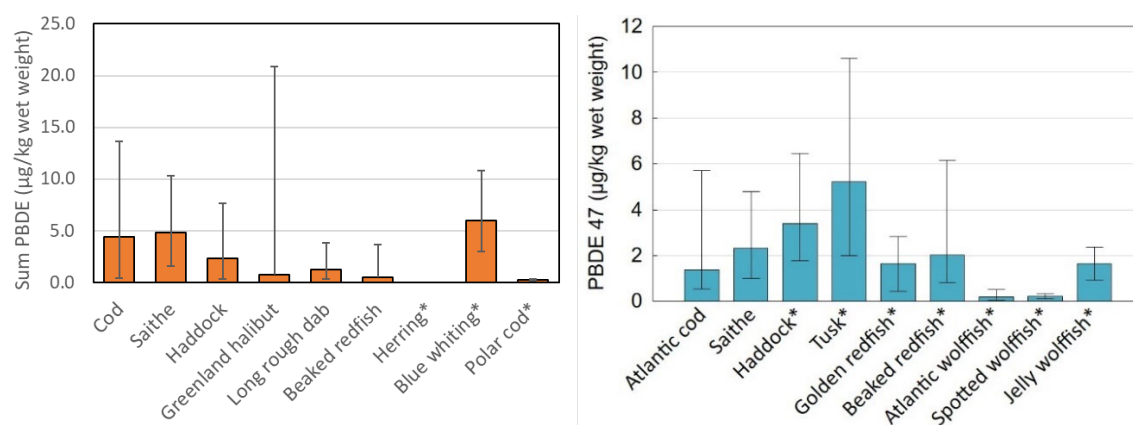


Figure 3.9.9.11 Left: Concentrations in 2015 of sum PBDE in liver of cod (2015, N=50), saithe (2015, N=25), haddock (2015, N = 49), Greenland halibut (2015, N = 50), long rough dab (2015, N = 26), beaked redfish (2015, N = 43), herring (2015, N = 10*), blue whiting (2015, N = 10*) and polar cod (2015, N = 5*). Right: Concentrations of PBDE 47 (µg/kg wet weight) in liver of cod (2018-2019, N=92), saithe (2018-2019, N=75), haddock (2014, N=8*), tusk (2014; N=9*), golden redfish (2018, N=2*), beaked redfish (2018, N = 14*), Atlantic wolffish (2014, N=6*), spotted wolffish (2014, N=4*) and jelly wolffish (2014, N=2*). Mean, minimum and maximum values are shown. * Composite samples analysed.

Levels of contaminants in forage fish and shrimp analysed whole are particularly interesting with regard to transfer of contaminants to higher trophic levels and ultimately to the top predators. Through the water framework directive, the EU has given a set of environmental quality standards (EQS) for harmful substances in the environment, including biota (Directive 2008/105/EC). In addition, Norway has established additional regional EQS values for substances not included by the EU (Miljødirektoratet 2016). The EQS are meant to protect the most sensitive organisms in the ecosystem. This means that levels of contaminants exceeding the EQS may

potentially have a harmful effect on animals at the highest trophic levels and animals feeding exclusively on fish. Therefore, the EQS have in general been set much lower than the maximum levels for food safety, where these exist.

Levels of selected compounds (PCB7, DDT, HCB, PBDE) in small organisms analysed whole, i.e. shrimp, capelin, polar cod and sandeel, are given in the graphs below (Figure 3.9.9.12). While mean levels of DDT, PCB7 and PBDE were higher in capelin than in polar cod, the mean level of HCB was higher in polar cod than in capelin. Sandeel had lower concentrations of both DDT, PCB and HCB than both capelin and polar cod. Shrimp (whole, boiled) had a mean PCB7 concentration similar to capelin, while levels of DDT and HCB were lower in shrimp than both capelin, polar cod and sandeel.

Concentrations of mercury, HCB and DDT in capelin and polar cod from the Barents Sea are below the EQS values (Figure 3.9.9.12; Figure 3.9.9.14). However, the levels of PCB7 and PBDE were mostly above the EQS. The concentrations of these substances are, however, very low in these species from the Barents Sea. Since capelin and polar cod are mainly found in the Barents Sea, there is no data to compare with from other Norwegian sea areas. For sandeel, there is data from the North Sea, where concentrations of Hg, DDT and PBDEs in 2016 were much higher than in the Barents Sea (miljostatus.no). On the other hand, the level of HCB was much higher in sandeel from the Barents Sea than in sandeel from the North Sea.

Concentrations of contaminants are found in fish and crustaceans at significant and measurable levels. The levels of the analysed substances are, however, relatively low in the Barents Sea compared to areas further south, except for the levels of cadmium and HCB, which seem to be higher in organisms from the Barents Sea. However, PCBs and PBDEs are above EQS values, which may indicate potentially harmful effects for animals at high trophic level such as for instance polar bears. It is not known, however, whether the levels of these substances in top predators and fish eaters such as marine mammals and seabirds in the Barents Sea actually have harmful effects on individual or population levels.

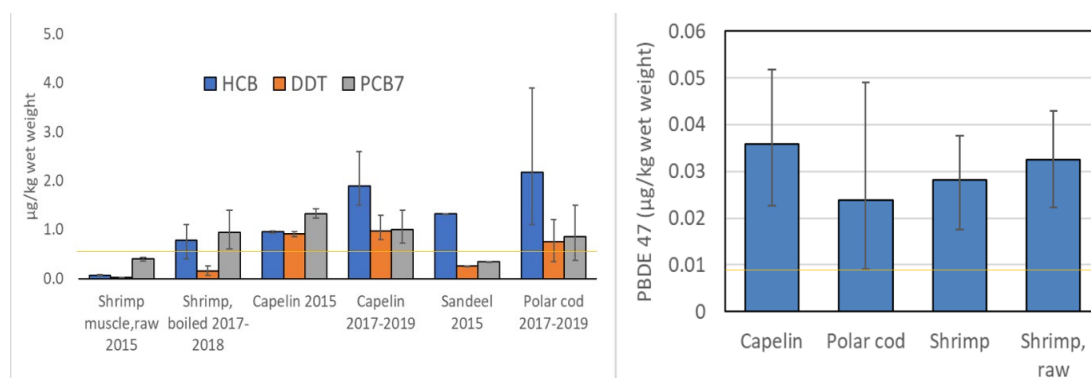


Figure 3.9.9.12 Left: Concentrations of HCB, DDT (sum of p,p'-DDD, p,p'-DDE and p,p'-DDT) and PCB7 in composite samples of whole boiled shrimp, capelin, sandeel and polar cod. Right: Concentration of PBDE 47 (the most dominating PBDE congener) in composite samples of whole

capelin, polar cod, boiled and raw shrimp. Yellow lines indicate EQS values for PCB7 (left panel) and PBDE (right panel).

Temporal trends of contaminant levels

In order to evaluate time trends for levels of different contaminants in the Barents Sea biota, data from cod, capelin and polar cod have been included (Figure 3.9.9.13-3.9.9.21).

Mercury levels appear to be very stable in the Barents Sea, based on concentrations measured in cod fillet as well as in capelin and polar cod (Figure 3.9.9.13, Figure 3.9.9.14). The lower limit of quantification (LOQ) for mercury prior to 2010 was higher than later on, which is why it may look like a decrease for polar cod after 2009.

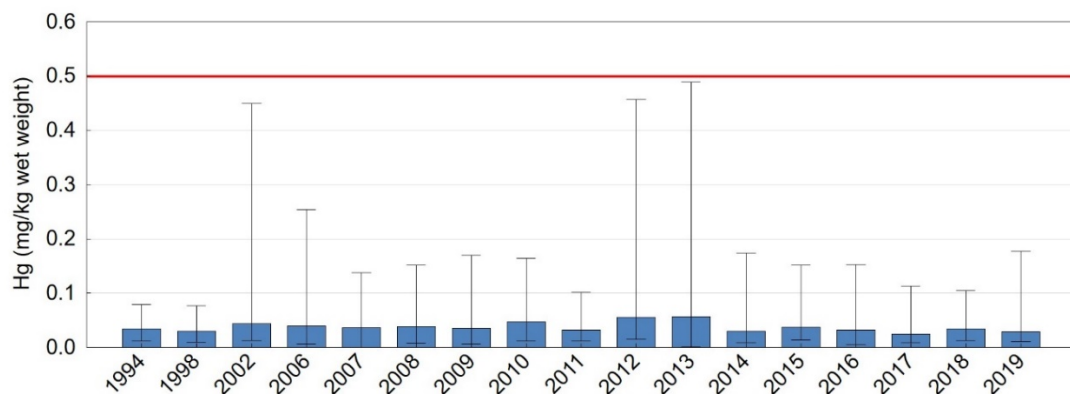


Figure 3.9.9.13 Annual concentrations of mercury in fillet of cod from 1994 to 2019. For each year, mean, minimum and maximum values are shown.

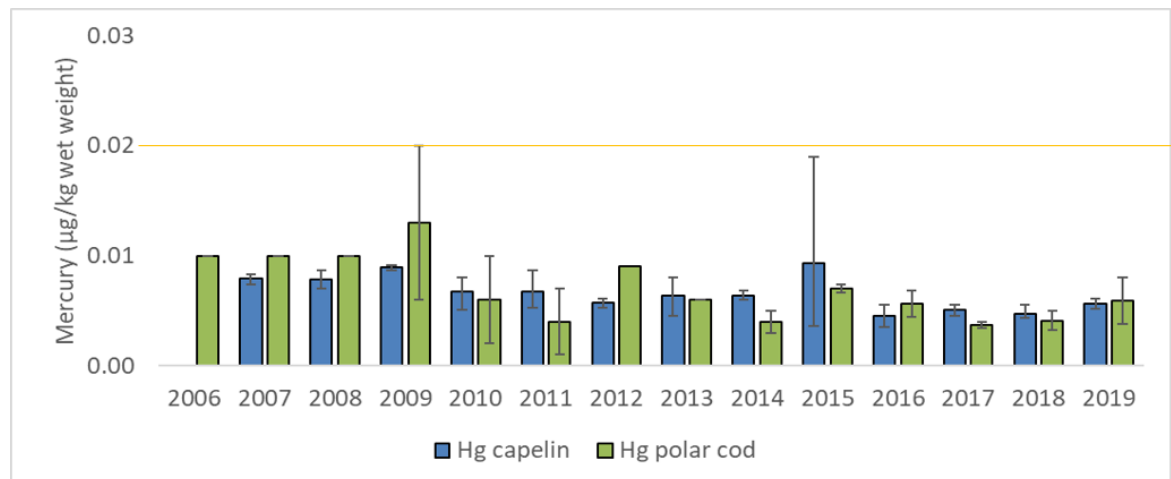


Figure 3.9.9.14 Annual concentrations of mercury in pooled samples of whole capelin and polar cod from 2006/2007 to 2019. For each year, mean, minimum and maximum values are shown.

Levels of dioxins and dioxin-like PCBs and PCB6 in cod liver analysed in program 2 seem to have decreased slightly since 2007 (Figure 3.9.9.15). Because sampling area and fish size may affect the results, results for samples taken south and north of 73°N have been shown separately, and only fish between 50 and 70 cm length were included.

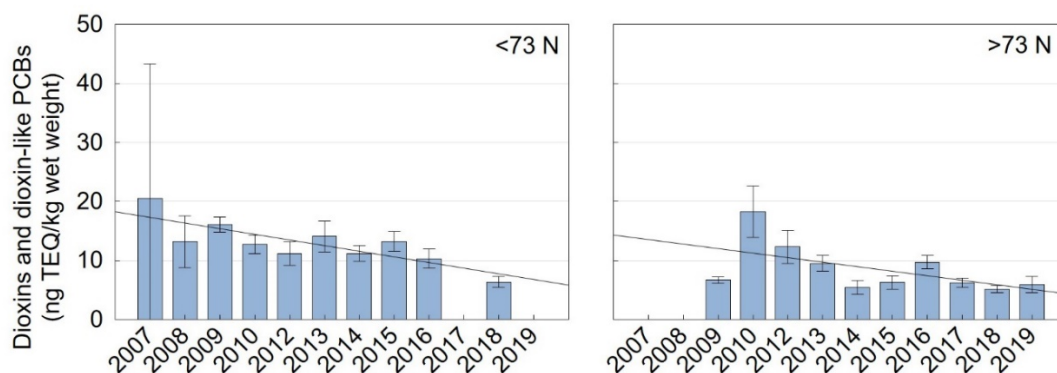


Figure 3.9.9.15 Annual concentrations of sum of dioxins and dioxin-like PCBs in liver of cod from 2007 to 2019, shown separately for the areas south of 73°N (<73 N; left) and north of 73°N (>73 N; right). Only individuals between 50 and 70 cm are included. For each year, mean \pm 95% confidence interval is shown.

Also, non-dioxinlike PCBs (given as PCB7 in program 1 and PCB6 in program 2) in cod liver, which has been analysed in prog. 1 since 1992, shows a decreasing trend (Figure 3.9.9.16). Most of the decrease occurred prior to 2008, although the levels also decreased until 2017-2019. For PCB6/PCB7 we did not separate between sampling areas or fish size, but when this was done, the pattern was similar as for dioxins and dioxin-like PCB. For PCB6/PCB7, results from both program 1 and 2 are included, and for the years when there is an overlap between the two programs, results were very similar in the two monitoring programs.

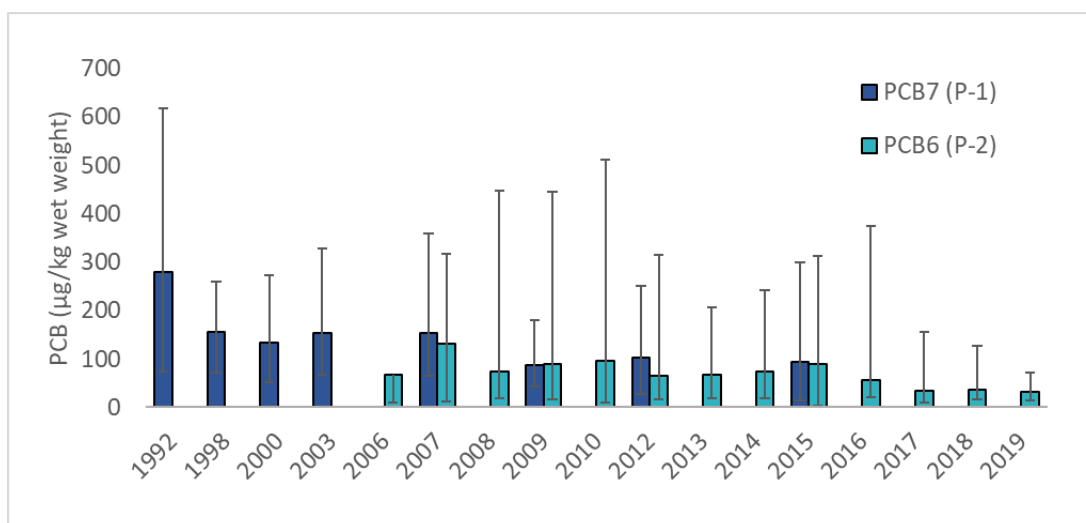


Figure 3.9.9.16 Annual concentrations of sum PCB7 (Program 1, P-1) and sum PCB6 (Program 2, P-2) in liver of cod from 1992 to 2019. For each year, mean, minimum and maximum values are shown.

The levels of PCB6/PCB7 in capelin and polar cod also seem to have decreased somewhat since 2006, and more so in polar cod than in capelin (Figure 3.9.9.17). It cannot be completely ruled out that a more northern distribution resulting in a more northern sampling in later years, may have resulted in a more decreasing trend than if sampling had been done in the same areas year after year.

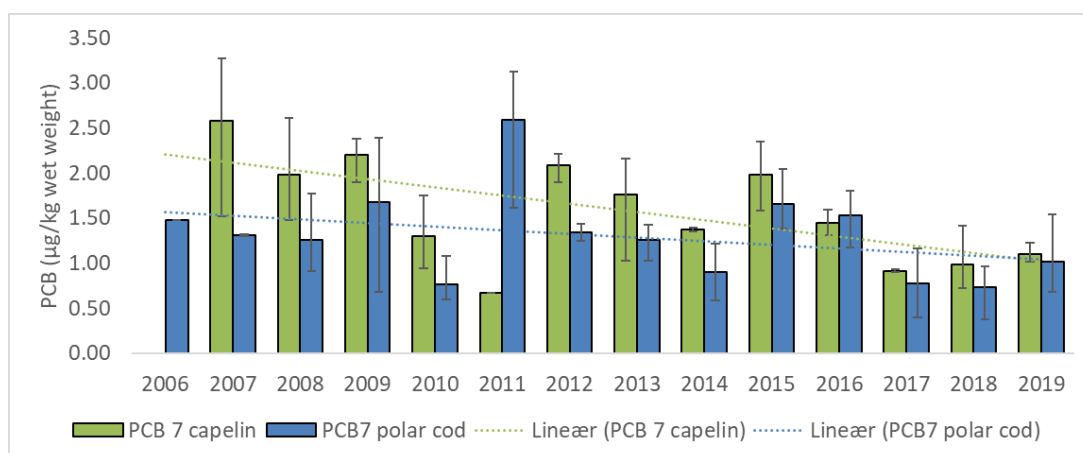


Figure 3.9.9.17 Annual concentrations of sum PCB7 in composite samples of whole capelin and polar cod from 2006 to 2019. For each year, mean, minimum and maximum values are shown.

For DDT, there has been a clear decrease in cod liver since 1992, while HCB levels have remained very stable (Figure 3.9.9.18). For polar cod, the level of HCB seems to be almost increasing in later years (Figure 3.9.9.19).

Levels of PBDE show clearly decreasing trends since 2006/2007, both in cod liver, capelin and polar cod (Figure 3.9.9.16 and 3.9.9.17).

There are thus indications that the levels of persistent organic contaminants such as dioxins, PCBs and DDTs have been decreasing and are still slowly decreasing in the Barents Sea. This pattern seems to be the most evident for PBDEs, which were banned around 2005, while HCB seems not to decrease at all. The latter may be because HCB can be breakdown product from other pesticides still in use. The level of mercury in cod fillet has remained very stable since 1994.

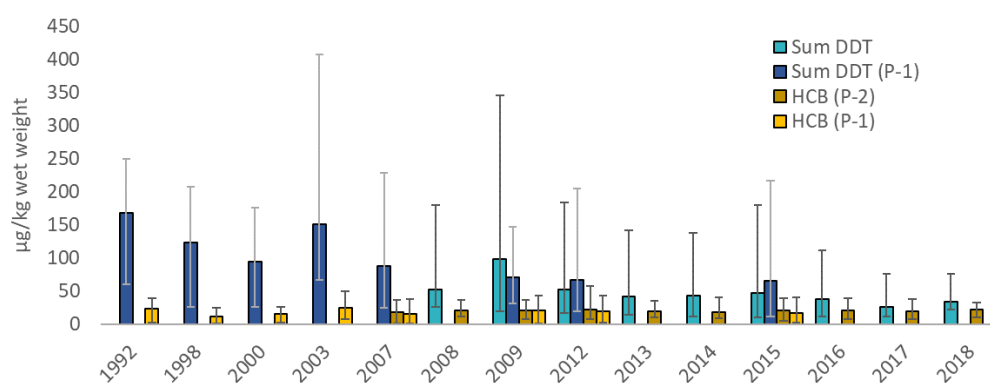


Figure 3.9.9.18 Annual concentrations of sum DDT and hexachlorobenzene (HCB) in composite samples of whole capelin and polar cod from 2006/2007 to 2019. Results from program 1 (P-1) and program 2 (P-2) are given separately. For each year, mean, minimum and maximum values are shown.

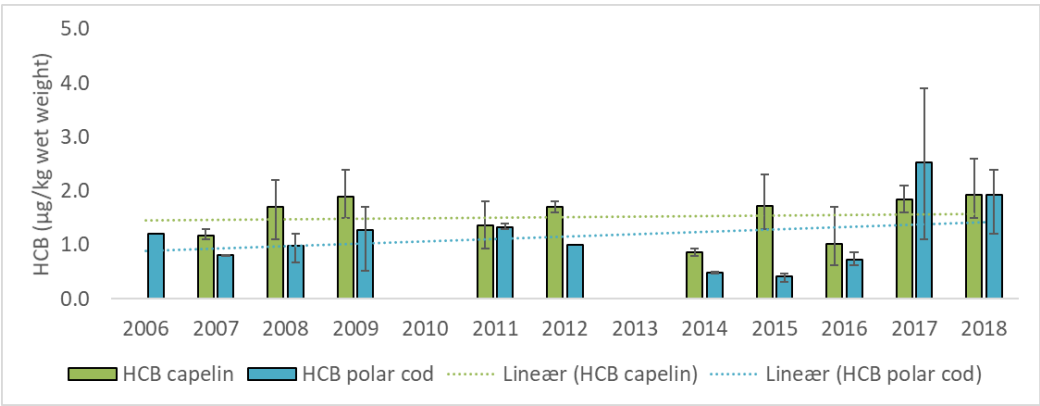


Figure 3.9.9.19 Annual concentrations of hexachlorobenzene (HCB) in composite samples of whole capelin and polar cod from 2006/2007 to 2019. For each year, mean, minimum and maximum values are shown.

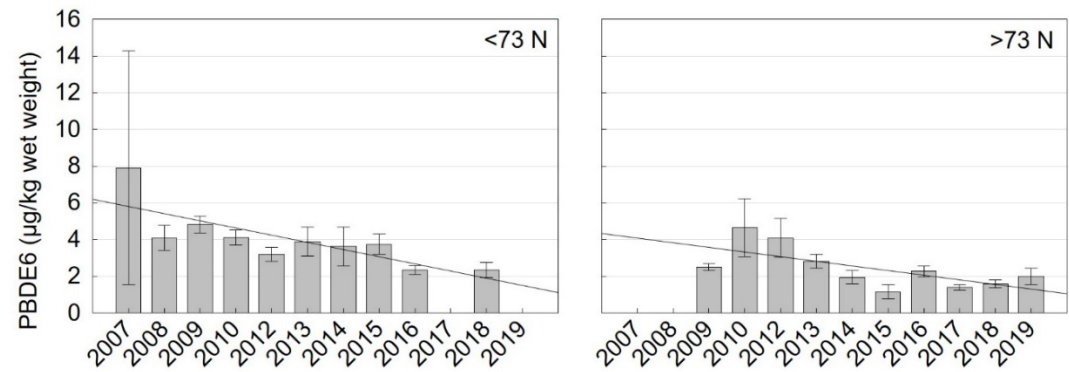


Figure 3.9.9.20 Temporal trend of concentrations of sum of 6 PBDEs in liver of cod from 2007 to 2019, shown separately for areas south of 73°N (<73 N) and north of 73°N (>73 N). Only individuals between 50 and 70 cm are included. For each year, mean ± 95% confidence interval is shown.

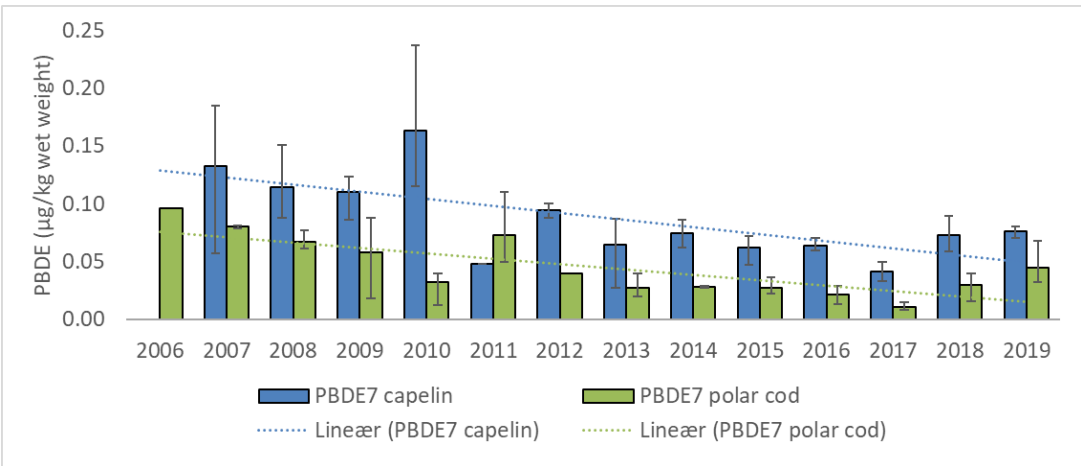


Figure 3.9.9.21 Temporal trend of concentrations of sum of 7 PBDEs in composite samples of whole capelin and polar cod from 2006 to 2019. For each year, mean, minimum and maximum values are shown.

References

EFSA (2009). EFSA panel on contaminants in the food chain (CONTAM); Scientific opinion on arsenic in food. EFSA Journal 2009 7(10): 199 pp.

- Frantzen, S. and Maage, A. (2016). Fremmedstoffer i villfisk med vekt på kystnære farvann. Brosme, lange og bifangstarter. Gjelder tall for prøver samlet inn i 2013-2015. 116 pp.
- Iulshamn, K., Nilsen, B.M., Frantzen, S., Valdersnes, S., Maage, A., Nedreaas, K., Sloth, I.I. (2012). Total and inorganic arsenic in fish samples from Norwegian waters. *Food Additives & Contaminants Part B-Surveillance* 5(4): 229-235.
- Iulshamn, K., Valdersnes, S., Duinker, A., Nedreaas, K., Sundet, I.H., Maage, A. (2015). Heavy metals and POPs in red king crab from the Barents Sea. *Food Chemistry* 167: 409-417.
- Miljødirektoratet (2016). Grenseverdier for klassifisering av vann, sediment og biota. Miljødirektoratet Veileder M-608. 25 s.
- Neff, J.M. (1997). Ecotoxicology of arsenic in the marine environment. *Environmental Toxicology and Chemistry* 16(5): 917-927.
- Nilsen, B.M., Frantzen, S., Iulshamn, K., Nedreaas, K., Måge, A. (2013a). Basisundersøkelse av fremmedstoffer i sei (*Pollachius virens*) fra Nordsjøen. Sluttrapport for prosjektet "Fremmedstoffer i villfisk med vekt på kystnære farvann". NIFES; Bergen. 56 s.
- Nilsen, B.M., Iulshamn, K., Duinker, A., Nedreaas, K. og Måge, A. (2013b). Basisundersøkelse av fremmedstoffer i sei (*Pollachius virens*) fra Norskehavet og Barentshavet. Sluttrapport. NIFES, Bergen. 44 s.
- Wiech, M., Frantzen, S., Duinker, A., Rasinger, J.D., Maage, A. (2020). Cadmium in brown crab *Cancer pagurus*. Effects of location, season, cooking and multiple physiological factors and consequences for food safety. *Science of the Total Environment* 703: 134922.
- Zauke, G.P., Krause, M., Weber, A. (1996). Trace metals in mesozooplankton of the North Sea: Concentrations in different taxa and preliminary results on bioaccumulation in copepod collectives (*Calanus finmarchicus*/*C. helgolandicus*). *Internationale Revue Der Gesamten Hydrobiologie* 81(1): 141-160.
- Zauke, G.P. og Schmalenbach, I. (2006). Heavy metals in zooplankton and decapod crustaceans from the Barents Sea. *Science of the Total Environment* 359(1-3): 283-294.

3.9.10 Radioactive contamination

Data accumulated over the past 10-15 years by the Joint Norwegian-Russian monitoring program has provided a reliable overview of the levels and trends of radioactive contamination in the Barents Sea marine environment. The data confirms that levels of the anthropogenic radionuclides Cs-137, Sr-90 and Pu-239,240 in seawater, sediments, fish and seaweed are currently low and generally decreasing. In recent decades, there has been a slow decrease in the levels of most anthropogenic radionuclides in the Barents Sea. Working document (WD2) present full report of the methodology and monitoring results.

The monitoring data reported by Norway and Russia has been demonstrated to be robust and comparable. Further effort to ensure data comparability is an important part of the ongoing work on future cooperation. To support this aim, a series of bilateral workshops on sampling, analysis and quality control have been launched (starting in 2016) to better understand and harmonise methodologies employed on each side of the border.

4 Interactions, drivers and pressures

By Bjarte Bogstad (IMR), Dmitri Prozorkevich (PINRO), Harald Gjøsæter (IMR), Alexey Russkikh (PINRO), Andrey Dolgov (PINRO), Irina Prokopchuk (PINRO), Padmini Dalpadado (IMR), Alina Rey (IMR), Johanna Fall (IMR), Lis Lindal Jørgensen (IMR), Natalia Strelkova (PINRO), and Denis Zakharov (PINRO)

4.1 Feeding and growth of capelin and polar cod

Capelin

Thirteen years (2006–2018) of capelin diet were examined from the Barents Sea where capelin is a key species in the food web, both as prey and predator. The PINRO/IMR mesozooplankton distribution usually shows low plankton biomass in the central Barents Sea, most likely due to predation pressure from capelin and other pelagic fish. This pattern was also observed in 2017-2019. In the Barents Sea, a pronounced shift in the diet from smaller (<14 cm) to larger capelin (≥ 14 cm) is observed. With increasing size, capelin shift their diet from predominantly copepods to euphausiids, (mostly *Thysanoessa inermis* - not shown separately), with euphausiids being the largest contributor to the diet weight in most years (Figure 4.1.1). Hyperiid amphipods contributed a small amount to the diet of capelin. The stomach fullness is highest in the central and northern areas of the Barents Sea, where the capelin concentrations usually are highest (Fig 4.1.2)

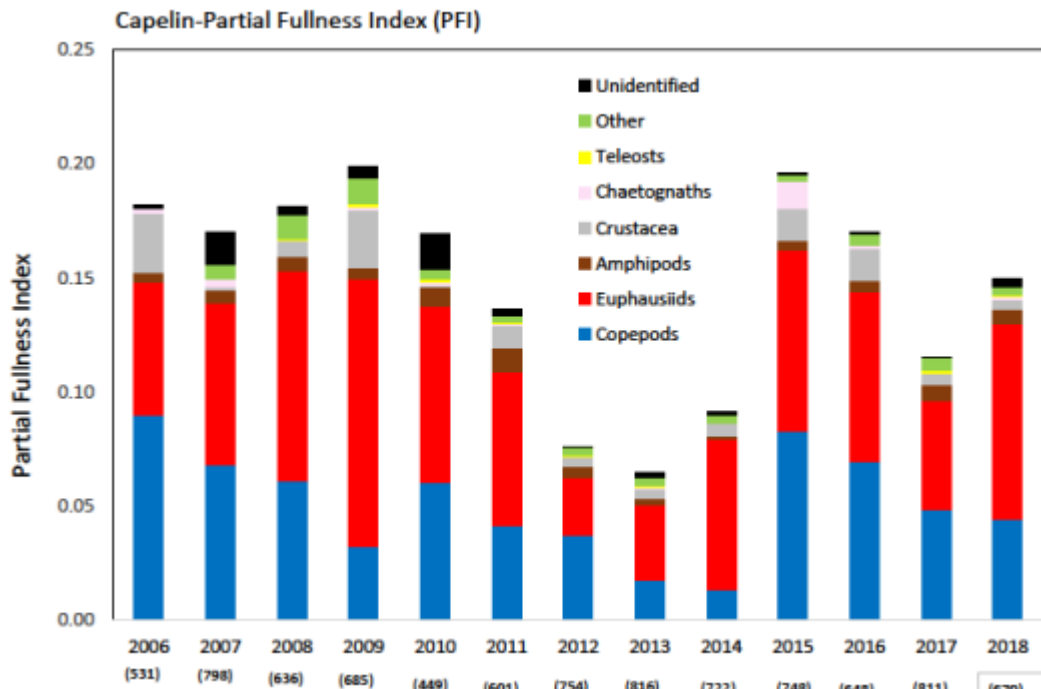


Figure 4.1.1. Stomach fullness (PFI, Lilly and Fleming 1981) of capelin during the BESS survey in August-September 2006-2018. Number of fish sampled each year in brackets.

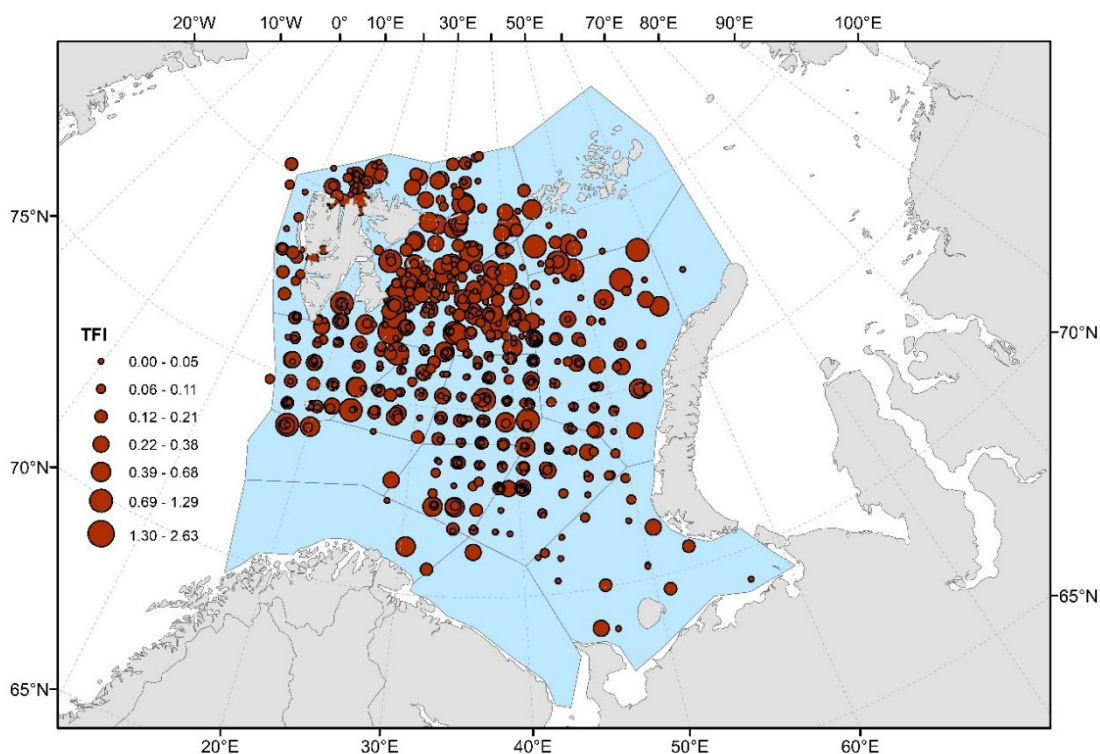


Figure 4.1.2 Geographic distribution of Total Fullness Index (TFI, Lilly and Fleming 1981) for capelin, all years 2006–2018 combined. For polygon areas we refer to chapter 3.

Capelin growth decreased from 2009 onwards in a way similar to earlier periods of relatively high capelin abundance (1990–1992, 1998–2002, Figure 4.1.3). There was a corresponding decrease in stomach fullness of capelin from 2009 onwards. These trends were reversed in 2014–2015 and both weight-at-age and stomach fullness are now at relatively high levels. Note that spatial coverage in the Russian EEZ in 2018 was poor (only 3 stations in that area).

The decrease in individual growth rate and condition of capelin observed before 2014 for the large capelin stock may have been caused by reduced food availability linked to strong grazing on the largest planktonic organisms; as suggested by reduction of the largest size fraction (>2 mm) in the Norwegian zone during the autumn survey (see section 3.3). Plankton species composition in the northeastern area has changed; abundance of large copepod species *Calanus finmarchicus* and *C. glacialis* (important prey items for capelin) had been decreasing since 2008 and was at a low level, while since 2015 an increasing trend has been observed. In 2017–2018 a substantial increase in both abundance and biomass were observed for large copepod *M. longa*, which is also prey for capelin as well as for polar cod. At the same time, the abundance of small copepod *Pseudocalanus* sp., which are not important to the capelin diet, was high in 2012–2015 and have been decreasing since 2016. The same trends were observed in biomass of mentioned copepod species. This change in species composition of the plankton community is most likely caused by the joint effect of warming in the Barents Sea, and high grazing pressure from different plankton consumers.

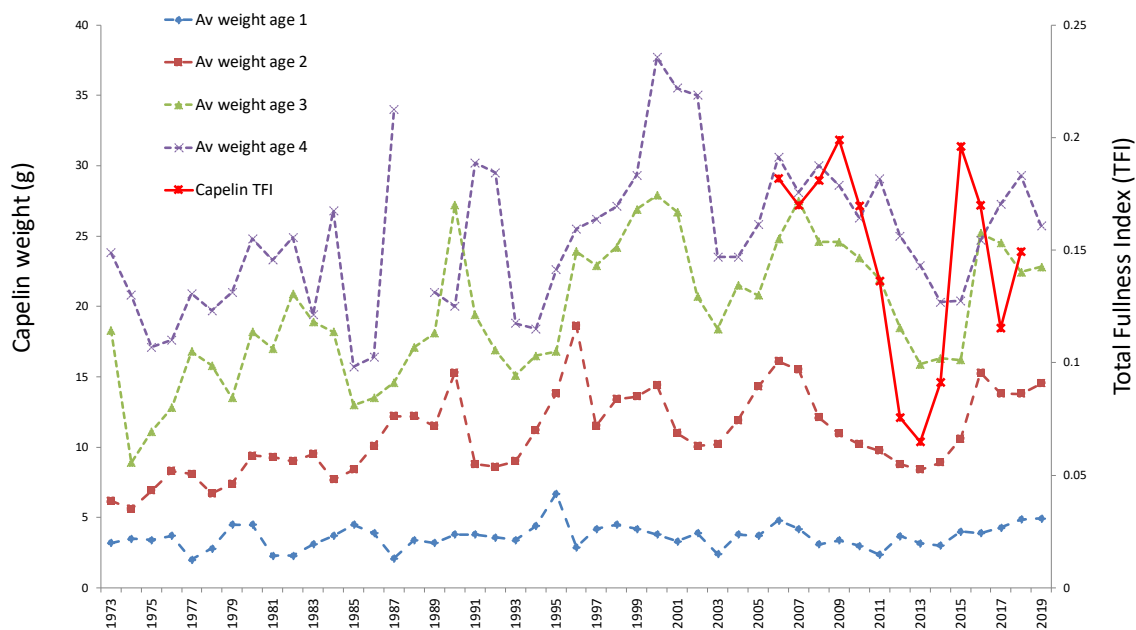


Figure 4.1.3 Growth (weight at age from ecosystem survey) and stomach fullness (TFI) of capelin in 1973–2019

Capelin growth depends on the state of the plankton community (Skjoldal *et al.*, 1992; Dalpadado *et al.*, 2002; Orlova *et al.*, 2010). Capelin produces a strong feedback mechanism on zooplankton stock levels through predation (Figure 4.1.4, Dalpadado *et al.*, 2003; Stige *et al.*, 2014); which has been found to be particularly pronounced for krill in the central Barents Sea (Dalpadado and Skjoldal, 1996).

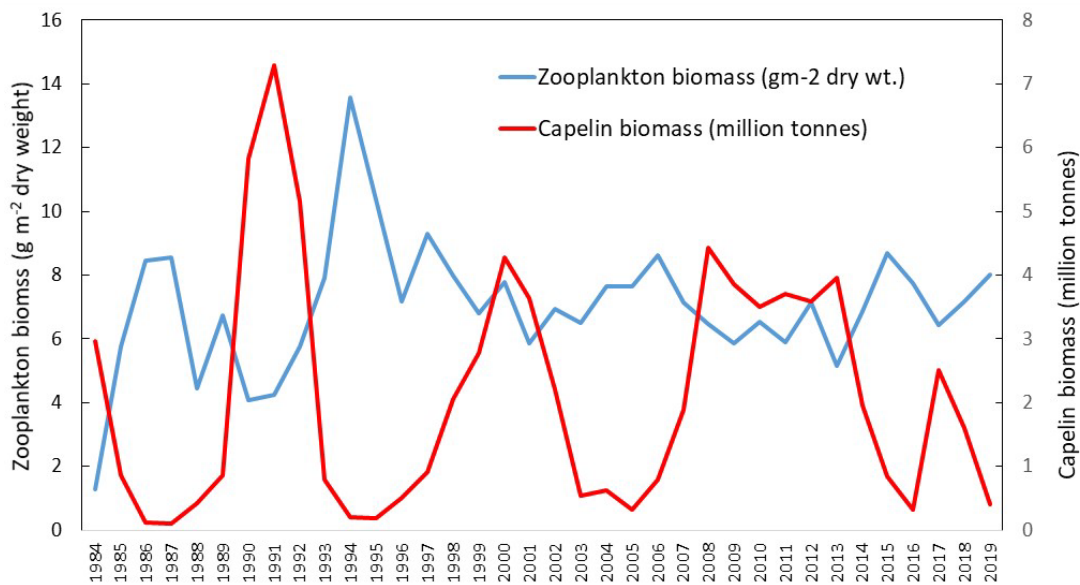


Figure 4.1.4. Fluctuation of capelin stock and zooplankton biomass in the Barents Sea in 1984–2019.

There is evidence of a density-dependent effect on capelin growth. This is reflected in decreasing length of individual (2- and 3-year old) capelin with increasing capelin abundance (Figure 4.1.5).

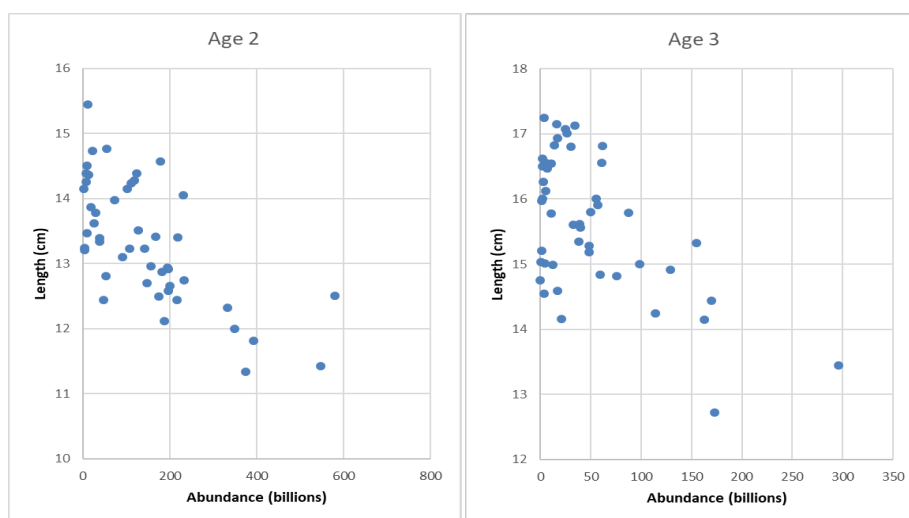


Figure 4.1.5. Average length as function of abundance for capelin at age 2 and 3. There are highly significant negative relationships between the variables; adjusted R^2 is 0.46 for the two-year-olds and 0.33 for the three-year-olds.

Polar cod

Diet data from 2007–2018 indicate that polar cod mainly feed on copepods, amphipods (mainly hyperiids *Themisto libellula* and occasionally gammarids), euphausiids, and other invertebrates (to a lesser degree) (Figure 4.1.6). Large polar cod also prey on fish. The total stomach fullness index decreased after 2011 and was at a fairly low level in 2012–2015; the index increased again in 2016 to the highest level measured in this 10-year time-series and remained relatively high in 2017–2018 (Figure 4.1.7). The growth rate of polar cod was low for age 3 and intermediate for ages 1–2 in 2016–2018 (Figure 4.1.8) and, thus, does not reflect the increase in stomach fullness from the 2012–2015 to the 2016–2018 period. It should be noted that spatial coverage for polar cod is incomplete during most years of the BESS; thus, growth and stomach fullness data may not reflect the status of the entire population. The stomach fullness was highest north of Spitsbergen and in the northern Barents Sea. The high proportion of amphipods in the diet especially in 2018, may reflect the high abundances of *Themisto* sp. in the region east of Spitsbergen.

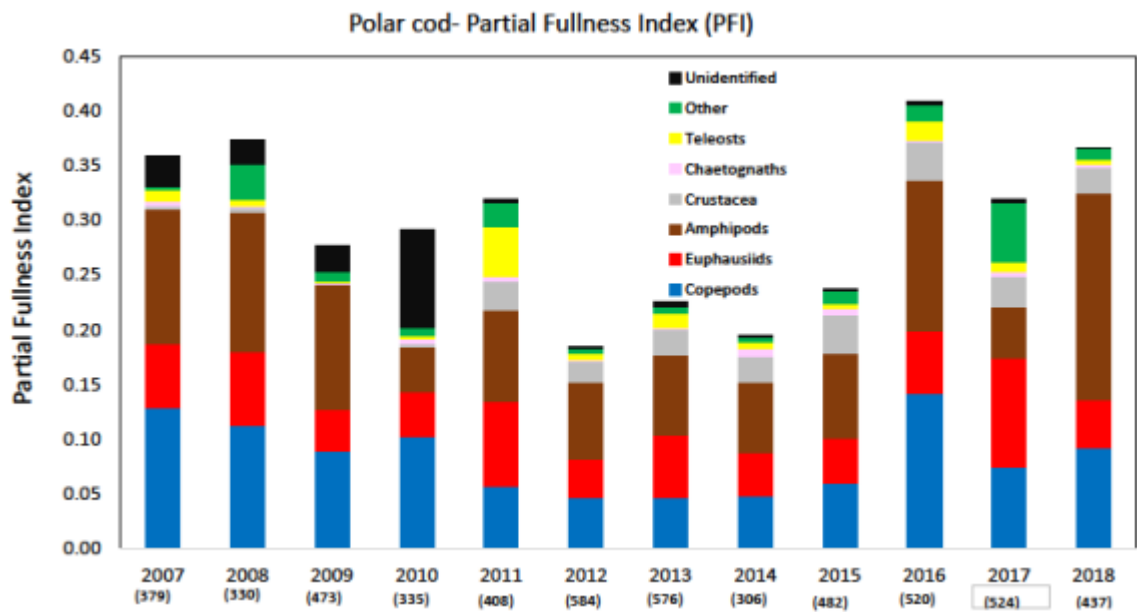


Figure 4.1.6. Stomach fullness (PFI) of polar cod during the BESS survey in August–September 2007–2018. Number of fish sampled each year in brackets.

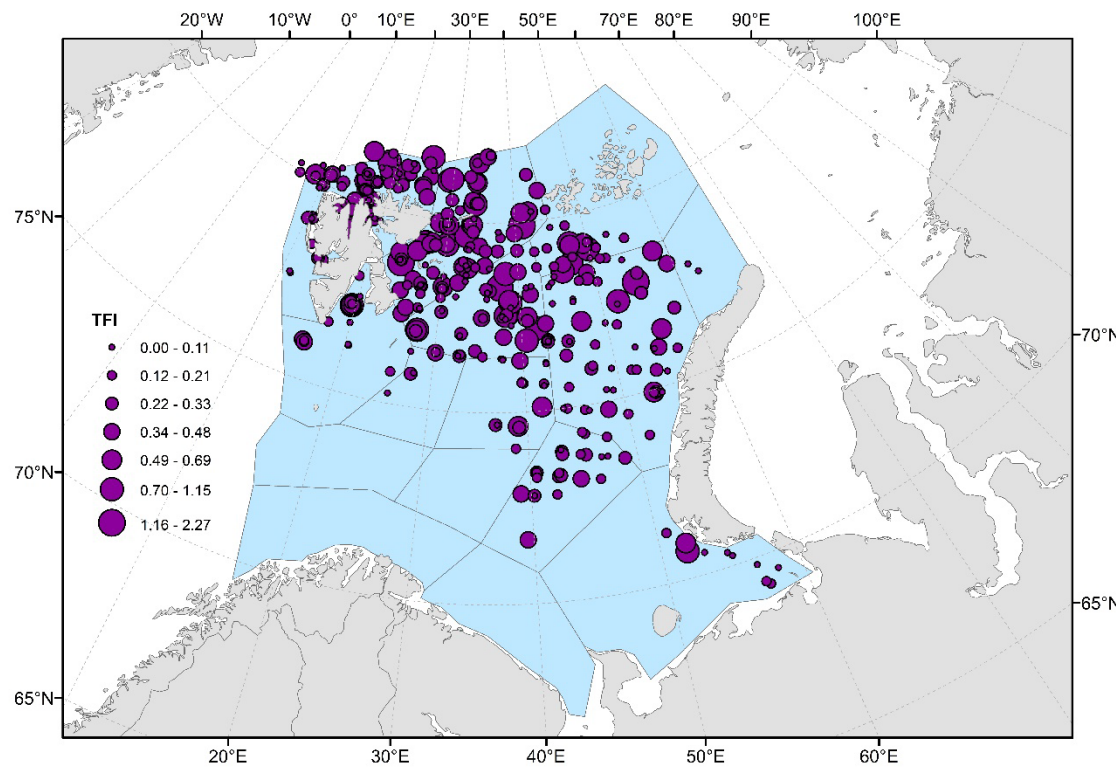


Figure 4.1.7 Geographic distribution of Total Fullness Index (TFI) for polar cod, all years 2007-2018 combined

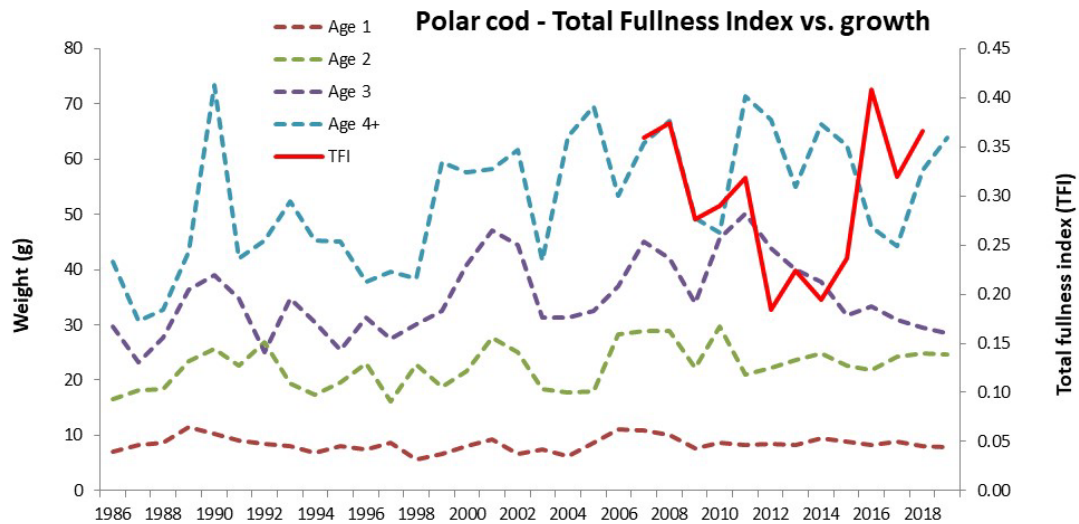


Figure 4.1.8 Growth (weight at age from ecosystem survey) and stomach fullness (TFI) of polar cod in 1986-2019

4.2 Feeding, growth, and maturation of cod

Feeding

Figures 4.2.1 and 4.2.2 show the consumption and diet composition of cod.

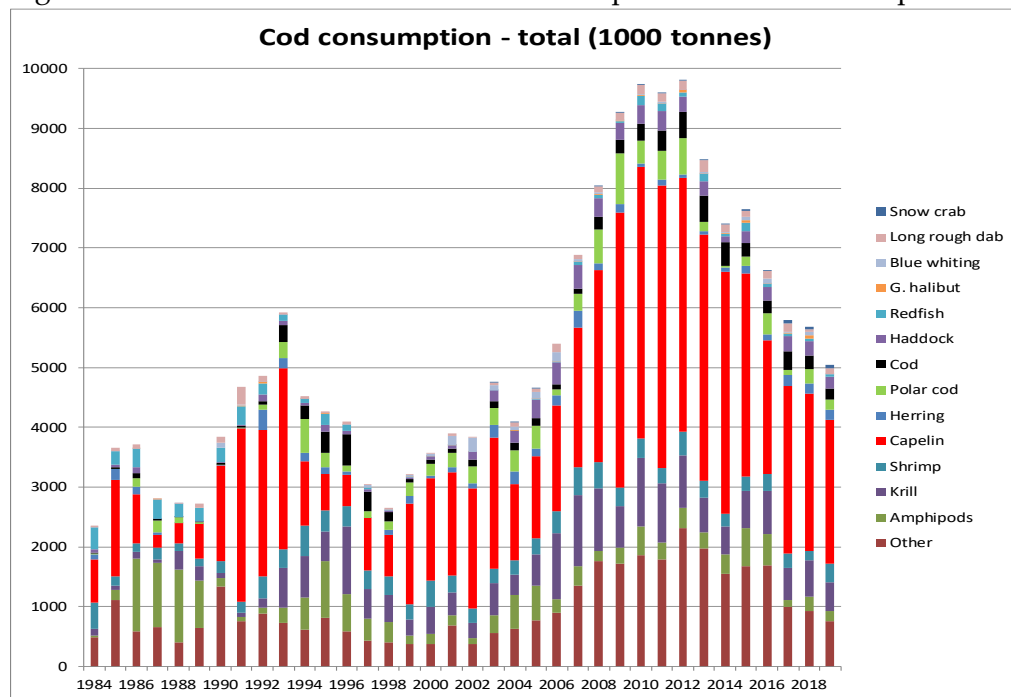


Figure 4.2.1 Cod consumption 1984–2019. Consumption by mature cod outside the Barents Sea (3 months during first half of year) not included. Norwegian calculations, preliminary figures, final numbers to be found in AFWG 2020.

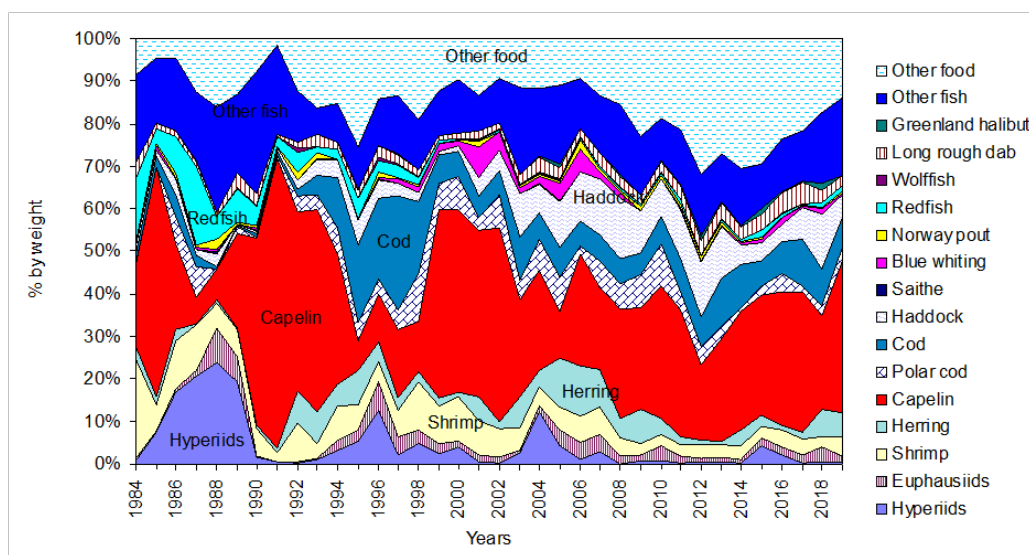


Figure 4.2.2. Cod stomach content composition in the Barents Sea in 1984–2019, by weight (aggregated over all size groups)

Cod is the major predator on capelin; although other fish species, seabirds and marine mammals are also important predators. The cod stock abundance in the Barents Sea peaked around 2013 and have declined since, although it is still above the long-term average. The cod spawning stock and thus the abundance of old, large fish is still very high. Estimated biomass of capelin consumed by cod in recent years has been close and in some years above the biomass of the entire capelin stock (Figure 4.2.3). Abundance levels of predators other than cod are also high and, to our knowledge, stable.

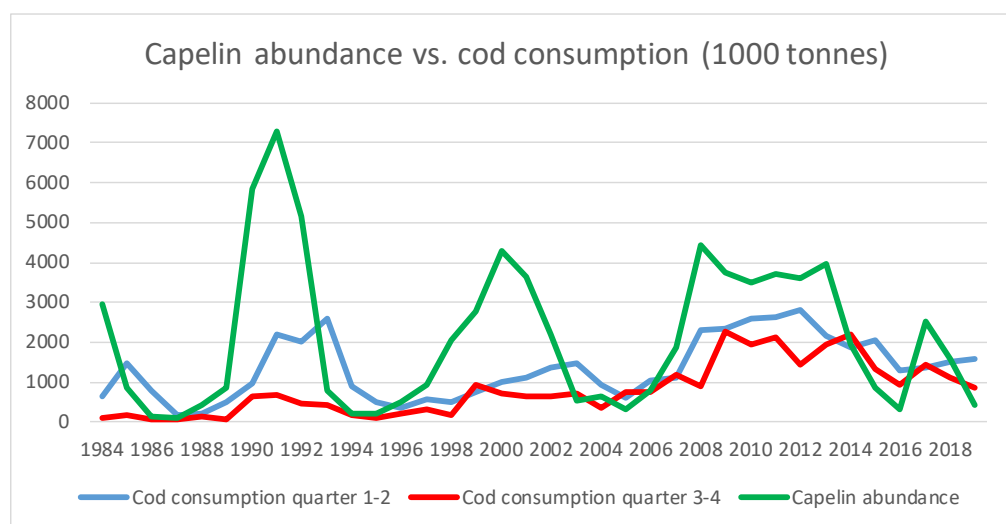


Figure 4.2.3 Size of the capelin stock and estimated consumption of capelin by cod. Note that the capelin biomass is estimated in September and may not be representative for the biomass available for cod during the year when year-to-year variability is high.

Estimated consumption of capelin by cod during first and second parts of the year has indicated different temporal patterns. Consumption during the 1st and 2nd quarters has been high during earlier periods and includes consumption during the spawning period, and during spring and early summer prior to seasonal capelin feeding

migrations. During the last decade, however, a major difference has been the pronounced increase to a much higher level of consumption in the 3rd and 4th quarters (Figure 4.2.3). This reflects the northward movement of cod stock, and a larger spatial overlap between cod and capelin under the recent warm conditions.

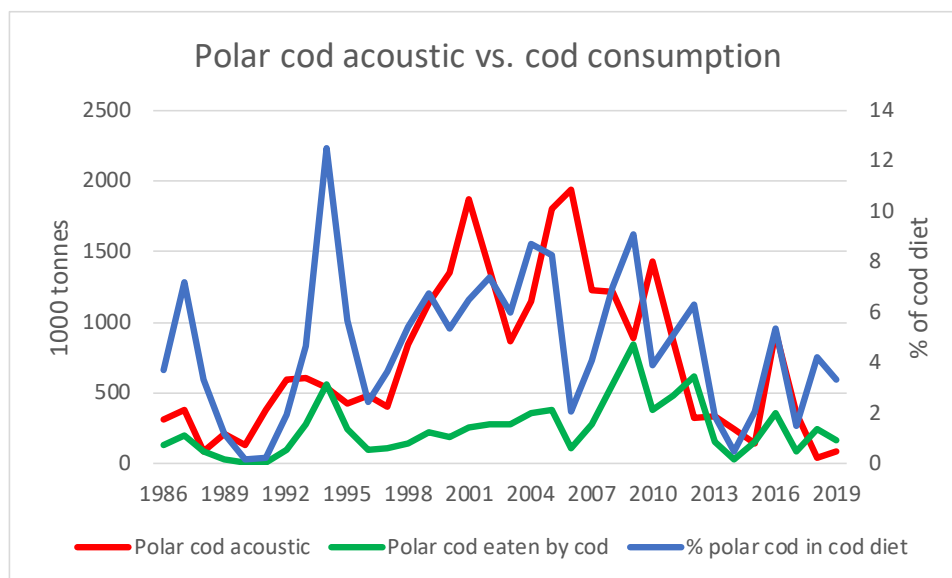


Figure 4.2.4 Acoustic estimates of polar cod compared to consumption of polar cod by cod and % of polar cod in cod diet, 1986-2019.

Figure 4.2.4 shows that there generally is a reasonable correspondence between the proportion of polar cod in the cod diet and acoustic estimates of polar cod. The very low acoustic abundance observed in 2018-2019 is, however, not consistent with the recent trends in amount of polar cod eaten by cod.

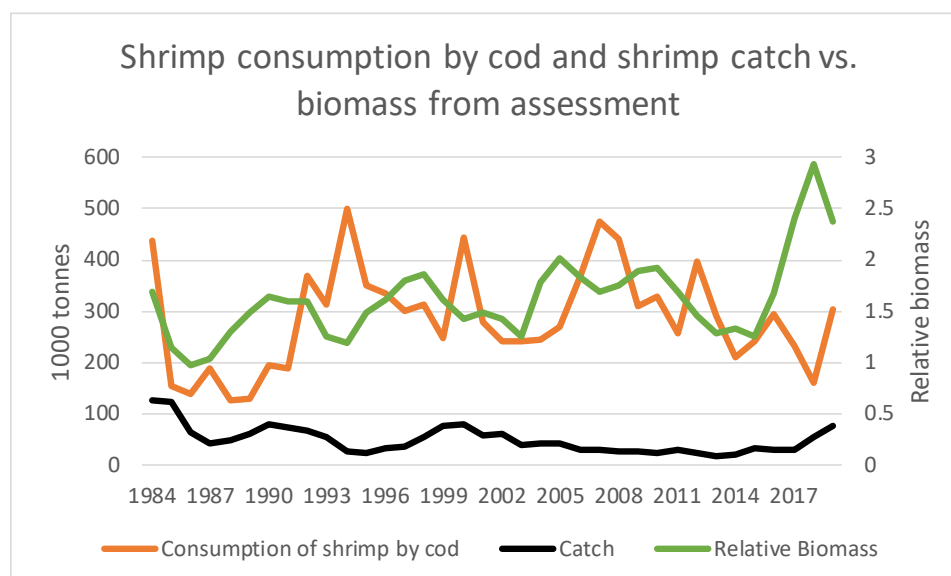


Fig 4.2.5. Cod consumption by shrimp and shrimp catch vs. biomass estimates of shrimp (ICES NIPAG 2019).

The estimated biomass as well as the catches of shrimp in the Barents Sea increased from 2017 to 2019. This increase is to some extent reflected in the cod diet (Fig. 4.2.5).

Note that the proportion of shrimp in the cod diet in 2019 was the highest since 2007.

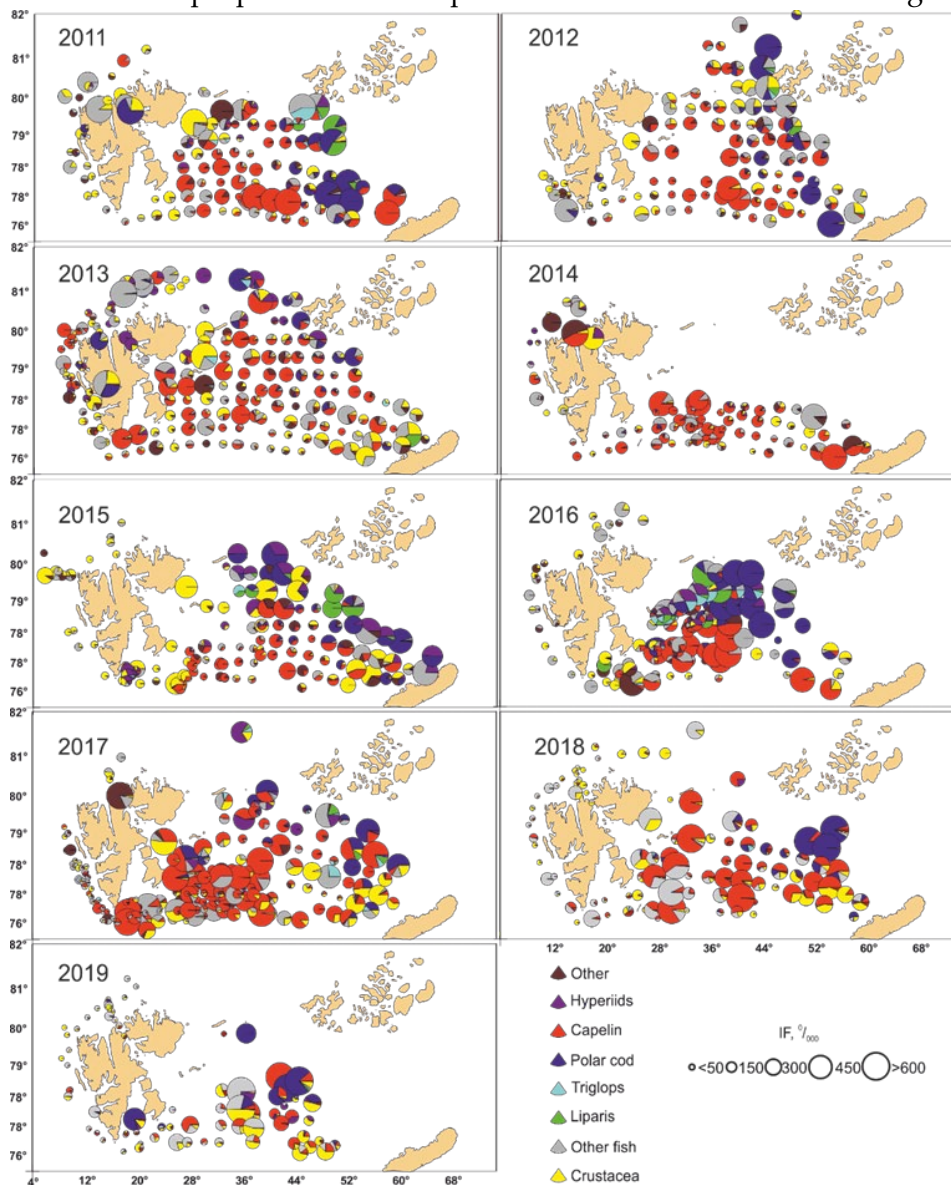


Figure 4.2.5. Cod diet composition in the northern part of the Barents Sea during the ecosystem survey in August–September 2011–2019. Red dots indicate capelin, and blue dots polar cod.

Capelin is the main prey item for cod. High or low stock biomass of capelin affect the biological state of cod.

During the first capelin collapse (1985–1989) the importance of capelin in cod diet decreased from 53% in 1985 to 20–22% (maximum) for the remainder of the collapse period. During that period, an increase of other prey was observed; in particular, hyperiids which constituted 7–23% of the capelin diet and redfish which constituted 3–18%.

During the second capelin collapse (1993–1997), the proportion (by weight) of capelin in the cod diet was high during the first 2 years (47% and 30%), followed by a decreased to 6–16%. During this period, cannibalism in cod increased sharply from 4–11% to 18–26% of the diet. In addition, more intensive consumption of hyperiids was observed

(1–12%), but the proportion of hyperiids consumed was still much lower than during the first collapse.

During the third capelin collapse (2003–2006), consumption of capelin by cod was rather high (10–26%). Several alternative prey groups were present in the cod diet in similar quantities: juvenile haddock (6–11%) and cod (5–10%); herring (3–11%); blue whiting (1–5%); and hyperiids (1–12%). Consumption of capelin by cod during the most recent years has remained somewhat stable (17–31%), but has been much lower than during earlier periods of high capelin abundance (average 36–51%). In recent years, a relatively diverse cod diet has been recorded: with stable high consumption of juvenile cod and haddock (6–11 and 5–11%, respectively); other fish species (11–15%); and other food types (21–33%) (mainly ctenophores and crabs).

Investigations of cod diet in the area north of 76°N showed different types of feeding intensity in three different local areas (Dolgov and Benzik, 2014). Cod feeding intensity was low (149–169^{0/000}) in areas near western and southern Spitsbergen — where cod feed on non-commercial fish. Other local areas were characterized by high feeding intensity (MFI 214–251–169^{0/000}) with capelin as dominant; non-target species (snailfish and sculpins), polar cod, and hyperiids were also consumed. These two are traditional areas of cod distribution during summer. The third area (Franz Josef Land, northern Novaya Zemlya, and adjacent areas) has become available habitat for cod only since 2008; in this area, cod (MFI 284–340^{0/000}) feed intensively on polar cod and capelin. Northward expansion of cod distribution, and their movement into northeastern Barents Sea results in better feeding conditions for cod under their high stock biomass and decreasing of main prey (capelin and polar cod). However, cod intensively fed on capelin and polar cod in 2015–2018 despite their low stocks (Figure 4.2.5). In 2019, consumption of these important prey was much lower and occurred in rather restricted areas in the northern Barents Sea compared to previous years.

In addition, some new prey items have recently appeared in the cod diet. The non-indigenous snow crab (*Chionoecetes opilio*) has become a rather important prey items for cod, especially in for large cod in the eastern Barents Sea alongside Novaya Zemlya (Dolgov and Benzik, 2016, Holt et al., submitted MS). The percentage (by weight) of snow crab in the cod diet sharply increased from 2014 onwards (Figure 4.2.6). In contrast, two other non-indigenous crab species (red king crab and deep water crab *Geryon trispinosus*) have not become more important in the cod diet. The difference is probably related to higher overlap between cod and snow crab, and more appropriate body shape and size of snow crab than the other crab species as prey for cod.

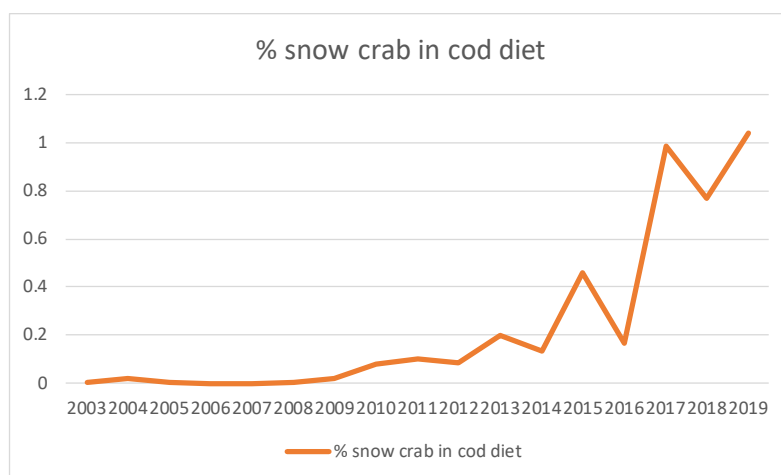


Figure 4.2.6. Importance of snow crab in cod diet (% weight of total consumption) in 1984–2019. Based on Norwegian consumption calculations.

Consumption and growth for young cod has been relatively stable in recent years (Figure 4.2.7); there has been a slight decrease for older cod (Figure 4.2.8). Maturity-at-age for cod decreased considerably in 2015–2016 but did in 2019 increase to the level seen in the early 2000s recent years, particularly for ages 6–9. The changes in maturity ogives were considerably larger than indicated by recent changes in weight-at-age estimates (Figures 4.2.9 and 4.2.10).

Biomass of the main prey species, relative to the cod stock size, has decreased somewhat in recent years (Figure 4.2.11). However, no consequences of the 2015–2016 ‘mini-collapse’ of the Barents Sea capelin stock on cod growth and condition have been observed. This may be related to ongoing expansion of cod stock to the northern Barents Sea, making previously untapped food resources now available for cod consumption.

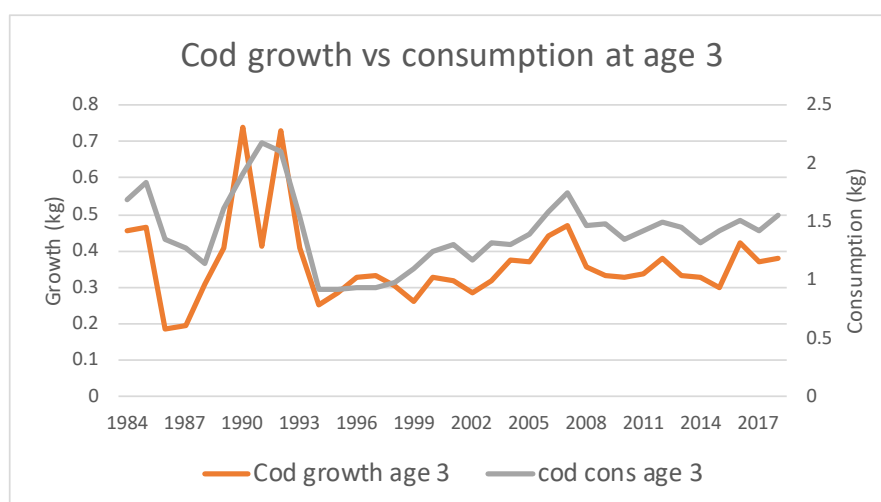


Figure 4.2.7 Cod growth and consumption at age 3 (ICES 2019a).

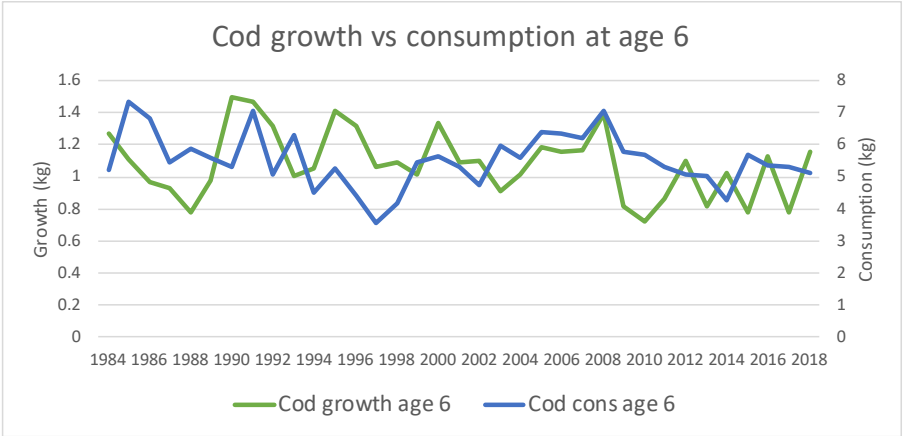


Figure 4.2.8 Cod growth and consumption at age 6 (ICES 2019a).

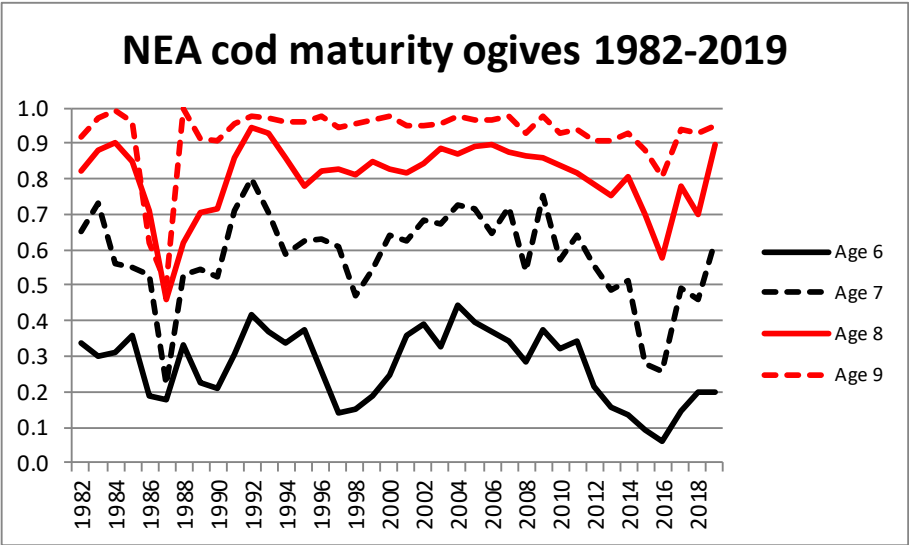


Figure 4.2.9 Maturity-at-age for cod ages 6-9 (ICES 2019a).

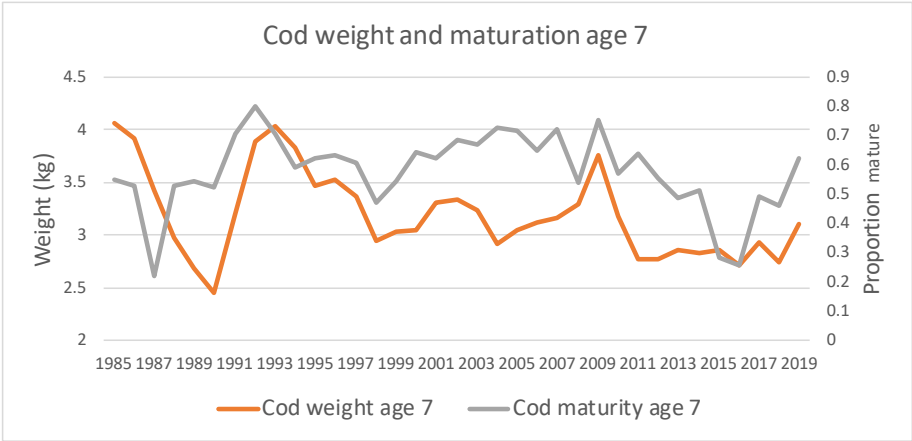


Figure 4.2.10 Cod maturity and weight at age 7 (ICES 2019a).

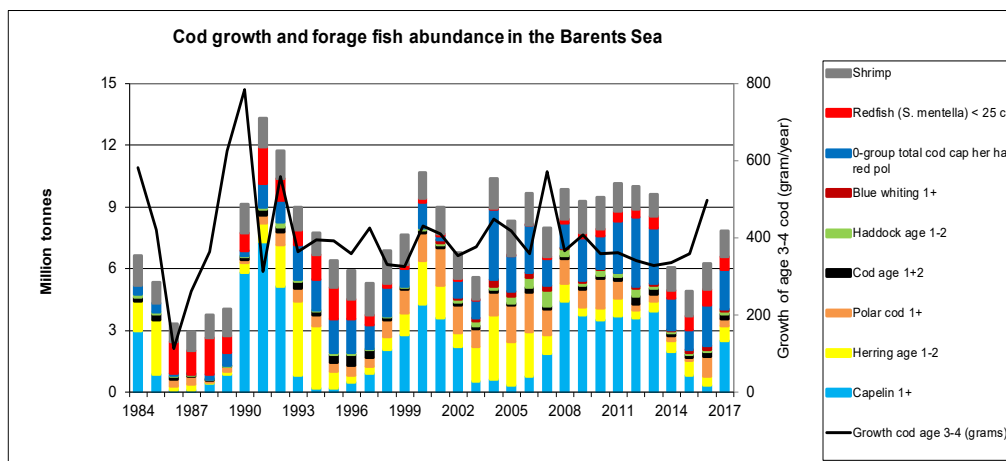


Figure 4.2.11. Abundance of major fish prey stocks and shrimp compared to cod growth.

4.3 Causes of capelin stock fluctuations

Stock size fluctuations

The Barents Sea capelin has undergone dramatic changes in stock size over the last four decades. Three stock collapses (when abundance was low and fishing moratoriums imposed) occurred during 1985–1989, 1993–1997, and 2003–2006. During the recent period 2014–2019 the stock estimates have fluctuated considerably. A rapid decline in stock size was recorded from 2014 onwards, and in 2016 the lowest biomass of capelin since 2005 was estimated from the joint Russian-Norwegian autumn Barents Sea Ecosystem Survey (BESS). The capelin stock size estimate from 2017, however, contrasted the two previous years and was so much higher that the results from 2016 and 2017 were incompatible when comparing cohorts (Skaret et al., 2019). For several reasons, the Arctic Fisheries Working Group concluded in 2017 that the 2017 survey was the more reliable of the two. Skaret et al. (2019) came to the same conclusion after having considered several possible reasons for either an underestimate in 2016 or an overestimate in 2017. Observations from the fisheries in 2018 and the autumn acoustic estimate of capelin in 2018, which was in line with the survey in 2017, strengthened this conclusion. However, the stock size estimate in autumn 2019 found the stock to be in very bad shape. It is unreasonable that the natural mortality should change so much from year to year, and one may question whether the surveys in recent years have given a reliable picture of the real trends in stock size. No firm conclusions can be drawn before one or more additional years of stock estimates have been added to the time series.

Previous collapses have had serious effects both up and down the foodweb. Reduced predation pressure from capelin has led to increased amounts of zooplankton during periods of capelin collapse. When capelin biomass was drastically reduced, its predators were affected in various ways. Cannibalism became more frequent in the cod stock, cod growth was reduced, and maturation delayed. Seabirds experienced increased rates of mortality, and total recruitment failures; breeding colonies were abandoned for several years. Harp seals experienced food shortages, and recruitment

failure, and increased mortality; partly because they invaded coastal areas and were caught in fishing gear. The effects were most serious during the 1985–1989 collapse, whereas, the effects could hardly be traced during the third collapse. Gjørøster *et al.* (2009) concluded that these differences in effect likely resulted from increased availability of alternative food sources during the second and third collapses (1990s and 2000s).

These collapses were caused by poor recruitment, most likely in combination with low growth and increased predation pressure. It is likely that high levels of fishing pressure during 1985–1986 amplified and prolonged the first collapse. After each collapse, the fishery has been closed and the stock has recovered within a few years due to good recruitment. Several authors have suggested that predation by young herring on capelin larvae has had a strong negative influence on capelin recruitment and, thus, has been a significant factor contributing to these capelin collapses (Gjørøster *et al.*, 2016), while others (Dolgov *et al.*, 2019) claim that other reasons for the periodic recruitment failures could be more important.

Recruitment of capelin and polar cod

Capelin is a short-lived species and thus the stock size variation is strongly influenced by the annual recruitment variability. This may indicate that the main reason of capelin stock collapses is poor recruitment (Figure 4.3.1). There was a better correspondence between the abundance of 0-group and one-year-olds in the first half of the time period where both estimates are available. In recent years, very high but fluctuating estimates of 0-group were obtained and the mortality from age 0 to age 1 has seemingly increased. Especially the year classes 2007-2010, 2012-2013 and 2016-17 were heavily reduced in size from the 0-group to the 1-group stage. While the three first capelin stock collapses were initiated by increased mortality at the early larval stage, between the larval survey in May-June and the 0-group survey in August, the increased mortality on young capelin in recent years is seemingly occurring later; between the 0-group survey and the acoustic measurement of the 1-year-olds. The reasons for this seemingly increased natural mortality at this stage is unknown but could likely be caused by other factors than those in effect during the collapses in the 1980s, the 1990s, and the 2000s.

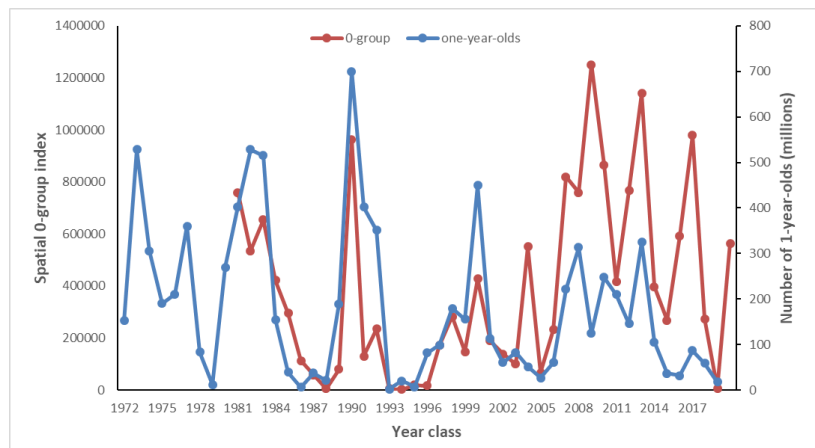


Figure 4.3.1. Fluctuation of capelin at age 0 (red line) and 1 (blue line) for the cohorts 1980–2019.

Mean length of 0-group capelin has varied somewhat during the data time-series. From a biological perspective, one may hypothesize that survival rates from age 0 to age 1 might be correlated with lengths-at-age 0. However, a plot of mean length-at-age 0 and total mortality, from age 0 to age 1, shows no such correlation; rather, this plot shows that 0-group and/or 1-group abundance estimates and, therefore also, mortality estimates from age 0 to age 1, are noisy; this could possibly mask possible relationships that might exist.

Figure 4.3.2 shows a stock–recruitment plot (updated from Gjøsæter *et al.* (2016)) for the year classes 1973–2018. The SSBs are those estimated by the assessment model for capelin (ICES 2019a). The points are coloured according to the amount of young herring estimated to be in the Barents Sea in the spawning year. Prior to 1991 the amount of herring is the abundance of age 1 and age 2 herring from the assessment model times the mean weight of these age groups; from 1991 it is the acoustic biomass estimate from herring survey in the Barents Sea in summer (ICES 2019b). The 1989-year class is the strongest year class at age 1 (700 billion). The average recruitment in the period is about 180 billion. It is seen that the recruitment in “red years” are below average recruitment in 11 out of 12 years, while in “green years” the recruitment is below average in 7 out of 12 years. In years with low numbers of young herring in the Barents Sea the recruitment is below average in 10 out of 22 years. This supports the hypothesis that capelin recruitment is negatively affected in years with substantial amounts of young herring in the Barents Sea (Gjøsæter *et al.* 2016). On the other hand, the general shape of the stock–recruitment relationship, where the highest recruitment is obtained for small to medium SSBs, points to the possibility of cannibalism or other density dependent mortality mechanisms (Dolgov *et al.*, 2019). In any case, the large variability in recruitment clearly indicates an interplay of many factors affecting the recruitment of capelin.

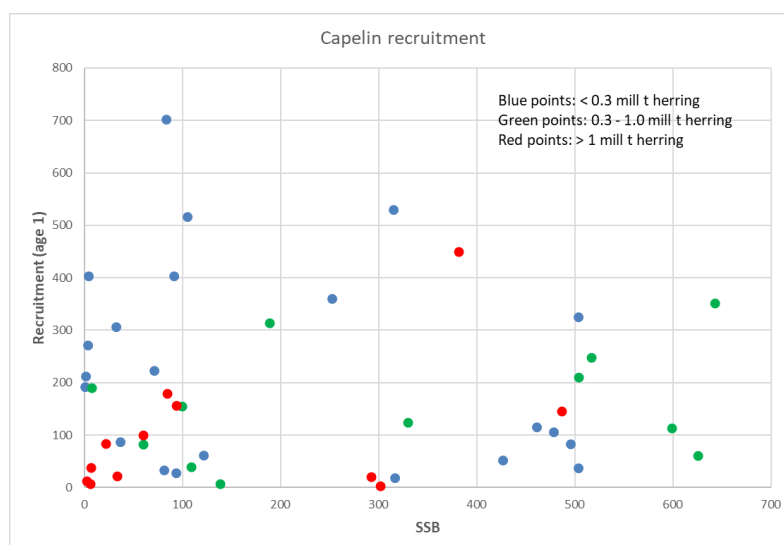


Figure 4.3.2. SSB/R plot for capelin. Cohorts 1973–2018. Points coded according to herring biomass as explained in the text. (Updated from Figure 7 in Gjøsæter *et al.* 2016).

Figure 4.3.3 depicts a stock-recruitment plot based on maturing stock size during autumn $\frac{1}{2}$ a year before spawning instead of estimated spawning stock size, and estimated number of 0-group capelin as an indicator of recruitment instead of one-year-olds.

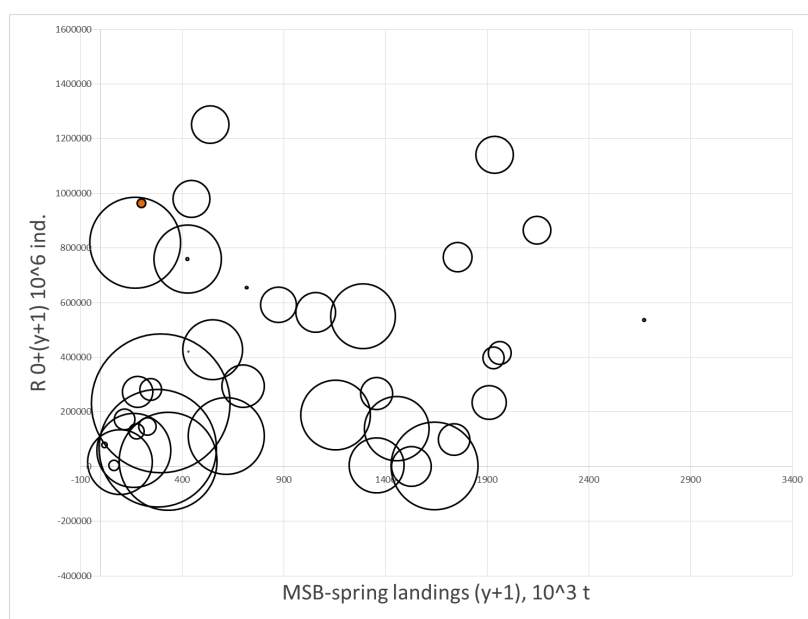


Figure 4.3.3. Relationship between mature stock biomass (>14 cm) with spring fishery subtracted (biomass at 1 Oct. Y, total landings from 1 January to 1 April. Y+1 are subtracted, 1000 tonnes) and 0-group index in billions (Y+1), covering the cohorts 1980–2019. The size of bubbles indicates the biomass of herring at age 1-3 (ICES WGIBAR data). Minimum diameter of bubble corresponds to 0.02 million tonnes of herring (1983), the maximum - 5.02 million tonnes. (1994). The red point is the 1989 cohort which is the basis for the current reference point (B_{lim}).

4.4 Causes of polar cod stock fluctuations

The Barents Sea polar cod stock was at a low level in 2017 and 2018. Norway conducted commercial fisheries on polar cod during the 1970s; Russia has fished this stock on

more-or-less a regular basis since 1970. However, the fishery has for many years been so small that it is believed to have very little impact on stock dynamics. Stock size has been measured acoustically since 1986 and has fluctuated between 0.1–1.9 million tonnes. Stock size declined from 2010 to a very low level in 2015, increased to 0.9 million tonnes in 2016, and again declined to 0.4 million tonnes in 2017. In 2018 the survey failed to cover the eastern parts of the Barents Sea and a reliable estimate of polar cod could not be obtained. However, the 2019 estimate confirmed that the polar cod stock is presently at a very low level. The rate of natural mortality for this stock appears to be quite high, relative to its importance as prey for cod and different stocks of seals.

It appears that polar cod mortality has increased in recent years. Since the mid-1990s, there has been a general trend of increase in both air and water temperature in the Barents Sea (See Section 3.1); record high temperatures have been recorded during the 2000s. The areal extent of sea ice coverage has never been lower than in 2016. In the Barents Sea, the area of Arctic water decreased, while a larger portion has been dominated by warmer Atlantic water. These climatic changes have likely affected the distribution and abundance of Arctic species like polar cod. It should be noted that during the three last years the temperatures have decreased somewhat, and the ice coverage has increased again.

0-group polar cod prey on small plankton organisms such as copepods and euphausiids, while adults feed mainly on large Arctic plankton organisms such as *Calanus hyperboreus* and *C. glacialis* and hyperiids. The biomass of Arctic forms of zooplankton decreased in recent years and most likely influenced negatively the feeding conditions for 0-group polar cod. However, no significant changes in the condition of adults were observed in recent years. This indicates a high degree of adaptability of this species to changes in the environment and enough available food resources.

The current fishing pressure is negligible now compared to the 1970s, when total catches were as high as 350 thousand tonnes. Thus, the total mortality is close to the natural mortality. Most likely predation by cod has contributed to the high natural mortality. Cod is a boreal species and associated with the temperate waters. The Barents Sea warming has been beneficial for cod and it has spread further north. In the northern areas cod overlapped with polar cod, and thus predation pressure on polar cod has increased, contributing to the declining stock trend in recent years. In the overlapping area cod feeds efficiently on polar cod (see Section 4.2).

The Barents Sea polar cod stock also has had a declining trend in recent years. Less is known about recruitment mechanisms of polar cod than of capelin, but some recent studies of recruitment of polar cod (Eriksen et al., 2019, Huserbråten et al., 2019, and Gjørseter et al., 2020) may shed some additional light on this topic. Based on a particle tracking model, Eriksen et al. (2019) studied simulated drift patterns of polar cod eggs in the Svalbard area. It has been inferred from 0-group distributions that some

spawning must have been taking place near Svalbard, but the location of this spawning is unknown. By releasing “eggs” several places around the Svalbard peninsula, from inner fjords to the outer coast, and letting these “eggs” drift with the currents until late summer and then compare their distribution with observed distributions of 0-group, the authors were able to backtrack the most probable spawning locations. Because there is a clockwise gyre flowing around Svalbard, they concluded that eggs spawned in outer coastal areas both at the western, northern and eastern coasts of Svalbard would be possible spawning areas, but that spawning locations under the ice east of Svalbard was the most probable spawning area for the western component of polar cod. This finding was confirmed by similar studies carried out by Huserbråten *et al.* (2019), who expanded the particle drift experiment to many more years and included the whole Barents Sea. The data-driven biophysical model of polar cod early life stages used in the latter study predicted a strong mechanistic link between survival and variation in ice cover and temperature; ice cover was positively related to survival of polar cod eggs and larvae, while temperature was negatively related to survival. The backtracking model also suggested a northward retreat of the spawning assemblages in the eastern Barents Sea, possibly in response to warming. Gjøsæter *et al.* (in review) used the same biophysical model to characterize the environmental and developmental properties of the early life history of individuals that reached the 0-group stage at the time and place of observations, and examined if and how ice cover, ice breakup time, maximum temperature, and spawning stock biomass relate to modelled larval survival. Results indicate that high ice coverage has a significant positive effect and high temperature a significant negative effect on survival of eggs and larvae from an eastern spawning component. No significant effects were found for the western spawning component, possibly because the variations in ice cover has been less noticeable there.

These recent studies support earlier findings that successful polar cod recruitment is associated with an ice cover until the eggs hatch. After hatching, however, larval survival depends on available food, which will only be available after ice break-up and onset of primary and secondary production. One may hypothesize, that ice break-up synchronizes these events, since the melting of ice and the associated stabilizing of the water column, warming of the surface layer, and deepening of the photic zone may initiate both hatching of eggs and onset of algal production.

4.5 Cod-capelin-polar cod interaction

The summer overlap between cod and capelin has increased, especially in the northern area, mainly due to the increased size of suitable habitat for cod, and the size of the cod stock. There is, however, a low correspondence between changes in horizontal overlap and changes in capelin consumption. The cod-capelin feeding interaction mainly takes place on the banks of the northern Barents Sea, where a vertical overlap with capelin is much more important for explaining variation in capelin consumption than capelin density. The northward expansion of

cod has probably also affected the polar cod negatively, since polar cod has become more available to cod.

The interaction among cod, capelin, and polar cod is one of the key factors regulating the state of these stocks. However, this interplay is far from fully understood. Cod prey on capelin and polar cod and can strongly influence the numbers of these species, while the availability of these species for cod varies. In addition, 0-group cod may also feed on 0-group capelin.

A prerequisite for feeding interactions is geographical overlap and both the overlap magnitude and the size of the overlap area will affect the consumption of forage fishes. In a recent analysis, it was found that increasing cod population size and water temperatures have influenced a northward shift of the late summer overlap area (Fall et al. 2018). The overlap between immature cod and capelin showed a rising trend, while the mature cod-capelin overlap had a less clear trend over time (Fig 4.5.1 B). The overlap area also increased in size, particularly for immature cod, which reflects the northeastwards expansion of the cod stock. The overlap was nevertheless relatively low, which was interpreted as a weak aggregative response of cod to capelin. The observed increased overlap over time could be interpreted as facilitating increased consumption of capelin per unit of cod stock in recent years. However, when comparing the amount of capelin consumed by cod in the summer-autumn period with the overlap, there is no obvious relationship (Figs 4.5.1 A-B). Consumption by immatures peaked during a period of average overlap, and for mature cod, the overlap trend is a near inverse of the trend in consumption. Generally, correlations between spatial overlap and consumption have been weak in summer, at several spatial scales (WD 1 by Johanna Fall).

Overlap is three-dimensional; two stocks may be overlapped in the horizontal dimension but still be segregated by depth, always or during parts of the day. The key to a better understanding of the feeding process may be the study of vertical overlap. One of the more important predictors of variation in cod feeding in summer was capelin depth distribution (Fall, 2019); more capelin was found in cod stomachs when capelin was distributed closer to the seafloor. Cod consumed more capelin at the Great and Central banks (100-250 m depth), where capelin was distributed closer to the seafloor throughout the diel cycle, than in deeper areas (Fig 4.5.2). An important factor that is likely to influence the distribution pattern of capelin is the near-bottom distribution of zooplankton on the banks (Aarflot et al. 2018). However, even when accounting for variation in capelin depth distribution, changes in capelin density did not have a strong effect on cod consumption. A potential explanation for this is that

once capelin is present, it is present in densities that allow cod to reach satiation (Fall and Fiksen 2019).

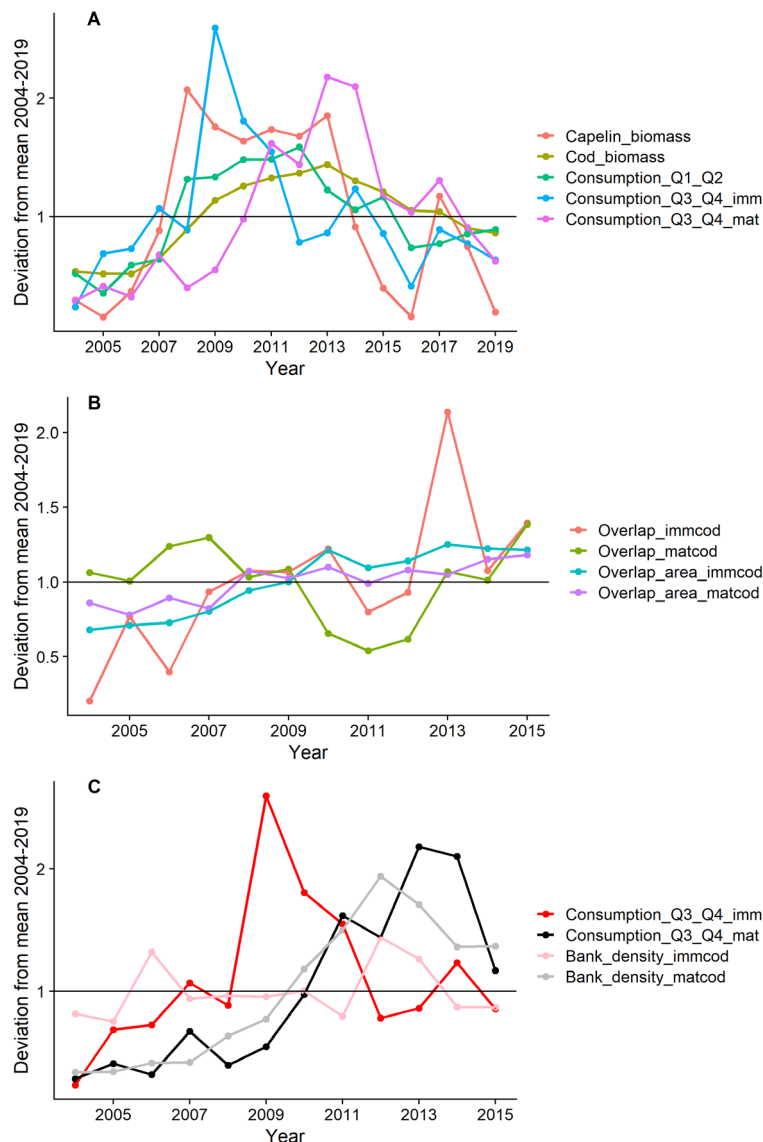


Figure 4.5.1: Deviations from mean A) capelin biomass, cod biomass, and estimated capelin consumption by cod, B) mean overlap and size of the overlap area, and C) density of cod on the banks across the period 2004-2015. Panel A shows the same data as Figure 4.2.3 divided by cod maturity (age 3-6 were considered immature) with the addition of cod stock biomass. Panel B shows mean overlap and size of the overlap area (overlap extent) from Fall et al. (2018) using predictions from the area north of 74 N. Bank density in panel C was calculated as the average predicted density of cod at 100-250 m depth using the distribution models in Fall et al. (2018).

Given the apparent importance of the banks for the cod-capelin interaction, it is of interest to examine trends in average cod density on these banks over time (Fig 4.5.1 C). Here, we see that the peak in immature cod consumption did not coincide with an increase in cod density on the banks, suggesting that the increased consumption resulted from behavioral changes in individual cod. For mature cod, on the other hand, consumption appears to follow the trend in bank density.

In conclusion, there seems to be a weak relationship between horizontal overlap and consumption of capelin by cod in summer, and capelin density is not an important

predictor of variation in cod's feeding on capelin beyond a very low-density threshold. On the other hand, behavioral responses to varying bottom depths by capelin may affect the feeding intensity of cod on capelin. How these findings reflect the feeding dynamics in other seasons should be further explored.

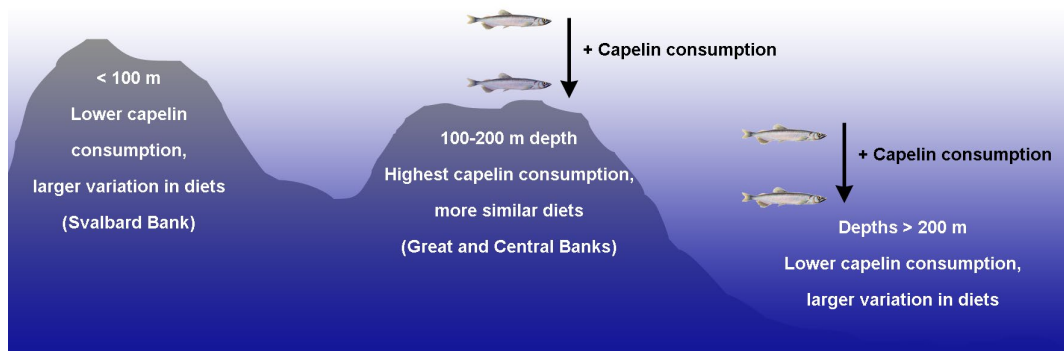


Figure 4.5.2 Schematic illustration of spatial variation in cod's consumption of capelin in the late summer overlap area in the central-northern Barents Sea.

Cod can prey intensively on polar cod. When polar cod and capelin occur in mixed concentrations, which they often do in northern and eastern areas, polar cod may be easier to catch because they may have a lower swimming speed (confirmed by trawl catch analyses) and are distributed closer to the bottom. However, capelin is a fatter and energetically a more valuable prey item. According to the estimated consumption of various prey species by cod (Fig 4.2.1-2) the consumption of polar cod is much smaller than for capelin. Possible under-sampling of cod stomachs where and when the most intense feeding on polar cod takes place may have biased the consumption estimates somewhat, but no doubt the capelin is a much more important prey for cod than polar cod is. The polar cod biomass in the Barents Sea is currently substantially less than the capelin biomass, thus, the effect of cod consumption on the stocks of these two species are different. Besides, the length of the period with cod and polar cod overlap is much shorter (September-December) compared to the overlapping time of cod and capelin. Interspecific interactions in this trophic system are very complex and require more detailed study.

References – Section 4.

- Aarflot, I., Aksnes, D., Opdal, A., Skioldal, H.R., & Fiksen, Ø. 2018. Caught in broad daylight: Topographic constraints of zooplankton depth distributions. *Limnology and Oceanography*, 64(3), 849-859. doi:10.1002/lno.11079
- Dalpadado, P. and Skioldal, H. R. 1996. Abundance, maturity and growth of the krill species, *Thysanoessa inermis* and *T. longicauda* in the Barents Sea. *Marine Ecology Progress Series*, 144:175–183
- Dalpadado, P., Bogstad, B., Gjøsaeter, H., Mehl, S., and Skioldal, H. R. 2002. Zooplankton–fish interactions in the Barents Sea. In *Large Marine Ecosystems of the North Atlantic*, pp. 269–291. Ed. by K. Sherman, and H. R. Skioldal. Elsevier Science, Amsterdam.
- Dalpadado, P., R. Ingvaldsen and A. Hassel. 2003. Zooplankton biomass variation in relation to climatic conditions in the Barents Sea. *Polar Biol.* 26: 233–241.
- Dolgov A.V., Benzik A.N. 2014. Feeding of cod in the northern Barents Sea. In: A.B. Karasev (ed.) *The formation of bioproductivity in the northern Barents Sea in the period of warming in the Arctic*. Murmansk: PINRO Press, P. 138-154. (in Russian)
- Dolgov A.V., Benzik A.N. 2016. Snow crab as a component of fish diet in the Barents Sea. In : K.M. Sokolov (ed.) *Snow crab Chionoecetes opilio in the Barents and Kara seas*. Murmansk:PINRO Press. P.140-153. (in Russian)

- Dolgov, A., Prokopchuk I., Gordeeva A. 2019. Fish predation on capelin larvae in the Barents Sea: myth or reality? In Influence of Ecosystem Changes on Harvestable Resources at High Latitudes. The Proceedings of the 18th Russian-Norwegian Symposium, Murmansk, Russia, 5–7 June 2018, pp. 142–148. Ed. by E. Shamray, G. Huse, A. Trofimov, S. Sundby, A. Dolgov, H. R. Skjoldal, K. Sokolov, L. L. Jørgensen, A. Filin, T. Haug, and V. Zabavnikov. IMR/PINRO Joint Report Series, No. 1-2019. 217 pp
- Eriksen, E., M. Huserbråten, H. Gjøsaeter, F. Vikebø and I. Albretsen (2019). "Polar cod eggs and larval drift pattern in the Svalbard archipelago." *Polar Biology*. <https://doi.org/10.1007/s00300-019-02549-6>
- Fall, J., Ciannelli, L., Skaret, G., & Johannesen, E. (2018). Seasonal dynamics of spatial distributions and overlap between Northeast Arctic cod (*Gadus morhua*) and capelin (*Mallotus villosus*) in the Barents Sea. *PLoS One*, 13(10), e0205921. doi:10.1371/journal.pone.0205921
- Fall, J. (2019). Drivers of variation in the predator-prey interaction between cod and capelin in the Barents Sea. PhD thesis, University of Bergen.
- Fall, J., & Fiksen, Ø. (2019). No room for dessert: A mechanistic model of prey selection in gut-limited predatory fish. *Fish and Fisheries*, 21(1), 63–79. doi:10.1111/faf.12415
- Gjøsaeter, H., Bogstad, B., and Tjelmeland, S. 2009. Ecosystem effects of the three capelin stock collapses in the Barents Sea. *Mar. Biol. Res.*: 40–53.
- Gjøsaeter, H., Hallfredsson, E. H., Mikkelsen, N., Bogstad, B., and Pedersen, T. 2016. Predation on early life stages is decisive for year-class strength in the Barents Sea capelin (*Mallotus villosus*) stock. *ICES J. Mar. Sci.*, 73: 182–195.
- Gjøsaeter, H., Huserbråten, M.B.O., Vikebø, F. and Eriksen, E. 2020. Key processes regulating the early life history of Barents Sea polar cod. *Polar Biology*.
- Holt, R. E., Hvingel, C., Agnalt, A-L., Dolgov, A. V., Hielset, A. M., and Bogstad, B. (submitted MS). Snow crab (*Chionoecetes opilio*), a new food item for North-East Arctic cod (*Gadus morhua*) in the Barents Sea?
- Huserbråten, M. B. O., E. Eriksen, H. Gjøsaeter and F. Vikebø (2019). "Polar cod in jeopardy under the retreating Arctic sea ice." *Communications Biology* 2 407. <https://doi.org/10.1038/s42003-019-0649-2>
- ICES 2019a. Arctic Fisheries Working Group (AFWG). ICES Scientific Reports. 1:30. 930 pp. <http://doi.org/10.17895/ices.pub.5292>
- ICES 2019b. Working Group on Widely Distributed Stocks (WGWISE). ICES Scientific Reports. 1:36. 948 pp. <http://doi.org/10.17895/ices.pub.5574>
- Lilly, G. R., and A. M. Fleming. 1981. Size relationships in the predation by Atlantic cod, *Gadus morhua*, on capelin, *Mallotus villosus*, and sand lance, *Ammodytes dubius*, in the Newfoundland area. *NAFO Sci. Coun. Studies*, 1: 41–45.
- Orlova, E. L., Rudneva, G. B., Renaud, P. E., Eiane, K., Vladimir, S., and Alexander, S. Y. 2010. Climate impacts on feeding and condition of capelin, *Mallotus villosus* in the Barents Sea. Evidence and mechanisms from a 30 year data set. *Aquatic Biology*, 10: 105–118.
- Skaret, G., D. Prozorkevich, H. Gjøsaeter, and B. Bogstad. 2019. Evaluation of potential sources of error leading to an underestimation of the capelin stock in 2016. Page 217 in Influence of Ecosystem Changes on Harvestable Resources at High Latitudes. The Proceedings of the 18th Russian-Norwegian Symposium. IMR/PINRO Joint Report Series, Murmansk, Russia.
- Skjoldal, H.R., Gjøsaeter, H., Loeng, H., 1992. The Barents Sea ecosystem in the 1980s: ocean climate, plankton and capelin growth. *ICES Marine Science Symposia* 195, 278–290.
- Stige, L.C., Dalpadado, P., Orlova, E., Boulav, A.C., Durant, I.M., et al. 2014. Spatiotemporal statistical analyses reveal predator-driven zooplankton fluctuations in the Barents Sea. *Progr Oceanogr*, 120: 243–253.

5 Expected changes in the coming years

5.1 Sea temperature

Oceanic systems have a “longer memory” than atmospheric systems. Thus, a priori, it seems feasible to predict oceanic temperatures realistically and much further ahead than atmospheric weather predictions. However, the prediction is complicated due to variations being governed by processes originating both externally and locally, which operate at different time-scales. Thus, both slow-moving advective propagation and rapid barotropic responses resulting from large-scale changes in air pressure must be considered.

According to the expert evaluation based on the analysis of the internal structure of the long-term variations in hydrometeorological parameters, over the next two years (2020–2021), the Atlantic water temperature in the Murman Current is expected to decline slightly but remain typical of warm years. Due to high temperatures and low sea-ice extent in recent years, the ice coverage is expected to remain below normal.

5.2 Possible development of some fish, shellfish and sea mammal stocks (near future)

Most of the commercial fish stocks found in the Barents Sea stocks are at or above the long-term mean level. The exceptions are polar cod and *Sebastes norvegicus*. In addition, the abundance of blue whiting in the Barents Sea is at present very low, but for this stock only a minor part of the younger age groups and negligible parts of the mature stock are found in the Barents Sea.

Concerning shellfish, the shrimp abundance has increased in 2018–2019 and is close to the highest observed. The abundance and distribution area of snow crab is also increasing.

Based on the current abundance and age structure of the main commercial stocks, the following lines of development are possible:

The haddock stock is expected to increase markedly, as the 2016 year class so far seems to be of the same order of magnitude as the strong 2004–2006 year classes and the 2017 year class is also above average. For cod and Greenland halibut, a slight decrease in total abundance is expected in the next couple of years, while the *S. mentella* stock is expected to stay at the present level.

The abundance of young herring in the Barents Sea in 2019 was high. However, most of this herring was from the strong 2016 year class. Thus, the abundance of herring is expected to decrease from 2019 to 2020 as this year class is expected to leave the Barents Sea in late 2019/early 2020. The capelin stock is currently very low, but abundance of 0-group capelin in 2019 was around average and this gives some promise for a recovery of the stock. Polar cod abundance will most likely stay low, although incomplete

survey coverage and migration of polar cod between the Barents and Kara Seas makes predictions of polar cod abundance in the Barents Sea very uncertain.

Shrimp abundance will stay high in the next couple of years. The westward expansion of snow crab leads to higher overlap between cod and snow crab and thus predation by cod on snow crab may slow down the rate of increase of the snow crab stock.

The populations of marine mammals change slowly and are thus likely to stay at the current level in the near future.

The sea temperature has decreased in 2018-2019 and this has pushed the northern boundary of cod distribution in the area between Svalbard and Frans Josef Land southwards. A further decrease of temperature to below the long-term average may strengthen such effects. The area covered by sea ice has increased, and this may also have direct and indirect effects on production and distribution of organisms in the northern areas of the Barents Sea.

Annex 5: Working documents

5.1 A weak relationship between cod-capelin spatial overlap and cod's consumption of capelin in late summer

By Johanna Fall, Institute of Marine Research

5.1.1 Summary

This document summarizes some of the work on cod-capelin interaction done in the CODFUN project (2015-2018, Research Council of Norway grant number 243676/E40) led by Edda Johannesen, which had the aim of quantifying and explaining spatial heterogeneity in the capelin-cod interaction at different spatial scales. The project has so far resulted in one PhD thesis¹ with three papers, two of which have been published in scientific journals^{2,3}. Here I highlight findings that are relevant for estimations of cod-capelin interaction strength. We found that cod had a weak aggregative response to capelin in both summer and winter, and that increasing population sizes and water temperatures have influenced a northward shift of the late summer overlap area. In the summer overlap area, a large proportion of the population-level diet was capelin, but individual consumption was highly variable. Variation in capelin density alone could not explain this variation since cod's functional response to capelin quickly reached saturation. In contrast, the vertical distribution of capelin strongly influenced variation in cod feeding, especially at the Great and Central banks where the main feeding interaction took place. A potential explanation for cod's weak aggregative response to capelin is that once capelin is present, it is present in densities that allow cod to reach satiation. I suggest further exploration of trends in vertical overlap and its relation to consumption, especially in winter.

5.1.2 Changes in spatial overlap in August-October 2004-2015

The spatial overlap between cod and capelin was estimated² using survey data from the Barents Sea Ecosystem Survey (BESS) and the Winter Survey. Results on winter overlap will not be discussed in detail here (but see last section). Capelin densities were taken from acoustic data (NASC) and cod data from bottom trawl (swept area density). Spatial distribution models were developed for each species, using geographical coordinates, survey day of the year, solar elevation angle, bottom depth, bottom/pelagic temperature, and stock size as predictors of local species density using the Generalized Additive Models (GAM) framework. These models were used to predict species densities on a regular grid of the Barents Sea with 65 x 65 km resolution, and overlap was calculated on these predictions using a simple overlap index. The overlap index ranged from 0 to 1, where 0 means that one or neither of the species were present in grid cell (x,y) in year t, while 1 means that both species were present in the highest densities predicted for that year (Equation 1).

$$O_{(x,y),t} = \frac{\widehat{Cap}_{(x,y),t}}{\max \widehat{Cap}_t} * \frac{\widehat{Cod}_{(x,y),t}}{\max \widehat{Cod}_t} \quad (1)$$

In the paper, we present the trend in mean overlap (mean across all grid cells) and overlap extent (number of grid cells where the species overlap) across the Barents Sea, as well as maps of spatial variation in the overlap (see [2] and [4]).

Cod showed a weak aggregative response to capelin, i.e., there was not a strong positive spatial association between cod and capelin densities. We found higher overlap in years with a large cod stock, even when the capelin stock was small. The overlap area also shifted to the northeast during the study period, concurrent with the cod stock increase and an increase in water temperature in the northeastern part of the Barents Sea.

Here, I show the overlap trend split into two geographical areas by 74°N latitude (Fig. 1), largely corresponding to a southern distribution area where immature capelin dominates, and a northern area dominated by matures. For each area, we show the overlap between immature cod and capelin (ICAC) and between mature cod and capelin (MCAC).

The trends in mean overlap and overlap extent differ between the southern and northern areas. The overlap was higher in the north than in the south throughout most of the time series (Figs 1 A-B). In both areas, the mature cod-capelin overlap was initially higher than the immature cod-capelin overlap, but became similar to or lower than the immature cod-capelin overlap later in the study period as the mature cod-capelin overlap decreased (south) or immature cod-capelin overlap increased (north). The size of the overlap area (overlap extent) of mature cod-capelin overlap decreased over time in the south (Fig. 1 C). After a low in 2013, both immature and mature cod-capelin overlap extent increased again. In the north, the overlap extent increased over time as the cod stock grew larger and moved farther north (Fig. 1 D).

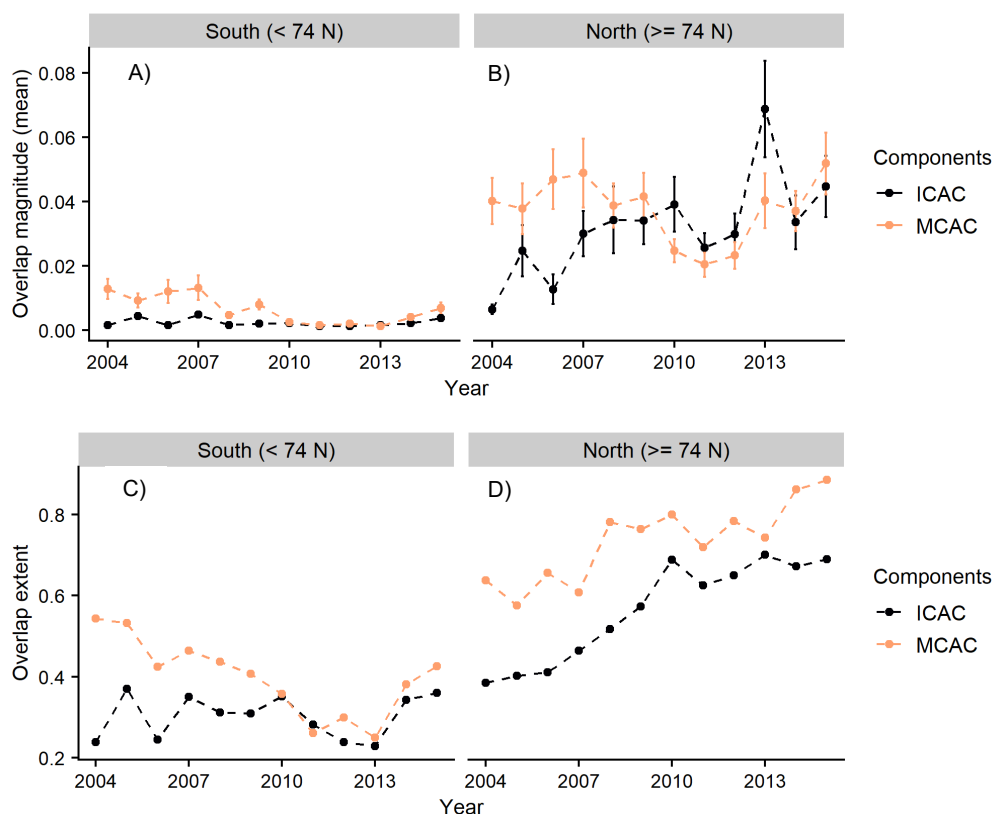


Figure 1: A-B) Changes in predicted overlap magnitude, i.e., mean overlap across a regular grid of the Barents Sea, and C-D) overlap extent, i.e., number of grid cells with overlap > 0.001 , in the southern and northern cod-capelin overlap area in 2004-2015. ICAC = immature cod-(acoustic) capelin, MCAC = mature cod-(acoustic) capelin.

5.1.3 Changes in relative consumption of capelin in August-October 2004-2018

For comparison, figure 2 shows the mass of capelin in cod stomachs sampled in the southern and northern areas for which we studied overlap. These are raw data from the cod stomach database from the months August-October and may contain some samples from commercial vessels. There is no obvious trend in consumption over time, and the relative ratio of capelin (kg capelin/kg cod) is similar in the southern and northern areas. We find the highest relative consumption in the south in 2008, but the cod sample was quite small. In the north, relative consumption by immature cod was highest in 2016 and 2017.

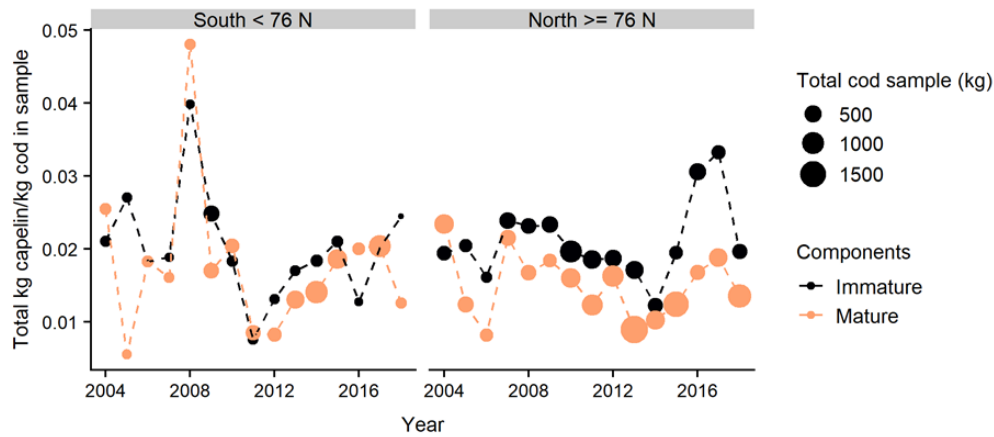


Figure 2: Trends in capelin consumption in the southern and northern areas. The y-axis shows the annual relative consumption of capelin for immature and mature cod, expressed as the total mass of capelin in all sampled stomachs divided by the total weight of the sampled cod. Cod < 75 cm in length are considered immature (same as in overlap calculations). The size of the points is proportional to the total cod sample in each year.

5.1.4 Relationship between horizontal overlap and consumption in the overlap area (Norwegian data only, 2004-2015)

In the PhD synthesis, I compared the spatial overlap with consumption (mass capelin in cod stomachs) in the overlap area at different spatial scales. The relationship was very weak, both at “station scale” where I compared the mean capelin consumption at each station with the estimated overlap at the scale of trawl hauls (approximately 2 km, comparing cod density in the trawl haul with overlapping acoustic measurements of capelin, Fig. 3 A), and when consumption was averaged across a 65 km grid cell and compared to predictions of overlap at this scale (Fig. 3 B). Thus, we see that changes in spatial predator-prey overlap does not necessarily reflect changes in prey consumption.

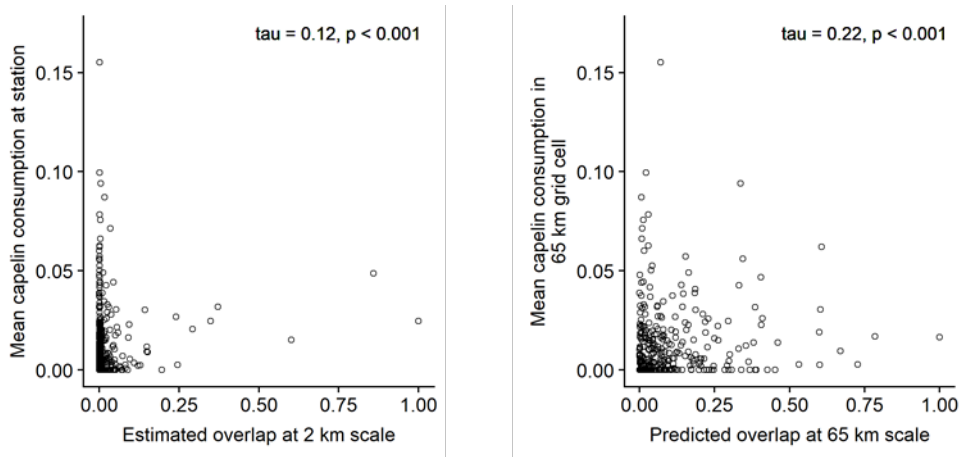


Figure 3: Cod-capelin overlap versus relative capelin consumption at two spatial scales in the overlap area. a) Overlap estimated at the 2 km “station scale” versus the mean consumption of cod caught at the same station. The overlap index from [2] was used, b) Predicted overlap from [2] (recalculated within the overlap area) versus the mean consumption of cod caught at stations within the 65 km grid cell. Relative consumption (mass capelin/mass cod) was calculated on data from paper 3 in [1].

5.1.5 Relationship between the local environment and cod's feeding on capelin in the overlap area (Norwegian data only, 2004-2015)

The final paper in the PhD thesis (unpublished) examines drivers of variation in cod's feeding on capelin in the overlap area by relating the amount of capelin in a cod stomach to the environment where the cod was sampled. Here we let the mass of capelin in individual cod stomachs be the response variable in a GAM with the predictors year, sampling day, capelin density, capelin weighted depth, cod density, bottom depth, and solar elevation angle (for details and hypotheses, see paper 3 in [1]).

Capelin dominated the diet of most cod that had managed to feed on this prey, but the majority of sampled cod had no capelin in their stomachs (Fig. 4). Nevertheless, half of the total prey mass consumed by the sampled cod was capelin. This means that the proportion of capelin in the population-level diet is not always representative of individual diets.

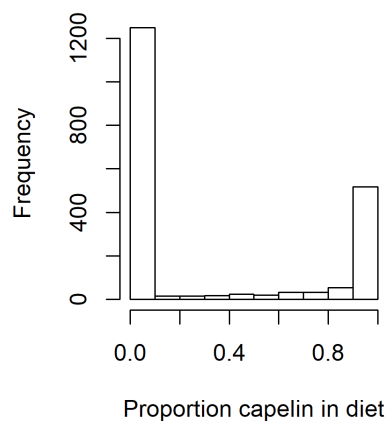


Figure 4: Capelin weight proportion of the total stomach contents in cod sampled by Norwegian vessels in the cod-capelin overlap area (data from paper 3 in [1]).

As already indicated by the weak relationship between horizontal overlap and consumption presented above, capelin density was not an important predictor of variation in cod's feeding on capelin beyond a very low-density threshold. Above this threshold, further increases in capelin density had a small effect on capelin consumption, i.e., the empirical functional response quickly reached saturation. Theoretical modelling of cod feeding using a foraging model combined with survey data³ suggested that capelin, when present, occur in densities that are high enough to satiate cod. Similar results have been found with stochastic modelling⁵ and bioenergetic calculations on for cod feeding on capelin in the Northwest Atlantic⁶. This therefore seems to be a likely explanation for the weak aggregative response of cod to capelin and the weak effect of capelin density on cod feeding.

One of the more important predictors of variation in cod feeding was capelin depth distribution; more capelin was found in cod stomachs when capelin was distributed closer to the seafloor. Cod consumed more capelin at the Great and Central banks (100-200 m depth), where capelin was distributed closer to the seafloor throughout the diel cycle, than in deeper areas.

This work also examined how cod diet breadth (weighted number of prey items) and individual diet variation (difference between individual diet and average diet) changed with the same local environmental variables. The results, summarized in figure 5, highlight the Great and Central banks as “hotspots” for cod’s feeding on capelin in late summer. Cod caught in shallower and deeper areas generally feed less on capelin and have more variable diets. At both the Great and Central banks and in deeper areas, capelin depth distribution influences the amount of capelin consumed by cod.

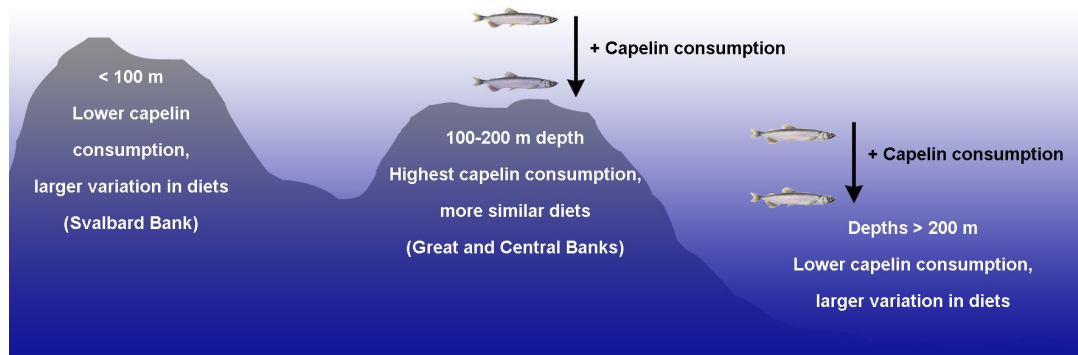


Figure 5: Schematic illustration of spatial variation in cod’s consumption of capelin in the late summer overlap area in the central-northern Barents Sea

5.1.6 Implications for estimates of cod-capelin interaction strength

Cod are distributed over a larger area than capelin in summer, and high cod densities are also found in areas where there is little or no capelin. We showed that spatial overlap between the species was weak at all spatial scales studied (entire Barents Sea @ overlap area @ 65 x 65 km grid @ scale of trawl hauls) and showed low correlation with capelin consumption. Even at the finest scale studied (the standard acoustic integration scale/trawl sampling scale of ~2 km), we found that vertically integrated capelin density was not a good indicator of capelin consumption.

Instead we found a clear signal showing higher capelin consumption in cod that were sampled in areas where capelin stood close to the seafloor. The depth distribution of capelin was estimated from vertically resolved acoustic data and showed that capelin generally stands closer to the seafloor on banks, especially during daylight hours. This may be related to the near-bottom distribution of their prey⁷. Changes in vertical overlap is therefore a potential indicator of changes in cod-capelin interaction strength. Vertical overlap may be quantified as changes in the proportion of the cod stock that are distributed on the Great and Central banks in summer, combined with changes in the proportion of capelin standing near the bottom in these areas.

A central question for further study is whether these vertical dynamics are valid also for the winter season. Predictions of capelin consumption by cod in the winter months are used in the capelin stock assessment, and assumptions on the duration and extent of spatial overlap are central to the prediction. The results on winter overlap from [2] reflected the dynamic species distributions during the cod and capelin spawning migrations. The relatively high overlap between immature cod and capelin in the

north, and between mature cod and capelin in the south gave support to the previously proposed revisions of the assessment model. The analysis also gave further insight into the methodological challenges of estimating the capelin stock in winter. One such challenge is the dynamic depth distribution of capelin at this time of year, where unknown proportions of the stock are distributed in acoustic dead zones near the surface and bottom during migration and spawning. These challenges make it difficult, but not impossible, to study capelin depth distribution and the effect of the vertical distribution on cod predation in winter.

The large variation in the amount of capelin eaten by cod can bias consumption estimates based on averaging across individual stomachs. The consumption estimate used in the capelin stock assessment is based on individual cod stomachs⁸, but cod cannibalism and the consumption of other prey species are estimated from pooled (averaged) stomachs⁹. A correction factor is applied to account for the bias introduced by averaging⁹. The correction factor is based on experiments by dos Santos and Jobling¹⁰, who showed that cod consumption based on pooled stomachs was always higher and had lower variance than consumption based on individual stomachs. Considering its importance for consumption estimates, the validity of the current correction factor for different years, seasons, cod sizes, and prey types should be explored in future work.

References

- Fall, I. (2019). Drivers of variation in the predator-prey interaction between cod and capelin in the Barents Sea. PhD thesis, University of Bergen.
- Fall, I., Ciannelli, L., Skaret, G., & Johannesen, E. (2018). Seasonal dynamics of spatial distributions and overlap between Northeast Arctic cod (*Gadus morhua*) and capelin (*Mallotus villosus*) in the Barents Sea. *PLoS One*, 13(10), e0205921. doi:10.1371/journal.pone.0205921
- Fall, I., & Fiksen, Ø. (2020). No room for dessert: A mechanistic model of prey selection in gut-limited predatory fish. *Fish and Fisheries*, 21(1), 63-79. doi:10.1111/faf.12415
- Spatial variation in overlap, by year. Supplementary material from Fall et al. (2018). This document also includes overlap estimates for winter (January-March).
- Strand, E., & Huse, G. (2007). Vertical migration in adult Atlantic cod (*Gadus morhua*). *Canadian Journal of Fisheries and Aquatic Sciences*, 64(12), 1747-1760. doi:10.1139/f07-135
- Horne, J. K., & Schneider, D. C. (1994). Lack of spatial coherence of predators with prey: a bioenergetic explanation for Atlantic cod feeding on capelin. *Journal of Fish Biology*, 45, 191-207. doi:10.1111/j.1095-8649.1994.tb01093.x
- Aarflot, I., Aksnes, D., Opdal, A., Rune Skioldal, H., & Fiksen, Ø. (2018). Caught in broad daylight: Topographic constraints of zooplankton depth distributions. *Limnology and Oceanography*, 64(3), 849-859. doi:10.1002/lno.11079
- Tiilmeland, S. (2005). Evaluation of long-term optimal exploitation of cod and capelin in the Barents Sea using the Bifrost model. Paper presented at the Proceedings of the 11th Russian-Norwegian Symposium, Murmansk, 15-17 August 2005, Bergen, Norway.
- Bogstad, B., & Mehl, S. (1997). Interactions between Atlantic cod (*Gadus morhua*) and its prey species in the Barents Sea Forage Fishes in Marine Ecosystems: Lowell Wakefield Fisheries Symposium Series, American Fisheries Society (Vol. 14, pp. 591-615).
- dos Santos, I., & Jobling, M. (1995). Test of a food consumption model for the Atlantic cod. *ICES Journal of Marine Science: Journal du Conseil*, 52(2), 209-219. doi:10.1016/1054-3139(95)80036-0

5.2 Radioactive contamination

By Louise k. Jensen (DSA), Hilde Elise Heldal (IMR), Margarita Katkova (RPA “Typhoon”), Justin Gwynn (DSA), Andrey Epifanov (RPA “Typhoon”) and Vladimir Bulgakov (RPA «Typhoon»)

Institute of Marine Research (IMR), Norway

Research and Production Association «Typhoon» (RPA “Typhoon”), Russia

Norwegian Radiation and Nuclear Safety Authority (DSA), Norway

Levels of the anthropogenic radionuclides Cs-137, Sr-90 and Pu-239,240 in seawater, sediments, fish and seaweed in the Barents Sea area are currently low. In recent decades, there has been a slow decrease in the levels of most anthropogenic radionuclides in the Barents Sea. Monitoring data reported by Norway and Russia has been demonstrated to be robust and comparable

5.2.1 Background

The Barents Sea has some of the richest fishing grounds in the world. The area has also been exposed to different sources of radioactive contamination for more than half a century. The main sources have been global fallout following atmospheric nuclear weapons testing in the 1950s and early 1960s, long-range transport of contamination from the European reprocessing plants Sellafield and La Hague and the Chernobyl accident in 1986. In addition, Russian scientists have documented that releases of radioactive contamination have occurred from the reactor of the sunken nuclear submarine “Komsomolets” which lies in the Northern part of the Norwegian Sea. A detailed overview of all past and present sources is given in e.g. AMAP (2015). In recent decades, there has been a slow decrease in the activity concentrations of most anthropogenic radionuclides in the Barents Sea as a result of decreasing discharges from the European reprocessing plants, the reduced impact of fallout from the Chernobyl accident, radioactive decay of radionuclides and their dilution in the water masses.

There are, however, numerous potential sources for radioactive contamination to the area. These include the Andreeva and Gremikha temporal storage sites for spent nuclear fuel and radioactive waste, the Kola Nuclear Power Plant, bases for nuclear powered vessels (e.g. Rosatomflot, Severomorsk and Severodvinsk) and large quantities of dumped solid radioactive waste (Figure 1). In addition to “Komsomolets”, there are two further sunken nuclear submarines containing spent nuclear fuel which could result in releases to the marine environment; K-159 in the Barents Sea and K-27 in the Kara Sea. Recent publications have shown that any leakages from these sunken nuclear submarines would not have any significant impacts on the marine ecosystem and that activity concentrations in fish in the Barents Sea would be well below the maximum permitted level for cesium-137 (Cs-137) 600 Bq/kg set by the Norwegian authorities after the Chernobyl accident (Heldal et al., 2013; Hosseini et al., 2016). However, any increases in radioactive contamination in the Barents Sea may have important socioeconomic consequences if consumers and international markets respond by decreasing their demand for seafood products from Norway. This effect was seen in Japan after the Fukushima Daiichi accident (Wakamatsu & Miyata, 2016).

In order to reassure fishery industries and consumers alike, there is a need for up-to-date information that can only be provided by regular monitoring of the levels of radionuclide contamination in the Barents Sea

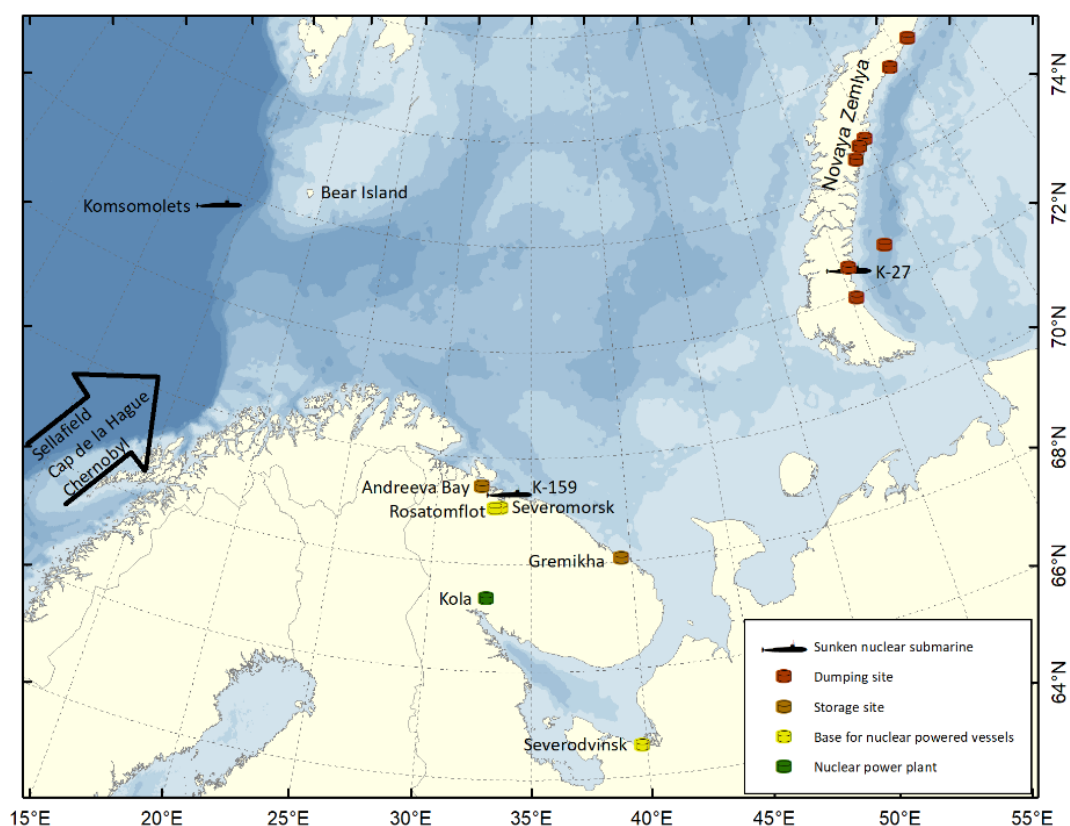


Figure 1. Potential sources of radioactive contamination in the Barents Sea area. The supply of long-range marine transport of contamination from European reprocessing plants and the Chernobyl accident is indicated. Illustration: Kjell Bakkeplass, IMR.

Cooperation between Russia and Norway on investigations of radioactive contamination of the marine environment began in 1992, when the first of three joint expeditions to the Kara Sea and fjords on the eastern coast of Novaya Zemlya was carried out (e.g. JNREG, 1996; Salbu et al., 1997). The «Joint Norwegian-Russian monitoring programme of radioactive contamination in the northern areas» was established in 2006. The main aim was to develop and implement a joint and integrated monitoring programme through the development of common observation targets (radionuclides and sample types) and methodological principles. Through such an initiative, data produced by both countries would be directly comparable and allow for common understanding of the levels of radioactive contamination in the Barents Sea area. To initiate the joint monitoring programme, a set of Norwegian and Russian sampling stations in coastal areas and in the open Barents Sea were agreed (Figure 2) (Jensen et al., 2017).

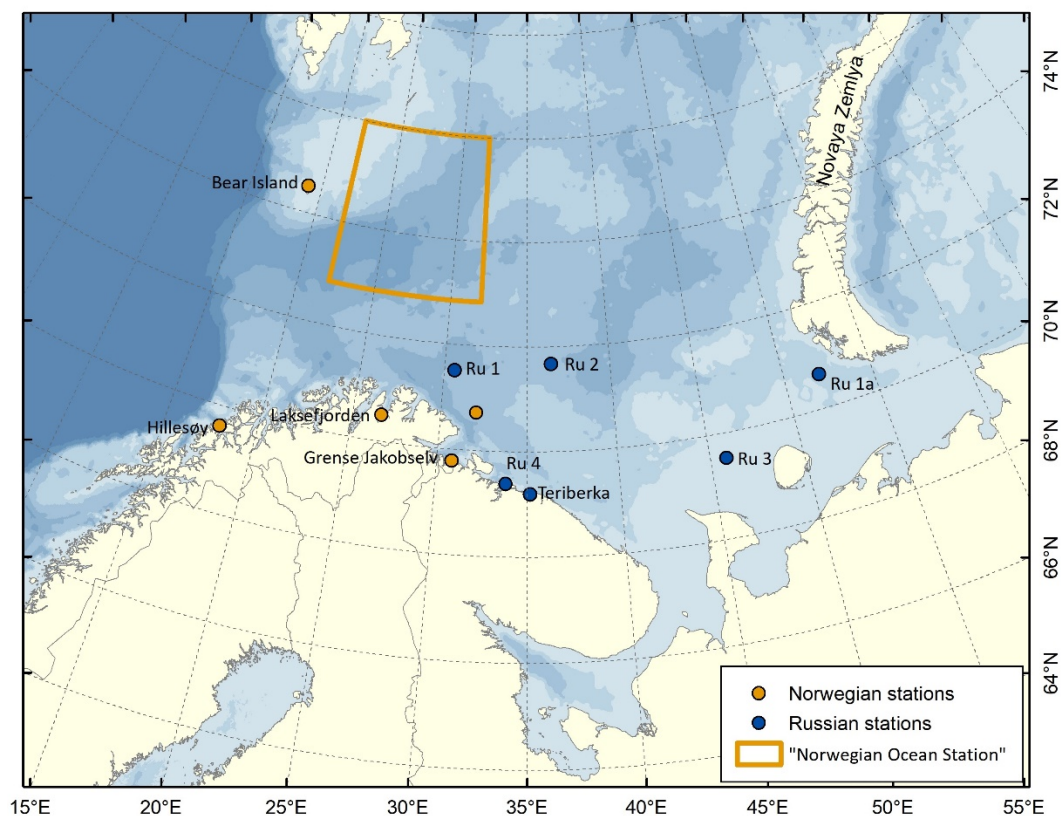


Figure 2. Marine monitoring stations included in the Joint monitoring programme. The «Norwegian Ocean Station» has been defined as the average of all data obtained from any sampling stations located between 72°50′-76°00′N and 22°00′-32°00′E. Ru 1-Ru 4 indicate different Russian stations. Since 2018, the Ru 1 station has been moved to a new location, Ru 1a. Illustration: Kjell Bakkeplass, IMR.

In Norway, monitoring of radioactive contamination in the marine environment is organised under the national monitoring programme, Radioactivity in the Marine Environment (RAME) (e.g. Skjerdal et al., 2015). This programme is coordinated by the Norwegian Radiation and Nuclear Safety Authority (DSA) and run in close cooperation with IMR. All Norwegian data are reported both to the Joint Norwegian-Russian monitoring programme and RAME.

In Russia, the monitoring programme is organised by the Research and Production Association «Typhoon» (RPA «Typhoon») jointly with the Murmansk Department for Hydrometeorology and Environment Monitoring (Murmansk Hydromet) and PINRO.

5.2.2 Sampling, analytical methods and data handling

Norwegian monitoring

Coastal samples are collected from the stations at Hillesøy, close to Tromsø, and Grense Jakobselv, close to the border with Russia. At these stations, samples of bladder wrack (*Fucus vesiculosus*) and seawater are collected by the DSA. In addition, coastal sediments are sampled on an annual basis by IMR at two stations in Laksefjorden, Troms and Finnmark.

Samples of seawater and sediments are collected from the open Barents Sea every third year during research cruises conducted by IMR. As sampling locations may vary

between different research cruises, a representative "Norwegian Ocean Station" has been defined in order to standardise the data from different years. A single data value for this representative station is derived by averaging all data from a given year for a particular radionuclide in a particular sample type collected from any station between 72°50'00"-76°00'00" N and 22°00'00"-32°00'00" E.

In addition, annual samples of cod are taken for IMR by Norwegian fishing vessels in the Bear Island area and along the coast of eastern Finnmark. Each sample is a pooled sample of muscle from either 25 or 100 individuals. An overview of the sampling stations is shown in Figure 2.

All sample preparation and analyses are performed by the DSA and IMR.

Russian monitoring

Sampling at the coastal monitoring station in Teriberka in the Murmansk Region includes annual sampling of surface seawater, surface layer sediments and marine biota (e.g. algae and fish). The sampling of seawater, sediments and bladder wrack (*Fucus vesiculosus*) is performed by RPA «Typhoon» and Murmansk Hydromet. Samples of cod (*Gadus morhua*) are taken by Murmansk Hydromet. Where more than one sample of a fish species was available, these were pooled into a single muscle sample weighing typically 2-3 kg before analysis. Otherwise, muscle samples from individual fish were analysed.

Sampling of surface seawater at three open sea stations (Ru 1-Ru 3) was carried out by PINRO on an annual basis until 2015 (Figure 2). Thereafter, the sampling frequency was reduced to every third years. In 2018, the station Ru 1 was moved to south of Novaya Zemlya as Ru 1a. In 2016, Ru 4, in the vicinity of K-159, was introduced. Surface seawater and surface sediments are sampled from this station on an annual basis to monitor for any possible releases from the sunken submarine.

All sample preparation and analyses are performed at the laboratories of RPA «Typhoon».

Selection of data

The joint monitoring programme focuses on radionuclides that are most relevant in terms of dose and on sample types that show temporal and spatial trends. Both Norway and Russia provide data on Cs-137, strontium-90 (Sr-90) and plutonium-239,240 (Pu-239,240) in one or more sample type (seawater, sediment, fish and seaweed).

5.2.3 Analytical methods and comparability of results

In 2012, a joint Norwegian-Russian expedition was carried out to Stepovogo Fjord on the eastern coast of Novaya Zemlya (JNREG, 2014; Gwynn et al., 2016). The main partners in the joint monitoring programme (RPA «Typhoon», IMR and DSA) all participated in the expedition. The analytical methods used for analysing samples collected during the expedition are the same as used in the joint monitoring

programme and are described in the final report from the expedition (JNREG, 2014). During the course of this expedition, a large volume sediment sample was obtained, homogenised and split for use as an intercomparison exercise between the different participants. The various analyses of this sediment showed good overall agreement between the results obtained by the partners (RPA «Typhoon», IMR and DSA) and the IAEA who were also involved in the expedition (JNREG, 2014).

More recently, intercomparison material of sample types relevant to the monitoring programme have been analysed by all participating laboratories. In each case, all results have been in good agreement.

Cesium-137 (Cs-137) in seawater

Activity concentrations of Cs-137 in seawater in the Barents Sea area have been low during the monitoring period (less than 3 Bq/m³), with a decreasing trend over the past 13 years (Figure 3). Activity concentrations observed at open ocean stations were generally comparable to values for coastal stations. Data reported under the joint monitoring programme shows good agreement with data from Icelandic and Greenlandic waters in the same time period (AMAP, 2015). The values and trend observed in the Barents Sea during the last 13 years reflect the overall reduction in the long-range transport of Cs-137 to the area. In the early 1980s, activity concentrations of Cs-137 in seawater in the southwestern Barents Sea reached nearly 50 Bq/m³ (Kershaw & Baxter, 1995; Matishov et al., 2005), as a result of peak discharges of this radionuclide from the European reprocessing facilities at Sellafield and La Hague in the mid-1970s.

In 2018, the levels of Cs-137 in the Skagerrak ranged from 2.5 to 13.6 Bq/m³ (RAME, unpublished data). The higher levels observed in the Skagerrak are due to the closer proximity to important contamination sources, namely outflowing Baltic seawater containing Chernobyl contamination, in addition to Sellafield and La Hague.

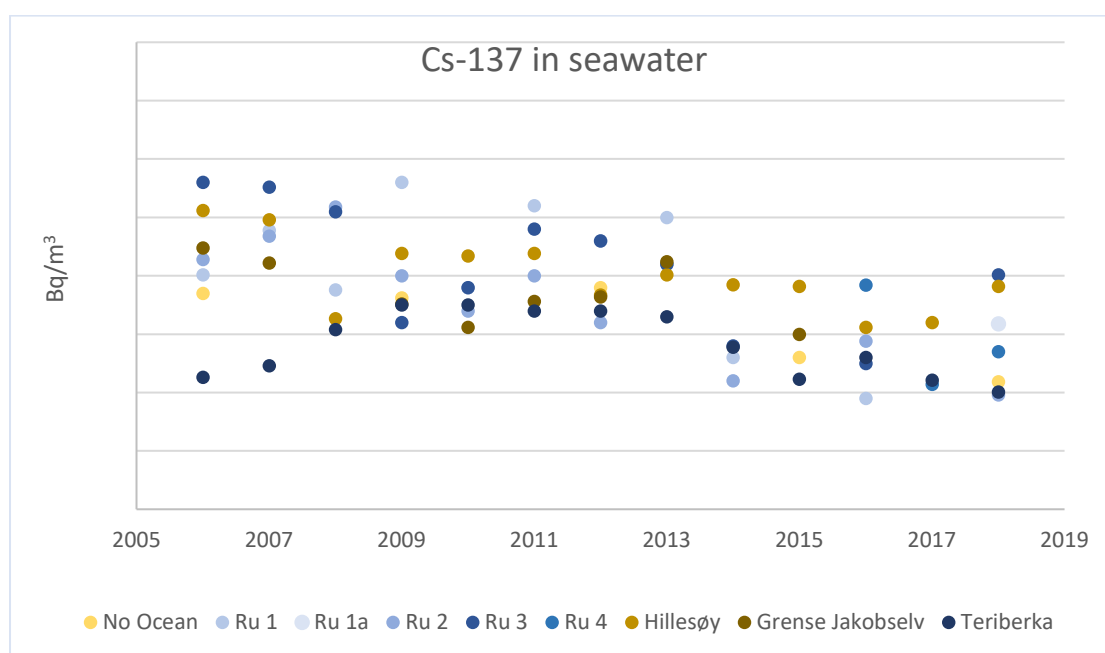


Figure 3. Activity concentrations (Bq/m^3) of Cs-137 in seawater from Norwegian and Russian sampling stations. See Figure 2 for the location of sampling stations.

Strontium-90 (Sr-90) in seawater

Activity concentrations of Sr-90 in seawater in the Barents Sea during the monitoring period were of a similar range to those observed for Cs-137, although with less of an obvious decreasing time trend over the last 13 years (Figure 4). The values reported under the joint monitoring programme are within the range of values observed by Leppänen et al. (2013) for the area for 2008 and 2009 (0.1 ± 0.1 to $10.4 \pm 0.7 \text{ Bq/m}^3$ ($n=25$)).

In comparison, Kershaw & Baxter (1995) reported activity concentrations of Sr-90 in the Barents Sea in 1981 of between 3.7 and 6.0 Bq/m^3 ($n=4$), that reflected the period of peak discharges of this radionuclide from European reprocessing facilities. Cs-137/Sr-90 activity ratios at this time were reported to be between 3.8 and 7.9 (Kershaw & Baxter, 1995), whereas during the time-span of the joint monitoring programme, this ratio has been closer to 1. The change in Cs-137/Sr-90 activity ratios observed in seawater follows the reduction in the ratio of Cs-137 and Sr-90 discharged from Sellafield from the mid-1970s until today (see e.g. Gray et al. (1995) and annual reports on discharges and environmental monitoring from Sellafield Ltd (<http://www.sellafieldsites.com>)).

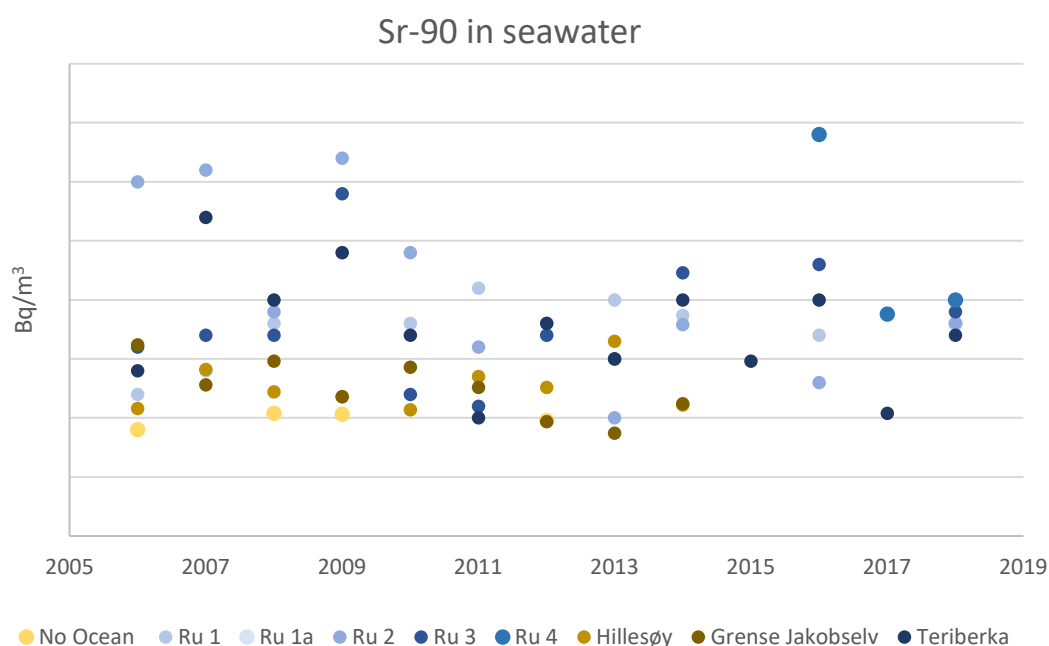


Figure 4. Activity concentrations (Bq/m^3) of Sr-90 in seawater from Norwegian and Russian sampling stations. See Figure 2 for the location of sampling stations.

Plutonium-239,240 (Pu-239,240) in seawater

Activity concentrations of Pu-239,240 in seawater in the Barents Sea during the monitoring period ranged from 2 to 11 mBq/m^3 (Figure 5). Only three samples have been analysed by Norway, and the results are in the lower range. These levels are comparable to data reported for other locations in the Barents Sea in the Norwegian

national monitoring programme RAME during the same period (Gäfvert et al., 2007; Gäfvert et al., 2011; Gwynn et al., 2012).

Similar values were reported by Strand et al. (1994) for the Barents and Kara Seas in the early 1990s. Since plutonium isotopes are more particle reactive than Cs-137 and Sr-90 in seawater, it would be expected that activity concentrations of Pu-239,240 would show less pronounced change over time at locations distant from any main source (e.g. Sellafield and la Hague), than any change in the magnitude of any actual releases. Although the values reported under the joint monitoring programme show some variation between years, an overall indication of decreasing activity concentrations over time can be observed.

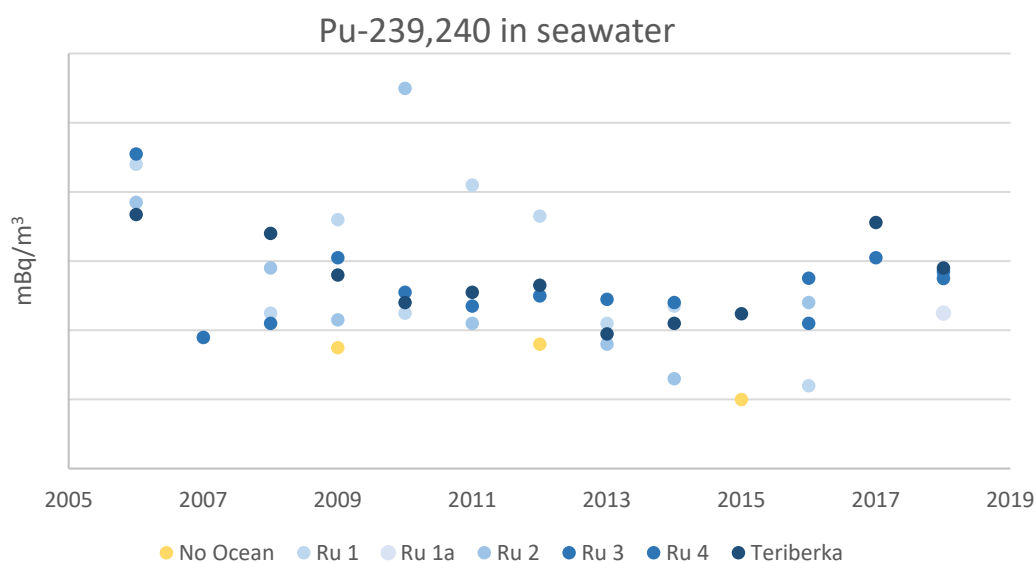


Figure 5. Activity concentrations of Pu-239,240 (mBq/m³) in seawater from Norwegian and Russian sampling stations. See Figure 2 for the location of sampling stations.

Cesium-137 (Cs-137) in sediments

The accumulation of radionuclides in sediments depends to a large extent on the activity concentrations in the overlying water column, the chemical properties of the radionuclide as well as the grain size and organic matter content of the sediment. As a result, different locations may show distinct differences in radionuclide levels despite similar fluxes of the radionuclide in question to the same areas. The activity concentration of Cs-137 in sediments in the Barents Sea collected in the joint monitoring programme were all below 10 Bq/kg dry weight (d.w.) (Figure 6). Although the activity concentrations of Cs-137 differ between the various stations, most likely due to differences in physical properties of the sediment, the values observed for each station have been relatively stable over the monitoring period. The results are comparable to the findings of e.g. Zaborska et al. (2010), Gwynn et al. (2012) and Leppänen et al. (2013).

The results obtained in the joint monitoring programme are also comparable to levels found at 102 stations in the Barents Sea and at the west coast of Spitsbergen in the early 1990s (values ranging from <1.0 to 8.6 Bq/kg d.w.) (Føyn & Sværen, 1997). Cs-137 is

generally considered to be conservative in seawater and so sediments are often less sensitive to relatively small changes in seawater activity concentrations over long time periods. It is for this reason, that the observed decreases in seawater are not reflected in the time series for sediments.

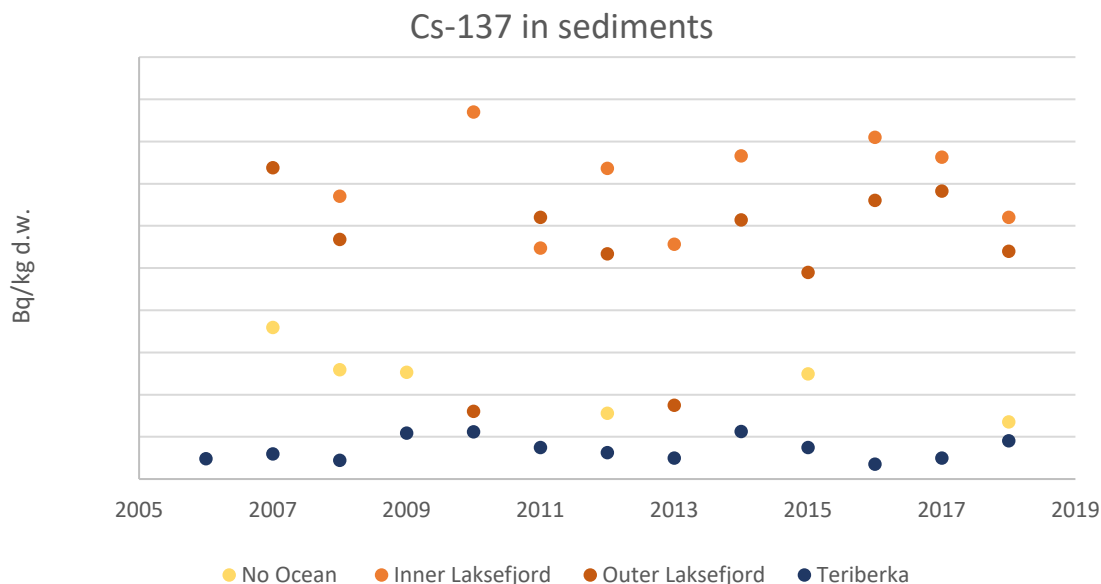


Figure 6. Activity concentrations (Bq/kg d.w.) of Cs-137 in surface sediments from Norwegian and Russian sampling stations. See Figure 2 for the location of sampling stations.

Cesium-137 (Cs-137) in Atlantic cod and brown seaweed

The activity concentrations of various anthropogenic radionuclides have been determined in a variety of marine biota within the joint monitoring programme. However, since the focus of the monitoring programme has been on fish and seaweed, we only present the results for these two indicators here. See e.g. Heldal et al. (2015) and Skjerdal et al. (2015) for information about radionuclides in other marine biota. Samples of Atlantic cod (*Gadus morhua*) analysed by Norway are pooled samples typically of 25 specimens. Some samples of fish species analysed by Russia consist of one individual only. The Norwegian results thus represent an average activity concentration in a fish stock, while the Russian results can represent activity concentrations in individual fish. This difference can introduce some variation between Norwegian and Russian results.

Due to its wide distribution and commercial importance, Atlantic cod has been chosen as an indicator species under Norwegian Marine Management Plans. Data reported under the joint monitoring programme by Norway is intended to represent different cod fish stocks. Fish caught around Bear Island are thought to represent the migrating northeast Arctic cod stock, while the fish caught near the Finnmark coast are thought to represent the stationary coastal cod stock. Cod caught by Russia at Teriberka are also thought to represent the stationary coastal stock. The activity concentrations of Cs-137 for all reported cod samples at all three different stations are low and comparable (<0.3 Bq/kg fresh weight (f.w.) (Figure 7). These levels are comparable to data reported for other locations in the Barents Sea in the Norwegian national monitoring programme

during the same period (Heldal et al., 2015). In the early 1980s, the activity concentration of Cs-137 in cod collected in the Barents Sea was reported to exceed 2 Bq/kg f.w. (Matishov et al., 2005), reflecting the higher activity concentrations of this radionuclide in seawater at this time. Overall, the time series for Cs-137 in cod from the monitoring programme shows a decreasing trend as a result of the concomitant decreasing activity concentration of Cs-137 in seawater.

The levels of Cs-137 in cod are very low compared with the maximum permitted level for radioactive cesium in food for commercial sale set by the Norwegian authorities after the Chernobyl accident (600 Bq/kg).

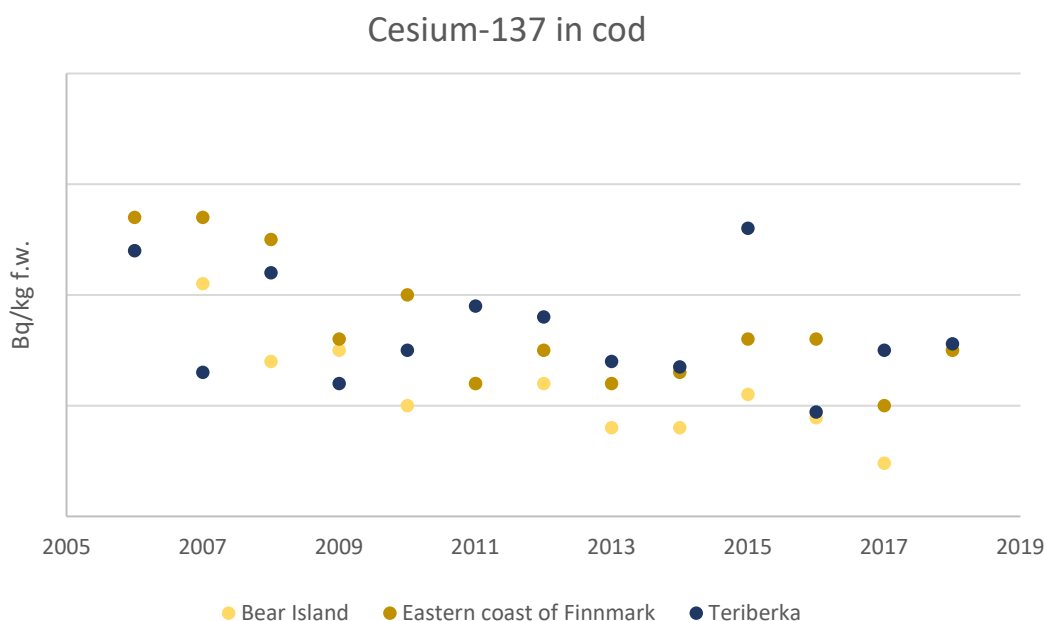


Figure 7. Activity concentrations (Bq/kg f.w.) of Cs-137 in Atlantic cod (*Gadus morhua*) from Norwegian and Russian sampling stations. See Figure 2 for the location of sampling stations.

Sessile organisms such as seaweed are often used as indicator species, as they can be repeatedly sampled from the same location and can integrate exposure concentrations over long time spans. The brown seaweed bladder wrack (*Fucus vesiculosus*) has been chosen as an indicator species under the Norwegian Marine Management Plans.

The activity concentrations of Cs-137 in bladder wrack from both Norwegian and Russian sampling stations were below 1 Bq/kg d.w. (Figure 8). The Norwegian results have been below the analytical detection limit since 2015.

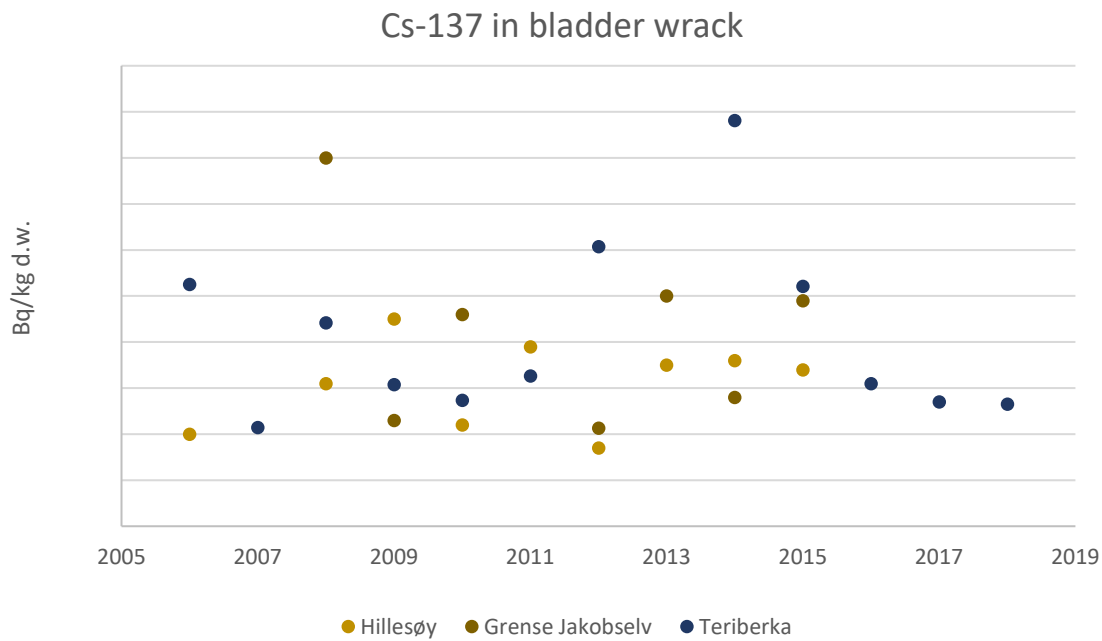


Figure 8. Activity concentrations (Bq/kg d.w.) of Cs-137 in bladder wrack from different Norwegian and Russian sampling stations. See Figure 2 for the location of sampling stations.

5.2.4 Monitoring of the nuclear submarine “Komsomolets”

Due to its proximity to the Barents Sea region and the previously documented release of radioactive contamination from its reactor, Norway has maintained a long term focus on monitoring the sunken nuclear submarine “Komsomolets”.

Norwegian monitoring of the area around the sunken nuclear submarine “Komsomolets” in the Norwegian Sea between 1993 and 2018 has not revealed any indication of releases from the reactor (Figure 9). Due to the depth at which the submarine lies and effect of sub-surface currents, it has not until recently been possible to know exactly how close to the wreck the samples have been collected. In 2013, 2015 and 2018, sampling was carried out using an acoustic transponder that allowed samples to be collected at a distance of <20 m from the hull of the submarine. Samples of seawater and sediment taken in these years showed similar activity concentrations to such samples collected in other years.

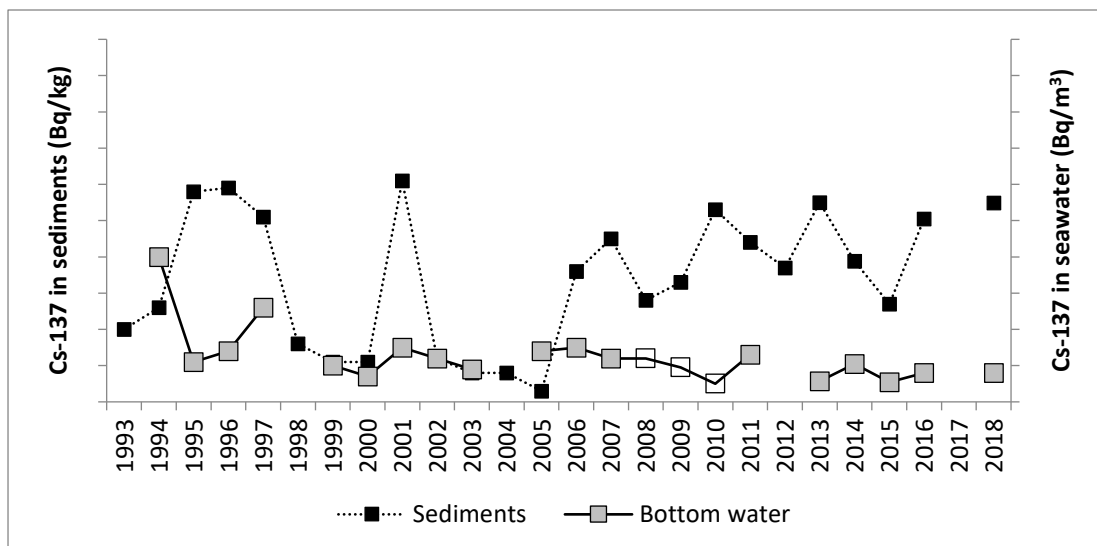


Figure 9. Activity concentrations of Cs-137 in sediments and bottom seawater collected in the area adjacent to the sunken nuclear submarine «Komsomolets» in the period 1993 to 2018. Open symbols represent values below detection limits. Values below detection limits are shown as half of the detection limit. Uncertainties on individual measurements were typically less than 10%.

In July 2019, a research cruise to “Komsomolets” was carried out with RV “G. O. Sars” and the advanced Remotely Operated Vehicle (ROV) Ægir 6000 (Figure 10). The expedition was organised under the Joint Norwegian Russian Expert Group for investigation of radioactive contamination in Northern Areas. Using the ROV, the condition of “Komsomolets” was visually documented and samples of seawater, sediment and biota were taken at specific locations in the immediate vicinity of the submarine (Figure 11). Onboard analyses of seawater sampled directly from the ventilation pipe where releases have previously been documented by Russian expeditions, showed activity concentrations of Cs-137 between <8.0 and 857 Bq/l. This indicates that releases from the reactor are still occurring, more than 30 years after “Komsomolets” sank. Based on our observations, the releases of Cs-137 from “Komsomolets” to the marine environment appear to vary in magnitude and duration. Samples collected during the expedition will now be further analysed in the laboratory for Cs-137, Sr-90, Pu-isotopes and other radionuclides as well as trace metals to further understand the nature of the releases from the reactor and to determine if any plutonium from the two nuclear warheads has been released into the marine environment. We aim to compile and publish the results in a report under the Joint Norwegian Russian Expert Group by the end of 2020.



Figure 10. The Remotely Operated Vehicle (ROV) Ægir 6000 investigating “Komsomolets”. Photo: Ægir 6000/IMR.

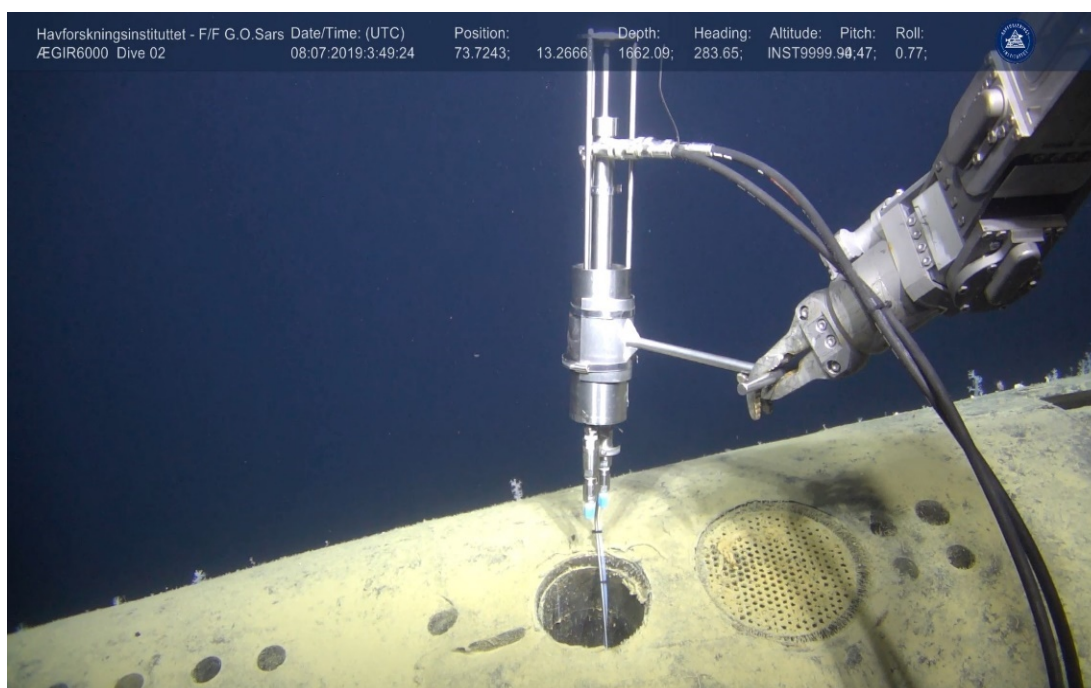


Figure 11. Collection of a 1l seawater sample from inside the ventilation pipe of “Komsomolets” with a biosyringe. Photo Ægir 6000/IMR.

5.2.5 Summary and conclusions

Data accumulated over the past 10-15 years by the Joint Norwegian-Russian monitoring program has provided a reliable overview of the levels and trends of radioactive contamination in the Barents Sea marine environment. The data confirms that levels of the anthropogenic radionuclides Cs-137, Sr-90 and Pu-239,240 in seawater, sediments, fish and seaweed are currently low and generally decreasing.

The monitoring data reported by Norway and Russia has been demonstrated to be robust and comparable. Further effort to ensure data comparability is an important part of the ongoing work on future cooperation. To support this aim, a series of bilateral workshops on sampling, analysis and quality control have been launched (starting in 2016) to better understand and harmonise methodologies employed on each side of the border.

References

- AMAP (2015). AMAP Assessment 2015: Radioactivity in the Arctic. In: Arctic Monitoring and Assessment Programme (AMAP), Oslo, Norway.
- Føyn L. & Sværen I. (1997). Distribution and sedimentation of radionuclides in the Barents Sea. *ICES J. Mar. Sci.*, 54, 333-340.
- Gray I., Jones S.R. & Smith A.D. (1995). Discharges to the environment from the Sellafield site, 1951-1992. *J. Radiol. Prot.*, 15, 99.
- Gwynn I.P., Heldal H.E., Gäfvert T., Blinova O., Eriksson M., Sværen I., Brungot A.L., Strålberg E., Møller B. & Rudiord A.L. (2012). Radiological status of the marine environment in the Barents Sea. *J. Environ. Radioact.*, 113, 155-162.
- Gwynn I.P., Nikitin A., Shershakov V., Heldal H.E., Lind B., Teien H.-C., Lind O.C., Sidhu R.S., Bakke G., Kazennov A., Grishin D., Fedorova A., Blinova O., Sværen I., Lee Liebig P., Salbu B., Wendell C.C., Strålberg E., Valetova N., Petrenko G., Katrich I., Logovda I., Osvath I., Levv I., Bartocci J., Pham M.K., Sam A., Nies H. & Rudiord A.L. (2016). Main results of the 2012 joint Norwegian– Russian expedition to the dumping sites of the nuclear submarine K-27 and solid radioactive waste in Stepovogo Fjord, Novaya Zemlya. *J. Environ. Radioact.*, 151, 417-426.
- Gäfvert T., Sværen I., Gwynn I.P., Brungot A.L., Kolstad A.K., Lind B., Alvestad P., Heldal H.E., Strålberg E., Christensen G.C., Drefvelin I., Dowdall M. & Rudiord A.L. (2007). Radioactivity in the Marine Environment 2005. Results from the Norwegian National Monitoring Programme (RAME). In: StrålevernRapport 2007:10 Norwegian Radiation Protection Authority, Østerås, Norway.
- Gäfvert T., Heldal H.E., Brungot A.L., Gwynn I.P., Sværen I., Kolstad A.K., Møller B., Strålberg E., Christensen G.C., Drefvelin I., Dowdall M., Lind B. & Rudiord A.L. (2011). Radioactivity in the Marine Environment 2008 and 2009. Results from the Norwegian National Monitoring Programme (RAME). In: StrålevernRapport 2011:4 Norwegian Radiation Protection Authority, Østerås, Norway.
- Heldal H.E., Vikebo F. & Johansen G.O. (2013). Dispersal of the radionuclide caesium-137 (¹³⁷Cs) from point sources in the Barents and Norwegian Seas and its potential contamination of the Arctic marine food chain: coupling numerical ocean models with geographical fish distribution data. *Environ. Pollut.*, 180, 190-8.
- Heldal H.E., Brungot A.L., Skierdal H., Gäfvert T., Gwynn I.P., Sværen I., Liebig P.L. & Rudiord A.L. (2015). Radioaktiv forurensning i fisk og sjømat i perioden 1991-2011. In: StrålevernRapport 2015:17: Norwegian Radiation Protection Authority, Østerås, Norway. (In Norwegian).
- Hosseini A., Amundsen I., Bartnicki I., Brown I., Dowdall M., Dvve I., Harm I., Karcher M., Kauker F., Klein H., Lind O., Salbu B., Schnur R. & Standring W. (2016). Environmental modelling and radiological impact assessment associated with hypothetical accident scenarios for the nuclear submarine K-27. In: StrålevernRapport 2016:8 Norwegian Radiation Protection Authority, Østerås, Norway, p. 140.
- Jensen, L. K., Shpinkov, V., Heldal, H. E., Gwynn, J. P., Møller, B. Bulgakov, V., Katkova, M., Artemyev, G., (2017). 10 years of joint monitoring of radioactive substances in the Barents Sea. Joint Norwegian-Russian expert Group for investigation of Radioactive Contamination in the Northern Areas (INREG).
- INREG (1996). Dumping of Radioactive Waste and Radioactive Contamination in the Kara Sea. Results from 3 Years of Investigations (1992-1994) by the Joint Norwegian Russian Expert Group. In: Joint Norwegian-Russian Expert Group for investigation of Radioactive Contamination in the Northern Areas. Norwegian Radiation Protection Authority, Østerås, Norway.
- INREG (2014). Investigation into the radioecological status of Stepovogo fiord. The dumping site of the nuclear submarine K-27 and solid radioactive waste. Results from the 2012 research cruise. In: Joint Norwegian-Russian Expert Group for investigation of Radioactive Contamination in the Northern Areas Norwegian Radiation Protection Authority, Østerås, Norway.
- Kershaw P. & Baxter A. (1995). The transfer of reprocessing wastes from north-west Europe to the Arctic. *Deep Sea Research Part II: Topical Studies in Oceanography*, 42, 1413-1448.
- Leppänen A.-P., Kasatkina N., Vaaramaa K., Matishov G.G. & Solatie D. (2013). Selected anthropogenic and natural radioisotopes in the Barents Sea and off the western coast of Svalbard. *J. Environ. Radioact.*, 126, 196-208.
- Matishov G.G., Matishov D.G., Kasatkina N.E., Usvagina I.S. & Kuklina M.M. (2005). Analysis of Distribution of Artificial Radionuclides in the Ecological System of Barents Sea. *Dokl Biol Sci.* 404, 375-378.
- Salbu B., Nikitin A.L., Strand P., Christensen G.C., Chumichev V.B., Lind B., Fjellidal H., Bergan T.D.S., Rudiord A.L., Sickel M., Valetova N.K. & Føyn L. (1997). Radioactive contamination from dumped nuclear waste in the Kara Sea — results from the joint Russian-Norwegian expeditions in 1992–1994. *Sci. Total Environ.*, 202, 185-198.
- Skierdal H., Heldal H.E., Gäfvert T., Gwynn I.P., Strålberg E., Sværen I., Liebig P.L., Kolstad A.K., Møller B., Komperød M., Lind B. & Rudiord A.L. (2015). Radioactivity in the Marine Environment 2011. Results from the

Norwegian National Monitoring Programme (RAME). In: StrålevernRapport 2015:3 Norwegian Radiation Protection Authority, Østerås, Norway.

Strand P., Nikitin A., Rudjord A.L., Salbu B., Christensen G., Føyn L., Krivshev I.I., Chumichev V.B., Dahlgaard H. & Holm E. (1994). Survey of artificial radionuclides in the Barents Sea and the Kara Sea. *J. Environ. Radioact.*, 25, 99-112.

Wakamatsu H. & Miyata T. (2016). Do Radioactive Spills from the Fukushima Disaster Have Any Influence on the Japanese Seafood Market? *Mar. Resour. Econ.*, 31, 27-45.

Zaborska A., Mietelski J.W., Carroll I., Papucci C. & Pempkowiak I. (2010). Sources and distributions of ^{137}Cs , ^{238}Pu , $^{239,240}\text{Pu}$ radionuclides in the north-western Barents Sea. *J. Environ. Radioact.*, 101, 323-331.